

**ENGINEERING AND IMPROVING A MOLECULAR SWITCH  
SYSTEM FOR GENE THERAPY APPLICATIONS**

A Dissertation  
Presented to  
The Academic Faculty

by

Jennifer Leigh Taylor

In Partial Fulfillment  
of the Requirements for the Degree  
Doctorate of Philosophy in the  
School of Chemistry & Biochemistry

Georgia Institute of Technology  
May 2011

# **ENGINEERING AND IMPROVING A MOLECULAR SWITCH SYSTEM FOR GENE THERAPY APPLICATIONS**

Approved by:

Dr. Donald Doyle, Advisor  
School of Chemistry & Biochemistry  
*Georgia Institute of Technology*

Dr. Bahareh Azizi, Advisor  
School of Chemistry & Biochemistry  
*Georgia Institute of Technology*

Dr. Loren Williams, Coadvisor  
School of Chemistry & Biochemistry  
*Georgia Institute of Technology*

Dr. H. Trent Spencer  
School of Medicine  
*Emory University*

Dr. Nicholas Hud  
School of Chemistry & Biochemistry  
*Georgia Institute of Technology*

Dr. Christoph Fahrni  
School of Chemistry & Biochemistry  
*Georgia Institute of Technology*

Dr. Joseph Le Doux  
Department of Biomedical Engineering  
*Georgia Institute of Technology*

Date Approved: [January 21, 2011]

I have learned that success is to be measured not so much by the position that one has reached in life as by the obstacles which he has had to overcome while trying to succeed.  
Booker T. Washington

During graduate school, I have lost two family members and gained three new ones. Therefore, I dedicate this work to my grandma Isabelle and my cousin Kellie, who I greatly miss. I also dedicate this work to my two nephews, Rome and Dave, and my niece, Milana, who I love dearly and I look forward to helping them achieve their goals in life.

## ACKNOWLEDGEMENTS

Being a graduate student has not been an easy task. I found that the road to graduation has been filled with obstacles, and when one challenge is conquered another obstacle is in your path. Although the path was not easy, I have learned a lot about my capability to strive through different situations, and I thank God for allowing me to triumph over the challenges I have faced so this work could be completed.

I want to first thank my entire family for all of their love and support. Thank you mom for your encouraging words and believing that I could get this degree. Thank you dad for instilling in me the value of an education. Thank you Robinson family and Wanzer family for your support throughout undergraduate and graduate school.

I would also like to thank my lab members: Michael Rood, Hally Schaffer, Amanda Ousley, Anna Duraj-Thatte, Hilda Castillo, and Dr. Bahareh Azizi. We have become a family over the past couple of years and words cannot explain how these people have impacted my life and the way I think about science. Dr. Bahareh Azizi has been a mentor and an advisor, and I would like to thank her for all the unrecognized effort she put into training this lab and the countless hours she put into make sure all group members could present and write scientifically.

Several other people have been involved in helping me through this process. I would like to thank Dr. Kenyetta Johnson for always encouraging me and listen to my presentations. I would like to thank Dr. Priyanka Rohatgi for training me and allowing me to continue this project. I would also like to thank Dr. Reagan McRae for being a

good sounding board to discuss scientific ideas and also training me to take beautiful pictures on the Fahrni lab microscope.

Finally, I would like to thank my committee members. A special thanks goes to Dr. Donald Doyle for allowing me to join your lab and sparking my interest in nuclear receptors. I look forward to hearing and reading about the research that will come out of your group in the future. A special thanks also goes to Dr. H. Trent Spencer for helping me trouble shoot the molecular switch project, training me and teaching me about gene therapy. I would like to thank Dr. Joseph Le Doux for helping me trouble shoot the retroviral studies, as well as, teaching me different ways to evaluate my data. I would also like to thank Dr. Christoph Fahrni for allowing me to use his microscope and the insight he provided throughout my graduate studies. Finally, I would like to thank Dr. Nicholas Hud and Dr. Loren Williams for their continual support especially in the last couple of years.

# TABLE OF CONTENTS

	Page
ACKNOWLEDGEMENTS	v
LIST OF TABLES	xi
LIST OF FIGURES	xii
LIST OF SYMBOLS AND ABBREVIATIONS	xvi
SUMMARY	xix
<u>CHAPTER</u>	
1 Introduction	1
1.1 Introduction to Nuclear Receptors	1
1.2 Nuclear Receptor Structure	2
1.3 Nuclear Receptor Function	5
1.4 Retinoid X Receptor (RXR)	8
1.5 Literature Cited	14
2 Gene Therapy and Molecular Switch Systems	24
2.1 Gene Therapy	24
2.1.1 Gene Delivery Methods	25
2.1.2 Gene Therapy Challenges	26
2.2 Criteria of a Molecular Switch System	30
2.3 Current Molecular Switch Systems	31
2.4 Literature Cited	37
3 Characterization of the Molecular Switch System with the GR130 Variant	45
3.1 Engineering RXR	45
3.1.1 Previous Work	48

3.2	GR130 in the Two-Component System	50
3.3	Characterization of the One-Component Molecular Switch System	51
3.4	Stable Expression of the Molecular Switch System	56
3.4.1	First Method: Retroviral Transduction	59
3.4.2	Second Method: Stable Expression Using a Selection Marker	64
3.4.3	Genomic Analysis of NIH3T3 cells transduced with GR130	68
3.5	Materials and Methods	70
3.6	Literature Cited	74
4	Characterization of the QCIMFI Variant in the Molecular Switch System	79
4.1	Engineering the QCIMFI Variant	79
4.2	Characterization of GRQCIMFI in the Two-Component System	81
4.3	Interference with Metabolic Pathways	83
4.4	Ligand Time Course	87
4.5	Characterization of GRQCIMFI in the One-Component System	89
4.6	Characterization of Stable Expression of GRQCIMFI in the Molecular Switch System	95
4.7	Materials and Methods	100
4.8	Literature Cited	102
5	Improving the Molecular Switch System	104
5.1	Improving the Fold Induction Using VP16	104
5.1.1	Addition of the Activation Domain	104
5.2	Discovery and Characterization of the Quadruple Mutant QCIMFILM	107
5.2.1	Chemical Complementation	109
5.2.2	Creation of RXR Libraries Using Random Mutagenesis	110
5.2.3	Results of Error Prone Libraries	115



5.2.4 Liquid Quantitation Assay	118
5.2.5 Activation Profile of the GRQCIMFILM Variant in Mammalian Cell Culture	124
5.2.6 Libraries of the QCIMFILM Variant	124
5.3 Determining the role of the L455M mutation	130
5.4 Summary	141
5.5 Materials and Methods	142
5.6 Literature Cited	144
6 The Effect of L455 Variants on Receptor Activation and Coactivation Association	147
6.1 The Importance of H12	147
6.2 Tolerance at the L455 position	150
6.2.1 Testing L455 Variants in Chemical Complementation	150
6.2.2 Testing L455 Variants in Mammalian Cell Culture	155
6.3 Assessment of the Double Variants L436V L455 and L436F L455	160
6.3.1 Testing the Double Variants in Chemical Complementation	160
6.3.2 Testing the Double Variants in Mammalian Cell Culture	163
ACTR 6.4 Ligand-Activated Growth Profiles of L455 Variants with SRC-1 and	169
ACTR 6.5 Ligand-Activation Growth Profiles of Double Variants with SRC-1 and	178
6.6 Materials and Methods	188
6.7 Literature Cited	189
7 Conclusions and Future Work	193
7.1 The Molecular Switch System	193
7.1.1 Conclusions	193
7.1.2 Future Work	199

7.2 The L455 Project	203
7.2.1 Conclusions	203
7.2.2 Future Work	204
7.3 Literature Cited	205

## LIST OF TABLES

	Page
Table 5.1: Transformation Results of RXR Libraries	116
Table 5.2: Sequencing Results of Error Prone Libraries	123
Table 5.3: QCIMFILM Libraries Transformation Results	127
Table 5.4: Activation of RXR Variants in Cell Culture	140
Table 6.1: EC <sub>50</sub> Values and Fold Activations of L455 Variants in Yeast	154
Table 6.2: EC <sub>50</sub> Values and Fold Activations of L455 Variants in Cell Culture	159
Table 6.3: EC <sub>50</sub> Values and Fold Activations of L455 Variants in Yeast with Coactivators	177
Table 6.4 EC <sub>50</sub> Values and Fold Activations of Double Variants in Yeast with Coactivators	186

## LIST OF FIGURES

	Page
Figure 1.1: Nuclear Receptor Structure	3
Figure 1.2: Structure of Nuclear Receptor Complex	6
Figure 1.3: Nuclear Receptor Function	9
Figure 1.4: <i>Apo</i> -Structure versus <i>Holo</i> -Structure	10
Figure 1.5: RXR Ligands	12
Figure 1.6: RXR Ligand Binding Pocket	13
Figure 2.1: Mechanism for Cationic Lipids	27
Figure 2.2: Mechanism of Action for Retroviruses	28
Figure 2.3: Schematic Diagram of Geneswitch®	33
Figure 2.4: Schematic Diagram of Tetracycline Inducible System	34
Figure 2.5: Schematic Diagram of Rheoswitch®	36
Figure 3.1: Engineering a Molecular Switch System	47
Figure 3.2: Schematic Diagram of Two-Component System	49
Figure 3.3: Activation Profile of G130 and GRXRwt	52
Figure 3.4: Schematic Diagram of One-Component System	53
Figure 3.5: Activation Profile in the One-Component System	55
Figure 3.6: Fluorescent Images of Transient Transfection with pMSCVGR130GFP	57
Figure 3.7: Fluorescent Image of Transient Transfection with pMSCVIRESGFP	58
Figure 3.8: Diagram of Packaging Cell Line	61
Figure 3.9: Flow Cytometry Histograms of NIH3T3 cells transduced with pMSCVIRESGFP	63
Figure 3.10: Fluorescent Images of Colonies transfected with GR130GFP and mRFP	66
Figure 3.11: Fluorescent Images of Cells stably transfected with GR130GFP and	

mRFP	67
Figure 3.12: Genomic Sequencing Analysis	69
Figure 4.1: Activation Profiles of RXRwt and QCIMFI	80
Figure 4.2: Fold Inductions of RXRwt and QCIMFI	82
Figure 4.3: Activation Profiles of GRQCIMFI and GRXRwt	84
Figure 4.4: Luciferase Assays in the Presence of 1 $\mu$ M Ligand	86
Figure 4.5: Ligand Time Course Flow Chart	90
Figure 4.6: Ligand Time Course Data	91
Figure 4.7: Transient Transfection of GRQCIMFIGFP	93
Figure 4.8: Transient Transfection of pMSCVIRESGFP	94
Figure 4.9: PCR of Genomic DNA of Cells Transduced with GRQCIMFIGFP	97
Figure 4.10: Fluorescent Images of Cells Transduced with GRQCIMFIGFP	98
Figure 4.11: Fluorescent Images of Cells Transduced with IRESGFP	99
Figure 5.1: Cloning VP16 into pMSCVGRQCIMFI	106
Figure 5.2: Activation profiles of VP16-GRQCIMFI and GRQCIMFI	108
Figure 5.3: Chemical Complementation System	111
Figure 5.4: Transformation of pGAD10BAACTR and pGBDRXR into the PJ69-4A strain	112
Figure 5.5: Creation of RXR Library and Transformation into PJ69-4A	114
Figure 5.6: Streaking Results of RXR Variants for Constitutive Activity	117
Figure 5.7: Streaking Results of RXR Variants Activated at Lower Concentrations of LG335	119
Figure 5.8: Liquid Quantitation Assay	120
Figure 5.9: Ligand-Activated Growth Profiles of Gal4, RXRwt, QCIMFI, and 23b	122
Figure 5.10: Activation Profile of GRQCIMFI and GRQCIMFILM	125
Figure 5.11: Streaking results for Constitutive Activity from QCIMFILM libraries	128

Figure 5.12: Ligand-Activated Growth Profiles of Gal4, RXRwt, 2-36, 2-43, 2-47	129
Figure 5.13 Crystal Structure of RXR Bound to 9cRA	131
Figure 5.14: Activation Profiles of RXRwt, L455M, Q275C L455M, I310M, and I310M L455M	134
Figure 5.15: Activation Profiles of F313I and F313I L455M	135
Figure 5.16: Activation Profiles of Q275C I310M and Q275C I310M L455M	136
Figure 5.17: Activation Profiles of Q275C F313I and Q275C F313I L455M	137
Figure 5.18: Activation Profiles of I310M F313I and I310M F313I L455M	138
Figure 5.19: Activation Profiles of Q275C I310M F313I and Q275C I310M F313I L455M	139
Figure 6.1: Sequence Alignment of H12 in Nuclear Receptor	149
Figure 6.2: Ligand-Activated Growth Profiles of L455 Variants	152
Figure 6.3: Activation Profiles of L455 Variants in Cell Culture	156
Figure 6.4: Activation Profiles of L455M Variants in Cell Culture	158
Figure 6.5: Ligand-Activated Growth Profiles of L436V L455 Variants	162
Figure 6.6: Ligand-Activated Growth Profiles of L436F L455 Variants	164
Figure 6.7: Activation Profiles of L436V L455M in Cell Culture	167
Figure 6.8: Activation Profiles of L436V L455S and L436V L455T in Cell Culture	168
Figure 6.9: Ligand-Activated Growth Profiles in Gal4 and RXRwt with ACTR and SRC-1	171
Figure 6.10: Ligand-Activated Growth Profiles of L455A, L455F, L455H, L455K, and L455Y with ACTR and SRC-1	173
Figure 6.11: Ligand-Activated Growth Profiles of L455C, L455T, and L455V with ACTR and SRC-1	174
Figure 6.12: Ligand-Activated Growth Profiles of L455S with ACTR and SRC-1	175
Figure 6.13: Ligand-Activated Growth Profiles of L455M with ACTR and SRC-1	176
Figure 6.14: Ligand-Activated Growth Profiles of L436V and L436F with ACTR and SRC-1	179

Figure 6.15: Ligand-Activated Growth Profiles of L436V L455A and L436F L455A with ACTR and SRC-1	180
Figure 6.16: Ligand-Activated Growth Profiles of L436V L455M and L436F L455M with ACTR and SRC-1	182
Figure 6.17: Ligand-Activated Growth Profiles of L436V L455T and L436F L455T with ACTR and SRC-1	183
Figure 6.18: Ligand-Activated Growth Profiles of L436V L455V and L436F L455V with ACTR and SRC-1	184
Figure 6.19: Ligand-Activated Growth Profiles of L436V L455S and L436F L455S with ACTR and SRC-1	185
Figure 7.1: Improvements in molecular switch system	202

## LIST OF SYMBOLS AND ABBREVIATIONS

AAV	Adeno-Associated Viral
ACTR	Activator for Thyroid Hormone and Retinoid Receptor
ADA	Adenosine Deaminase
AF-1	Activation Function 1
AF-2	Activation Function 2
CC	Chemical Complementation
CoAc	Coactivator
CSC	Chondroitin Sulfate C
DBD	DNA Binding Domain
DHA	Docosaheptaenoic Acid
DIC	Differential Interference Contrast Microscopy
Dox	Doxycycline
EcR	Ecdysone Receptor
epPCR	Error Prone Polymerase Chain Reaction
ER	Estrogen Receptor
G418	Geneticin
GAD	Gal4 Activation Domain
GFP	Green Fluorescent Protein
H12	Helix 12
HAT	Histone Acetyltransferase
HDAC	Histone Deacetylases
HSC	Hematopoietic Stem Cells



IRES	Internal Ribosome Entry Site
LBD	Ligand Binding Domain
LBP	Ligand Binding Pocket
LTR	Long Terminal Repeat
LXR	Liver X Receptor
N-CoR	Nuclear Receptor Corepressor
NR	Nuclear Receptor
Nurr1	Nuclear Receptor Related 1
OD	Optical Density
OLRP	Orthogonal Ligand/Receptor Pair
PB	Polybrene
PR	Progesterone Receptor
PXR	Pregnane X Receptor
RE	Response Element
RFP	Red Fluorescent Protein
RU486	Mifepristone
RXR	Retinoid X Receptor
SC	Synthetic Complete
SCID	Severe Combined Immunodeficiency
SF-1	Steroidogenic Factor 1
SHP	Short Heterodimer Partner
SMRT	Silence Mediator of Retinoic Acid and Thyroid Receptor
SNRMS	Selective Nuclear Receptor Modulators
TBP	TATA-Binding Protein
Tet	Tetracycline

TLX	Tailess Homolog
USP	Ultraspirale Receptor
VDR	Vitamin D Receptor
wt	Wild Type

## SUMMARY

Molecular switch systems that activate gene expression by a small molecule are effective technologies that are widely used in applied biological research. Previously, two orthogonal ligand receptor pairs (OLRP) were developed as potential molecular switch systems by modifying nuclear receptors, ligand-activated transcription factors, to bind and activate gene expression with the synthetic ligand LG335 and not with the natural ligand 9-*cis* retinoic acid (9cRA). The two OLRP previously discovered were RXR variant 130 (I268A, I310A, F313A, and L436F) (also known as GR130) and the RXR variant QCIMFI (Q275C, I310M, and F313I) and (also known as GRQCIMFI).

The OLRP were further developed into molecular switches to provide controlled gene expression and potentially benefit gene therapy applications by replacing the DNA binding domain (DBD) with a Gal4 DBD, a yeast transcription factor. Both molecular switches are able to bind Gal4 RE in response to LG335 and activate expression of a luciferase or GFP reporter gene in either a two- or one-component system. When characterizing the GR130 variant in the two-component system, no activation was observed with the natural ligand 9cRA, and the variant displayed a  $19 \pm 5$ -fold activation and a 50 nM EC<sub>50</sub> value in the presence of LG335. When the GRQCIMFI variant was evaluated in the two-component system, activation was observed in the presence of LG335 with a 10 nM EC<sub>50</sub> value and a  $6 \pm 2$ -fold induction, and 9cRA induced activation only at the highest concentration. The GRQCIMFI variant was also characterized with the one-component system containing the reporter gene GFP in a transient transfection as

well as through retroviral transduction, displaying green fluorescence in 30% of the cells in the presence of 10  $\mu$ M LG335.

Several attempts were made to improve the molecular switch system. The VP16 activation domain was fused to GRQCIMFI in an effort to increase the fold induction; however, the addition of the VP16 created a constitutively active protein. Another approach to improve the molecular switch incorporated error-prone PCR and the discovery of a variant, Q275C, I310M, F313I, L455M (QCIMFILM), which displayed a 10-fold increase in sensitivity towards LG335 with a 5 nM EC<sub>50</sub> value. Examination of the L455 position in the crystal structure of RXR revealed this residue is located outside of the ligand binding pocket on helix 12 (H12), but is able to significantly enhance receptor function. In fact, the single variant, L455M, was able to enhance receptor activation, compensate for a nonfunctional variant, as well as influence coactivator association.

The long-term goal of this research is to develop a gene regulation system that would be used in human gene therapy trials. In the process of creating this system a deeper assessment of the nuclear receptor structure and function is made, which can be used for the enhancement and development of transcriptional regulation mechanisms.

# **CHAPTER 1**

## **INTRODUCTION**

### **1.1 Introduction to Nuclear Receptors**

Nuclear receptors (NR) are a superfamily of proteins that have the ability to bind ligands and regulate transcription [1-3]. When a small molecule binds to a NR, a conformational change occurs in the receptor's structure allowing recruitment of the transcription machinery. This role in transcription makes NR crucial for the induction of gene expression and regulation of a variety of cellular processes, such as proliferation, differentiation, intracellular signalling, reproduction, and metabolism [3-5].

The sequencing of the human genome has lead to the identification of 48 human nuclear receptors [4, 6, 7]. This family is further divided into three sub-groups based on physiological ligands [8, 9]. The first class of receptors are called the endocrine receptors, binding hormones and vitamins. Examples of these receptors include the estrogen receptor (ER) and the vitamin D receptor (VDR), which are activated by  $17\beta$ -estradiol and  $1\alpha, 25$ -dihydroxy vitamin  $D_3$ , respectively [10, 11]. The adopted orphan NR are another class, and were identified based on sequence homology, but lacked a natural occurring ligand. However, their status was changed to “adopted” once the ligand for these receptors was identified. Examples in this class include the retinoid X receptor (RXR) and the pregnane X receptor (PXR), which bind phytanic acids and xenobiotics, respectively [12, 13]. “True” orphan receptors, the final subfamily, currently do not possess a natural or synthetic ligand. Examples of this class include short heterodimer partner (SHP) and tailless homolog (TLX).

Nuclear receptors have been implicated in various diseases including cancer, diabetes, obesity, and Parkinson's disease. Due to their role in these diseases, researchers are vastly interested in studying nuclear receptor pathways, as well as, discovering drug therapies for NR-based diseases [9, 14-16]. In fact, many nuclear receptors are significant drug targets: 10-20% of drugs currently on the market are nuclear receptors ligands [4, 17]. Examples of these drugs include tamoxifen, an anticancer drug targeting the estrogen receptor (ER) [18, 19], and bexarotene (Targretin®), a ligand that binds the retinoid X receptor (RXR) and is used to treat skin cancer [20, 21]. In attempt to discover potential new drug targets for NR, much focus has been put forth on understanding the structure and function of these proteins.

## **1.2 Nuclear Receptor Structure**

As shown in Figure 1.1, most nuclear receptors consist of five main domains. The first domain is the A/B domain, containing the transcriptional activation function 1 (AF-1). This domain is not well conserved, and varies in length within the nuclear receptor family [22]. However, this domain is known to interact with transcription factors, and undergoes post-translational modifications, such as phosphorylation, to enhance the signalling of transcription [8, 23-29].

The C domain or the DNA binding domain (DBD) is highly conserved among the NR family and is responsible for binding specific DNA sequences called response elements (RE). Structurally, the DBD has two  $\alpha$ -helices packed together in a perpendicular fashion, shown in green in Figure 1.1. Within the DBD are two zinc finger motifs, composed of four cysteine residues forming a tetrahedral arrangement coordinated by two zinc ions [30]. In order for the DBD to bind to these response

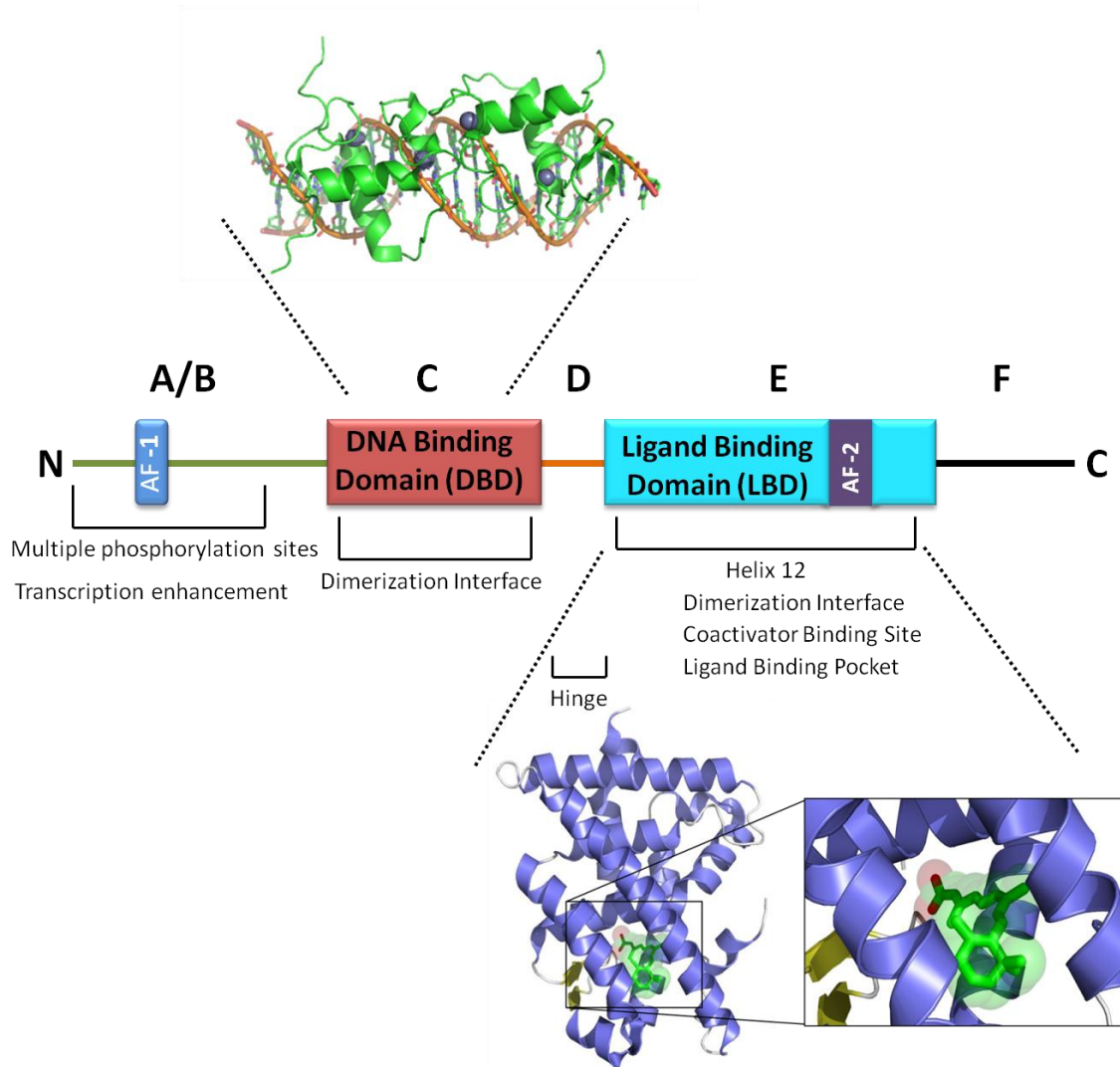


Figure 1.1: **Nuclear Receptor Structure:** Schematic illustration of nuclear receptor domains with the visual structure of the DBD (green) and the LBD (blue). (PDB files:1R4R and1FBY)

elements, the recognition helix of the DBD, residues 19-30, must insert itself into the major groove of the DNA. Therefore, this helix is important for allowing the receptor to bind alternate response elements [31].

The D domain, which is composed of a flexible hinge region, connects the DBD to the ligand binding domain (LBD). The hinge region is not well conserved within the nuclear receptor family; however, this region allows the DBD and the LBD to have the flexibility to adopt different conformations without steric hindrance [8].

The ligand binding domain (LBD) or the E domain, shown in blue in Figure 1.1, has several components, and is responsible for the binding of small lipophilic molecules. Most nuclear receptors consist of an overall composition of 12  $\alpha$ -helices and a short  $\beta$ -turn arranged in three layers to form an antiparallel “ $\alpha$ -helical sandwich” [32-34]. One key feature of this domain is the activation function 2 (AF-2), also known as helix 12 (H12). The conformational flexibility of AF-2 is essential for NR function and is also crucial for coregulator interaction [8, 33, 35]. The LBD also contains the strong dimerization interface. The majority of residues encompassed in this interface are located in helices 9 and 10 [36, 37].

Divergence within the LBD is primarily seen in the shape and in residues forming the ligand binding pocket (LBP). The size of the pocket varies from no space for constitutively active receptors, such as the nuclear receptor related 1 (Nurr1), to receptors like steroidogenic factor 1 (SF-1), which has a pocket size of about 1600 Å [38, 39]. Other receptors have a LBP that can accommodate a variety of molecules, such as



cholesterol derivatives and large macrolides [40]. The location of the LBP is usually between helices 3, 7, 10, and the  $\beta$ -turn, and is lined with hydrophobic residues and a few hydrophilic residues at the deep ends of the pocket [8, 41]. The hydrophilic residues at the deep ends of the pocket anchor the ligand into place, while the hydrophobic residues determine the pocket size and shape [32].

Previously, solved crystal structures of nuclear receptors have provided insight into the structure, but lacked information on how different domains interact with each other, as well as, with other transcription factors. Recently, the crystal structure of the heterodimer PPAR $\gamma$  and RXR $\alpha$  and their corresponding ligands rosiglitazone and 9cRA, respectively, was published (PDB file 3DZU) (Figure 1.2). The domains were bound to the PPAR response element (DR1) and associated with two coactivator peptides [42]. Structural information obtained from this complex is consistent with previously solved structures; however, new details revealed insight into the nuclear receptor complex, previously unknown. For example, the DBD was known to interact with the DNA, but this study provided insight that the DBD interacts with the LBD as well. The hinge region, previously not crystallized, is significantly organized in the PPAR structure, and able to interact with the DNA, as well as the DBD of RXR. The A/B domain could not be visualized, leading to the hypothesis that this region lacks a folded motif [32, 42]. The value in understanding the structure of these complexes is important for gaining knowledge on the physiology of these receptors, which has implications in understanding NR-based diseases and impacts the design of new drug targets for these receptors.

### **1.3 Nuclear Receptor Function**

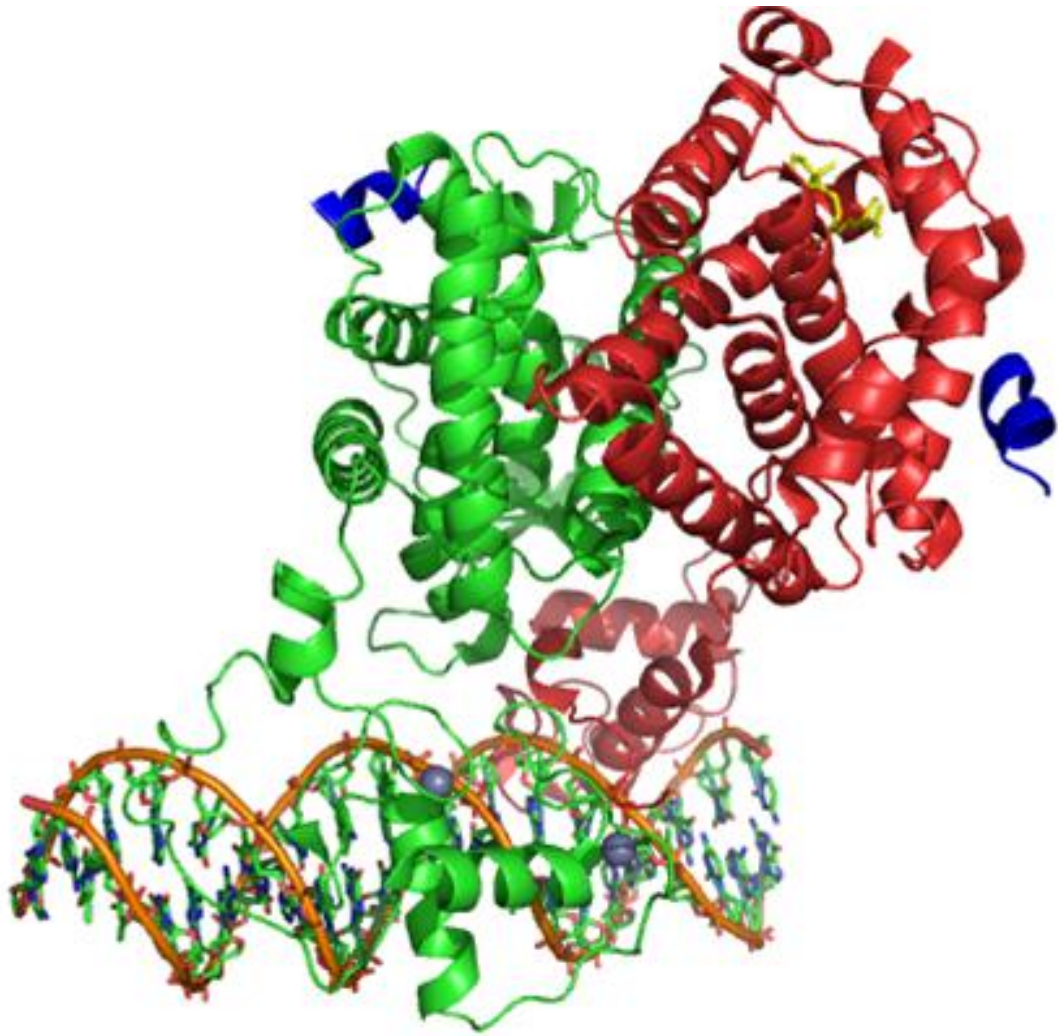


Figure 1.2: **Structure of Nuclear Receptor Complex:** Peroxisome proliferated-activated receptor (PPAR) (green) and the heterodimerization partner retinoid X receptor (RXR) (red) bound to coactivators (blue) and PPAR response elements. (PDB file: 3DZU)

Most NR function as homo- or heterodimers, which increases the binding efficiency to various DNA sequences called response elements (RE) [30, 43]. RE can be classified according to the receptor's dimerization partner [8, 30]. For instance, steroid receptors bind to RE containing palindromic repeats of hexameric half site sequences [31, 44, 45], while RXR homo- and heterodimers bind to direct repeat sequences (5'-AGGTCA-3'). The direct repeat sequences are separated by one to five base-pair inter-half site spacing (DR-1-DR-5) [30, 46, 47]. Previous research has shown that the spacing between the half sites is crucial for the DBD to recognize the proper DNA sequence [43, 48].

As transcription factors, nuclear receptors are involved in activating the transcription process, which is controlled by the binding of a specific small molecule or ligand. When a ligand binds to the receptor, a conformational change occurs, transforming the receptor to the active conformation. NR ligands can be classified into several groups: agonists, antagonists, and selective nuclear receptor modulators (SNRMs) [1]. Ligands able to bind and activate the receptor, initiating the transcription process, are called agonists. Ligands that are able to bind without activating the receptor are called antagonists. The last class of ligands, SNRMs, have both agonistic and antagonistic characteristics [49].

Nuclear receptors can repress transcription by recruiting corepressors in the absence of a ligand, or in the presence of antagonist [50-53]. Corepressors are complexes of proteins known to silence genes by recruiting or possessing enzymatic activity, such as histone deacetylases (HDAC). These enzymes deacetylate the histone, allowing the DNA backbone to tightly wrap around the histones, denying access to the RNA polymerase (Figure 1.3). Corepressors such as N-CoR (nuclear receptor corepressor) and SMRT (silence mediator of retinoic acid and thyroid receptor) bind to the nuclear receptor

through a LXX[I/H]IXX[I/L] motifs (L represents leucine, X represents any amino acid, I represents isoleucine, and H represents histidine) also known as CoR-NR boxes [4, 49, 54, 55].

Figure 1.4 depicts the differences in the NR structure in the process of ligand binding and activating the receptor. The crystal structure of RXR LBD in the absence of ligand (*apo*-crystal structure) shows the C-terminal helix extended away from the core of the protein and exposed to the solvent [56]. The RXR crystal structure in the presence of ligand (*holo*-crystal structure) shows H12 positioned in a conformation sealing the ligand binding pocket [57]. The positioning of H12 is critical in recruiting the CoAc complex, composed of several proteins such as histone acetyltransferase (HAT), kinase, and ATPase, which interact with the receptor and remodels the chromatin [58, 59]. Acetylation of the histones causes the DNA to unwind, allowing the RNA polymerase complex to access the DNA and initiate transcription (Figure 1.3). Previously, analysis of NR/coactivator interaction has shown that coactivators interact with NR through distinct LXXLL motifs (L represents leucine and X represents any amino acid). These motifs, present in the CoAc, serve as the interaction surface between the receptor and the CoAc [60].

#### **1.4 Retinoid X Receptor (RXR)**

RXR is a 463-residue protein that belongs to the class of retinoid receptors [61], and plays important roles in cellular morphogenesis and differentiation [62, 63]. There are three different isotypes and several isoforms of this receptor: RXR $\alpha$  ( $\alpha 1$  and  $\alpha 2$ ),  $\beta$  ( $\beta 1$  and  $\beta 2$ ), and  $\gamma$  ( $\gamma 1$  and  $\gamma 2$ ) [12]. RXR $\alpha$  and  $\gamma$  are tissue specific. RXR $\alpha$  is expressed in the liver, kidney, epidermis, intestine, and skin [62, 64, 65], whereas RXR $\gamma$  is expressed

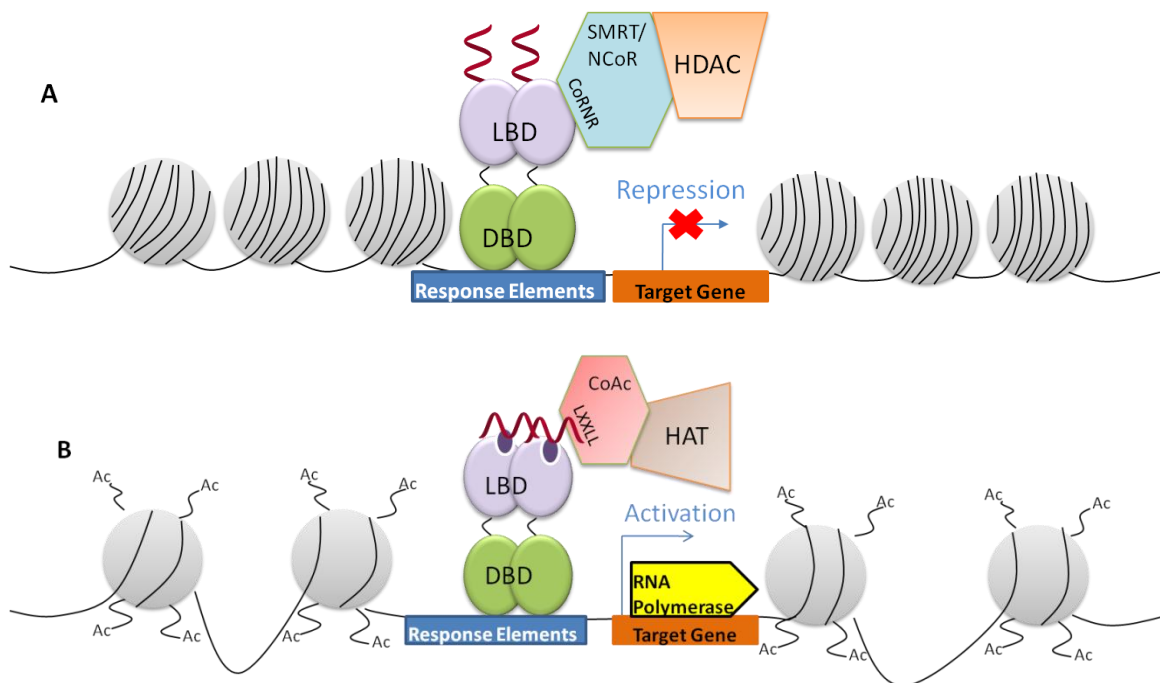


**Figure 1.3: Nuclear Receptor Function:** (A) In the absence of ligand, the corepressor complex associates with NR, which deacetylate the histones, wrapping the DNA tightly around the histones. (B) In the presence of ligand, the coactivator complex associates with NR, which acetylate the histone, allowing DNA to unwind giving access to the RNA polymerase.

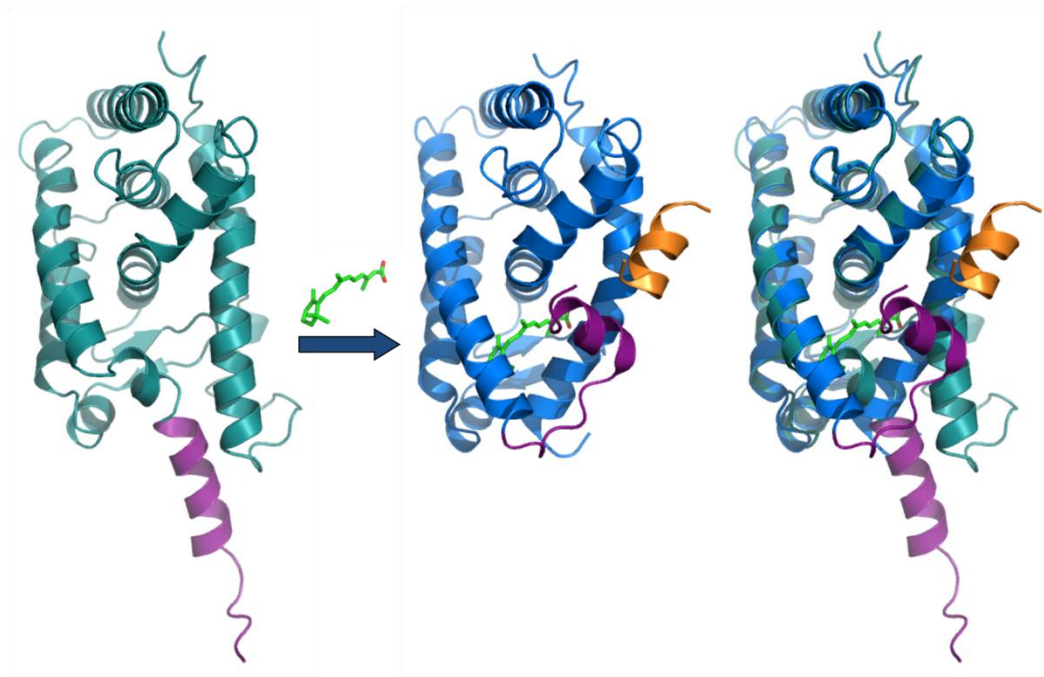
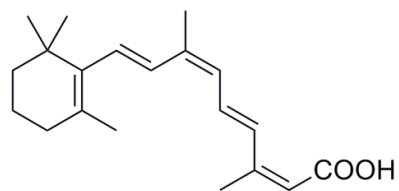


Figure 1.4: ***Apo*-Structure versus *Holo*-Structure**: Schematic illustration of the conformational change of nuclear receptor upon ligand binding, and overlay of *apo*- (teal) and *holo*- (blue) structures. Helix 12 is visualized in purple and the ligand is visualized in green.

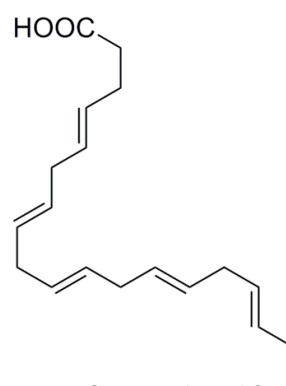
in the muscle, brain, and pituitary gland [64-67]. On the other hand, RXR $\beta$  is ubiquitously expressed. Ligands for this receptor are various endogenous small lipophilic compounds, such as 9-*cis*-retinoic acid (9cRA), docosahexanoic acid, as well as the synthetic ligand bexarotene (Figure 1.5) [64, 68-71]. The most potent ligand for RXR is 9cRA, with an EC<sub>50</sub> value of 1.7 nM [72]. However, studies have suggested that 9cRA is not the natural ligand for RXR [73, 74]. Other molecules, such as the unsaturated fatty acids docosahexaenoic acid (DHA) and linoleic acid found in animal tissues close to the EC<sub>50</sub> concentration are thought to be the “natural” ligand for this receptor [75].

Crystal structures of RXR bound to numerous ligands have provided considerable insight into the structure of this receptor. The crystal structure of RXR with 9cRA (Figure 1.6) reveals a hydrophobic ligand binding pocket formed by residues located on helices H3, H5, H7, H11, and the  $\beta$ -turn [57]. These residues are well conserved in all RXR isoforms, indicating the lack of an existing isoform-specific ligand for RXR. H11 plays a crucial role in both the *apo* and *holo* conformations. In the absence of ligand, H11 lines the pocket with hydrophobic residues [57]; however, upon binding of ligand, H3 displaces H11, permitting the helix to rotate 180° and generating adequate space for ligand binding, as well as, stabilizing H12 [57].

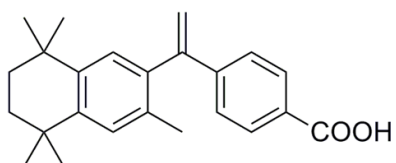
One of RXR's main functions is to serve as a heterodimerization partner for other nuclear receptors [43]. Most researchers classify the RXR dimerization partners as permissive and nonpermissive [15, 76, 77]. Permissive partners can activate transcription by the agonist of RXR and the partner nuclear receptor independently or together for an additive effect [12, 78]. Members of this group include the pregnane X receptor



**9-*cis* retinoic acid (9cRA)**



**Docosahexanoic acid**



**Bexarotene**

Figure 1.5: **RXR ligands:** 9-*cis* retinoic acid (9cRA), Docosahexanoic acid, and Bexarotene.



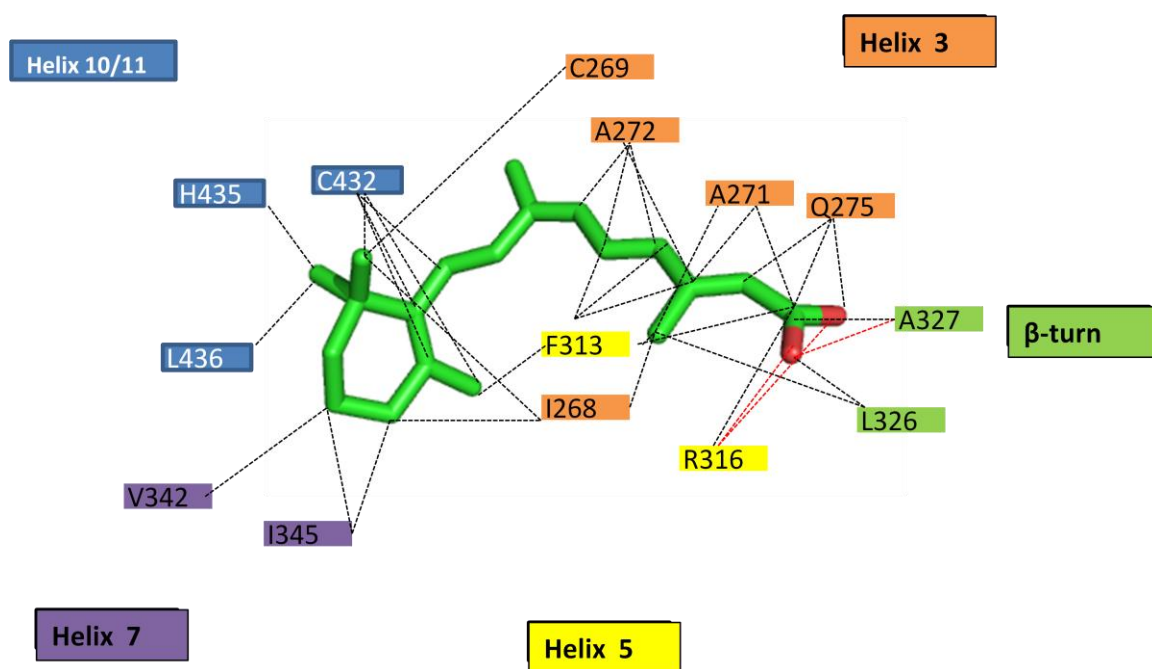


Figure 1.6: **RXR ligand binding pocket:** The ligand, 9cRA, is shown in green and the residues in the ligand binding pocket of RXR are colored by their corresponding helix.

(PXR), the PPAR, and the liver X receptor (LXR). Nonpermissive partners are not activated by a RXR agonist [12, 78]. Members of this group include the thyroid receptor (TR) and the vitamin D receptor (VDR). Shulman *et al* further defined RXR as acting as a “conditional permissive” heterodimerization partner [79]. Conditional permissive partners are activated by the ligand of the partner in the pair, but the RXR ligand is required for full activation. RXR is not only found in dimers; this receptor can self-associate into a tetramer complex in the absence of ligand; possibly the transcriptionally silent form of this receptor since it cannot interact with other receptors or coregulators [80-82].

In summary, nuclear receptors are involved in many metabolic processes, and as a result they are implicated in many diseases, ranging from diabetes to Parkinson’s disease. Much interest and research is put forth towards discovering drugs that target these receptors. Gaining insight into the structure and function of nuclear receptors allows pharmaceutical companies to develop novel agonists, antagonists, and SNRMs to treat NR-based diseases. In addition, nuclear receptors can also be used for applications such as protein engineering and gene therapy [83]. This work presented in this dissertation focuses on engineering RXR for controlling gene expression in mammalian cell culture for future use in gene therapy applications.

### **1.5 Literature Cited**

1. Gronemeyer, H., J.A. Gustafsson, and V. Laudet, *Principles for modulation of the nuclear receptor superfamily*. Nat Rev Drug Discov, 2004. **3**(11): p. 950-64.
2. Katzenellenbogen, J.A. and B.S. Katzenellenbogen, *Nuclear hormone receptors: ligand-activated regulators of transcription and diverse cell responses*. Chem Biol, 1996. **3**(7): p. 529-36.

3. Chambon, P., *The nuclear receptor superfamily: a personal retrospect on the first two decades*. Mol Endocrinol, 2005. **19**(6): p. 1418-28.
4. Gronemeyer, H., J.A. Gustafsson, and V. Laudet, *Principles for modulation of the nuclear receptor superfamily*. Nature Reviews Drug Discovery, 2004. **3**(11): p. 950-964.
5. Mangelsdorf, D.J., Thummel, C., Beato, M., Herrlich, P., Schutz, G., Umesono, K., Blumberg, B., Kastner, P., Mark, M., Chambon, P., and Evans, R. M., *The nuclear receptor superfamily: the second decade*. Cell, 1995. **83**(6): p. 835-9.
6. Zhang, Z.D., P.E. Burch, A.J. Cooney, R.B. Lanz, F.A. Pereira, J.Q. Wu, R.A. Gibbs, G. Weinstock, and D.A. Wheeler, *Genomic analysis of the nuclear receptor family: New insights into structure, regulation, and evolution from the rat genome*. Genome Research, 2004. **14**(4): p. 580-590.
7. Robinson-Rechavi, M., A.S. Carpentier, M. Duffraisse, and V. Laudet, *How many nuclear hormone receptors are there in the human genome?* Trends in Genetics, 2001. **17**(10): p. 554-556.
8. Germain, P., B. Staels, C. Dacquet, M. Spedding, and V. Laudet, *Overview of nomenclature of nuclear receptors*. Pharmacological Reviews, 2006. **58**(4): p. 685-704.
9. Sonoda, J., L.M. Pei, and R.M. Evans, *Nuclear receptors: Decoding metabolic disease*. Febs Letters, 2008. **582**(1): p. 2-9.
10. Levin, E.R., *Integration of the extranuclear and nuclear actions of estrogen*. Molecular Endocrinology, 2005. **19**(8): p. 1951-1959.
11. Moore, D.D., S. Kato, W. Xie, D.J. Mangelsdorf, D.R. Schmidt, R. Xiao, and S.A. Kliewer, *International Union of Pharmacology. LXII. The NR1H and NR1I receptors: Constitutive androstane receptor, pregnene X receptor, farnesoid X receptor alpha, farnesoid X receptor beta, liver X receptor alpha, liver X receptor beta, and vitamin D receptor*. Pharmacological Reviews, 2006. **58**(4): p. 742-759.
12. Germain, P., P. Chambon, G. Eichele, R.M. Evans, M.A. Lazar, M. Leid, A.R. de Lera, R. Lotan, D.J. Mangelsdorf, and H. Gronemeyer, *International Union of Pharmacology. LXIII. Retinoid X receptors*. Pharmacological Reviews, 2006. **58**(4): p. 760-772.

13. Moore, D.D., S. Kato, W. Xie, D.J. Mangelsdorf, D.R. Schmidt, R. Xiao, and S.A. Kliewer, *International Union of Pharmacology. LXII. The NR1H and NR1I receptors: constitutive androstane receptor, pregnene X receptor, farnesoid X receptor alpha, farnesoid X receptor beta, liver X receptor alpha, liver X receptor beta, and vitamin D receptor*. Pharmacol Rev, 2006. **58**(4): p. 742-59.
14. Mukherjee, S. and S. Mani, *Orphan Nuclear Receptors as Targets for Drug Development*. Pharmaceutical Research, 2010. **27**(8): p. 1439-1468.
15. Nohara, A., J. Kobayashi, and H. Mabuchi, *Retinoid X Receptor Heterodimer Variants and Cardiovascular Risk Factors*. Journal of Atherosclerosis and Thrombosis, 2009. **16**(4): p. 303-318.
16. Fitzgerald, M.L., K.J. Moore, and M.W. Freeman, *Nuclear hormone receptors and cholesterol trafficking: the orphans find a new home*. Journal of Molecular Medicine-Jmm, 2002. **80**(5): p. 271-281.
17. McDonnell, D.P., E. Vegeto, and M.A. Gleeson, *Nuclear hormone receptors as targets for new drug discovery*. Biotechnology (N Y), 1993. **11**(11): p. 1256-61.
18. Shao, W.L. and M. Brown, *Advances in estrogen receptor biology: prospects for improvements in targeted breast cancer therapy*. Breast Cancer Research, 2003. **6**(1): p. 39-52.
19. Kramer, R. and P. Brown, *Should tamoxifen be used in breast cancer prevention?* Drug Safety, 2004. **27**(13): p. 979-989.
20. Tanaka, T. and L.M. De Luca, *Therapeutic Potential of "Retinoids" in Cancer Prevention and Treatment*. Cancer Research, 2009. **69**(12): p. 4945-4947.
21. Tooker, P., W.C. Yen, S.C. Ng, A. Negro-Vilar, and T.W. Hermann, *Bexarotene (LGD1069, targretin), a selective retinoid X receptor agonist, prevents and reverses gemcitabine resistance in NSCLC cells by modulating gene amplification*. Cancer Research, 2007. **67**(9): p. 4425-4433.
22. Moore, J.T., J.L. Collins, and K.H. Pearce, *The nuclear receptor superfamily and drug discovery*. ChemMedChem, 2006. **1**(5): p. 504-23.

23. Bommer, M., A. Benecke, H. Gronemeyer, and C. Rochette-Egly, *TIF2 mediates the synergy between RAR alpha 1 activation functions AF-1 and AF-2*. Journal of Biological Chemistry, 2002. **277**(40): p. 37961-37966.
24. Tian, H.H., M.A. Mahajan, C.T. Wong, I. Habeos, and H.H. Samuels, *The N-terminal A/B domain of the thyroid hormone receptor-beta 2 isoform influences ligand-dependent recruitment of coactivators to the ligand-binding domain*. Molecular Endocrinology, 2006. **20**(9): p. 2036-2051.
25. Benecke, A., P. Chambon, and H. Gronemeyer, *Synergy between estrogen receptor alpha activation functions AF1 and AF2 mediated by transcription intermediary factor TIF2*. EMBO Rep, 2000. **1**(2): p. 151-7.
26. Onate, S.A., V. Boonyaratanakornkit, T.E. Spencer, S.Y. Tsai, M.J. Tsai, D.P. Edwards, and B.W. O'Malley, *The steroid receptor coactivator-1 contains multiple receptor interacting and activation domains that cooperatively enhance the activation function 1 (AF1) and AF2 domains of steroid receptors*. J Biol Chem, 1998. **273**(20): p. 12101-8.
27. Tian, H., M.A. Mahajan, C.T. Wong, I. Habeos, and H.H. Samuels, *The N-Terminal A/B domain of the thyroid hormone receptor-beta2 isoform influences ligand-dependent recruitment of coactivators to the ligand-binding domain*. Mol Endocrinol, 2006. **20**(9): p. 2036-51.
28. Webb, P., P. Nguyen, J. Shinsako, C. Anderson, W. Feng, M.P. Nguyen, D. Chen, S.M. Huang, S. Subramanian, E. McKinerney, B.S. Katzenellenbogen, M.R. Stallcup, and P.J. Kushner, *Estrogen receptor activation function 1 works by binding p160 coactivator proteins*. Mol Endocrinol, 1998. **12**(10): p. 1605-18.
29. Kobayashi, Y., T. Kitamoto, Y. Masuhiro, M. Watanabe, T. Kase, D. Metzger, J. Yanagisawa, and S. Kato, *p300 mediates functional synergism between AF-1 and AF-2 of estrogen receptor alpha and beta by interacting directly with the N-terminal A/B domains*. J Biol Chem, 2000. **275**(21): p. 15645-51.
30. Khorasanizadeh, S. and F. Rastinejad, *Nuclear-receptor interactions on DNA-response elements*. Trends in Biochemical Sciences, 2001. **26**(6): p. 384-390.
31. Zilliacus, J., A.P. Wright, J. Carlstedt-Duke, and J.A. Gustafsson, *Structural determinants of DNA-binding specificity by steroid receptors*. Mol Endocrinol, 1995. **9**(4): p. 389-400.

32. Huang, P.X., V. Chandra, and F. Rastinejad, *Structural Overview of the Nuclear Receptor Superfamily: Insights into Physiology and Therapeutics*. Annual Review of Physiology, 2010. **72**: p. 247-272.
33. Moras, D. and H. Gronemeyer, *The nuclear receptor ligand-binding domain: structure and function*. Current Opinion in Cell Biology, 1998. **10**(3): p. 384-391.
34. Benoit, G., M. Malewicz, and T. Perlmann, *Digging deep into the pockets of orphan nuclear receptors: insights from structural studies*. Trends in Cell Biology, 2004. **14**(7): p. 369-376.
35. Nettles, K.W. and G.L. Greene, *Ligand control of coregulator recruitment to nuclear receptors*. Annu Rev Physiol, 2005. **67**: p. 309-33.
36. Bourguet, W., V. Vivat, J.M. Wurtz, P. Chambon, H. Gronemeyer, and D. Moras, *Crystal structure of a heterodimeric complex of RAR and RXR ligand-binding domains*. Molecular Cell, 2000. **5**(2): p. 289-298.
37. Gampe, R.T., V.G. Montana, M.H. Lambert, A.B. Miller, R.K. Bledsoe, M.V. Milburn, S.A. Kliewer, T.M. Willson, and H.E. Xu, *Asymmetry in the PPAR gamma/RXR alpha crystal structure reveals the molecular basis of heterodimerization among nuclear receptors*. Molecular Cell, 2000. **5**(3): p. 545-555.
38. Wang, Z.L., G. Benoit, J.S. Liu, S. Prasad, P. Aarnisalo, X.H. Liu, H.D. Xu, N.P.C. Walker, and T. Perlmann, *Structure and function of Nurr1 identifies a class of ligand-independent nuclear receptors*. Nature, 2003. **423**(6939): p. 555-560.
39. Li, Y., M. Choi, G. Cavey, J. Daugherty, K. Suino, A. Kovach, N.C. Bingham, S.A. Kliewer, and H.E. Xu, *Crystallographic identification and functional characterization of phospholipids as ligands for the orphan nuclear receptor steroidogenic factor-1*. Molecular Cell, 2005. **17**(4): p. 491-502.
40. le Maire, A., W. Bourguet, and P. Balaguer, *A structural view of nuclear hormone receptor: endocrine disruptor interactions*. Cell Mol Life Sci. **67**(8): p. 1219-37.
41. Moras, D. and H. Gronemeyer, *The nuclear receptor ligand-binding domain: structure and function*. Curr Opin Cell Biol, 1998. **10**(3): p. 384-91.

42. Chandra, V., P.X. Huang, Y. Hamuro, S. Raghuram, Y.J. Wang, T.P. Burris, and F. Rastinejad, *Structure of the intact PPAR-gamma-RXR-alpha nuclear receptor complex on DNA*. Nature, 2008. **456**(7220): p. 350-U33.
43. Lefebvre, P., Y. Benomar, and B. Staels, *Retinoid X receptors: common heterodimerization partners with distinct functions*. Trends in Endocrinology & Metabolism. **In Press, Corrected Proof**.
44. Schoenmakers, E., G. Verrijdt, B. Peeters, G. Verhoeven, W. Rombauts, and F. Claessens, *Differences in DNA binding characteristics of the androgen and glucocorticoid receptors can determine hormone-specific responses*. Journal of Biological Chemistry, 2000. **275**(16): p. 12290-12297.
45. Gewirth, D.T. and P.B. Sigler, *The basis for half-site specificity explored through a non-cognate steroid receptor-DNA complex*. Nat Struct Biol, 1995. **2**(5): p. 386-94.
46. Takeshita, A., Y. Ozawa, and W.W. Chin, *Nuclear receptor coactivators facilitate vitamin D receptor homodimer action on direct repeat hormone response elements*. Endocrinology, 2000. **141**(3): p. 1281-1284.
47. Xie, W., J.L. Barwick, C.M. Simon, A.M. Pierce, S. Safe, B. Blumberg, P.S. Guzelian, and R.M. Evans, *Reciprocal activation of Xenobiotic response genes by nuclear receptors SXR/PXR and CAR*. Genes & Development, 2000. **14**(23): p. 3014-3023.
48. Luisi, B.F., W.X. Xu, Z. Otwinowski, L.P. Freedman, K.R. Yamamoto, and P.B. Sigler, *Crystallographic analysis of the interaction of the glucocorticoid receptor with DNA*. Nature, 1991. **352**(6335): p. 497-505.
49. Nettles, K.W. and G.L. Greene, *Ligand control of coregulator recruitment to nuclear receptors*. Annual Review of Physiology, 2005. **67**: p. 309-333.
50. Chambon, P., *A decade of molecular biology of retinoic acid receptors*. FASEB J, 1996. **10**(9): p. 940-54.
51. McKenna, N.J., R.B. Lanz, and B.W. O'Malley, *Nuclear receptor coregulators: cellular and molecular biology*. Endocr Rev, 1999. **20**(3): p. 321-44.

52. Glass, C.K. and M.G. Rosenfeld, *The coregulator exchange in transcriptional functions of nuclear receptors*. Genes Dev, 2000. **14**(2): p. 121-41.
53. Nagy, L. and J.W. Schwabe, *Mechanism of the nuclear receptor molecular switch*. Trends Biochem Sci, 2004. **29**(6): p. 317-24.
54. Chambon, P., *(T)he nuclear receptor superfamily: A personal retrospect on the first two decades*. Molecular Endocrinology, 2005. **19**(6): p. 1418-1428.
55. Smith, C.L. and B.W. O'Malley, *Coregulator function: A key to understanding tissue specificity of selective receptor modulators*. Endocrine Reviews, 2004. **25**(1): p. 45-71.
56. Bourguet, W., M. Ruff, P. Chambon, H. Gronemeyer, and D. Moras, *Crystal structure of the ligand-binding domain of the human nuclear receptor RXR-alpha*. Nature, 1995. **375**(6530): p. 377-82.
57. Egea, P.F., A. Mitschler, N. Rochel, M. Ruff, P. Chambon, and D. Moras, *Crystal structure of the human RXR alpha ligand-binding domain bound to its natural ligand: 9-cis retinoic acid*. Embo Journal, 2000. **19**(11): p. 2592-2601.
58. Lonard, D.M. and B.W. O'Malley, *Nuclear receptor coregulators: Judges, juries, and executioners of cellular regulation*. Molecular Cell, 2007. **27**(5): p. 691-700.
59. Wolf, I.M., M.D. Heitzer, M. Grubisha, and D.B. DeFranco, *Coactivators and nuclear receptor transactivation*. Journal of Cellular Biochemistry, 2008. **104**(5): p. 1580-1586.
60. Stallcup, M.R., J.H. Kim, C. Teyssier, Y.H. Lee, H. Ma, and D. Chen, *The roles of protein-protein interactions and protein methylation in transcriptional activation by nuclear receptors and their coactivators*. J Steroid Biochem Mol Biol, 2003. **85**(2-5): p. 139-45.
61. Mangelsdorf, D.J. and R.M. Evans, *The RXR heterodimers and orphan receptors*. Cell, 1995. **83**(6): p. 841-850.
62. Mangelsdorf, D.J., E.S. Ong, J.A. Dyck, and R.M. Evans, *Nuclear receptor that identifies a novel retinoic acid response pathway*. Nature, 1990. **345**(6272): p. 224-229.



63. Shulman, A.I. and D.J. Mangelsdorf, *Mechanisms of disease: Retinoid X receptor heterodimers in the metabolic syndrome*. New England Journal of Medicine, 2005. **353**(6): p. 604-615.
64. Mangelsdorf, D.J., U. Borgmeyer, R.A. Heyman, J.Y. Zhou, E.S. Ong, A.E. Oro, A. Kakizuka, and R.M. Evans, *Characterization of three RXR genes that mediate the action of 9-cis retinoic acid*. Genes Dev, 1992. **6**(3): p. 329-44.
65. Dolle, P., V. Fraulob, P. Kastner, and P. Chambon, *Developmental expression of murine retinoid X receptor (RXR) genes*. Mech Dev, 1994. **45**(2): p. 91-104.
66. Haugen, B.R., N.S. Brown, W.M. Wood, D.F. Gordon, and E.C. Ridgway, *The thyrotrope-restricted isoform of the retinoid-X receptor-gamma 1 mediates 9-cis-retinoic acid suppression of thyrotropin-beta promoter activity*. Molecular Endocrinology, 1997. **11**(4): p. 481-489.
67. Chiang, M.Y., D. Misner, G. Kempermann, T. Schikorski, V. Giguere, H.M. Sucov, F.H. Gage, C.F. Stevens, and R.M. Evans, *An essential role for retinoid receptors RAR beta and RXR gamma in long-term potentiation and depression*. Neuron, 1998. **21**(6): p. 1353-1361.
68. Boehm, M.F., L. Zhang, B.A. Badea, S.K. White, D.E. Mais, E. Berger, C.M. Suto, M.E. Goldman, and R.A. Heyman, *Synthesis and structure activity relationships of novel retinoid X receptor selective retinoids*. Journal of Medicinal Chemistry, 1994. **37**(18): p. 2930-2941.
69. Boehm, M.F., L. Zhang, L. Zhi, M.R. McClurg, E. Berger, M. Wagoner, D.E. Mais, C.M. Suto, P.J.A. Davies, R.A. Heyman, and A.M. Nadzan, *Design and synthesis of potent retinoid X receptor selective ligands that induce apoptosis in leukemia-cells*. Journal of Medicinal Chemistry, 1995. **38**(16): p. 3146-3155.
70. Hallenbeck, P.L., S. Minucci, P. Lippoldt, M. Phyllaier, V. Horn, K. Ozato, and V.M. Nikodem, *Differential 9-cis-retinoic acid-dependent transcriptional activation by murine retinoid X receptor alpha (RXR alpha) and RXR beta - Role of cell type and RXR domains*. Journal of Biological Chemistry, 1996. **271**(18): p. 10503-10507.
71. Tate, B.F., A.A. Levin, and J.F. Grippo, *The discovery of 9-cis retinoic acid: a hormone that binds the retinoid-X receptor*. Trends Endocrinol Metab, 1994. **5**(5): p. 189-94.

72. Wolf, G., *Is 9-cis-retinoic acid the endogenous ligand for the retinoic acid-X receptor?* Nutr Rev, 2006. **64**(12): p. 532-8.
73. Mic, F.A., A. Molotkov, D.M. Benbrook, and G. Duester, *Retinoid activation of retinoic acid receptor but not retinoid X receptor is sufficient to rescue lethal defect in retinoic acid synthesis.* Proceedings of the National Academy of Sciences of the United States of America, 2003. **100**(12): p. 7135-7140.
74. Wolf, G., *Is 9-cis-retinoic acid the endogenous ligand for the retinoic acid-X receptor?* Nutrition Reviews, 2006. **64**(12): p. 532-538.
75. Egea, P.F., A. Mitschler, and D. Moras, *Molecular recognition of agonist Ligands by RXRs.* Molecular Endocrinology, 2002. **16**(5): p. 987-997.
76. Shulman, A.I. and D.J. Mangelsdorf, *Retinoid x receptor heterodimers in the metabolic syndrome.* N Engl J Med, 2005. **353**(6): p. 604-15.
77. Lammi, J., T. Perlmann, and P. Aarnisalo, *Corepressor interaction differentiates the permissive and non-permissive retinoid X receptor heterodimers.* Arch Biochem Biophys, 2008. **472**(2): p. 105-14.
78. de Lera, A.R., W. Bourguet, L. Altucci, and H. Gronemeyer, *Design of selective nuclear receptor modulators: RAR and RXR as a case study.* Nat Rev Drug Discov, 2007. **6**(10): p. 811-20.
79. Shulman, A.I., C. Larson, D.J. Mangelsdorf, and R. Ranganathan, *Structural determinants of allosteric ligand activation in RXR heterodimers.* Cell, 2004. **116**(3): p. 417-29.
80. Lin, B.C., C.W. Wong, H.W. Chen, and M.L. Privalsky, *Plasticity of tetramer formation by retinoid X receptors - An alternative paradigm for DNA recognition.* Journal of Biological Chemistry, 1997. **272**(15): p. 9860-9867.
81. Kersten, S., D. Kelleher, P. Chambon, H. Gronemeyer, and N. Noy, *Retinoid X receptor alpha forms tetramers in solution.* Proc Natl Acad Sci U S A, 1995. **92**(19): p. 8645-9.

82. Kersten, S., P.R. Reczek, and N. Noy, *The tetramerization region of the retinoid X receptor is important for transcriptional activation by the receptor*. J Biol Chem, 1997. **272**(47): p. 29759-68.
83. Taylor, J., P. Rohatgi, H.T. Spencer, D. Doyle, and B. Azizi, *Characterization of a molecular switch system that regulates gene expression in mammalian cells through a small molecule*. BMC Biotechnology. **10**(1): p. 15.

## **CHAPTER 2**

### **GENE THERAPY AND MOLECULAR SWITCH SYSTEMS**

#### **2.1 Gene Therapy**

Gene therapy is the use of DNA as a drug to treat genetic disorders, as well as other diseases by replacing a defective gene(s) with a normal gene(s) [1-3]. The fundamentals of gene therapy show great promise and is a highly pursued research area due to the frequency of human diseases based on genetic or inherited defects [4]. Severe combined immunodeficiency (SCID) disorders are a primary target of gene therapy applications. These disorders usually have a characteristic defect in both the T and B-lymphocyte systems, which results in an onset of serious infections [5, 6]. One of the first successful gene therapy trials took place about twenty years ago, involving the transfer of an adenosine deaminase (ADA) gene into the lymphocytes of a patient with the defective enzyme [7, 8]. This clinical trial treated 18 patients and 17 of them benefited from this life-saving technology. Since then over 1300 gene therapy clinical trials have been conducted [9]. One of the many success stories includes the gene therapy trial in 2007, involving a retinal disease caused by a mutation in the RPE65 gene. This gene encodes for an enzyme that converts all *trans* retinyl ester to 11-*cis* retinal, a natural ligand for G protein-coupled receptors in photoreceptor cells [10-12]. A recombinant adeno-associated virus was used to safely deliver the RPE65 gene for long-term restoration of vision [10, 13, 14].

Despite the appeal of gene therapy in treating patients, the failures of this method have posed several safety and ethical issues. For example, several years after the clinical

trials were conducted for the treatment of the X linked form of SCID (XSCID), cases of leukemia developed in five of the twenty subjected treated [5]. XSCID is an inherited defect in a gene that encodes a mutation in a common cytokine needed for lymphocyte development and function [5, 6]. Another setback of gene therapy occurred in 1999 with the death of 18-year-old Jesse Gelsinger, a patient who passed away due to a severe immune response from treatment with large amounts of adenoviral particles [15]. Although there are numerous advantages of gene therapy, these failed attempts have affected the progression of this promising technology.

### **2.1.1 Gene Delivery Methods**

In order to treat these diseases, genetic material must be delivered to target cells or tissue. Currently, two methods, nonviral and viral, have been developed to deliver DNA to cells or tissue. Examples of nonviral methods include DNA electroporation, which involves delivering a high-voltage electric pulse to the cell, allowing DNA diffusion through the cell membrane [16-18]. Another common example of a nonviral method is the use of cationic lipids, which condenses and encapsulates the DNA into a liposome, also known as a lipoplex [19]. As shown in Figure 2.1, cationic lipids are polymers with positively charged heads that can directly interact with the DNA backbone [20], and hydrophobic tails. X-ray diffraction studies have revealed insight into the three dimensional structure of these complexes. These studies have revealed that a lipoplex can arrange in two structures: a “DNA sandwich” where the DNA is packed inside monolayers formed by the cationic lipid or a “honeycomb” structure where the DNA is encapsulated in monolayer tubes that form a hexagonal shape [21]. These lipoplexes can

enter the cell via nonspecific endocytosis [22], and this technique is used quite often in transient transfections, as well as in clinical trials [23-27].

Common viral methods used for gene therapy include the retroviral, adenoviral, and adeno-associated viral (AAV) delivery systems [28]. Viruses are infectious agents or pathogens that cause disease to its host [29]. However, new DNA delivery methods have been engineered based on the fundamentals of the function of viruses, and have been used in several gene therapy applications. The viral systems that will be discussed in this chapter have been modified to infect a host; however, the pathogenesis of these viruses that cause the virus to replicate and cause damage to the host have been excluded [22]. Retroviruses are RNA viruses that can integrate genetic material into the genome of a host, allowing transcription of the therapeutic gene to take place. Figure 2.2 shows the mechanism of the virus' entry to the cell via receptor-mediated endocytosis. Once the virus enters the cell, the RNA is released and transcribed into double stranded DNA by the reverse transcriptase. Finally, the DNA enters the nucleus, integrates into the host genome, and enabling the expression of viral proteins. Adenoviruses are double-stranded DNA viruses that remain episomal in the nucleus but exploit the host's nuclear machinery to facilitate gene expression. Adeno-associated viruses (AAV) are single-stranded DNA viruses that integrate genetic material into the genome of the host; however, the virus remains inactivate or in the latent stage until a subsequent virus infects the host [19].

### **2.1.2 Gene Therapy Challenges**

Numerous challenges need to be overcome before gene therapy can be implemented as a standard treatment. For instance, the appropriate delivery system as discussed in the

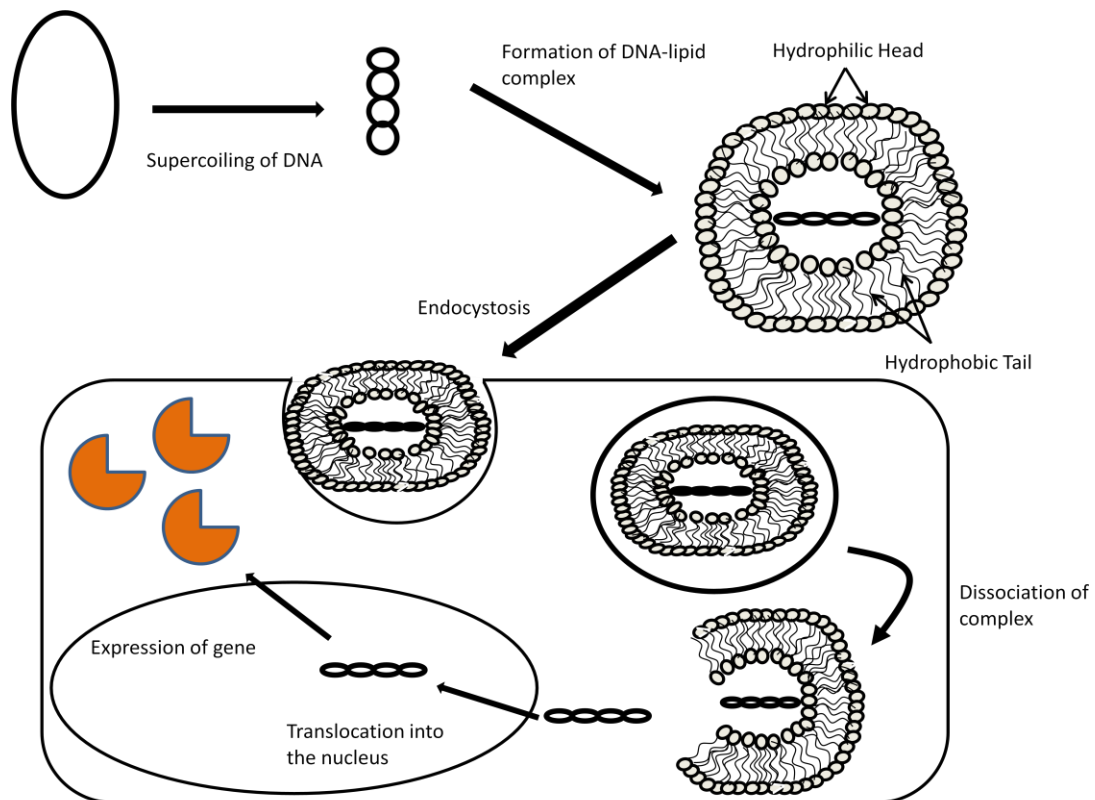


Figure 2.1: **Mechanism for Cationic Lipids:** DNA can supercoil and form a complex with the cationic lipids. The lipoplex then enters into the cell through endocytosis where DNA is released, translocated into the nucleus, and transcription of gene occurs.

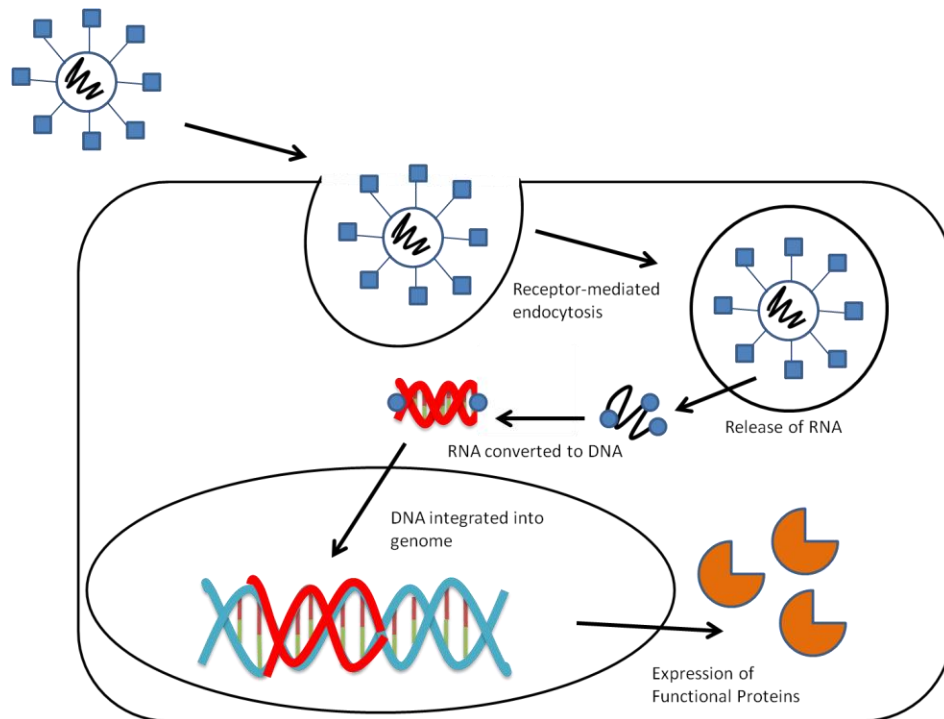


Figure 2.2: **Mechanism of action for retroviruses:** The virion enters the cell through receptor-mediated endocytosis. The RNA and virion proteins are released into the cell where reverse transcription takes place. Finally, the DNA enters the nucleus and integrates into the genome of the host, and then expression of viral genes occurs.



section above has been one of the challenges with this area of research. Viruses have been the choice of most gene therapy studies. However, each viral delivery system has advantages and limitations depending on the type of tissue or cells targeted and the duration of expression of the therapeutic gene. For example, retroviruses are able to transfer genetic material efficiently and allow long-term expression of the therapeutic gene. However, the lack of control of gene integration site has caused leukemia in various XSCID case studies [30].

Another challenge in gene therapy is the short-lived gene expression, which introduces the problem of retention of exogenous genes or the silencing of gene expression over an extended period of time. For example, nonviral methods are known to transfer genes inefficiently [31], causing inefficient gene expression. Therefore, this method is not ideal when treating certain diseases, such as primary immune deficiency disorders, that require long-term gene expression.

Immunogenic responses, another challenge of gene therapy, can be induced by introducing a foreign object into a host. All gene therapy methods have the potential of inducing an immunogenic response, reducing the effectiveness of gene therapy, as well as causing severe illnesses. This challenge is a main disadvantage of the adenovirus delivery system, since acute and chronic immune responses have been observed in several animal model studies [32].

Finally, the lack of transcriptional control of the therapeutic gene is another problem faced within this area of research. Most endogenous genes are turned on or off by the addition or removal of a specific signal that causes a cascade of proteins to initiate the transcription process. When a foreign gene is introduced into cells, the expression of that

gene is primarily controlled by the promoter region that recruits the transcription machinery, which in many cases instantly induces gene expression. However, if the therapeutic gene is overexpressed, then other complications, as well as other diseases within the host may occur. Therefore, there is a need to develop new regulation systems to control expression of the therapeutic gene.

Bone marrow transplantation has been a beneficial treatment to treating patients with inherited disorders such as SCID, since bone marrow contains hematopoietic stem cells (HSC) that are known to restore the immune response system [5, 6]. However the lack of donor matches and the frequency of transplantations have limited the benefits of this treatment. The repopulation of healthy HSC *in vitro* and *in vivo* would offer a novel treatment to permanently cure these life-threatening diseases. One potential target gene known to expand HSC count is the homeobox gene *HOXB4* [33-35]; however, high expression of this gene impairs HSC differentiation. Hence the need to develop molecular switch systems that would provide the appropriate gene expression levels when needed by the administration of a drug, resulting in HSC repopulation that would restore an impaired immune response system.

## **2.2 Criteria of a Molecular Switch System**

Gene regulation systems are important research tools for studying gene function and can provide numerous benefits for clinical applications. Several systems have been designed that place a target transgene under the control of an engineered transcription factor that is activated in the presence of an exogenous ligand [36]. These systems have been successfully used to control expression of a target transgene in a cellular

environment with high expression levels in response to an extensive range of ligand concentrations [37].

As a mechanism for controlling gene expression, several researchers have focused on the development of molecular switch systems. According to Toniatti and coworkers, there are several criteria for an effective molecular switch system. First, the switch should be an “ON-switch” and not an “OFF-switch”, meaning the switch should be able to be turned on and off based on the addition or removal of drug. “OFF-switches” have two drawbacks. One drawback is a prolonged exposure of drug to silence the gene, and the second is the rate of gene expression is determined by the drug clearance. The second criterion is the drug and the molecular switch should be target specific and not interfere with endogenous metabolic pathways. The potential drug should have appropriate pharmacological properties, which include a metabolism profile that is compatible with prolonged usage. Third, target gene expression should correlate with the dose of the ligand. The system should have low basal activity, be inactive in the absence of the ligand but strongly stimulated by ligand administration, hence high fold induction levels. Finally, the system should not induce an immune response in humans. [38].

### **2.3 Current Molecular Switch Systems**

To date, several research groups have developed molecular switch systems to control transgene expression in both cell culture assays, as well as, animal models. Some of the most commonly used examples include the progesterone receptor (PR)/ mifepristone (RU486) inducible system (also known as GeneSwitch®), the tetracycline inducible system [39], and the ecdysone-responsive regulation system (also known as Rheoswtich®) [40].

The progesterone receptor (PR) inducible system regulates gene expression using RU486, a synthetic PR antagonist. This ligand binds to a chimeric regulator composed of a truncated PR fused to a Gal4 DNA binding domain, a yeast transcription factor, and the p53 activation domain [41-44], a human transcription factor involved in chromatin remodelling [45]. As shown in Figure 2.3, the regulator then binds a DNA sequence composed of six Gal4 response elements (RE) and activates gene expression. This system has been used in animal models, regulating human growth hormone (hGH) expression in the liver of mice using the adenoviral delivery system. One major disadvantage of the GeneSwitch® system is the usage of RU486, a female contraceptive drug used to induce abortion [46]. Long term usage of this drug could lead to significant side effects, making this system difficult for animal studies [47, 48].

The tetracycline (Tet) inducible system is based on the prokaryotic repressor protein (TetR) that binds to a specific DNA sequence called *tetO*. In the absence of tetracycline (Tet) or its derivative doxycycline (dox), the TetR proteins are tightly bound to the DNA sequence [49]. In the presence of ligand, the TetR is released from DNA and gene expression occurs [50]. Over the years, the TetR protein has been involved in many molecular switch systems. The first molecular switch system this protein was involved in had the TetR protein fused to the VP16 transactivator of the herpes simplex virus [39]. VP16 is a very strong transactivator and is known to have a strong interaction with the TATA-binding protein (TBP), TFIIB, and the Spt-Ada-Gcn5 (SAGA) histone acetyltransferase complex allowing transcription to occur more efficiently [51, 52]. This system can function as both an “ON-switch” as well as an “OFF-switch” [53]. The “OFF-switch” is composed of the TetR fused to VP16 (tTA), and gene expression takes place in

# Geneswitch®

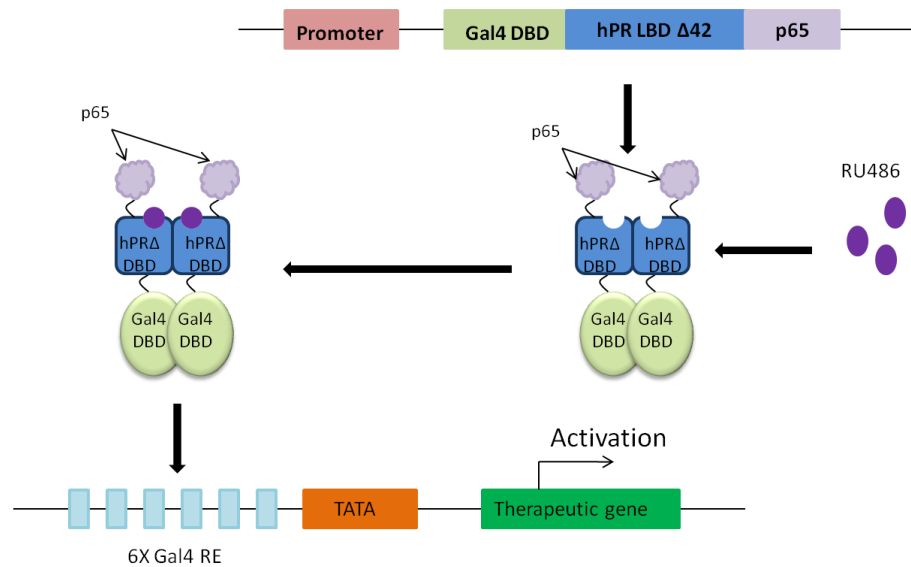


Figure 2.3: **Schematic Diagram of Geneswitch®:** The fusion protein composed of a Gal4 DBD, a mutant progesterone receptor LBD, and a p65 activation domain is constitutively expressed. Upon the addition of the ligand, RU486, the fusion protein can then bind an artificial promoter contain six Gal4 RE controlling expression of the therapeutic gene.

## Tetracycline inducible system

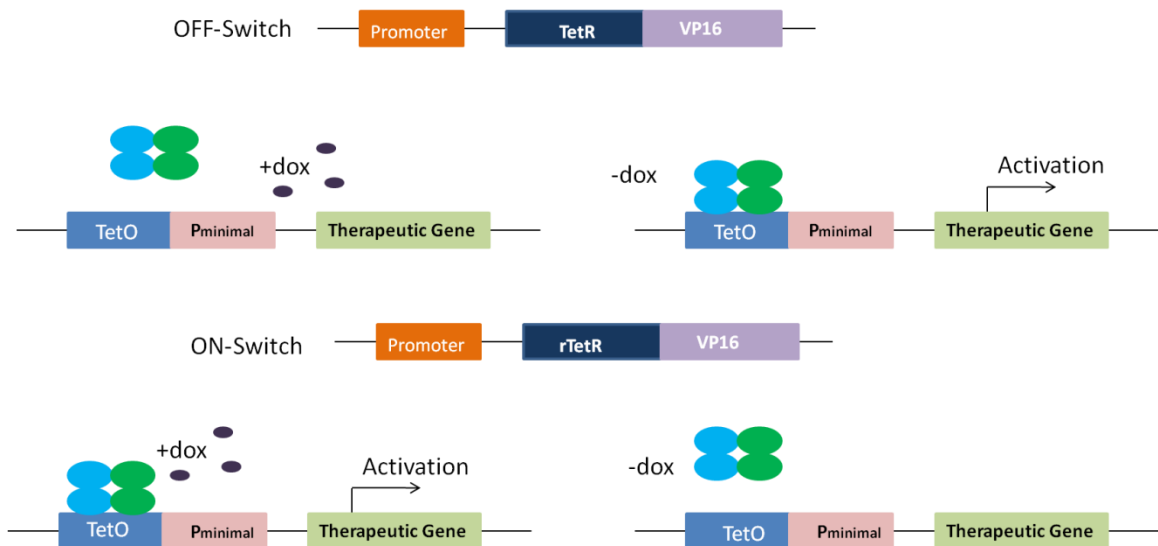


Figure 2.4: **Schematic Diagram of Tetracycline Inducible System:** OFF-Switch is composed of the TetR and VP16 fusion protein that is constitutively expressed. In the presence of ligand doxycycline (dox) represses gene expression and in the absence of ligand gene expression takes place. The OFF-Switch constitutively expressed the chimeric protein with a mutant TetR (rTetR) activates gene expression the presence of ligand and represses gene expression in the absence of ligand.

the absence of ligand (Figure 2.4). Upon the addition of ligand, tTA is released from the promoter region and gene expression is silenced. Four mutations in the TetR domain (rtTA) reversed the activity of this protein, only interacting with the *tetO* sequence in the presence of ligand, which created the “ON-switch” [52].

An advantage of the Tet inducible system is that the ligand dox is inexpensive and “bioavailable” [54, 55]. This molecular switch system has also been used in several *in vitro* and *in vivo* models including rodents and monkeys, and has been delivered in various viral vectors including AAV, adenovirus, and lentivirus [47, 56]. However, one drawback of this system is the utilization of bacterial proteins, which may induce an immunogenic response in human gene therapy trials [57, 58].

Finally, the ecdysone-responsive regulation system is based on a heterodimer between the insect steroid hormone receptor, ecdysone receptor (EcR), and the retinoid X receptor (RXR) (Figure 2.5) [59]. The ecdysone receptor is a nuclear receptor in insects, involved in molting and metamorphosis, and consists of the heterodimer partner ultraspirale (USP) [60-62]. In this system the DBD of EcR was altered to resemble the glucocorticoid receptor (GR), binding to a hybrid DNA sequence of the GR response elements (RE) and the EcR RE (EGRE). VP16 is fused to the RXR LBD; RXR serves as the human ortholog of USP [40]. The LBD of EcR carries a transcriptional silencer; therefore, the absence of ligand can recruit corepressors to silence gene expression [60]. Upon the addition of ecdysteroids, insect steroids that are structurally different than mammalian steroids, the EcR chimera heterodimerizes with RXR-VP16 and expression of target gene occurs. Despite low basal expression and high fold induction of this system [63, 64], the overexpression of two transgenes (EcR and RXR) simultaneously

## Ecdysone system

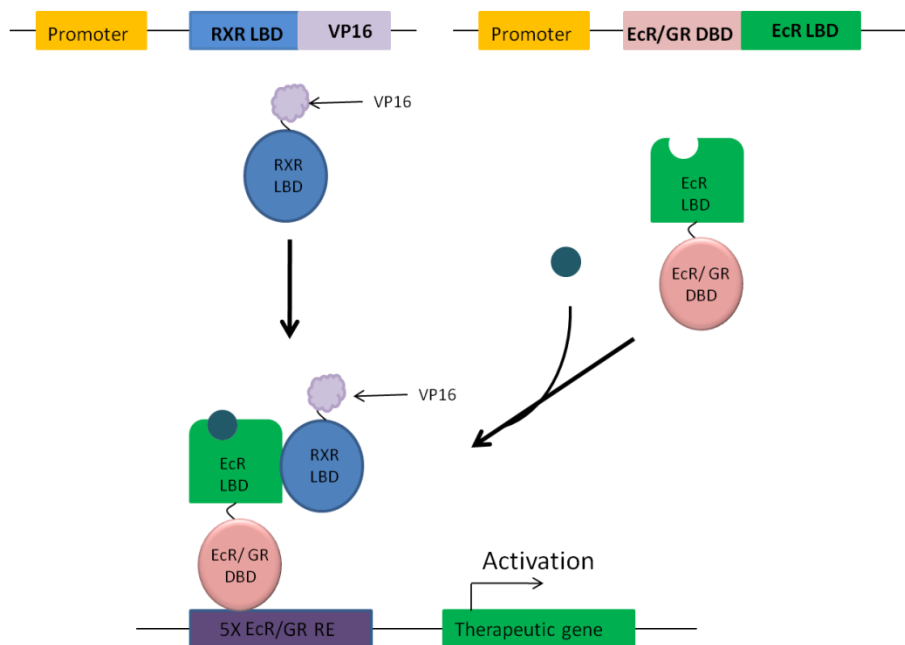


Figure 2.5: **Schematic Diagram of Rheoswitch®**: Two fusion proteins are constitutively expressed: RXR fused the VP16 activation domain and a hybrid EcR and GR DBD fused to the EcR LBD. Upon the addition of ecdysteroids, both fusion protein are recruited to the promoter region and activate expression of the therapeutic gene.



complicates viral delivery. Another disadvantage of this system is the overexpression of RXR poses a safety concern, since RXR plays a significant role in many metabolic pathways [62, 65-68].

These three successful ligand-dependent molecular switch systems have been used for various cellular studies; however, these systems contain certain limitations for *in vivo* applications. The concerns posed by these systems permit the development of new or improved molecular switch systems. This thesis will describe a molecular switch system based on an engineered nuclear receptor and a synthetic small molecule. The characterization of this molecular switch system will be discussed in the following chapters and provide a new potential system for gene therapy applications.

### 2.3 Literature Cited

1. Mulligan, R.C., *The basic science of gene therapy*. Science, 1993. **260**(5110): p. 926-932.
2. Muller, H., *Human gene therapy: possibilities and limitations*. Experientia, 1987. **43**(4): p. 375-8.
3. Kantoff, P.W., S.M. Freeman, and W.F. Anderson, *Prospects for gene therapy for immunodeficiency diseases*. Annu Rev Immunol, 1988. **6**: p. 581-94.
4. SoRelle, R., *Who owns your DNA? who will own it?* Circulation, 2000. **101**(5): p. E67-E68.
5. Kohn, D.B., *Update on gene therapy for immunodeficiencies*. Clin Immunol, 2010. **135**(2): p. 247-54.
6. Kohn, D.B., *Gene therapy for childhood immunological diseases*. Bone Marrow Transplantation, 2008. **41**(2): p. 199-205.
7. Anderson, W.F., *Human gene therapy*. Science, 1992. **256**(5058): p. 808-13.

8. Miller, A.D., *Human gene therapy comes of age*. Nature, 1992. **357**(6378): p. 455-60.
9. Edelstein, M.L., M.R. Abedi, and J. Wixon, *Gene therapy clinical trials worldwide to 2007 - an update*. Journal of Gene Medicine, 2007. **9**(10): p. 833-842.
10. Maguire, A.M., F. Simonelli, E.A. Pierce, E.N. Pugh, F. Mingozzi, J. Bennicelli, S. Banfi, K.A. Marshall, F. Testa, E.M. Surace, S. Rossi, A. Lyubarsky, V.R. Arruda, B. Konkle, E. Stone, J.W. Sun, J. Jacobs, L. Dell'Osso, R. Hertle, J.X. Ma, T.M. Redmond, X.S. Zhu, B. Hauck, O. Zeleniaia, K.S. Shindler, M.G. Maguire, J.F. Wright, N.J. Volpe, J.W. McDonnell, A. Auricchio, K.A. High, and J. Bennett, *Safety and efficacy of gene transfer for Leber's congenital amaurosis*. New England Journal of Medicine, 2008. **358**(21): p. 2240-2248.
11. Moiseyev, G., Y. Chen, Y. Takahashi, B.X. Wu, and J.X. Ma, *RPE65 is the isomerohydrolase in the retinoid visual cycle*. Proceedings of the National Academy of Sciences of the United States of America, 2005. **102**(35): p. 12413-12418.
12. Redmond, T.M., E. Poliakov, S. Yu, J.Y. Tsai, Z.J. Lu, and S. Gentleman, *Mutation of key residues of RPE65 abolishes its enzymatic role as isomerohydrolase in the visual cycle*. Proceedings of the National Academy of Sciences of the United States of America, 2005. **102**(38): p. 13658-13663.
13. Bennicelli, J., J.F. Wright, A. Komaromy, J.B. Jacobs, B. Hauck, O. Zeleniaia, F. Mingozzi, D. Hui, D. Chung, T.S. Rex, Z.Y. Wei, G. Qu, S.Z. Zhou, C. Zeiss, V.R. Arruda, G.M. Acland, L.F. Dell'Osso, K.A. High, A.M. Maguire, and J. Bennett, *Reversal of blindness in animal models of Leber congenital amaurosis using optimized AAV2-mediated gene transfer*. Molecular Therapy, 2008. **16**(3): p. 458-465.
14. Maguire, A.M., K.A. High, A. Auricchio, J.F. Wright, E.A. Pierce, F. Testa, F. Mingozzi, J.L. Bennicelli, G.S. Ying, S. Rossi, A. Fulton, K.A. Marshall, S. Banfi, D.C. Chung, J.I.W. Morgan, B. Hauck, O. Zeleniaia, X.S. Zhu, L. Raffini, F. Coppieters, E. De Baere, K.S. Shindler, N.J. Volpe, E.M. Surace, C. Acerra, A. Lyubarsky, T.M. Redmond, E. Stone, J.W. Sun, J.W. McDonnell, B.P. Leroy, F. Simonelli, and J. Bennett, *Age-dependent effects of RPE65 gene therapy for Leber's congenital amaurosis: a phase I dose-escalation trial*. Lancet, 2009. **374**(9701): p. 1597-1605.

15. Raper, S.E., N. Chirmule, F.S. Lee, N.A. Wivel, A. Bagg, G.P. Gao, J.M. Wilson, and M.L. Batshaw, *Fatal systemic inflammatory response syndrome in a ornithine transcarbamylase deficient patient following adenoviral gene transfer*. Molecular Genetics and Metabolism, 2003. **80**(1-2): p. 148-158.
16. Rols, M.P., C. Delteil, M. Golzio, P. Dumond, S. Cros, and J. Teissie, *In vivo electrically mediated protein and gene transfer in murine melanoma*. Nature Biotechnology, 1998. **16**(2): p. 168-171.
17. Wong, T.K. and E. Neumann, *Electric field mediated gene transfer*. Biochem Biophys Res Commun, 1982. **107**(2): p. 584-7.
18. Neumann, E., M. Schaefer-Ridder, Y. Wang, and P.H. Hofschneider, *Gene transfer into mouse lyoma cells by electroporation in high electric fields*. EMBO J, 1982. **1**(7): p. 841-5.
19. Brooks, G., *Gene Therapy*. The use of DNA as a drug. 2002: Pharmaceutical Press. 39-41.
20. Felgner, P.L., T.R. Gadek, M. Holm, R. Roman, H.W. Chan, M. Wenz, J.P. Northrop, G.M. Ringold, and M. Danielsen, *Lipofection: a highly efficient, lipid-mediated DNA-transfection procedure*. Proc Natl Acad Sci U S A, 1987. **84**(21): p. 7413-7.
21. de Ilarduya, C.T., Y. Sun, and N. Duezgues, *Gene delivery by lipoplexes and polyplexes*. European Journal of Pharmaceutical Sciences, 2010. **40**(3): p. 159-170.
22. Brooks, G., ed. *Gene Therapy*. The use of DNA as a drug. 2002, Pharmaceutical Press: London. 23-43.
23. Mumper, R.J., J.J. Wang, S.L. Klakamp, H. Nitta, K. Anwer, F. Tagliaferri, and A.P. Rolland, *Protective interactive noncondensing (PINC) polymers for enhanced plasmid distribution and expression in rat skeletal muscle*. Journal of Controlled Release, 1998. **52**(1-2): p. 191-203.
24. Tang, M.X. and F.C. Szoka, *The influence of polymer structure on the interactions of cationic polymers with DNA and morphology of the resulting complexes*. Gene Therapy, 1997. **4**(8): p. 823-832.

25. Boussif, O., F. Lezoualc'h, M.A. Zanta, M.D. Mergny, D. Scherman, B. Demeneix, and J.P. Behr, *A versatile vector for gene and oligonucleotide transfer into cells in culture and in vivo: polyethylenimine*. Proc Natl Acad Sci U S A, 1995. **92**(16): p. 7297-301.
26. Wadhwa, M.S., D.L. Knoell, A.P. Young, and K.G. Rice, *Targeted gene delivery with a low molecular weight glycopeptide carrier*. Bioconjug Chem, 1995. **6**(3): p. 283-91.
27. Caplen, N.J., E.W. Alton, P.G. Middleton, J.R. Dorin, B.J. Stevenson, X. Gao, S.R. Durham, P.K. Jeffery, M.E. Hodson, C. Coutelle, and et al., *Liposome-mediated CFTR gene transfer to the nasal epithelium of patients with cystic fibrosis*. Nat Med, 1995. **1**(1): p. 39-46.
28. Lattime, E.C., *Retroviral Vector Design for Cancer Gene Therapy*, in *Gene Therapy of Cancer*. 2002, Academic Press: San Diego. p. 3-23.
29. Koonin, E.V., T.G. Senkevich, and V.V. Dolja, *The ancient Virus World and evolution of cells*. Biol Direct, 2006. **1**: p. 29.
30. Kohn, D.B., *Update on gene therapy for immunodeficiencies*. Clinical Immunology, 2010. **135**(2): p. 247-254.
31. Li, S. and L. Huang, *Nonviral gene therapy: promises and challenges*. Gene Therapy, 2000. **7**(1): p. 31-34.
32. Seiler, M.P., V. Cerullo, and B. Lee, *Immune response to helper dependent adenoviral mediated liver gene therapy: Challenges and prospects*. Current Gene Therapy, 2007. **7**(5): p. 297-305.
33. Sauvageau, G., U. Thorsteinsdottir, C.J. Eaves, H.J. Lawrence, C. Largman, P.M. Lansdorp, and R.K. Humphries, *Overexpression of HOXB4 in hematopoietic cells causes the selective expansion of more primitive populations in vitro and in vivo*. Genes Dev, 1995. **9**(14): p. 1753-65.
34. Thorsteinsdottir, U., G. Sauvageau, and R.K. Humphries, *Enhanced in vivo regenerative potential of HOXB4-transduced hematopoietic stem cells with regulation of their pool size*. Blood, 1999. **94**(8): p. 2605-12.

35. Antonchuk, J., G. Sauvageau, and R.K. Humphries, *HOXB4 overexpression mediates very rapid stem cell regeneration and competitive hematopoietic repopulation*. Exp Hematol, 2001. **29**(9): p. 1125-34.
36. Pollock, R. and T. Clackson, *Dimerizer-regulated gene expression*. Current Opinion in Biotechnology, 2002. **13**(5): p. 459-467.
37. Clackson, T., *Controlling mammalian gene expression with small molecules*. Current Opinion in Chemical Biology, 1997. **1**(2): p. 210-218.
38. Toniatti, C., H. Bujard, R. Cortese, and G. Ciliberto, *Gene therapy progress and prospects: transcription regulatory systems*. Gene Therapy, 2004. **11**(8): p. 649-657.
39. Gossen, M. and H. Bujard, *Tight control of gene-expression in mammalian-cells by tetracycline-responsive promoters*. Proceedings of the National Academy of Sciences of the United States of America, 1992. **89**(12): p. 5547-5551.
40. No, D., T.P. Yao, and R.M. Evans, *Ecdysone-inducible gene expression in mammalian cells and transgenic mice*. Proceedings of the National Academy of Sciences of the United States of America, 1996. **93**(8): p. 3346-3351.
41. Wang, Y.L., B.W. Omalley, and S.Y. Tsai, *A regulatory system for gene-transfer*. Proceedings of the National Academy of Sciences of the United States of America, 1994. **91**(17): p. 8180-8184.
42. Vegeto, E., G.F. Allan, W.T. Schrader, M.J. Tsai, D.P. McDonnell, and B.W. Omalley, *The mechanism of RU486 antagonism is dependent on the conformation of the carboxy-terminal tail of the human progesterone-receptor*. Cell, 1992. **69**(4): p. 703-713.
43. Wang, Y., J. Xu, T. Pierson, B.W. Omalley, and S.Y. Tsai, *Positive and negative regulation of gene expression in eukaryotic cells with an inducible transcriptional regulator*. Gene Therapy, 1997. **4**(5): p. 432-441.
44. Burcin, M.M., G. Schiedner, S. Kochanek, S.Y. Tsai, and B.W. O'Malley, *Adenovirus-mediated regulable target gene expression in vivo*. Proceedings of the National Academy of Sciences of the United States of America, 1999. **96**(2): p. 355-360.

45. Mankan, A.K., M.W. Lawless, S.G. Gray, D. Kelleher, and R. McManus, *NF-kappa B regulation: the nuclear response*. Journal of Cellular and Molecular Medicine, 2009. **13**(4): p. 631-643.
46. Sarkar, N.N., *Mifepristone: bioavailability, pharmacokinetics and use-effectiveness*. European Journal of Obstetrics Gynecology and Reproductive Biology, 2002. **101**(2): p. 113-120.
47. Goverdhana, S., M. Puntel, W. Xiong, J.M. Zirger, C. Barcia, J.F. Curtin, E.B. Soffer, S. Mondkar, G.D. King, J. Hu, S.A. Sciascia, M. Candolfi, D.S. Greengold, P.R. Lowenstein, and M.G. Castro, *Regulatable gene expression systems for gene therapy applications: Progress and future challenges*. Molecular Therapy, 2005. **12**(2): p. 189-211.
48. Nordstrom, J.L. *The antiprogesterin-dependent GeneSwitch (R) system for regulated gene therapy*. 2003: Elsevier Science Inc.
49. Wissmann, A., I. Meier, L.V. Wray, Jr., M. Geissendorfer, and W. Hillen, *Tn10 tet operator mutations affecting Tet repressor recognition*. Nucleic Acids Res, 1986. **14**(10): p. 4253-66.
50. Orth, P., F. Cordes, D. Schnappinger, W. Hillen, W. Saenger, and W. Hinrichs, *Conformational changes of the Tet repressor induced by tetracycline trapping*. Journal of Molecular Biology, 1998. **279**(2): p. 439-447.
51. Hall, D.B. and K. Struhl, *The VP16 activation domain interacts with multiple transcriptional components as determined by protein-protein cross-linking in vivo*. Journal of Biological Chemistry, 2002. **277**(48): p. 46043-46050.
52. Gossen, M., S. Freundlieb, G. Bender, G. Muller, W. Hillen, and H. Bujard, *Transcriptional activation by tetracyclines in mammalian cells*. Science, 1995. **268**(5218): p. 1766-9.
53. Salucci, V., A. Scarito, L. Aurisicchio, S. Lamartina, G. Nicolaus, S. Giampaoli, O. Gonzalez-Paz, C. Toniatti, H. Bujard, W. Hillen, G. Ciliberto, and F. Palombo, *Tight control of gene expression by a helper-dependent adenovirus vector carrying the rtTA2(s)-M2 tetracycline transactivator and repressor system*. Gene Therapy, 2002. **9**(21): p. 1415-1421.

54. Zhu, Z., T. Zheng, C.G. Lee, R.J. Homer, and J.A. Elias, *Tetracycline-controlled transcriptional regulation systems: advances and application in transgenic animal modeling*. Seminars in Cell & Developmental Biology, 2002. **13**(2): p. 121-128.
55. Agwuh, K.N. and A. MacGowan, *Pharmacokinetics and pharmacodynamics of the tetracyclines including glycyclines*. Journal of Antimicrobial Chemotherapy, 2006. **58**(2): p. 256-265.
56. Stieger, K., B. Belbellaa, C. Le Guiner, P. Moullier, and F. Rolling, *In vivo gene regulation using tetracycline-regulatable systems*. Adv Drug Deliv Rev, 2009. **61**(7-8): p. 527-41.
57. Favre, D., V. Blouin, N. Provost, R. Spisek, F. Porrot, D. Bohl, F. Marme, Y. Cherel, A. Salvetti, B. Hurtrel, J.M. Heard, Y. Riviere, and P. Moullier, *Lack of an immune response against the tetracycline-dependent transactivator correlates with long-term doxycycline-regulated transgene expression in nonhuman primates after intramuscular injection of recombinant adeno-associated virus*. Journal of Virology, 2002. **76**(22): p. 11605-11611.
58. Latta-Mahieu, M., M. Rolland, C. Caillet, M.P. Wang, P. Kennel, I. Mahfouz, I. Loquet, J.F. Dedieu, A. Mahfoudi, E. Trannoy, and V. Thuillier, *Gene transfer of a chimeric trans-activator is immunogenic and results in short-lived transgene expression*. Human Gene Therapy, 2002. **13**(13): p. 1611-1620.
59. Betz, S.F., J.L. Marmorino, A.J. Saunders, D.F. Doyle, G.B. Young, and G.J. Pielak, *Unusual effects of an engineered disulfide on global and local protein stability*. Biochemistry, 1996. **35**(23): p. 7422-8.
60. Riddiford, L.M., P. Cherbas, and J.W. Truman, *Ecdysone receptors and their biological actions*, in *Vitamins and Hormones - Advances in Research and Applications*, Vol 60. 2001, Academic Press Inc: San Diego. p. 1-73.
61. Zelhof, A.C., T.P. Yao, R.M. Evans, and M. McKeown, *Identification and characterization of a drosophila nuclear receptor with the ability to inhibit the ecdysone response*. Proceedings of the National Academy of Sciences of the United States of America, 1995. **92**(23): p. 10477-10481.
62. Yao, T.P., W.A. Segraves, A.E. Oro, M. McKeown, and R.M. Evans, *Drosophila ultraspiracle modulates ecdysone receptor function via heterodimer formation*. Cell, 1992. **71**(1): p. 63-72.

63. Karns, L.R., A. Kisielewski, K.M. Guldin, J.M. Seraj, and D. Theodorescu, *Manipulation of gene expression by an ecdysone-inducible gene switch in tumor xenografts*. BMC Biotechnol, 2001. **1**: p. 11.
64. Palli, S.R., M.Z. Kapitskaya, M.B. Kumar, and D.E. Cress, *Improved ecdysone receptor-based inducible gene regulation system*. Eur J Biochem, 2003. **270**(6): p. 1308-15.
65. Subbarayan, V., M. Mark, N. Messadeq, P. Rustin, P. Chambon, and P. Kastner, *RXRalpha overexpression in cardiomyocytes causes dilated cardiomyopathy but fails to rescue myocardial hypoplasia in RXRalpha-null fetuses*. J Clin Invest, 2000. **105**(3): p. 387-94.
66. Subbarayan, V., M. Mark, N. Messadeq, P. Rustin, P. Chambon, and P. Kastner, *RXR alpha overexpression in cardiomyocytes causes dilated cardiomyopathy but fails to rescue myocardial hypoplasia in RXR alpha-null fetuses*. Journal of Clinical Investigation, 2000. **105**(3): p. 387-394.
67. Thomas, H.E., H.G. Stunnenberg, and A.F. Stewart, *Heterodimerization of the drosophila ecdysone receptor with retinoid X receptor and ultraspirale*. Nature, 1993. **362**(6419): p. 471-475.
68. Yao, T.P., B.M. Forman, Z.Y. Jiang, L. Cherbas, J.D. Chen, M. McKeown, P. Cherbas, and R.M. Evans, *Functional ecdysone receptor is the product of ECR and ultraspiracle genes*. Nature, 1993. **366**(6454): p. 476-479.



## **CHAPTER 3**

### **CHARACTERIZATION OF A MOLECULAR SWITCH WITH THE GR130 VARIANT**

This chapter will discuss the characterization of the GR130 variant in a two- and one-component system. This work was performed with plasmids containing the GR130 variant inherited from a previous Doyle lab member Priyanka Rohatgi; therefore, it was assumed that the plasmid contained the corrected variant [1]. However, when the variant was sequenced at the end of this study, it was found to be the GRQCIMFI variant. The data collected with the two- and one-component system that contained the luciferase reporter gene was resequenced and confirmed to be the GR130 variant. The data collected with the one-component system containing the GFP reporter gene, was not confirmed and is unclear if the GR130 or the GRQCIMFI variant was tested.

#### **3.1 Engineering RXR**

The first step in engineering a molecular switch system is to create an orthogonal ligand/receptor pair (OLRP). An OLRP consists of a modified protein designed to bind a new small molecule, and not possess the ability to bind its natural ligand [2]. Figure 3.1 describes criteria for an OLRP in relation to the retinoid X receptor (RXR) and a synthetic compound structurally similar to an RXR agonist but that does not activate this receptor. As previously mentioned in Chapter 1, RXR can transcriptionally activate an endogenous gene with its natural ligand 9-*cis* retinoic acid (9cRA), but not the synthetic ligand LG335, an inactive analog of the FDA approved drug Targretin (Figure 3.1A) [3]. To develop an OLRP, RXR variants were created to bind the synthetic ligand, LG335. At

the same time, these variants should not activate transcription with the natural ligand, 9cRA (Figure 3.1B). Thus the OLRP involves an engineered variant that binds and activates in response to a synthetic small molecule not present in mammalian cells and should not activate endogenous receptors.

The compound LG335 was selected as the ligand target since previous studies showed the compound does not activate the wild-type receptor. The ligand was developed by the company Ligand Pharmaceuticals that was in pursuit of a selective RXR agonist [4, 5]. A series of compounds were synthesized included LG335 and the FDA approved drug Targretin. Targretin is a drug currently on the market used as an anticancer agent used in several therapies [6]. Doyle and coworkers previously discovered a RXR variant Q275C, I310M, F313I (QCIMFI) that was orthogonal to the ligand LG335 and will be characterized in Chapter 4; therefore, this ligand was chosen to engineer new OLRP [7].

Since nuclear receptors (NR) naturally contain DNA binding domains (DBD) that bind to NR response elements (RE), the OLRP in the molecular switch system must be further engineered so that interference with endogenous pathways is not observed. To address this issue, the DBD of RXR was replaced by the Gal4 DBD (Figure 3.1C). The Gal4 protein is a yeast transcription factor that activates transcription of genes involved in galactose catabolism, and is not present in mammalian cells [8-11]. The modularity of both nuclear receptors and the Gal4 protein allows their DBD to be switched. Thus, this new transcription factor will not bind to the RXR RE and activate endogenous genes, but will bind to an artificial promoter containing Gal4 RE and active transcription of a therapeutic gene, and can be used for *in vivo* applications (Figure 3.1D).

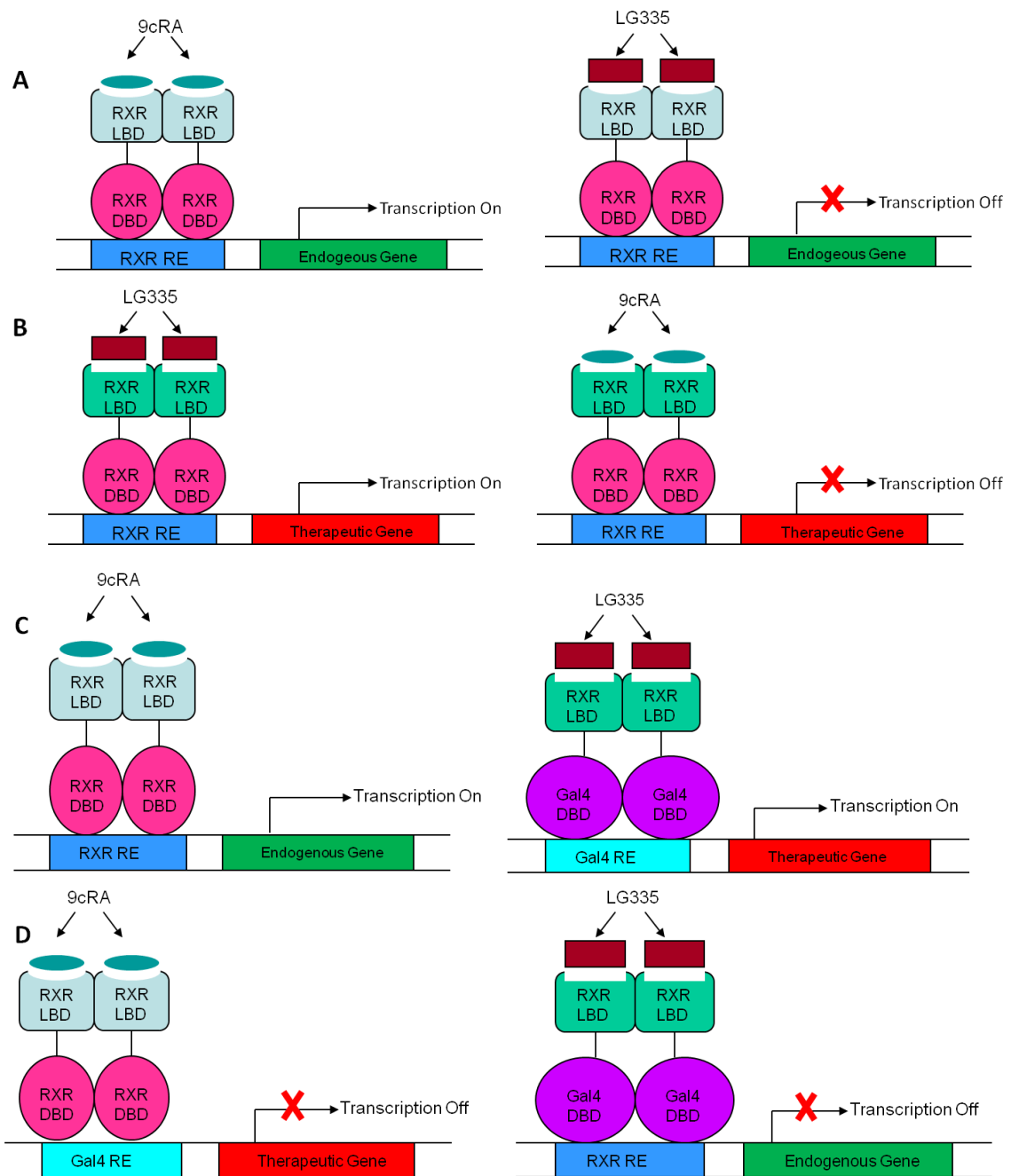


**Figure 3.1: Engineering a Molecular Switch System:** (A) 9cRA binds to RXRwt and activates expression of endogenous genes, and LG335 does not activate expression of endogenous genes. (B) RXR LBD was engineered to bind LG335 and activate gene expression, but not bind 9cRA. (C) RXR DBD was replaced with the Gal4 DBD that binds Gal4 RE. (D) RXRwt should not bind Gal4 RE and activate expression of therapeutic gene and the molecular switch should not bind RXR RE and activate expression of endogenous genes.

### 3.4.1 Previous Work

Previously, Doyle *et al* and Schwimmer *et al* engineered RXR variants to bind and activate in response to the novel small molecule, LG335. The best candidate, variant 130, obtained from a library of  $3.2 \times 10^4$  variants displayed a 30 nM EC<sub>50</sub> value with LG335 and no activation with 9cRA. This variant was determined to have four mutations: I268A, I310A, F313A, and L436F [12], and was chosen as a candidate for this molecular switch system and further characterized.

In order to use this variant in a molecular switch system, the DBD of this variant was switched from a RXR DBD to a Gal4 DBD. The Gal4 DBD binds four multiple repeats of a 17-mer DNA sequence called Gal4 RE [13]. This sequence, unique to yeast, provides specificity to a target promoter region containing Gal4 RE, and should not bind to endogenous mammalian DNA sequences. Thus, the fusion of the Gal4 DBD and the LBD of the RXR variant 130 (GR130) creates a new transcription factor involved in this molecular switch system.

Previously, GR130 was cloned into the retroviral vector pMSCV, creating a new plasmid, pMSCVGR130 [1]. This plasmid contains two long terminal repeat (LTR) regions. The 5' LTR region is composed of enhancer elements and the promoter that allows GR130 to be constitutively expressed (Figure 3.2). Both LTRs and the  $\Psi$  region also possess retroviral signals. The second part of the molecular switch system is the reporter system. On a separate plasmid, the Gal4 RE located upstream from a minimal thymidine kinase promoter ( $P_{tk}$ ) controls expression of the reporter gene, *Renilla* luciferase (Figure 3.2).

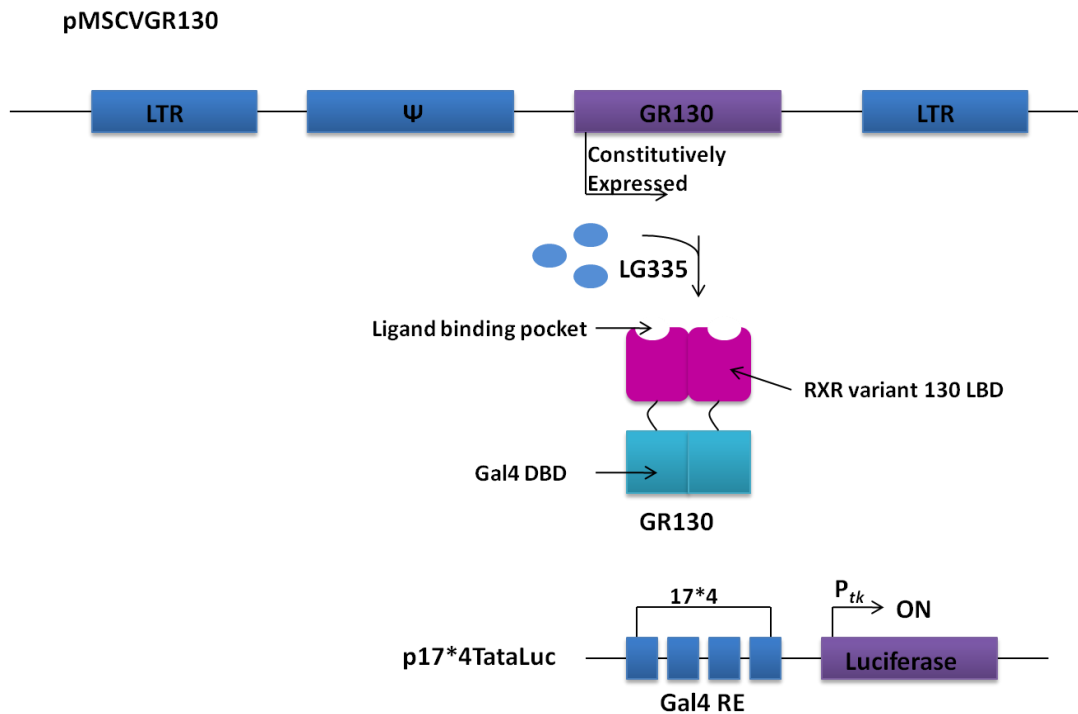


Figure 3.2: **Schematic diagram of two-component switch system:** The pMSCVGR130 plasmid constitutively expresses GR130. Upon the addition of LG335, GR130 binds to four Gal4 RE upstream from a minimal *thymidine kinase* promoter controlling expression of the luciferase reporter gene.

This chapter will address the characterization of this molecular switch system through transient transfections in a two-component and one-component system. The difference between the two systems is that the two-component system involves two plasmids, whereas the one-component system only involves one plasmid. Lastly, stable expression of the one component system was also characterized using a retrovirus, as well as, transient transfection with a selection marker.

### 3.2 GR130 in the Two-Component System

As shown in Figure 3.2, the two component system is composed of two plasmids. The first plasmid, pMSCVGR130, is a retroviral vector that has two LTR regions, a  $\Psi$  region, and the GR130 gene. The 5' LTR region allows GR130 to be constitutively expressed. Upon binding of LG335, GR130 binds to the reporter plasmid, p17\*4TataLuc, containing four tandem Gal4 RE located upstream from a minimal thymidine kinase promoter ( $P_{tk}$ ). The binding of GR130 to the promoter region induces expression of the *Renilla* luciferase gene.

The molecular switch was first tested in a luciferase assay to determine the activity of the GR130 variant with LG335 and 9cRA. HEK293T cells, human embryonic kidney cells, were cotransfected with a 1:2 molar ratio of pMSCVGR130 and p17\*4TataLuc using the transfection agent Lipofectamine 2000, a cationic lipid. As a positive control, the pCMXGRXRwt was transfected alongside. This plasmid contains the Gal4 DBD fused to RXRwt (GRXRwt), and the fusion protein is constitutively expressed under the control of the cytomegalovirus (CMV) promoter.

The results in Figure 3.3 show that GR130 is not activated by 9cRA, but activation is observed in response to LG335, displaying a  $19 \pm 5$ -fold induction and 50 nM

EC<sub>50</sub> value, comparable to results found by Schwimmer *et al* [12]. The control, GRXRwt, showed activation with both LG335 and 9cRA. Maximal activation was observed at 1 μM 9cRA (280 nM EC<sub>50</sub> value) with a 9±1-fold induction, and maximal activation was observed at 3.2 μM LG335 (690 nM EC<sub>50</sub> value) and a 5±1-fold induction. The activation of GRXRwt by the synthetic ligand is not of any concern since the fusion of the Gal4 DBD and the RXRwt LBD does not exist *in vivo*. Therefore, the molecular switch system developed has the ability to regulate transgene expression upon the addition of ligand, and the receptor is orthogonal to the ligand LG335.

### 3.3 Characterization of the One-Component Molecular Switch System

The previous section shows the two-component system is capable of regulating gene expression. However, cotransfecting two plasmids are less desirable than transfecting a single plasmid due to the fact that introducing two plasmids decreases the transfection efficiency. To increase the versatility for stable expression in cell culture, the components in the p17\*4TataLuc plasmid were cloned into the pMSCVGR130 vector, called pMSCVGR130Talu (Figure 3.4). In this vector, GR130 is constitutively expressed, as shown in Figure 3.4, and in the presence of LG335 will bind to the Gal4 RE located on the same plasmid and induces expression of the *Renilla* luciferase reporter gene. Another reporter, the enhanced green fluorescent protein (eGFP), was also tested in order to visualize protein expression.

When GR130 was tested in the one-component system with the luciferase gene, as shown in Figure 3.5, reduced luciferase activity is observed, displaying a 2-fold increase in the EC<sub>50</sub> value (100 nM) compared to the two component system (50 nM EC<sub>50</sub> value). Also, a low fold induction of 3±1-fold was observed and compared to GRQCIMFI. The

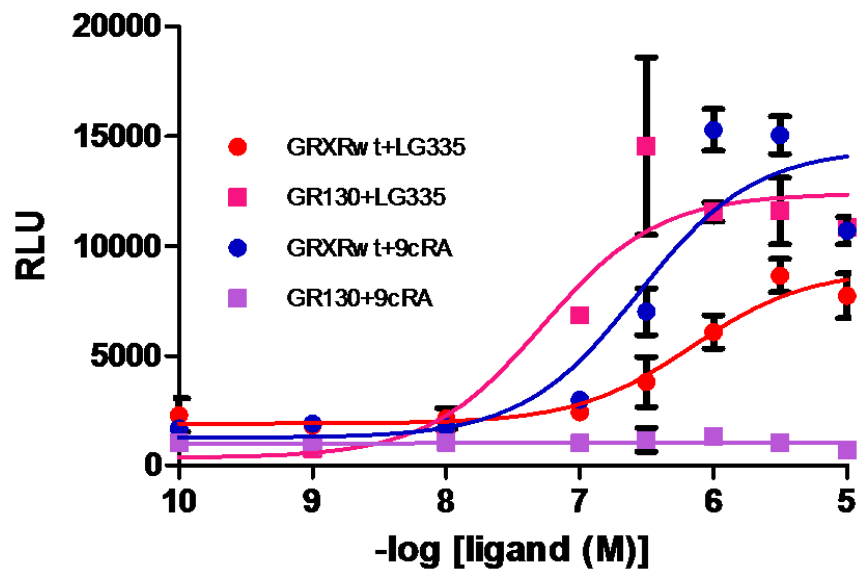


Figure 3.3: **Activation Profile of G130 and GRXRwt:** Activation profiles of GR130 and GRXRwt in HEK293T cells in response to LG335 and 9cRA.



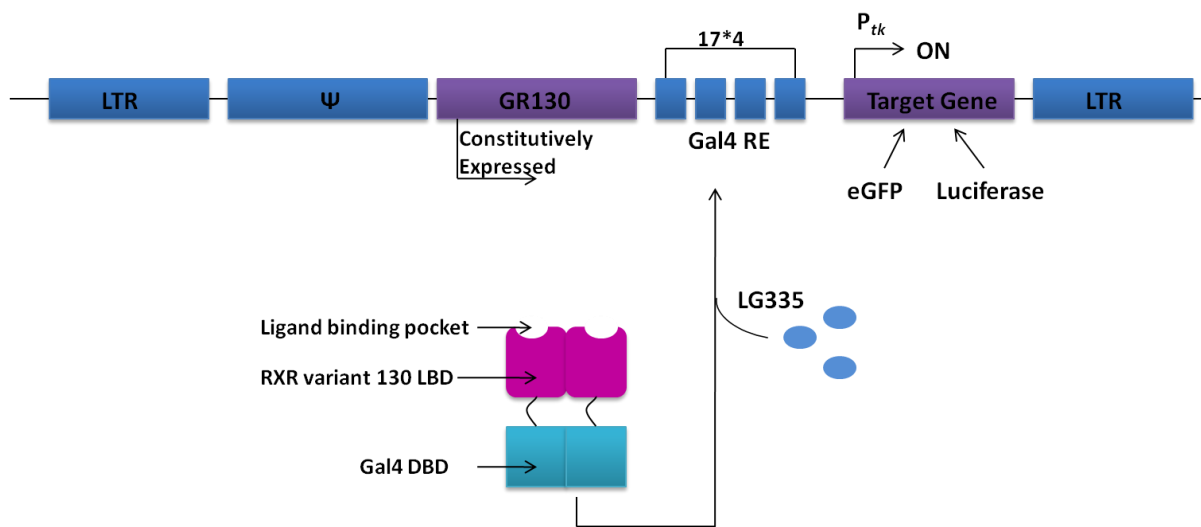


Figure 3.4: **Schematic diagram of one-component system:** The pMSCVGR130GFP plasmid constitutively expressed GR130. Upon the addition of LG335, GR130 binds to the same plasmid containing Gal4 RE located upstream from a minimal *thymidine kinase* promoter controlling expression of the target gene, eGFP or luciferase.

GR130 variant was compared to the Q275C, I310M, F313I (GRQCIMFI) variant, previously developed by Doyle *et al* and also showed reverse ligand specificity with LG335. The GRQCIMFI variant shows a  $6\pm 1$ -fold induction and a 271 nM EC<sub>50</sub> value in the one-component system. These results show the GRQCIMFI variant is able to induce activation, while the GR130 variant does not; therefore the GR130 variant needs further improvement if this variant will be used in the molecular switch system.

Since a low fold induction was observed with the one-component system, the green fluorescent protein (GFP) was used to determine if the amount of activation provided sufficient gene expression to visualize GFP. The pMSCVGR130GFP plasmid, constitutively expresses GR130 and upon the addition of LG335, GR130 can bind to the same plasmid and induce expression of eGFP (Figure 3.4) [1]. After the pMSCVGR130GFP plasmid was transfected into HEK293T cells, cells were then treated with and without 10  $\mu$ M LG335 eight hours after the transfection. Fluorescent images of the cells were taken 48 hours after the transfection.

To evaluate the fluorescent images, the percentage of fluorescent cells was determined by manually counting the number of the fluorescent cells and taking into account the total number of cells, multiplying by a factor of 100. As shown in Figure 3.6, very little background is seen when no ligand is added to the system; however, when 10  $\mu$ M LG335 is added, GFP expression is observed in approximately 30% of the cells. To evaluate transfection efficiency, these results were compared to a control plasmid pMSCVIRESGFP, which contains an internal ribosome entry site (IRES) and constitutively expresses eGFP (Figure 3.7). IRES is a DNA sequence that initiates translation of RNA by recruiting ribosomal subunits to a site on the RNA other than the

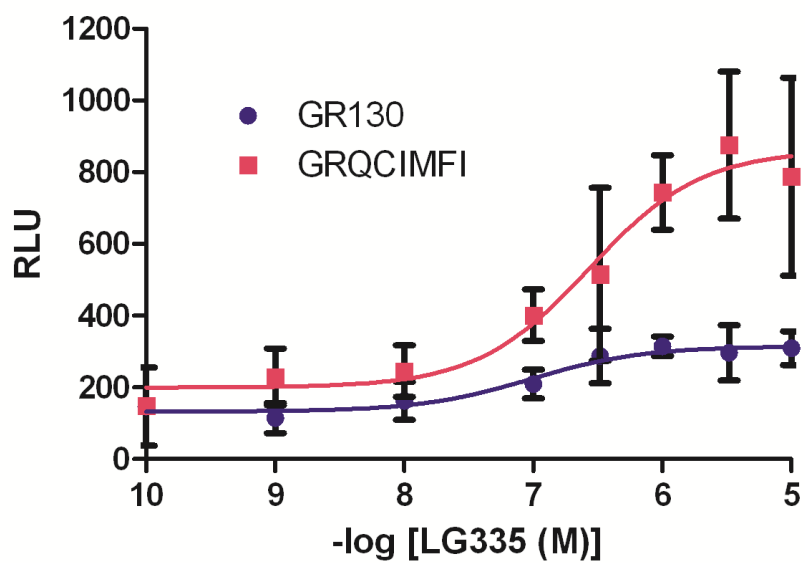


Figure 3.5: **Activation Profile in the One-Component System:** Activation profile of the one-component system with GR130 (●) and GRQCIMFI (■) with LG335.

5' end region, allowing the translation of protein to occur more efficiently [14, 15]. The transfection efficiency with the IRESGFP plasmid was observed to be approximately 60%. Despite the low fold induction observed with the luciferase reporter gene, the molecular switch system is able to induce a reasonable amount of GFP expression in the one component system with the GR130 variant.

In comparing the one-component and the two-component systems, both systems were able to regulate target gene expression proficiently; however, each system has advantages and disadvantages. The two-component system displays a high fold induction and a lower  $EC_{50}$  values, but the presence of two plasmids reduces transfection efficiency and is not desirable in gene therapy applications. The one-component system provides versatility by decreasing the amount of exogenous DNA required [16]; however, a decrease in gene expression is also observed when all components are combined into one plasmid.

### **3.4 Stable Expression of the Molecular Switch System**

Since the potential molecular switch GR130 was able to turn on gene expression with the eGFP reporter. The next step was to characterize stable expression of the molecular switch system. Stable expression allows the components of the molecular switch system to be expressed in a cell over an extended period of time, which would be more favorable in gene therapy applications. In transient transfections, a two-fold problem exists. First, cationic lipids do not enter cells very efficiently because they are easily degraded [17]. Second, expression of target gene is lost over time, since cells do not retain plasmid. In this section, two types of methods will be used to characterize stable expression of the molecular switch system. The first section will discuss using retroviral particles, which

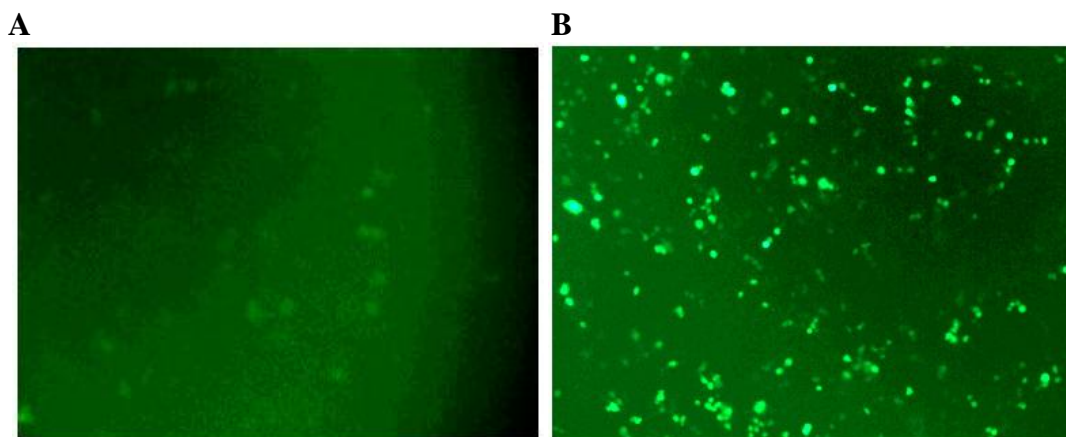


**Figure 3.6: Fluorescent Images of Transient Transfection with pMSCVGR130GFP:** Fluorescent images of HEK293T cells transiently transfected with GR130GFP in the presence of (A) no ligand or (B) 10  $\mu$ M LG335

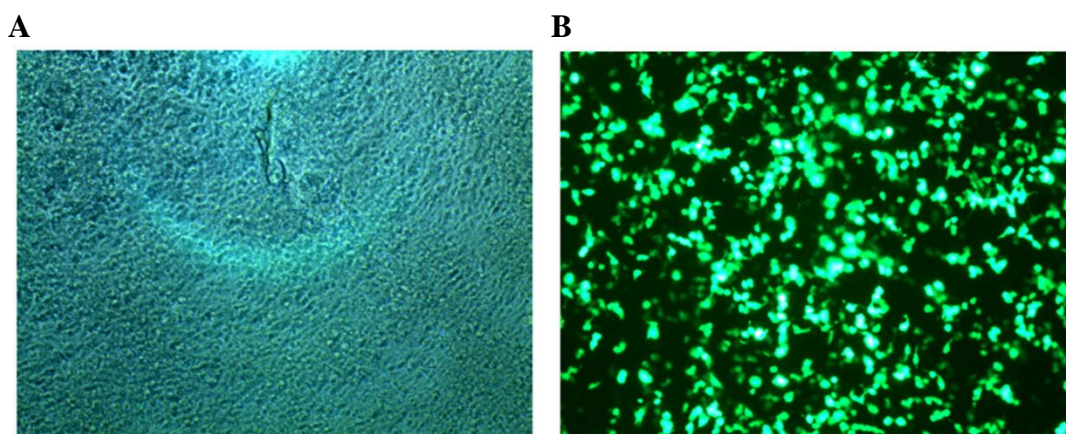


**Figure 3.7: Fluorescent Image of Transient Transfection with pMSCVIRESGFP:** (A) The DIC and (B) fluorescent image of HEK293T cells transiently transfected with pMSCVIRESGFP.

integrate the DNA of the molecular switch system into the genome of the host. The second section will discuss using transient transfection and a selection marker. This method forces cells to retain the episomal DNA, since the same plasmid expresses an antibiotic resistant gene, allowing cells to survive in media treated with antibiotics.

### **3.4.1 First Method: Retroviral transduction**

As previously discussed in Chapter 2, viral systems allow long-term expression of the therapeutic gene, and can enter cells very efficiently. Several viral systems exist; however, the retrovirus system was chosen for the molecular switch system. Retroviruses enter the cells and integrate DNA into the genome of the host. Retroviral infectious particles are created by transiently transfecting a retroviral plasmid into a packaging cell line (Figure 3.8). Packaging cell lines possess *trans*-elements, such as the *gag*, *pol*, and *env* genes [18]. These genes produce essential proteins such as reverse transcriptase, integrase, and viral envelope proteins that make retroviruses effective at entering cells and integrating genetic material into the genome of host [19]. The packaging cell line lacks the packaging and regulation signals, the *cis*-elements, which prevent mobilization of virion particles. Therefore, viral particles cannot be produced until the retroviral plasmid is transfected into the packaging cell line.

As shown in Figure 3.8, the viral vector enters the nucleus and is transcribed into RNA. The packaging signal,  $\Psi$ , on the RNA sequence is recognized by the viral proteins, allowing the packaging of the virus. Lastly, the virions bud off the cell membrane, and retains the envelope and cell membrane proteins that allow the virus to infect a specific host [19]. The virus used for the molecular switch system is an ecotropic retrovirus, which specifically infects rodents, and was used for testing in a murine cell line.

To optimize the viral transduction, the control plasmid, pMSCVIRESGFP was used. This plasmid constitutively expresses eGFP and contains an internal ribosomal entry site (IRES) prior to the eGFP DNA sequence. EcoPack 2-293 cells were transfected with pMSCVIRESGFP using the transfection reagent, Lipofectamine 2000. Viral particles released in the media were collected every 12 hours for four to five days, and then transduced into NIH3T3 cells, mouse fibroblast cells. Previously, viral particles were shown to infect cells more efficiently when incubated with two charged polymers [20-22]; therefore, two polymers were used to transduce the virus.

The first polymer, polybrene (PB), a positively charged polymer, is known to neutralize charges between virions and sugars on the cell surface [23, 24]. The second polymer, chondroitin sulfate C (CSC), an anionic glycosaminoglycan, has been shown to increase viral mediated transfer [21, 25]. The optimal concentration of polymers was assessed by incubating viral stocks with a range of polymer concentrations (8-200  $\mu\text{g/mL}$ ). The optimal protocol found for retroviral transductions was to first incubate with 80  $\mu\text{g/mL}$  of CSC for 10 minutes, and then incubate with 80  $\mu\text{g/mL}$  of PB for 10 minutes. The viral stock was then added to NIH3T3 cells with 8  $\mu\text{g/mL}$  of PB. To further enhance this protocol, the stock solution composed of retroviral infectious particles was concentrated in an effort to increase the amount of viral particles that can infect cells. However, the concentrated stocks did not enhance the transduction efficiency.

NIH3T3 cells transduced with the IRESGFP virus were analyzed using flow cytometry to measure the efficiency of the viral transduction. Flow cytometry is a technique used to analyze thousands of cells or particles that are in liquid suspension [26-28]. Individual cells or particles are examined for physical and/or chemical



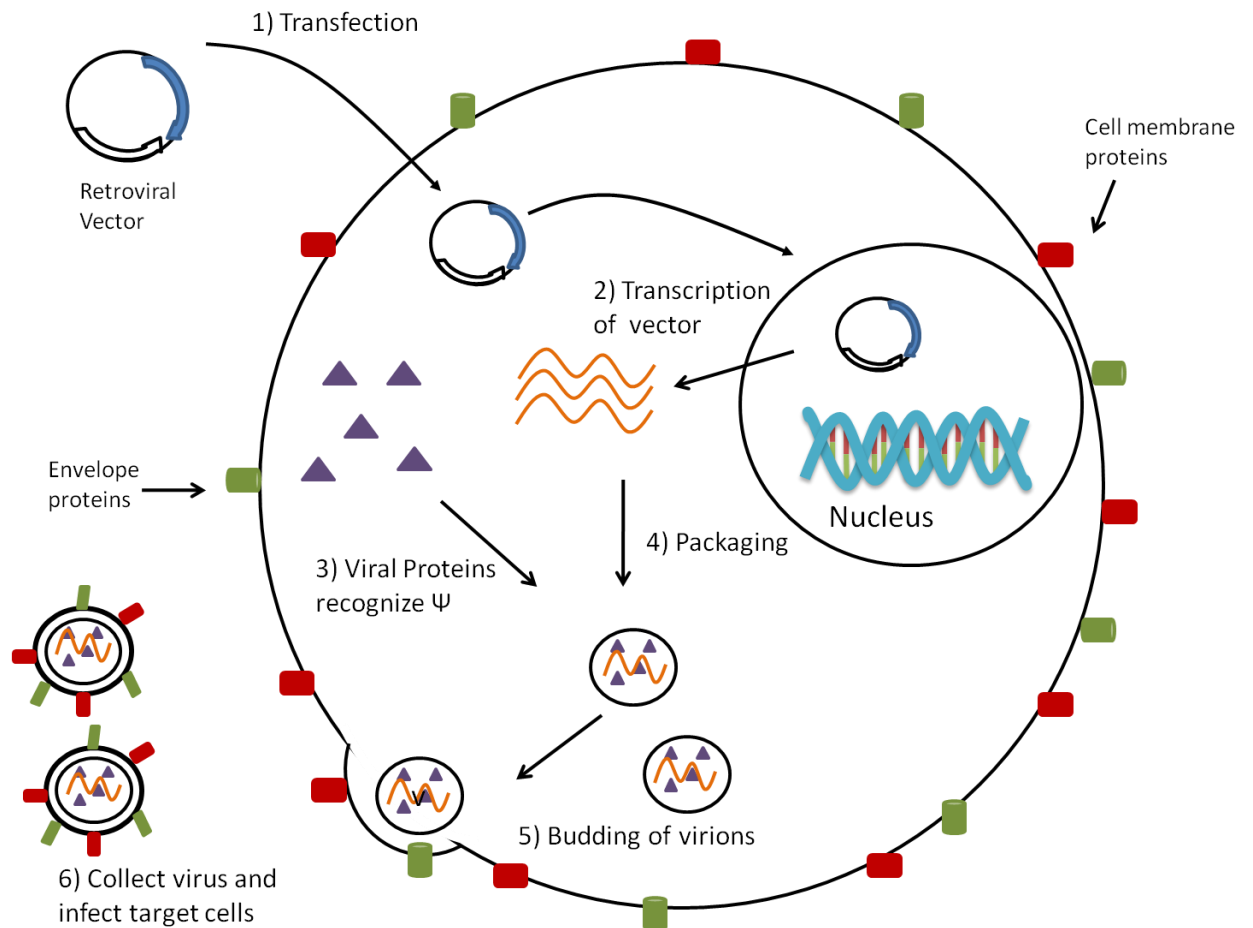


**Figure 3.8: Diagram of Packaging Cell Line:** The retroviral vector is transiently transfected into the packaging cell line. The vector enters the nucleus where it is transcribed into RNA. The  $\Psi$  region on the RNA is recognized by the viral proteins expressed in the packaging cells line and is packaged into virions. The virions then bud from the cell retaining the envelope and cell membrane proteins. Collected from the media and transduced onto target cells.

characteristics as they pass through a laser [26-28]. Data collected from samples can be plotted on a histogram, which produces a graph displaying a single parameter on the x-axis against the number of cells analyzed on the y-axis. A gate can be placed on the histogram that selects for a subpopulation of cells that exhibit a specific characteristic, which allows the percentage of cells displaying a specific characteristic to be determined.

Figure 3.9 is a histogram, indicating the number of fluorescent cells in a given sample. Cells transduced with no virus, 10  $\mu$ L of virus, and 100  $\mu$ L of virus were subjected flow cytometry, analyzed, and plotted on a histogram. The negative control, cells not transduced with virus, were first analyzed by setting a gate above the fluorescent intensity of these cells, indicating autofluorescence. From this control, cell emitting a fluorescent intensity above autofluorescence can be evaluated and the percentage of GFP positive cell can be determined. When evaluating cells transduced with 10  $\mu$ L of virus, GFP fluorescence was observed in 30% of the cells, and cells transduced with 100  $\mu$ L of virus were 77% positive for GFP fluorescence (Figure 3.9).

These results show a successful transduction in NIH3T3 cells with the IRESGFP retroviral particles. The optimal conditions to transduce cells were by incubating cells with the charged polymers CSC and PB, then adding 100  $\mu$ L of the viral stock to NIH3T3 cells. When cells were transduced with pMSCVGR130GFP, GFP fluorescence was barely observed; therefore, another route to evaluate stable expression of the molecular switch system was pursued.

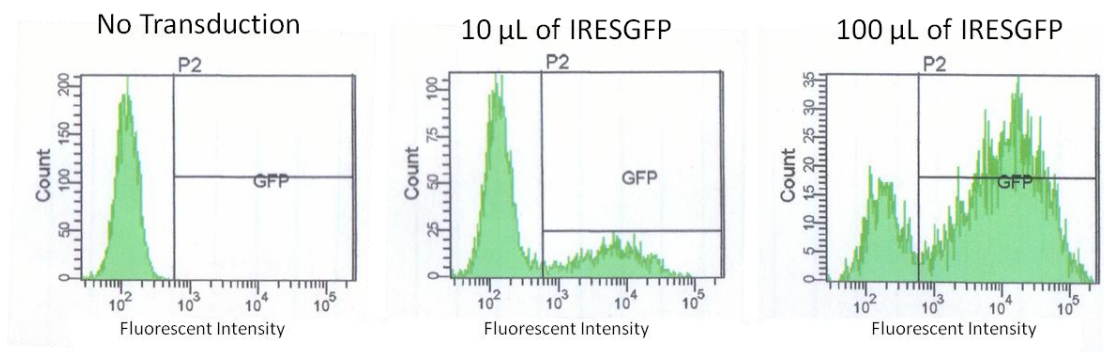


**Figure 3.9: Flow Cytometry Histograms of NIH3T3 cells transduced with pMSCVIRESGFP:** Histogram displaying flow cytometry data of NIH3T3 cells transduced with no virus, 10  $\mu$ L, or 100 $\mu$ L of IRESGFP.

### 3.4.2 Second Method: Stable Expression Using a Selection Marker

Despite the advantage of using viral methods for the introduction of the molecular switch system, a considerably low fluorescent intensity of GFP was observed in comparison to transient transfections. Therefore, characterization of stable expression of the molecular switch system was attempted by adding selective pressure to the transient transfection method using a plasmid that contained a selection marker. This method utilizes the power of genetic selection to maintain the gene of interest over an extended period of time. A selection marker in this case is an antibiotic resistance gene, the neomycin resistance gene (*neo*), providing resistance in the presence of the antibiotic geneticin (G418). G418, an aminoglycoside antibiotic produced by *Micromonospora rhodorangea*, can block peptide synthesis by inhibiting the elongation step in both prokaryotes and eukaryotes [29-31]. The *neo* gene expresses a phosphotransferase enzyme, able to hydrolyze G418, allowing cells to survive in media containing this antibiotic [32, 33].

The initial step in this experiment was to determine the optimal G418 concentration to kill the majority of the cells over an extended period of time. NIH3T3 cells grown in media containing G418 (50-800  $\mu\text{g/mL}$ ) were observed for cell viability over a four to five day period, known as a kill curve. The appropriate concentration of G418 was determined to be 400  $\mu\text{g/mL}$ , killing NIH3T3 cells in four days.

As stated above, in order to develop stable cell lines using a selection marker, the plasmid of interest must contain a selection marker resistant gene. Unfortunately, the pMSCVGR130GFP plasmid lacked a neomycin resistance marker; therefore, a cotransfection was performed with the pmRFP plasmid, which contains the *neo* gene and

constitutively expresses the red fluorescent protein (RFP). The hypothesis is that the cotransfection with the pmRFP plasmid and the pMSCVGR130GFP plasmid will allow the cells to survive in media treated with G418, as well as stably express the molecular switch system.

A 1:20 cotransfection (mRFP: GR130) with the transfection reagent Polyfect was performed in a cell culture dish. G418 (400 µg/mL) was added to the cells daily until colonies formed. Once colonies formed, they were placed in a 48-well plate with media containing G418 to screen for colonies that expressed the molecular switch system proteins. LG335 was added to the colonies, and then colonies were analyzed for green and red fluorescence. Green fluorescence indicated that the colonies possessed the functional molecular switch system, while red fluorescence showed that the colonies contained the plasmid with the antibiotic resistant gene.

Figure 3.10 is a image of one of several colonies chosen that exhibited both green and red fluorescence, as well as daughter cells that are also fluorescent. Colonies possessing both green and red fluorescent were selected and then placed in 6-well plates with media containing 400 µg/mL of G418 to allow the generation of daughter cells to occur. Once daughter cells were generated, they were also examined for green and red fluorescence. As shown in Figure 3.11, a number of daughter cells emitted both green and red fluorescence (purple circle); however, this was not observed in all the daughter cells generated. Fluorescence was lost in the other daughter cells, black arrow.

pMSCVIRESGFP was used as a positive control. This plasmid is not missing the selection marker gene; hence cells cotransfected with pMSCVIRESGFP and mRFP were able to sustain green fluorescence. The transient transfection of the one-component

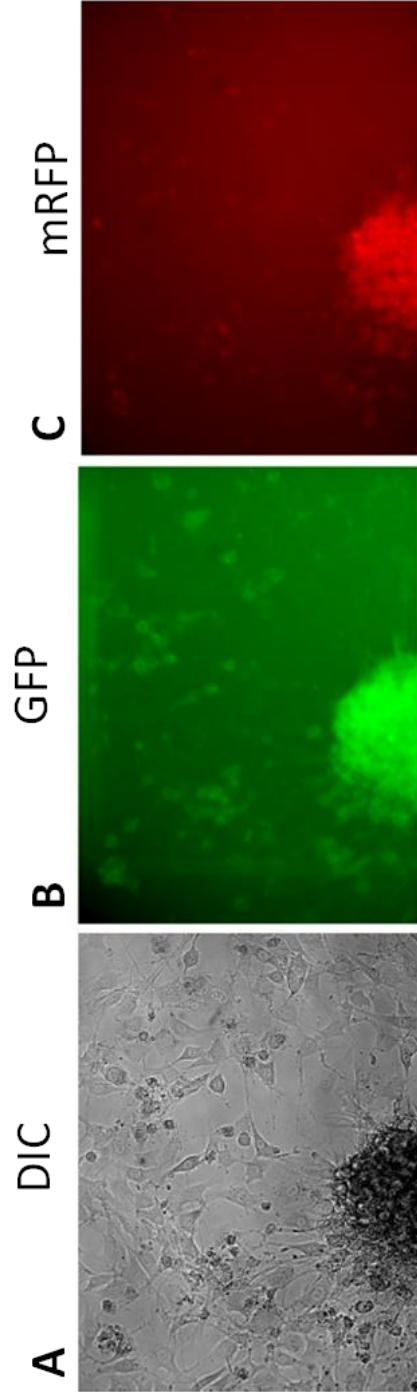


Figure 3.10: **Fluorescent Images of Colonies transfected with GR130GFP and mRFP:** A colony from the NIH3T3 stable cell line made through transient transfection with GR130GFP and mRFP, (A) is the differential interference contrast microscopy picture, (B) is the image of GFP expression, and (C) is the image of mRFP expression.

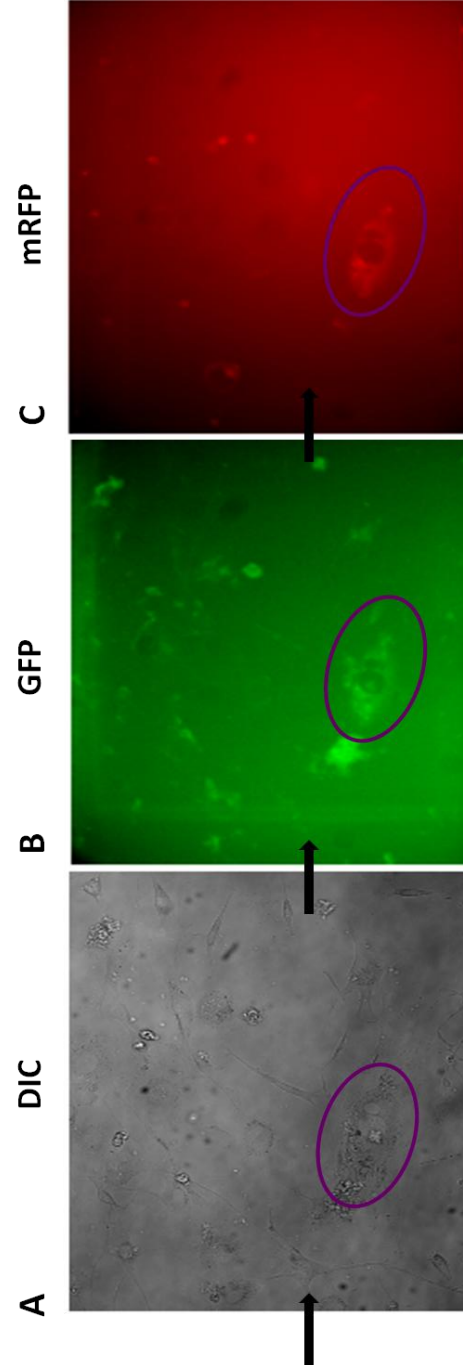


Figure 3.1.1: **Fluorescent Images of Cells stably transfected with GR130GFP and mRFP:** Fluorescent images of cells stably transfected with GR130GFP and mRFP, (A) is the differential interference contrast microscopy picture, (B) is the image of GFP expression, and (C) is the image of mRFP expression.

system with the selection marker plasmid allowed the production of cells that expressed the molecular switch system; however, expression of this system was lost over time, due to the fact that the colonies only needed the mRFP plasmid to survive.

### **3.4.3 Genomic Analysis of NIH3T3 cells transduced with GR130**

Since stable expression of the molecular switch system could not be characterized through transient transfection and a selection marker, troubleshooting was performed with the retroviral transduced cells. Retroviral transductions provide the ability to integrate the molecular switch into the genome of the host. Integration of the transgene allows for the stable expression of a target gene for an extended period of time and over multiple generations of cells. To determine whether integration was successful, genomic DNA was purified from the transduced cells and primers were used to amplify regions of the molecular switch system. Sequencing results showed that the variant was not I268A, I310A, F313A, and L436F (GR130) but was Q275C, I310M, and F313I (GRQCIMFI). This plasmid was inherited prior to this thesis work from a previous lab member, and must have been mislabeled.

In summary, a molecular switch system was characterized with what was thought to be the orthogonal ligand receptor pair (OLRP), GR130, which has a Gal4 DBD fused to a RXR variant (I268A, I310A, F313A, and L436F). In the presence of LG335, this transcription factor is shown to bind to Gal4 RE and activate both a luciferase and GFP genes. This system shows efficient gene expression in both two-component and one-component systems. The one-component system was then transduced in NIH3T3 cells using retroviral particles after optimization with the control plasmid, pMSCVIRESGFP. Unfortunately, sequencing of the genomic DNA revealed the actual RXR OLRP was



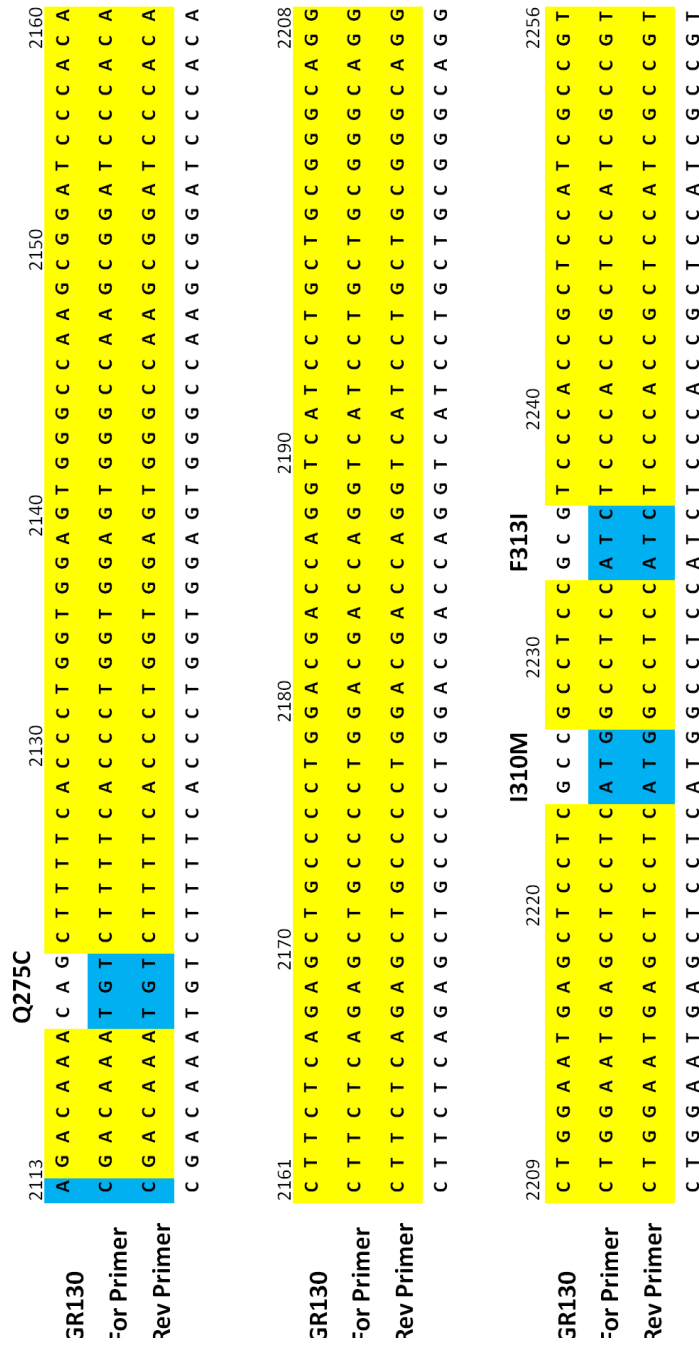


Figure 3.12: **Genomic Sequencing Analysis:** Sequencing analysis of genomic DNA purified from cells transduced with GR130 retroviral particles.

QCIMFI (Q275C, I310M, F313I) rather than the GR130 variant. Therefore, the next chapter focuses on characterizing the molecular switch system using the QCIMFI variant.

### 3.5 Materials and Methods

#### Ligands

9-*cis*-retinoic acid (MW 304.44 g/mol) and all-*trans*-retinoic acid (MW 300.44 g/mol) were purchased from MP Biomedicals (Solon, OH). LG335 was synthesized in the lab [12, 34]. 10 mM stocks of the ligand were dissolved in 80% ethanol:20% DMSO and stored at 4°C.

#### Plasmids

The p17\*4TataRluc plasmid was previously constructed from p17\*4TataFLuc (a gift from Dr Sofia Tsai, Baylor College, Houston, TX) [35, 36] by replacing the *firefly* luciferase with *Renilla* luciferase. The *Renilla* luciferase was cloned from pHRL (Clontech, USA) with *NotI* and *SacII* restriction sites. The internal standard plasmid pCMX-βGAL constitutively expresses β-galactosidase under control of the CMV promoter. The plasmids pCMXRXRwt, pCMXRXR130, pMSCVGR130, pMSCVGR130Talu, and pMSCVGRQCIMFITalu have been previously described [1, 12]. The pLuc\_CRPBII was made by site-directed mutagenesis from pLucMCS (Stratagene, USA). Site-directed primers were designed to incorporate a CRPBII response element in the multiple cloning site (MCS).

#### Cell culture conditions

All cell types were maintained at 37°C in humidified air with 5% CO<sub>2</sub>. NIH3T3 (ATCC, Manassas, VA) and HEK293T (ATCC, Manassas, VA) cells were cultured in Dulbecco's Modified Eagle Medium (DMEM, Mediatech Inc, Manassas, VA) supplemented with 10% fetal bovine serum (FBS, PAA Australia, ) and 1% penicillin/streptomycin (PS) (VWR, West Chester, PA), also known as growth media.

#### Mammalian luciferase assays

Transfections of HEK293T cells were performed in 48-well plates with Lipofectamine 2000 (Invitrogen, Carlsbad, CA) as the cationic lipid as recommended by the manufacturer. Briefly, 20 ng of pMSCVGR130 or pCMXGRXRwt expression plasmid, 40 ng of p17\*4TataLuc reporter plasmid, and 40 ng of pCMX-βGAL expression plasmid (used as an internal standard) were mixed with 0.3 μL of Lipofectamine 2000 in 40 μL of Opti-Mem (Invitrogen, Carlsbad, CA) reduced serum media per transfected well. After incubating for 30-60 minutes, an additional 160 μL of Opti-Mem was added. The mixture with a total volume of 200 μL mixture was added to a well previously washed with 250 μL of Opti-Mem. Eight hours after the transfection, wells were aspirated and ligands diluted in growth media were added to the wells. Cells were harvested after 36-40 hours and assayed for luciferase and β-galactosidase activities. All data points represent the mean of triplicate experiments normalized against β-galactosidase activity. Error bars represent the standard deviation. The one-component system, pMSCVGR130GFP was transfected as described above; however the p17\*4TataLuc plasmid was not added to the transfection mixture. Data was analyzed in the graphing program Graph Pad Prism® using the nonlinear regression curving program called Dose-Response Stimulation: log(agonist) vs. response (three parameters).

Standard Deviation Calculation:

$$s_N = \sqrt{\frac{1}{N} \sum_{i=1}^N (x_i - \bar{x})^2}.$$

Where  $x_i$  is the RLU value,  $N$  is the number of samples measured, and  $\bar{x}$  is the average RLU value.

#### Mammalian GFP analysis

Transfections of HEK293T cells were performed in 12-well plates with Lipofectamine 2000 cationic lipid as recommended by the manufacturer. Briefly, 1.6  $\mu$ g of pMSCVGR130GFP or pMSCVIRESGFP was mixed with four  $\mu$ L of Lipofectamine 2000 in 200  $\mu$ L of Opti-Mem reduced serum media per transfected well. After 30-60 minutes, an additional 1600  $\mu$ L of Opti-Mem was added and the 2 mL mixture was added to a well previously washed with 2 mL of Opti-Mem. After eight hours of transfection the wells were aspirated and ligands diluted in growth media were added to the wells. Images of transfected cells were taken using a 40X objective on a Zeiss LSM microscope. Images were processed on Adobe Photoshop. To obtain the percentage of fluorescent cells, the number of fluorescent cells counted was divided by the total number of cells counted multiplied 100.

#### Transfection into Packaging Cell Line

EcoPack-293T cells (Clontech, USA) were transiently transfected with 16  $\mu$ g of pMSCVGRQCIMFIGFP or pMSCVIRESGFP plasmid with 20  $\mu$ L of Lipofectamine 2000 and 6 mL of Opti-Mem in a 100 mm cell culture dish. After eight hours, the media was changed to 7 mL of growth media. Collected viral particles in media on cells every

10-15 hours and filtered with a 0.45 µm syringe filter (Pall Corporation, USA) for five consecutive days.

#### Concentration of Virus

Viral stock were thawed in a waterbath at 37°C, and centrifuged at 13800 x g overnight (minimum 16 hours) at 4°C. Supernatant was removed and viral pellet was resuspended in 1/20<sup>th</sup> to 1/40<sup>th</sup> of the original volume of media.

#### Retroviral Transduction

Media contain retroviral infectious particles was incubated with 80 µg/mL of chondroitin 6-sulfate sodium salt from shark cartilage (CSC, Sigma Aldrich, USA) for 10 minutes, and then with 80 µg/mL of polybrene (PB, Millipore Corporation, USA) for 10 minutes. Media was then added to NIH3T3 cells grown on 6-well plates with 8 µg/mL of polybrene.

#### Flow Cytometry Data

NIH3T3 cells transduced with the IRESGFP retroviral infectious particles were trypsinized and resuspended in growth media. Fluorescent intensity was then measured and analyzed using the BD LSR instrument.

#### Transfection using selection marker

NIH3T3 cells were cotransfected with 1 µg of pmRFP and 20 µg pMSCVGR130GFP with 44 µL of the transfection reagent PolyFect (Qiagen, USA). Geneticin (HyClone Laboratories, Utah) was diluted in growth media to a concentration of 400 µg/mL and 10 mL of media containing the antibiotic was added to the cells daily until colonies formed. Colonies were picked with a pipette tip and placed in a 48-well

plate with 250  $\mu$ L of growth media containing 400  $\mu$ g/mL of geneticin. Colonies were analyzed for green and red fluorescence using the 40X objective on a Zeiss LSM microscope. Cells displaying both green and red fluorescence were placed in 6-well plates with 2 mL of growth media containing 400  $\mu$ g/mL of geneticin for further growth. Once cells reached confluency in the 6-well plate were then trypsinized and then placed in 35 mm dish with 4 mL of growth media containing 400  $\mu$ g/mL of geneticin. Cells were then analyzed again for green and red fluorescence using a 40X objective on a Zeiss LSM microscope. Images were processed on Adobe Photoshop.

### Genomic Analysis

NIH3T3 cells transduced with retrovirus were harvested and purified using the DNeasy kit (Qiagen, USA). Sections of the molecular switch system were amplified from the genomic DNA and submitted for sequencing (Eurofins/MWG/Operon, Alabama). Sequencing primers used to confirm variant were: 1f', ATT CTT TAC AGG ATA TAA AAG CAT TGT TAA CAG GAT; 1r', CGC CTC CAG CAT CTC CAT AAG G.

## **3.6 Literature Cited**

1. Rohatgi, P., *Engineering protein molecular switches to regulate gene expression with small molecules*. 2006, Atlanta, Ga. :: Georgia Institute of Technology.
2. Bishop, A., O. Buzko, S. Heyeck-Dumas, I. Jung, B. Kraybill, Y. Liu, K. Shah, S. Ulrich, L. Witucki, F. Yang, C. Zhang, and K.M. Shokat, *Unnatural ligands for engineered proteins: New tools for chemical genetics*. Annual Review of Biophysics and Biomolecular Structure, 2000. **29**: p. 577-606.
3. Qu, L.Y. and X.W. Tang, *Bexarotene: a promising anticancer agent*. Cancer Chemotherapy and Pharmacology. **65**(2): p. 201-205.

4. Boehm, M.F., M.R. McClurg, C. Pathirana, D. Mangelsdorf, S.K. White, J. Hebert, D. Winn, M.E. Goldman, and R.A. Heyman, *Synthesis of high specific activity [3H]-9-cis-retinoic acid and its application for identifying retinoids with unusual binding properties*. J Med Chem, 1994. **37**(3): p. 408-14.
5. Boehm, M.F., L. Zhang, B.A. Badea, S.K. White, D.E. Mais, E. Berger, C.M. Suto, M.E. Goldman, and R.A. Heyman, *Synthesis and structure activity relationships of novel retinoid X receptor selective retinoids*. Journal of Medicinal Chemistry, 1994. **37**(18): p. 2930-2941.
6. Qu, L.Y. and X.W. Tang, *Bexarotene: a promising anticancer agent*. Cancer Chemotherapy and Pharmacology, 2010. **65**(2): p. 201-205.
7. Doyle, D.F., D.A. Braasch, L.K. Jackson, H.E. Weiss, M.F. Boehm, D.J. Mangelsdorf, and D.R. Corey, *Engineering orthogonal ligand-receptor pairs from "near drugs"*. Journal of the American Chemical Society, 2001. **123**(46): p. 11367-11371.
8. Laughon, A. and R.F. Gesteland, *Primary structure of the Saccharomyces cerevisiae GAL4 gene*. Mol Cell Biol, 1984. **4**(2): p. 260-7.
9. Traven, A., B. Jelacic, and M. Sopta, *Yeast Gal4: a transcriptional paradigm revisited*. Embo Reports, 2006. **7**(5): p. 496-499.
10. Bhat, P.J. and T.V.S. Murthy, *Transcriptional control of the GAL/MEL regulon of yeast Saccharomyces cerevisiae: mechanism of galactose-mediated signal transduction*. Molecular Microbiology, 2001. **40**(5): p. 1059-1066.
11. Johnston, M., *A model fungal gene regulatory mechanism: the GAL genes of Saccharomyces cerevisiae*. Microbiol Rev, 1987. **51**(4): p. 458-76.
12. Schwimmer, L.J., P. Rohatgi, B. Azizi, K.L. Seley, and D.F. Doyle, *Creation and discovery of ligand-receptor pairs for transcriptional control with small molecules*. Proceedings of the National Academy of Sciences of the United States of America, 2004. **101**(41): p. 14707-14712.
13. Lohr, D., P. Venkov, and J. Zlatanova, *Transcriptional regulation in the yeast gal gene family - A complex genetic network*. Faseb Journal, 1995. **9**(9): p. 777-787.

14. Kieft, J.S., *Viral IRES RNA structures and ribosome interactions*. Trends in Biochemical Sciences, 2008. **33**(6): p. 274-283.
15. Pfingsten, J.S. and J.S. Kieft, *RNA structure-based ribosome recruitment: Lessons from the Dicistroviridae intergenic region IRESes*. Rna-a Publication of the Rna Society, 2008. **14**(7): p. 1255-1263.
16. Lattime, E.C., *Retroviral Vector Design for Cancer Gene Therapy*, in *Gene Therapy of Cancer*. 2002, Academic Press: San Diego. p. 3-23.
17. Li, S. and L. Huang, *Nonviral gene therapy: promises and challenges*. Gene Ther, 2000. **7**(1): p. 31-4.
18. Clontech. *Retroviral Gene Transfer and Expression User Manual*. 2006; Available from: <http://www.clontech.com/images/pt/PT3132-1.pdf>.
19. Gerson, E.C.L.a.S.L., *Retroviral Vector Design for Cancer Gene Therapy*, in *Gene Therapy of Cancer*. 2002, Academic Press: San Diego. p. 3-23.
20. Davis, H.E., M. Rosinski, J.R. Morgan, and M.L. Yarmush, *Charged polymers modulate retrovirus transduction via membrane charge neutralization and virus aggregation*. Biophys J, 2004. **86**(2): p. 1234-42.
21. Le Doux, J.M., N. Landazuri, M.L. Yarmush, and J.R. Morgan, *Complexation of retrovirus with cationic and anionic polymers increases the efficiency of gene transfer*. Hum Gene Ther, 2001. **12**(13): p. 1611-21.
22. Landazuri, N. and J.M. Le Doux, *Complexation of retroviruses with charged polymers enhances gene transfer by increasing the rate that viruses are delivered to cells*. J Gene Med, 2004. **6**(12): p. 1304-19.
23. Davis, H.E., M. Rosinski, J.R. Morgan, and M.L. Yarmush, *Charged polymers modulate retrovirus transduction via membrane charge neutralization and virus aggregation*. Biophysical Journal, 2004. **86**(2): p. 1234-1242.
24. Abe, A., A. Miyahara, and T. Friedmann, *Polybrene increases the efficiency of gene transfer by lipofection*. Gene Ther, 1998. **5**(5): p. 708-11.



25. McMillin, D.W., N. Landazuri, B. Gangadharan, B. Hewes, D.R. Archer, H.T. Spencer, and J.M. Le Doux, *Highly efficient transduction of repopulating bone marrow cells using rapidly concentrated polymer-complexed retrovirus*. Biochem Biophys Res Commun, 2005. **330**(3): p. 768-75.
26. Laerum, O.D. and T. Farsund, *Clinical application of flow cytometry: a review*. Cytometry, 1981. **2**(1): p. 1-13.
27. Traganos, F., *Flow cytometry: principles and applications. II*. Cancer Invest, 1984. **2**(3): p. 239-58.
28. Traganos, F., *Flow cytometry: principles and applications. I*. Cancer Invest, 1984. **2**(2): p. 149-63.
29. Jimenez, A. and J. Davies, *Expression of a transposable antibiotic resistance element in Saccharomyces*. Nature, 1980. **287**(5785): p. 869-71.
30. Colbere-Garapin, F., F. Horodniceanu, P. Kourilsky, and A.C. Garapin, *A new dominant hybrid selective marker for higher eukaryotic cells*. J Mol Biol, 1981. **150**(1): p. 1-14.
31. Bar-Nun, S., Y. Shneyour, and J.S. Beckmann, *G-418, an elongation inhibitor of 80 S ribosomes*. Biochim Biophys Acta, 1983. **741**(1): p. 123-7.
32. Xu, M.Z. and J. Stavnezer, *Regulation of transcription of immunoglobulin germ-line gamma 1 RNA: analysis of the promoter/enhancer*. EMBO J, 1992. **11**(1): p. 145-55.
33. Moritz, O.L., K.E. Biddle, and B.M. Tam, *Selection of transgenic Xenopus laevis using antibiotic resistance*. Transgenic Res, 2002. **11**(3): p. 315-9.
34. Schwimmer, L.J., *Engineering ligand-receptor pairs for small molecule control of transcription*. 2005, Georgia Institute of Technology: Atlanta.
35. Wang, Y., B.W. O'Malley, Jr., S.Y. Tsai, and B.W. O'Malley, *A regulatory system for use in gene transfer*. Proc Natl Acad Sci U S A, 1994. **91**(17): p. 8180-4.

36. Wang, Y., J. Xu, T. Pierson, B.W. O'Malley, and S.Y. Tsai, *Positive and negative regulation of gene expression in eukaryotic cells with an inducible transcriptional regulator*. *Gene Ther*, 1997. **4**(5): p. 432-41.

## CHAPTER 4

# CHARACTERIZATION OF THE QCIMFI VARIANT IN THE MOLECULAR SWITCH SYSTEM

### 4.1 Engineering the QCIMFI Variant

As mentioned in Chapter 3, the retinoid X receptor (RXR) variant that was thought to be GR130 (adopted from the previous Doyle lab member Priyanka Rohatgi) was actually the Q275C, I310M, and F313I (QCIMFI) variant. Previously, the QCIMFI variant was engineered through rational design and site directed mutagenesis to have reverse ligand specificity, binding and activating in response to LG335 and not RXR's natural ligand 9cRA [1].

The luciferase activation profile of this variant was determined using a reporter plasmid containing RXR response elements controlling expression of the *firefly* luciferase gene (pLuc\_CRBP2) [2]. As shown in Figure 4.1, the QCIMFI variant, in the mammalian expression vector pCMXRXRQCIMFI, and the pLuc\_CRBP2 plasmids were cotransfected into HEK293T cells at a 1:2 molar ratio, and then cells were treated with a range of LG335 and 9cRA concentrations. The activation profiles show the QCIMFI variant is activated in response to LG335 (pink line) at concentrations as low as 100 nM ( $EC_{50}$  value is 38 nM) with a  $14.5 \pm 1.6$ -fold induction. No activation was observed with 9cRA (purple line shown in Figure 4.1). Conversely, the wild type (wt) RXR is activated by 1  $\mu$ M 9cRA ( $EC_{50}$  value is 597 nM) with a  $13.4 \pm 4.2$ -fold induction (blue line) and is activated by LG335 at the same concentration ( $EC_{50}$  value is 338 nM) but only at a fold induction of  $6.0 \pm 2.3$  (green line). This data confirms that the QCIMFI

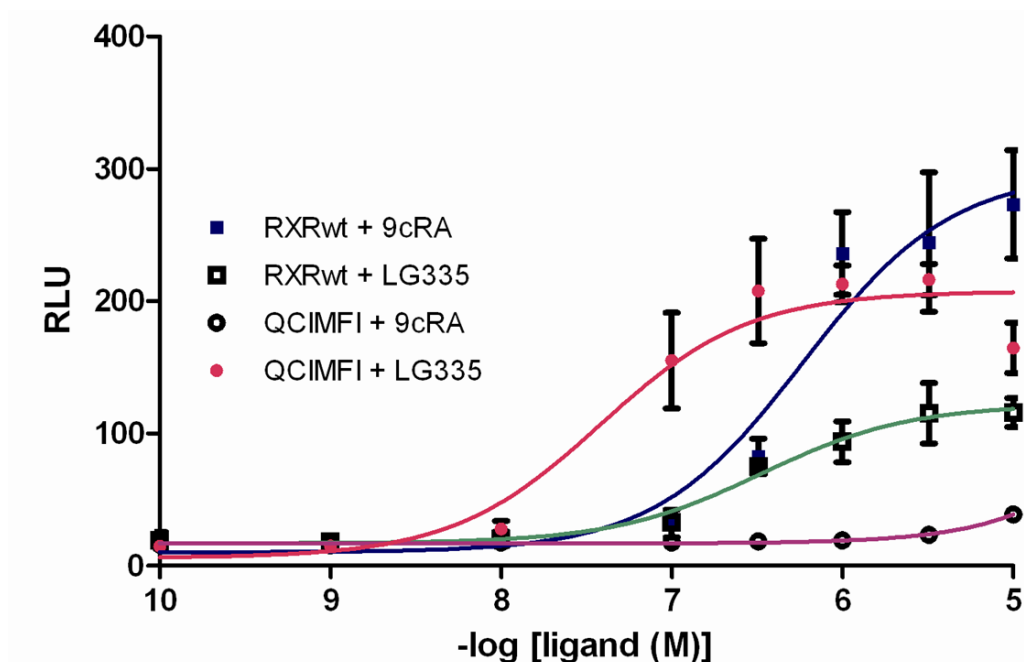


Figure 4.1: **Activation Profiles of RXRwt and QCIMFI:** Dose response curves for the activation of full length wild-type RXR (RXRwt) and RXR variant Q275C I310M F313I (QCIMFI) in response to 9cRA and LG335.

variant is orthogonal to the synthetic ligand LG335 and is not activated by the endogenous ligand 9cRA.

Figure 4.2 displays the fold induction at different concentrations of LG335 with QCIMFI and RXRwt. QCIMFI is activated at lower concentrations of LG335 and has much higher fold inductions, displaying a 10-fold induction at 100 nM LG335, when compared to RXRwt, which shows a 4-fold induction at 0.3  $\mu$ M LG335. The reverse ligand specificity, high fold induction, and relatively low EC<sub>50</sub> value were comparable to results observed by Doyle *et al* and led to the development of a molecular switch system using the QCIMFI variant and the ligand LG335. This chapter will address the characterization of the QCIMFI variant as a potential molecule switch. Characterization of this system involves first assessing the system through transient transfection in a two-component and a one-component system, as well as through stable expression of the one component system using retroviral particles.

#### **4.2 Characterization of GRQCIMFI in the Two-Component System**

As mentioned in Chapter 3, the DNA binding domain (DBD) of nuclear receptors (NR) must be switched to a Gal4 DBD in order to prevent binding of the molecular switch to endogenous NR response elements (RE). Gal4 is a yeast transcription factor that initiates transcription of genes controlled by Gal4 RE [3-5]. Removal of the NR's natural DBD provides specificity towards the molecular switch, allowing the expression of a therapeutic gene in response to the synthetic ligand and an artificial promoter.

To assess the activation of the QCIMFI variant in the two-component molecular switch system, the variant was previously cloned into the pMSCV plasmid and fused to the Gal4 DBD [6]. As stated in Chapter 3, the two-component system consists of two

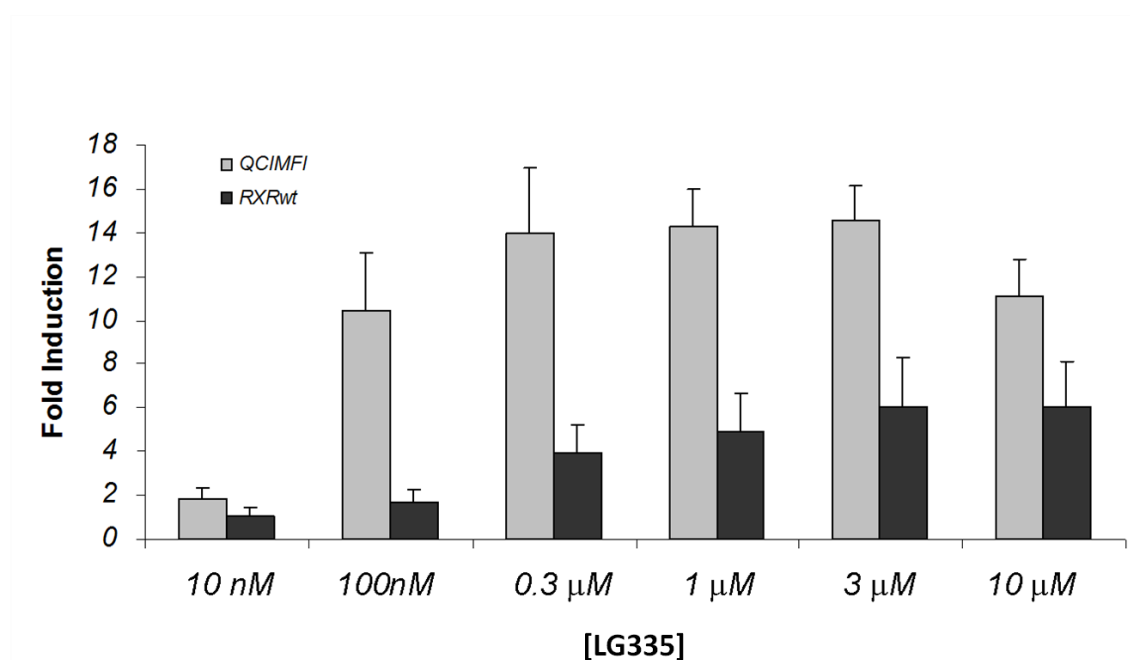


Figure 4.2: **Fold Inductions of RXRwt and QCIMFI:** Fold inductions of RXRwt (black bars) and QCIMFI (grey bars) in the presence of various LG335 concentrations.

plasmids. The first plasmid, pMSCVGRQCIMFI, constitutively expresses the GRQCIMFI variant (Gal4 DBD fused to the RXR variant QCIMFI LBD). The second plasmid, p17\*4TataLuc, contains four Gal4 RE located upstream from the *thymidine kinase* promoter controlling expression of *Renilla* luciferase. These two plasmids were cotransfected into HEK293T cells at a 1:2 molar ratio respectively, and tested with a range of both LG335 and 9cRA concentrations.

As shown in Figure 4.3A, the two-component system induces expression of luciferase at 100 nM LG335 ( $EC_{50}$  value of 11 nM) leading to a  $6 \pm 2$ -fold induction ratio of luciferase activity, shown in pink. Activation with 9cRA, shown in blue, only occurs at the highest concentration of ligand, 10  $\mu$ M 9cRA ( $EC_{50}$  value is greater than 10  $\mu$ M) with a  $5 \pm 1$ -fold induction. As a positive control, the Gal4 DBD was fused to the RXRwt LBD (GRXRwt) and assessed for luciferase activity (Figure 4.3B). GRXRwt displayed an  $EC_{50}$  value of 100 nM and a  $4 \pm 1$ -fold induction in the presence of 9cRA, shown in blue; a 320 nM  $EC_{50}$  value and a  $5 \pm 2$ -fold induction were observed with LG335, shown in pink. The GRQCIMFI variant has a lower  $EC_{50}$  values in response to LG335 when compared to the control GRXRwt, as well as comparable fold induction. As stated in Chapter 3, the activation of GRXRwt by LG335 is not of any concern since the fusion protein does not exist *in vivo*. As expected, these results show that the GRQCIMFI variant is specific to the synthetic ligand LG335 in the molecular switch system.

### 4.3 Interference with Metabolic Pathways

To determine if GRQCIMFI was only able to bind the Gal4 RE and turn on transcription with LG335, a series of luciferase activity assays were performed with endogenous ligands and RXR RE. These assays also determined if RXRwt was able to

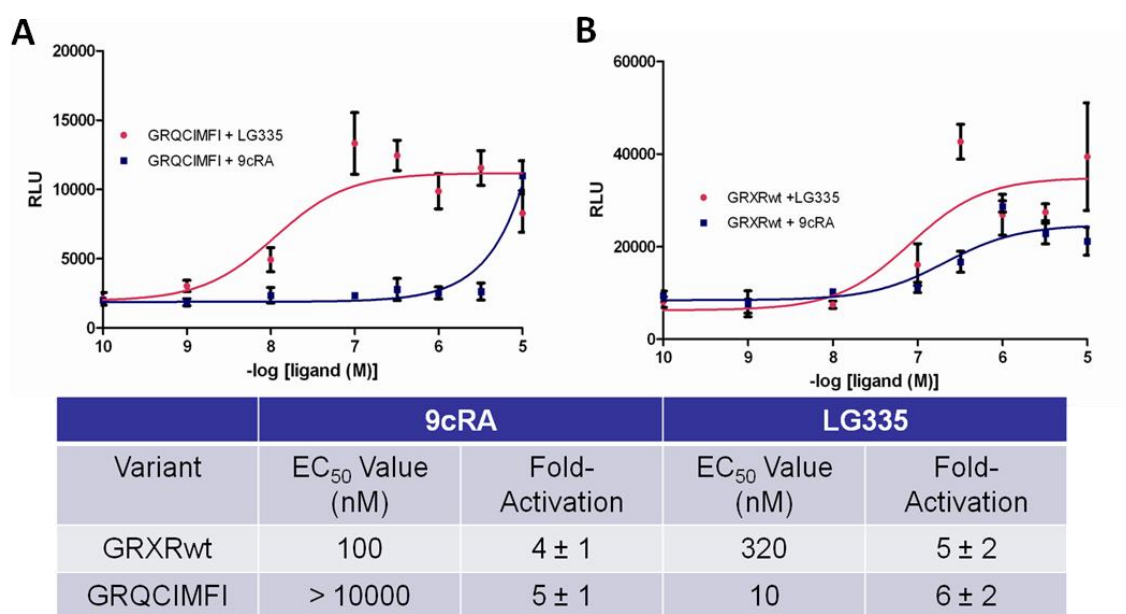


**Figure 4.3: Activation Profiles of GRQCIMFI and GRXRwt:** Luciferase assay of GRQCIMFI (Gal4 DBD-RXR variant QCIMFI LBD) and GRXRwt (Gal4 DBD-RXRwt) in the presence of LG335 (—●—) or 9cRA (—■—).



induce expression of the target gene controlled by Gal4 RE. A combination of plasmids containing GRQCIMFI or RXRwt (pMSCVGRQCIMFI or pCMXRXRwt) along with reporter plasmid (p17\*4TataLuc or pLuc\_CRBP2) were cotransfected into HEK293T cells at a 1:2 molar ratio, respectively, with no ligand and with 1  $\mu$ M ligand (LG335, 9cRA, and *all-trans* retinoic acid (atRA)). The plasmid pCMXRXRwt contains full length RXRwt under the control of a cytomegalovirus (CMV) promoter, and as stated previously, the pLuc\_CRBP2 plasmid contains RXR response elements controlling expression of *firefly* luciferase. The concentration 1  $\mu$ M of ligand was chosen, since previous results showed that 9cRA activates the molecular switch at a concentration of 10  $\mu$ M. Therefore, this experiment examines the activation of GRQCIMFI and RXRwt with ligands at a lower concentration.

Figure 4.4 shows the cotransfection of pMSCVGRQCIMFI and p17\*4TataLuc resulted in a  $4.5 \pm 1.1$ -fold induction in the presence of 1  $\mu$ M LG335. Only a  $1.2 \pm 0.3$ -fold induction is observed with 9cRA, and a  $2.1 \pm 0.5$ -fold induction with atRA. Activation does not occur when pMSCVGRQCIMFI is cotransfected with pLuc\_CRBP2, as expected, due to the fact that the Gal4 DBD should not and does not bind to the RXR RE. Conversely, when pCMXRXRwt and pLuc\_CRBP2 plasmids are cotransfected, the highest activation occurs in the presence of both 9cRA and atRA, with fold inductions of  $10.1 \pm 3.0$  and  $5.7 \pm 1.0$ , respectively. RXRwt is slightly activated in response to LG335 with a  $4.5 \pm 1.1$ -fold induction; however, this result was not surprising since previous results showed activation of RXR at 1  $\mu$ M LG335 (Figure 4.1). When pCMXRXRwt is cotransfected with p17\*4TataLuc, minimal activation occurs since the RXR DBD does not recognize the Gal4 RE. The lack of activation of the molecular switch with

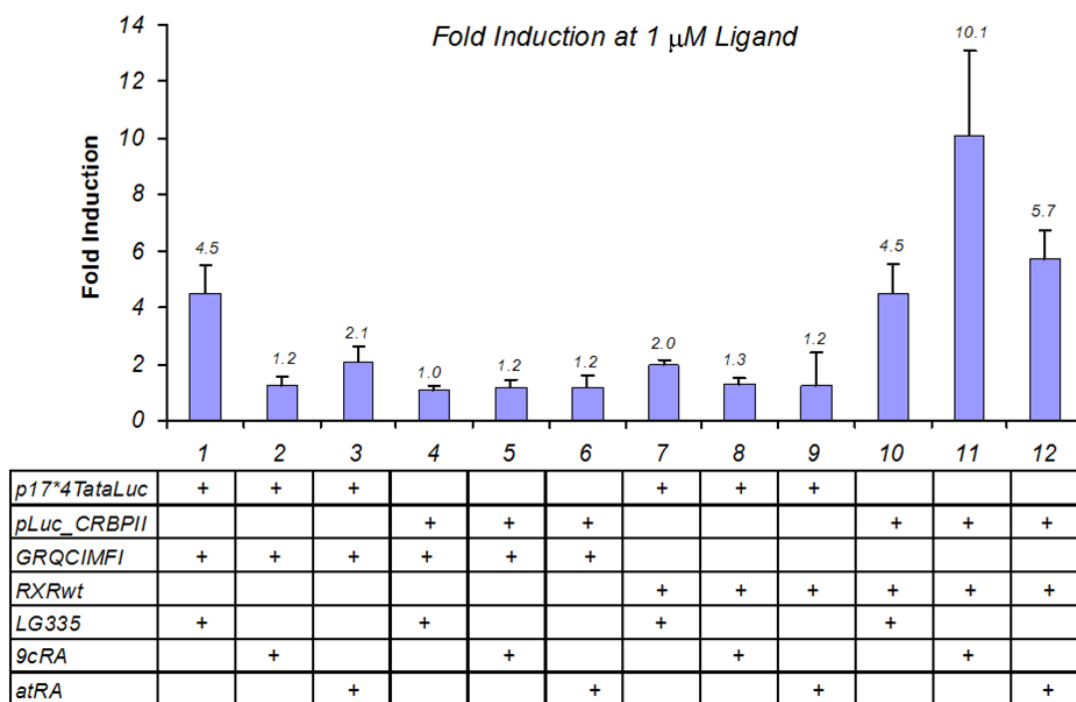


**Figure 4.4: Luciferase Assays in the Presence of 1  $\mu$ M Ligand:** Luciferase assays in the presence of 1  $\mu$ M different ligands: LG335, 9cRA, or atRA. Constitutively expressed GRQCIMFI or RXRwt were cotransfected with p17\*4TataLuc or pLuc\_CRBP11. These plasmids have either Gal4 or RXR response elements respectively as well as the target gene, luciferase.

endogenous RE and ligands shows that the engineered transcription factor has specificity to its target enhancer region and is orthogonal to the ligand LG335. [7, 8]. One drawback to this system is the slight activation observed with RXRwt in response to LG335; however, the fold induction is approximately half the fold induction of RXR with 9cRA.

The results above show a two-component molecular switch system was developed using the ligand LG335 and the fusion of the Gal4 DBD and the RXR variant QCIMFI LBD. Activation of a transgene with LG335 occurred at levels as low as 100 nM, and was only observed with the wild-type ligand at a concentration of 10  $\mu$ M. GRQCIMFI displays orthogonal behavior with LG335, activating expression of a target gene 6-fold, and binding specific DNA sequences called Gal4 RE, exhibiting tight control over the target gene. Activation occurs only when pMSCVGRQCIMFI and p17\*4TataLuc, the plasmid containing Gal4 RE, were cotransfected and 100 nM LG335 was added to the cells. No activation above basal activity occurred when pMSCVGRQCIMFI was transfected under different conditions. The engineered switch with the Gal4 DBD responds appropriately to the Gal4 RE and not with endogenous RE.

#### **4.4 Ligand Time Course**

As previously described in Chapter 2, the activation of a molecular switch system should correlate with the ligand dosage. The addition of ligand should rapidly induce target gene expression, and the removal of ligand should show a rapid decrease of target gene expression. Many molecular switch systems have evaluated how ligand dosage correlates to gene expression in various systems. For instance, the GeneSwitch regulation system has shown protein expression 24 hours after administration of mifepristone (RU485) in a mouse model, and expression of this protein returned to basal expression

levels 72 hours after the ligand is removed [9]. The doxycycline ligand, a tetracycline analog used in the tetracycline inducible system, is a well documented ligand and has been used for over 30 years [10]. This ligand has been shown to induce gene expression in animal models five years after administration of the viral vector [11-13].

To understand the rate at which LG335 induces expression of the target gene, as well as the rate that the target gene expression decreases, a ligand time course assay was performed. As shown in Figure 4.5, several subsets of data were collected and averaged, where HEK293T cells were cotransfected with pMSCVGRQCIMFI and p17\*4TataLuc at a 1:2 molar ratio. In the first data set, shown in red, the basal activity of this system was tested by transfecting cells with plasmids and assaying for luciferase activity. No ligand was added in this data set. The second and third data set, shown in blue and green respectively, were also transfected with the pMSCVGRQCIMFI and p17\*4TataLuc plasmids, but 100 nM LG335 was added eight hours after the transfection. Both data sets were also assayed for luciferase activity; however, data set three was washed with growth media 32 hours after the transfection to remove LG335, a time point chosen after full activation is reached.

As shown in Figure 4.6, LG335 induces luciferase activity 24 hrs after ligand is added, and activation increases up to 56 hours after the transfection. This is observed if the ligand is not removed from the media, as shown in data set two (blue bars). A slight decrease in luciferase activity is observed after 56 hours, which could be due in part to the viability of the cells. In the third data set (green bars), when ligand is removed 32 hours after transfection, an immediate decrease in luciferase activity is observed at the 40

hour time point. The decrease of activation is observed until the 88 hour time point; however, basal activity is not observed.

These results show LG335 can induce transgene activation within 24 hours of adding ligand, and the ligand activation increases for about 56 hours after induction. The prolonged activation by the ligand, as well as the slow decrease to basal levels is not surprising, due to the fact that LG335 is a very stable compound. LG335 has a high melting temperature of 250-252°C and the parent compound, Targretin, is known to have a seven hour half-life when introduced into the body [14]. To further understand how this ligand behaves in this molecular switch system, the ligand time course needs to be assessed when stable expression of this system is achieved. Stable expression allows a more accurate assessment of the rate of gene activation and decrease since transient transfection factors are eliminated, such as the retention of the plasmid. Also to further understand the pharmacology of this ligand, *in vivo* analysis of LG335 would be extremely useful for toxicity studies, as well as determining the rate of metabolism of LG335.

#### **4.5 Characterization of GRQCIMFI in the One-Component System**

As established in Chapter 3, the one-component system has higher transfection efficiency than the two-component system. Therefore, GRQCIMFI was cloned into the one-component system plasmid by removing GR130 from the retroviral vector (pMSCVGR130GFP), replacing the gene with GRQCIMFI (pMSCVGRQCIMFIGFP). As stated previously, this plasmid constitutively expresses GRQCIMFI, and upon the addition of LG335, the molecular switch can bind to the Gal4 RE on the same plasmid and induce expression of GFP. The pMSCVGRQCIMFIGFP plasmid was transiently

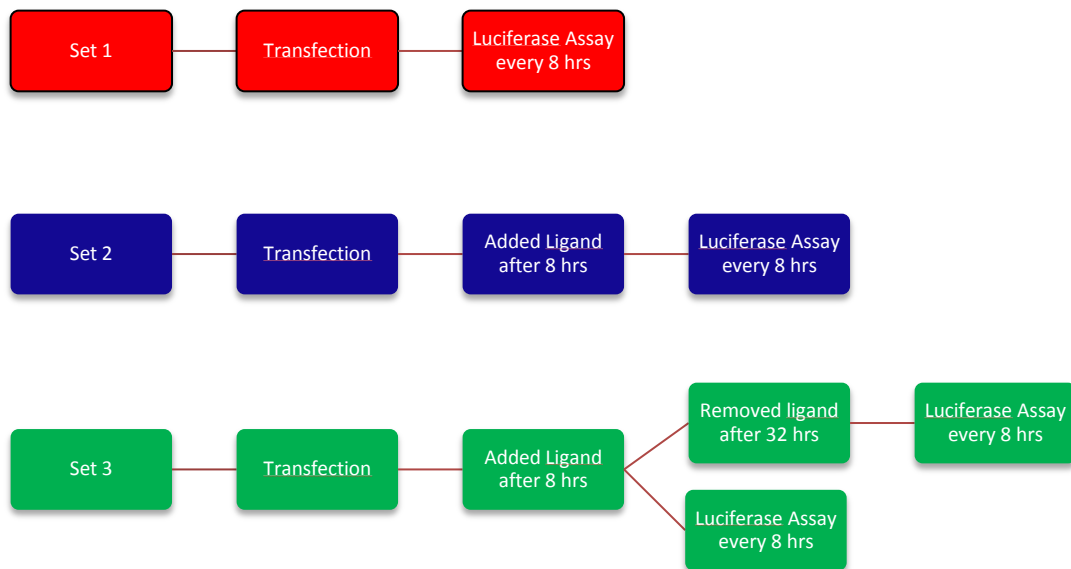


Figure 4.5: **Ligand Time Course Flow Chart:** Experimental design of three sets of data collected to determine basal expression levels (set 1), when gene expressed is induced (set 2), and when gene expressed is decreased (set 3).

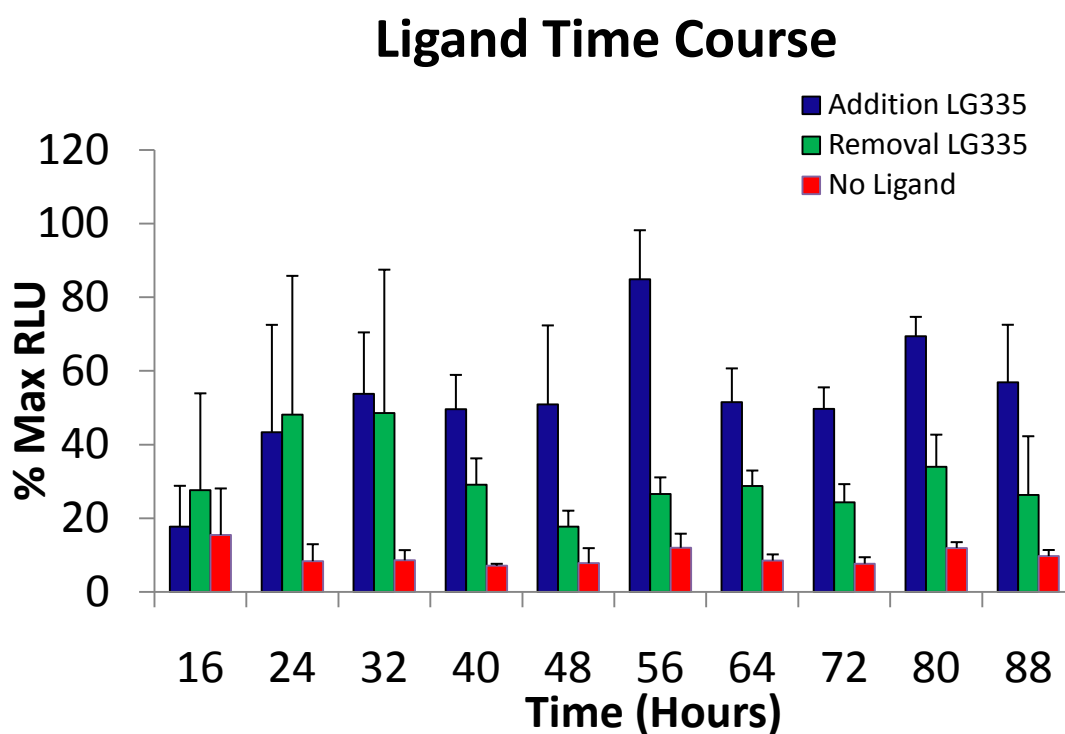


Figure 4.6: **Ligand Time Course Data:** HEK293T cells were transfected with pMSCVGRQCIMFI and p17\*4TataLuc and 8 hours after transfection 100 nM of LG335 was added to cells. Ligand was removed 32 hours after transfection. Cells were harvested every 8 hours for the ligand time course. The addition of LG335 is shown in (■), the removal of ligand is shown in (■), and the no ligand data set is shown in (■).

transfected into HEK293T cells and treated with no ligand, 10 nM and 10  $\mu$ M LG335 to evaluate this variant in the one-component system (Figure 4.7). Images of transfected cells were taken 48 hours after the transfection, and the percentage of fluorescent cells was obtained.

The results in Figure 4.7 show that without ligand, basal GFP expression is observed where approximately 7% of the cells are dimly fluorescent. Upon the addition of 10 nM LG335 the intensity of the fluorescence increases and approximately 10% exhibit GFP expression. In the presence of 10  $\mu$ M LG335 the expression of GFP is detected in about 30% of HEK293T cells, verifying the increase in percent fluorescent cells as the ligand concentration increases (Figure 4.7). The GFP expression in the one-component system was compared to a control plasmid pMSCVIRESGFP, which constitutively expresses eGFP. This plasmid contains an internal ribosome entry site (IRES) that allows the translation of RNA to occur more effectively, and was used to evaluate transfection efficiency. As shown in Figure 4.8, the IRESGFP plasmid shows GFP expression in approximately 60% of the cells. As expected, the one-component system with the GRQCIMFI variant shows tight regulation of GFP expression. Therefore, both two-component and one-component systems showed that the molecular switch system is able to regulate gene expression.



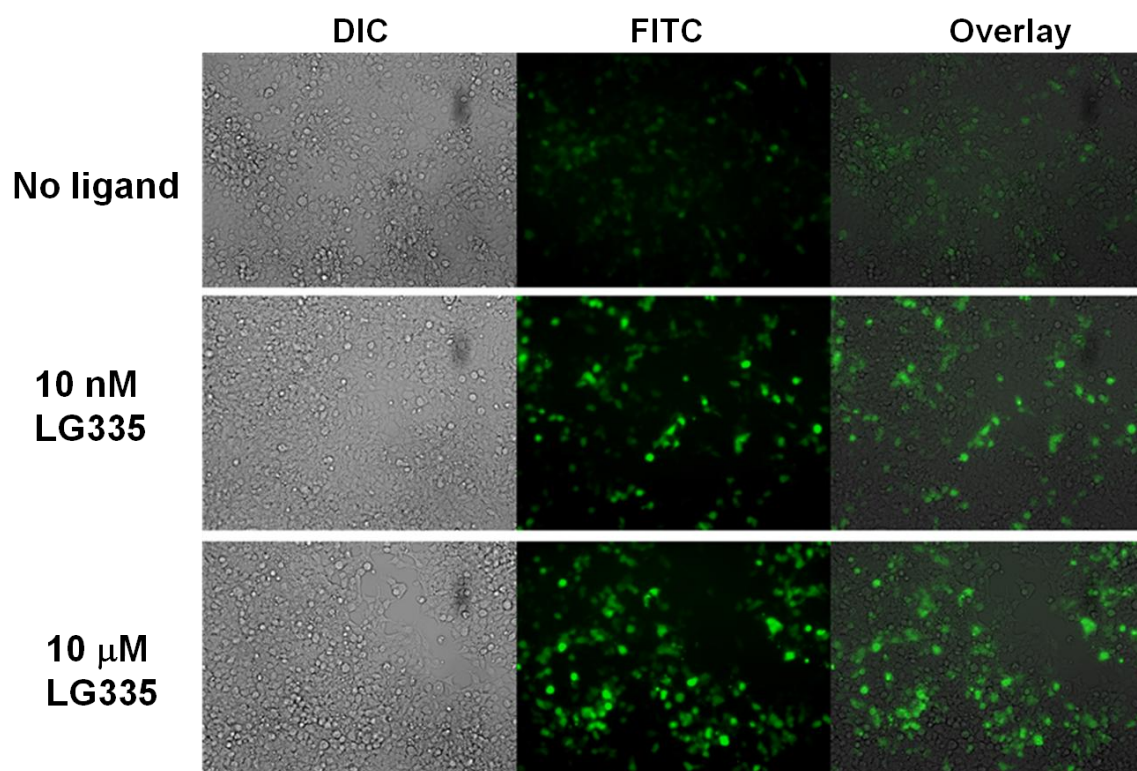


Figure 4.7: **Transient Transfection of GRQCIMFIGFP**: DIC, fluorescent, and overlay images of HEK293T cells transfected with GRQCIMFIGFP in the presence of no ligand, 10 nM, and 10  $\mu$ M LG335.

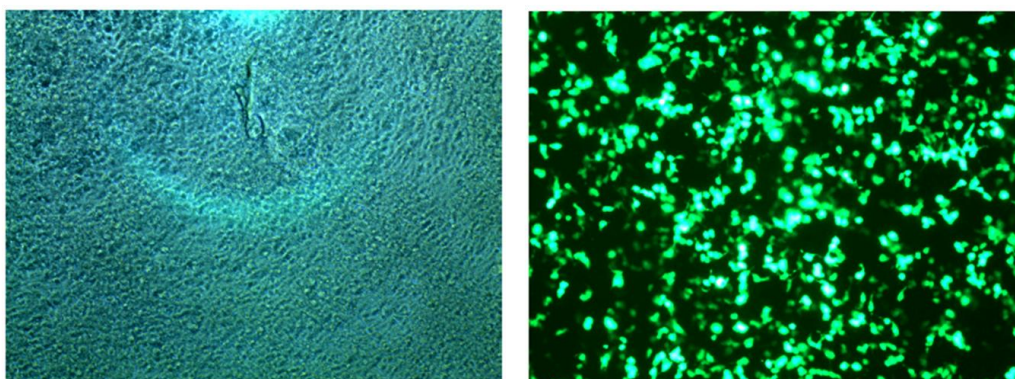


Figure 4.8: **Transient transfection of pMSCVIRESGFP:** The DIC and fluorescent image of HEK293T cells transfected with IRESGFP.

## **4.6 Characterization of Stable Expression of GRQCIMFI in the Molecular Switch System**

As mentioned in Chapter 3, stable expression of the molecular switch system was assessed by transducing cells with retroviral particles. Retroviral particles can be made by transiently transfecting the pMSCVGRQCIMFIGFP vector into the EcoPack 2-293 packaging cell line and infectious retroviral particles were collected and transduced into NIH3T3 cells. These cells were then analyzed for integration of the virus into the cellular genome.

To determine integration of the molecular switch sequence, a genomic extraction of NIH3T3 cells was collected using the Qiagen DNeasey Blood & Tissue kit and analyzed by nesting PCR. Nesting PCR is a technique where two sets of primers are used to amplify DNA in two consecutive polymerase chain reactions (PCR). The second set of primers is needed to eliminate amplification of non-specific DNA strands. As shown in Figure 4.9, PCR experiments were performed with primers that annealed to separate regions of the four kilobase one-component system. Primer set 1 (1f and 1r) annealed to the GRQCIMFI region; whereas primer set 2 (2f and 2r) amplify the region containing Gal4 RE and eGFP. Both primer sets 1 and 2 were used in PCRs with genomic DNA, and secondary PCRs were done with primer sets 1' (1f' and 1r') and 2' (2f' and 2r') to confirm the sequence of interest was being amplified. As a positive control, these experiments were performed with plasmid DNA, and the sizes of the amplified cassettes were compared with the sizes of the genomic DNA. Figure 4.9 shows the PCR fragments from the genomic DNA are the same size as predicted, suggesting that cellular integration occurs without transgene rearrangement. Genomic PCR fragments were also confirmed

by sequencing. These results indicated that administrating this system through a retrovirus successfully integrated the molecular switch sequence into target cells.

To assess the regulation of the stable molecular switch system, NIH3T3 cells transduced with GRQCIMFIGFP were grown in media with no LG335 or 10  $\mu$ M LG335 for 24 hours. These results show that without the presence of ligand, GFP fluorescence is not observed (Figure 4.10), whereas 34% of the cells were fluorescent upon the addition of 10  $\mu$ M LG335, further confirming this system as a useful tool for controlling gene expression. The positive control pMSCVIRESGFP shows GFP expression in 70% of cells with a higher fluorescent intensity in comparison to the molecular switch system (Figure 4.11). The low fluorescence intensity led to the evaluation of the transduction efficiency of the molecular switch system.

In summary, the molecular switch was developed to address the criteria stated in Chapter 2, which include the turning on and off of transgene expression upon the addition of LG335. Even though the molecular switch system can proficiently regulate gene expression, improvements are needed to make this system more versatile for gene therapy applications. The ligand, LG335, is specific to the engineered protein GRQCIMFI; however, this exogenous ligand can slightly activate RXRwt, which may cause interference in metabolic pathways. Therefore, this switch could be further engineered to be activated at a lower dosage in order to reduce activation by the wild type receptor. The molecular switch system is able to induce expression of the target gene in transient transfections, as well as retroviral transduction; however, the stable expression of GFP is only observed at a low fluorescent intensity. The next chapter will attempt to address improvements in this molecular switch system.

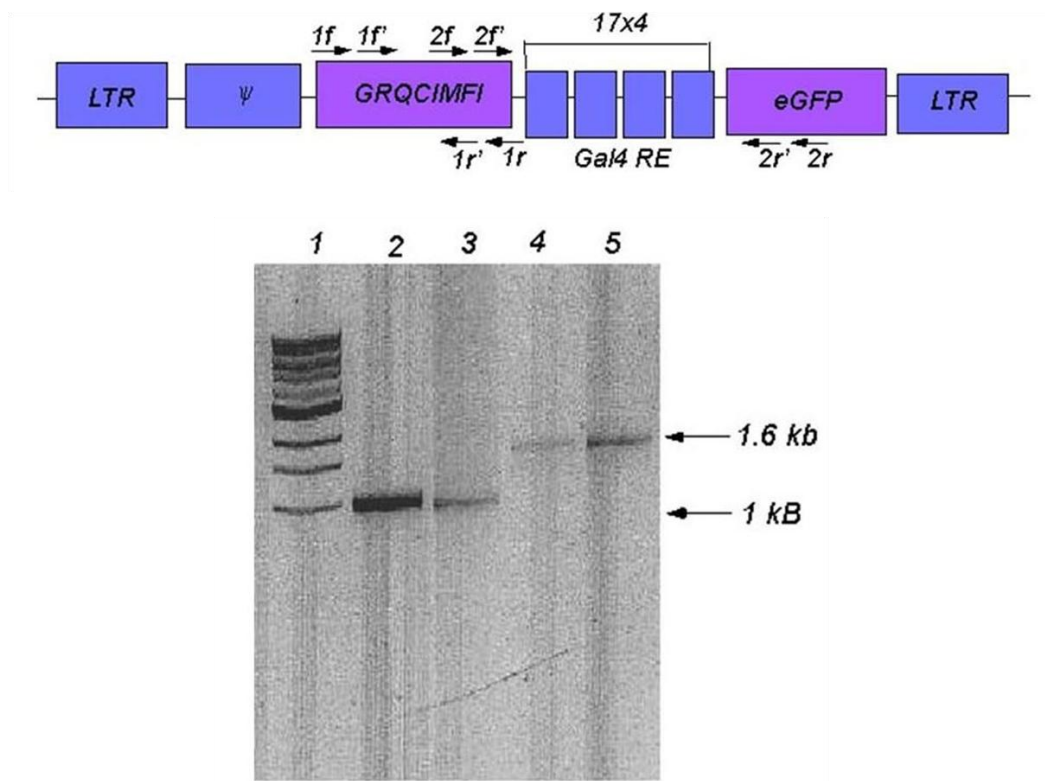


Figure 4.9: **PCR of Genomic DNA of Cells Transduced with GRQCIMFIGFP:** PCR of genomic DNA purified from NIH3T3 cells transduced with virus. (A) is a schematic diagram of where the primers bind in the molecular switch system, and (B) the electrophoresis gel of the PCR fragments.

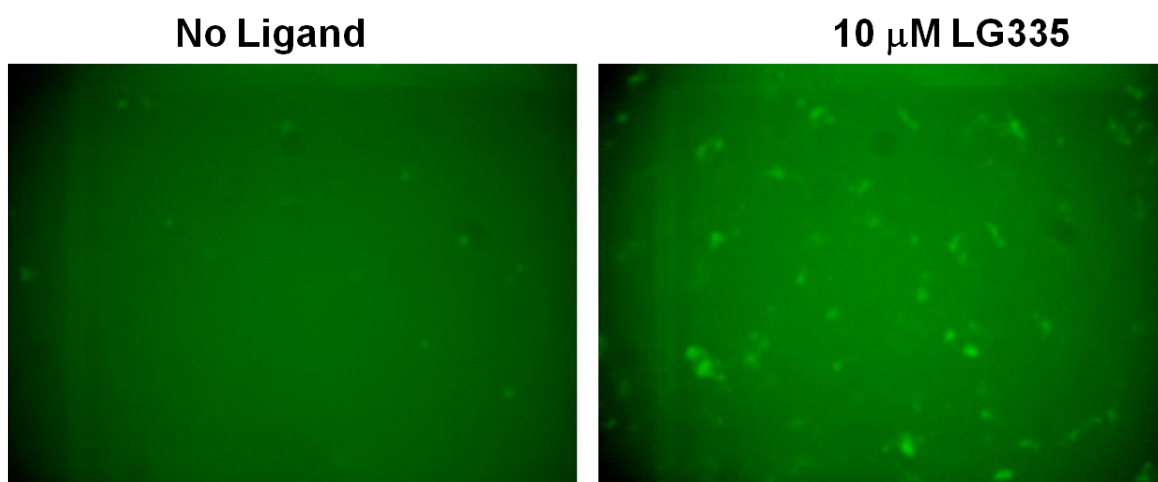


Figure 4.10: **Fluorescent Images of Cells Transduced with GRQCIMFIGFP:**  
Fluorescent images of NIH3T3 cells transduced with GRQCIMFIGFP in response to no ligand or 10  $\mu$ M LG335.

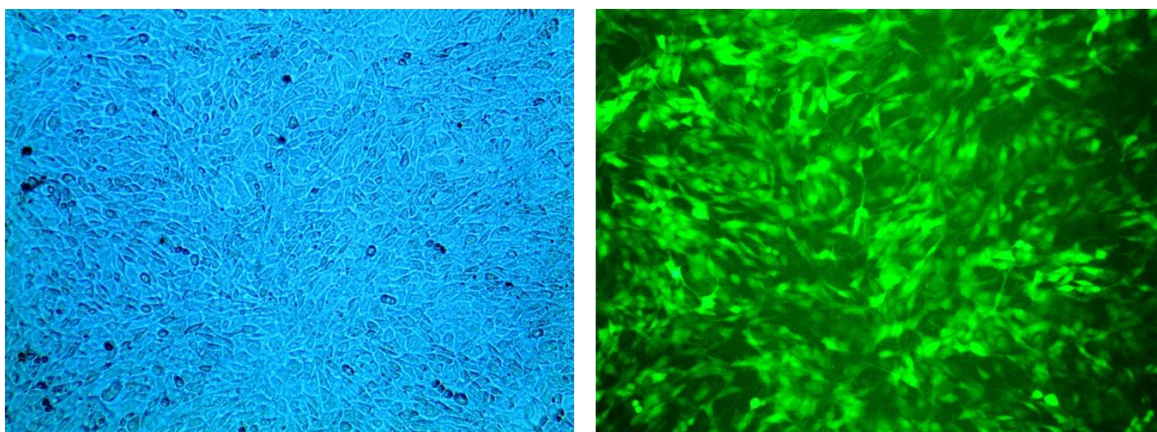


Figure 4.11: **Fluorescent Images of Cells Transduced with IRESGFP:** The DIC and fluorescent image of NIH3T3 cells transduced with pMSCVIRESGFP.

## 4.7 Materials and Methods

### Mammalian Luciferase Assay

Transfections of the two-component systems with the GRQCIMFI variant were performed as described in Chapter 3.

### Ligand time course

The transfection for this assay was performed as described in Chapter 3. HEK293T cells were transfected with the pMSCVGRQCIMFI and p17\*4TataLuc plasmids at a 1:2 ratio. Eight hours after the transfection, the batch of cells from data set 1 were placed in growth media lacking ligand, and the batch of cells from data set 2 and 3 were placed in growth media with 100 nM LG335. As described in Chapter 3, growth media is DMEM with 10% FBS and 1% P/S. Cells were harvested every 8 hours for luciferase and  $\beta$ -galactosidase activity, also described in Chapter 3. Media with 100 nM LG335 was removed from the batch of cells from data set 3, 32 hours after transfection and placed in growth media with no ligand. Cells were continuously harvested for 88 hours after transfection. Two experimental data sets were taken and each set was divided by the maximum RLUs and multiplied by 100 to receive the percent maximal RLUs. Then the average and standard deviation of both sets were calculated.

### Mammalian GFP Analysis

HEK293T cells were transfected with the pMSCVGRQCIMFIGFP plasmid as described in Chapter 3. Eight hours after the transfection, wells were aspirated and then growth media containing no ligand, 100 nM LG335, and 10  $\mu$ M LG335 were added to



the wells. Fluorescent images and data processing was evaluated as described in Chapter 3.

#### Retroviral Transduction

Retroviral infectious particles were made with the pMSCVGRQCIMFIGFP vector as described in Chapter 3. NIH3T3 cells were transduced with 100  $\mu$ L of viral incubated with CSC and PB, and then 10  $\mu$ M LG335 was added to a subset of transduced cells. To obtain the percentage of fluorescent cells, the number of fluorescent cells counted was divided by the total number of cells counted multiplied by 100. Images of transduced cells were taken using a 40X objective on a Zeiss LSM microscope, and processed using Adobe Photoshop.

#### Genomic PCR

Genomic DNA was extracted from NIH3T3 cells transduced with GRQCIMFIGFP retrovirus using the DNeasy kits (Qiagen, USA). To clone the 1029 bp DNA sequence GR130 from genomic DNA, a primary PCR was performed using the following primers: 1f, CCT TGA CAT GAT TTT GAA AAT GG; 1r, GCC GCC TAA GTC ATT TGG TG. Then a secondary PCR was performed with the following primers: 1f', ATT CTT TAC AGG ATA TAA AAG CAT TGT TAA CAG GAT; 1r', CGC CTC CAG CAT CTC CAT AAG G. To clone out the 1650 bp DNA sequence, containing the Gal4 RE and eGFP, a primary PCR was done with the following primers: 2f, GAG GTG GAG TCG ACC AGC AG; 2r, TTA CTT GTA CAG CTC GTC CAT GC. A secondary PCR was done with the following primers: 2f', CGC CAA CGA GGA CAT GCC G; 2r', CGA GAG TGA TCC CGG CGG C. The same sets of primers were used on the

pMSCVGR130GFP plasmid for size comparisons. *Pfu* polymerase (Stratagene, USA) was used, and the PCR fragments were analyzed on a 1.2% agarose gel.

#### 4.8 Literature Cited

1. Doyle, D.F., et al., *Engineering orthogonal ligand-receptor pairs from "near drugs"*. Journal of the American Chemical Society, 2001. **123**(46): p. 11367-11371.
2. Mangelsdorf, D.J., et al., *A direct repeat in the cellular retinol-binding protein type-II gene confers differential regulation by RXR and RAR*. Cell, 1991. **66**(3): p. 555-561.
3. Laughon, A. and R.F. Gesteland, *Primary structure of the Saccharomyces cerevisiae GAL4 gene*. Mol Cell Biol, 1984. **4**(2): p. 260-7.
4. Johnston, M., *A model fungal gene regulatory mechanism: the GAL genes of Saccharomyces cerevisiae*. Microbiol Rev, 1987. **51**(4): p. 458-76.
5. Traven, A., B. Jelacic, and M. Sopta, *Yeast Gal4: a transcriptional paradigm revisited*. Embo Reports, 2006. **7**(5): p. 496-499.
6. Rohatgi, P., *Engineering protein molecular switches to regulate gene expression with small molecules*. 2006, Atlanta, Ga. :: Georgia Institute of Technology.
7. Mulligan, R.C., *The basic science of gene therapy*. Science, 1993. **260**(5110): p. 926-932.
8. Goverdhana, S., et al., *Regulatable gene expression systems for gene therapy applications: Progress and future challenges*. Molecular Therapy, 2005. **12**(2): p. 189-211.
9. Nordstrom, J.L. *The antiprogestin-dependent GeneSwitch (R) system for regulated gene therapy*. 2003: Elsevier Science Inc.

10. Agwuh, K.N. and A. MacGowan, *Pharmacokinetics and pharmacodynamics of the tetracyclines including glycyclines*. J Antimicrob Chemother, 2006. **58**(2): p. 256-65.
11. Stieger, K., et al., *In vivo gene regulation using tetracycline-regulatable systems*. Adv Drug Deliv Rev, 2009. **61**(7-8): p. 527-41.
12. Stieger, K., et al., *Long-term doxycycline-regulated transgene expression in the retina of nonhuman primates following subretinal injection of recombinant AAV vectors*. Mol Ther, 2006. **13**(5): p. 967-75.
13. Stieger, K., et al., *Oral administration of doxycycline allows tight control of transgene expression: a key step towards gene therapy of retinal diseases*. Gene Ther, 2007. **14**(23): p. 1668-73.
14. *Targretin (Bexarotene) - Description and Clinical Pharmacology* 2006 [cited 2010 November 11]; Available from: [http://www.druglib.com/druginfo/targretin/description\\_pharmacology/](http://www.druglib.com/druginfo/targretin/description_pharmacology/).

# **CHAPTER 5**

## **IMPROVING THE MOLECULAR SWITCH SYSTEM**

### **5.1 Improving the Fold Induction Using VP16**

The molecular switch system described in Chapter 4 is shown to be able to regulate gene expression. However, the fluorescence intensity of GFP (green fluorescent protein) was significantly lower in cells infected with the GRQCIMFIGFP retrovirus in comparison to cells transiently transfected with the one-component system. Therefore, the next goal was to increase the fold induction of the molecular switch system and increase the sensitivity towards the ligand LG335. This chapter will discuss adding an activation domain to the molecular switch system, as well as performing mutagenesis in an attempt to discover a new variant with a higher fold induction and/or increased sensitivity towards LG335.

#### **5.1.1 Addition of the Activation Domain**

The VP16 protein consists of 490-amino acids, the key protein in the herpes simplex virus, and contains a core region and a C-terminal transcriptional activation domain [1, 2]. The activation domain of VP16 is considered to be a very potent transactivator, since the amino acid sequence is known to have strong interactions with several general transcription factors, such as the TATA-binding protein (TBP), TFIIB, and the Spt-Ada-Gcn5 (SAGA) histone acetyltransferase complex [1]. Hence, transcription occurs more efficiently in the presence of this domain.

Several molecular switch systems have used an activation domain as a means to improving the fold induction of their molecular switch system. In the initial development of the GeneSwitch® system, the Gal4 DBD was fused to a mutant progesterone receptor (PR) ligand binding domain (LBD), and when tested in mammalian cell culture, no significant activation was observed with the RU486 ligand. Therefore, the VP16 activation domain was fused to the C-terminus region of this chimeric protein, enhancing the activation approximately 50-fold [3]. The VP16 activation domain was then replaced with the human p65 activation domain, a transcription factor that is a member of the NFκB family, to minimize basal activation levels and reduce possible immunogenic reactions [4-6]. The Ecodyson (EcR) responsive system (also known as Rheoswitch®) has also gone through several rounds of improvement. The VP16 activation domain was fused to the chimeric protein composed of the Gal4 DBD fused to the ecodyson receptor, as well as to the LBD of RXR [7-9]. The most current Rheoswitch® system, which consists of two fusion proteins, a hybrid DBD between EcR and the glucocorticoid receptor fused to an EcR LBD, and a RXR LBD fused to the VP16 activation domain, has approximately a 10,000-fold induction [9].

In an effort to increase the fold induction of the molecular switch described in Chapter 4, the VP16 activation domain was fused to GRQCIMFI. The fusion protein was created by amplifying VP16 from pVP16, a mammalian plasmid, and cloning the gene into the pMSCVGRQCIMFI plasmid, which contains the molecular switch GRQCIMFI (Figure 5.1). GRQCIMFI consists of the Gal4 DNA binding domain (DBD) fused to a RXR variant LBD with the following mutations: Q275C, I310M, and F313I. The first step in the cloning process was to insert the restriction enzyme sites *MfeI* and

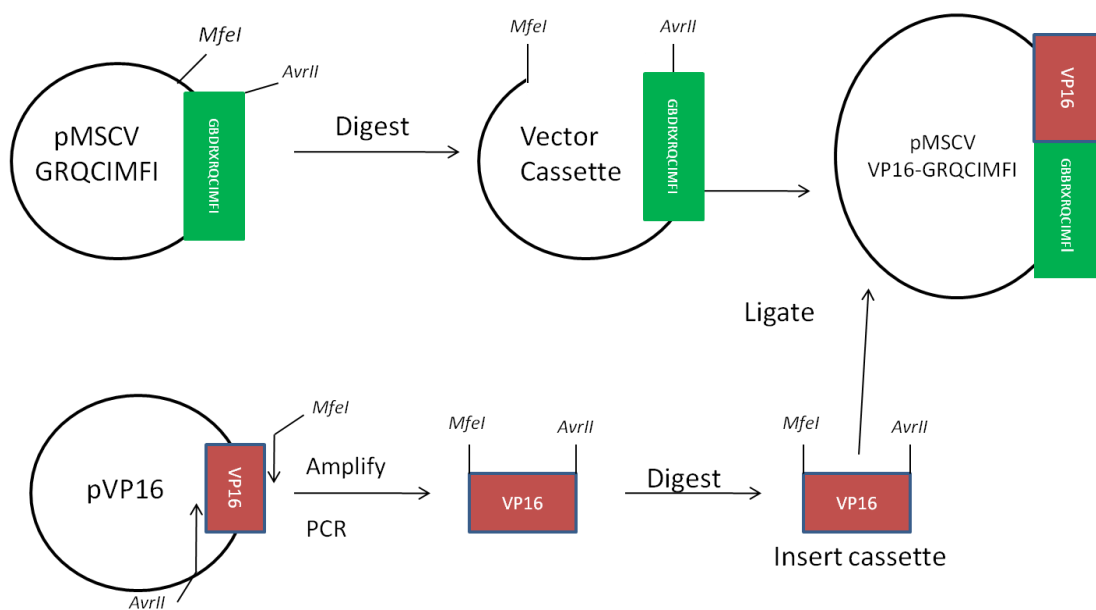


**Figure 5.1 Cloning VP16 into pMSCVGRQCIMFI:** *MfeI* and *AvrII* restriction enzyme sites were inserted into the pMSCVGRQCIMFI plasmid. VP16 was amplified from the pVP16 plasmid with primers containing *MfeI* and *AvrII* restriction sites. The vector cassette and insert cassette wither digested and ligated together to create the pMSCV VP16-GRQCIMFI plasmid.

*AvrII* into the pMSCVGRQCIMFI vector at the N-terminus region of GRQCIMFI via site-directed mutagenesis. Then the VP16 domain was cloned out the pVP16 plasmid (provided by the Ortlund lab, Emory University) using primers containing *MfeI* and *AvrII* restriction enzyme sites. The VP16 insert cassette and the pMSCVGRQCIMFI vector cassette were then digested with the *MfeI* and *AvrII* restriction enzymes, and ligated together to create the new plasmid, pMSCV VP16-GRQCIMFI, confirmed by sequencing (Figure 5.1).

The pMSCV VP16-GRQCIMFI plasmid, which constitutively expresses VP16-GRQCIMFI, was cotransfected with the p17\*4TataLuc plasmid into HEK293T cells. The plasmid, p17\*4TataLuc, contains Gal4 response elements (RE) controlling expression of *Renilla* luciferase. As shown in Figure 5.2A, the addition of VP16 to GRQCIMFI displayed a  $1.8 \pm 0.2$ -fold induction in response to 9cRA and a  $0.8 \pm 0.2$ -fold induction with LG335. Since high relative light units (RLU) were observed, the addition of the VP16 activation domain created a constitutively active protein. This activation profile was compared to the GRQCIMFI profile, which lacked the activation domain, and showed a  $5 \pm 1$ -fold induction with 9cRA and a  $6 \pm 1$ -fold induction with LG335. This data confirms results observed previously by Lipkin *et al*, who also observed a constitutively active receptor upon the addition of the VP16 AD to the C-terminus domain of wild type RXR [10]. The addition of VP16 did not increase the fold activation of this system; hence, another route was pursued in order to improve the molecular switch system.

## **5.2 Discovery and Characterization of the Quadruple Mutant QCIMFILM**

The next approach used to improve the molecular switch was exploring mutations that might increase fold induction and lower sensitivity towards LG335. Previously

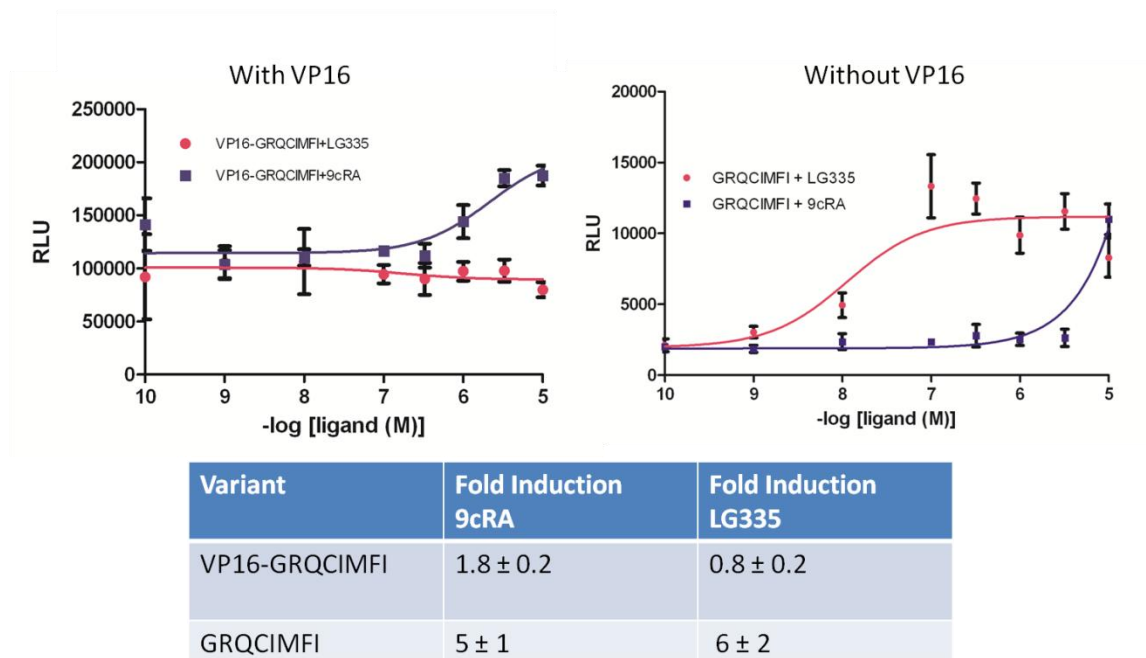


**Figure 5.2 Activation profiles of VP16-GRQCIMFI and GRQCIMFI:** Activation profile of HEK29T cells transfected with VP16-GRQCIMFI and GRQCIMFI in response to LG335 (●) or 9cRA (■) Table of fold inductions for each ligand.



engineered RXR libraries using rational design produced two RXR variants discussed in previous chapters, GR130 (I268A, I310A, F313A, and L436F) and QCIMFI (Q275C, I310M, and F313I) that displayed reverse specificity, activated by the synthetic ligand LG335 and not the natural ligand 9-*cis* retinoic acid (9cRA) [11, 12]. However, further rational design approaches did not produce RXR variants with increased sensitivity towards LG335 without also increasing sensitivity towards the natural ligand. Therefore, random mutagenesis was used to develop libraries of RXR variants that were subjected to chemical complementation, in an attempt to discover a new variant that is able to activate the receptor at lower concentrations of LG335 than the QCIMFI variant.

### 5.2.1 Chemical Complementation

Chemical complementation (CC) is a genetic selection system that links the binding and activation of a nuclear receptor by a small molecule to the survival of *Saccharomyces cerevisia*. CC was established in the PJ69-4A strain, based on a third generation yeast-two hybrid system [13]. This strain contains Gal4 response elements (RE) controlling expression of genetic selection genes, such as *ADE2* or *HIS3*. Gal4 is a ligand independent yeast transcription factor, containing a DNA binding domain (DBD) that binds the Gal4 RE and a activation domain, involved in recruiting the transcription machinery [14].

To develop CC, the genetic selection genes, specifically *ADE2*, which encodes for a key enzyme involved in the adenine biosynthetic pathway, was utilized. Expression of the *ADE2* gene allows the yeast to survive in media lacking adenine. To link a small molecule to the expression of the *ADE2* gene, a three-component system was created, consisting of a Gal4 DBD fused to the RXR LBD (GBD-RXR), the coactivator ACTR

(activator for thyroid hormone and retinoid receptor) fused to the Gal4 activation domain (ACTR-GAD), and a small molecule [11, 15]. When a ligand binds to GBD-RXR, a conformation change takes place, allowing the recruitment of ACTR-GAD, leading to the expression of the *ADE2* gene (Figure 5.3). Therefore, in the presence of a small molecule the yeast are able to survive in media lacking adenine (ligand-activated growth).

In order to use CC experimentally, yeast expression plasmids must be transformed into the PJ69-4A strain. As shown in Figure 5.4, the GBD-RXR fusion protein contains a tryptophan (W) marker (pGBDRXR), and the plasmid containing the ACTR-GAD fusion protein contains a leucine (L) marker (pGAD10BAACTR). Both plasmids were transformed in the yeast strain and plated on synthetic complete media (SC) lacking leucine and tryptophan (SC-LW). This media is called nonselective media, since the presence of a ligand is not needed for the yeast to survive.

### **5.2.2 Creation of RXR Libraries Using Random Mutagenesis**

Chemical complementation is a relatively easy and fast method used to evaluate ligand-activated growth of NR, and is comparable to mammalian cell assays. This selection system can also be used as a tool to evaluate variant receptors that are engineered to bind novel small molecules. RXR has been characterized in chemical complementation with several ligands, and several RXR libraries have been transformed in this yeast strain to select for variants activated by novel small molecules [11, 16, 17]. Hence, this system was used to select for RXR variants that were activated at a lower concentration of LG335.

Previously, rational design has been used to engineer nuclear receptor variant to bind novel small molecules. Although this approach is valid, rational design is limited in

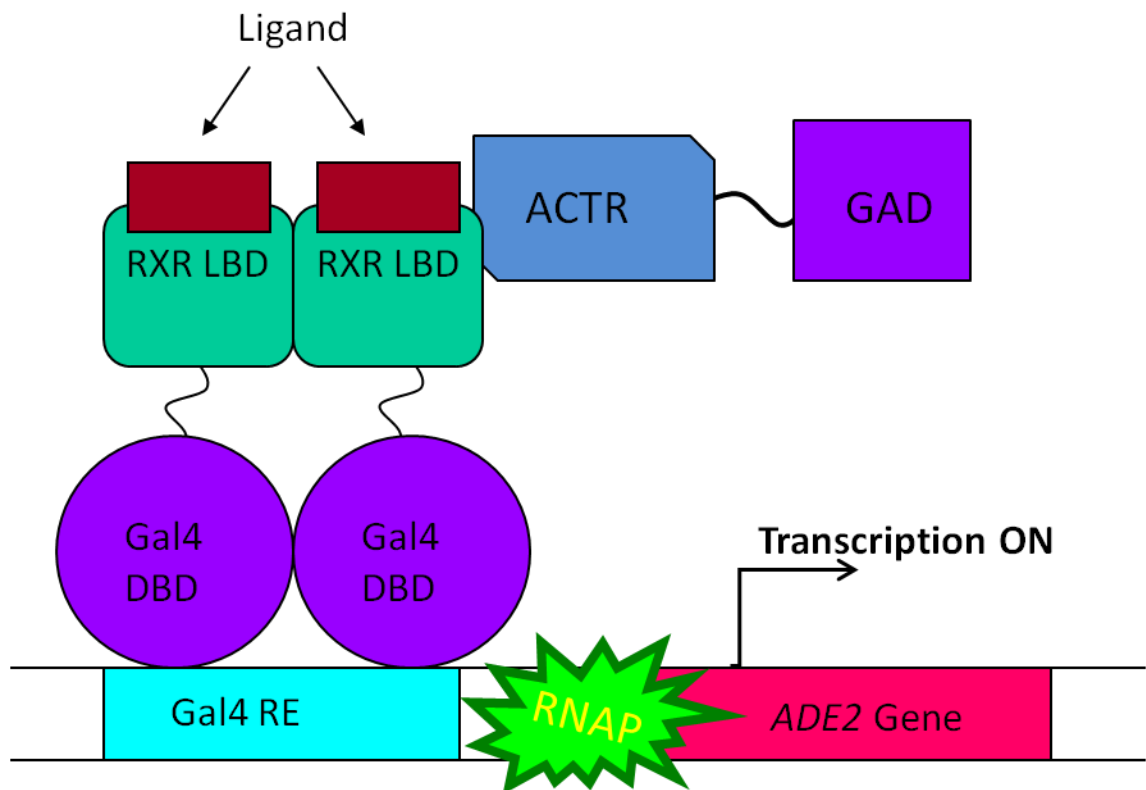
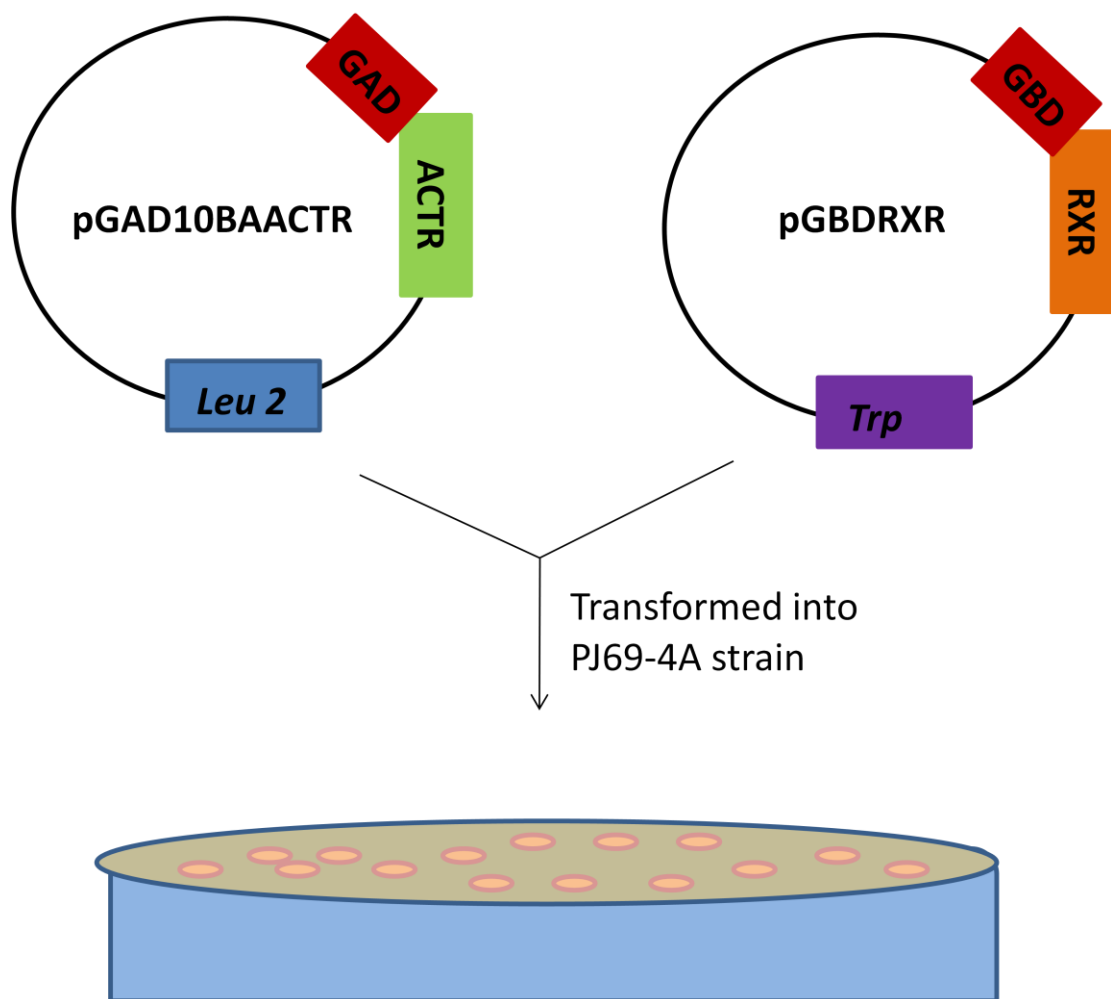


**Figure 5.3: Chemical Complementation System:** This system is established in the PJ69-4A strain, which contains Gal4 RE controlling expression of the genetic selection gene, *ADE2*. When the ligand LG335 binds to the RXR LBD-Gal4 DBD fusion protein, the ACTR-GAD fusion protein is recruited, turning on expression of the *ADE2* gene.



Nonselective Media: Synthetic Complete Media – Leu and Trp

Figure 5.4: **Transformation of pGAD10BAACTR and pGBDRXR into the PJ69-4A strain:** The yeast plasmids pGAD10BAACTR and pGBDRXR were transformed into the yeast strain PJ69-4A and then placed on nonselective plates containing synthetic complete media lacking leucine and tryptophan (SC-LW).

exploring mutation space. Error prone polymerase chain reaction (epPCR) is a simplistic and versatile method that allows a larger mutational range to be explored [18]. In this method, DNA strands are amplified using a commercial polymerase. The fidelity or the error rate of the polymerase can be increased by manipulating the parameters of the PCR conditions [18]. The *Taq* polymerase is a thermostable enzyme from *Thermus aquaticus* that catalyzes the synthesis of DNA, but lacks proofreading capability, hence, a high error rate [18, 19]. To further increase the error rate of *Taq* polymerase,  $\text{MnCl}_2$  was added to the PCR reaction. Manganese II is a metal that has the same oxidation number as magnesium, the cofactor of the *Taq* polymerase, but increases the mismatching frequency of this enzyme [18, 20]. Various concentrations of  $\text{MnCl}_2$  (2  $\mu\text{M}$ , 20  $\mu\text{M}$ , and 200  $\mu\text{M}$ ) were used to amplify three different RXR templates, GR130, GRQCIMFI, and RXRwt, making a variety of insert cassettes. The insert cassettes have ends that are complementary to the background plasmid (pGBDRXRBP).

The previously cloned background plasmid, pGBDRXRBP, contains the Gal4 DBD fused to the RXR LBD; however, a random DNA sequence is inserted into the RXR LBD, creating multiple stops in the sequence [17]. The purpose of introducing stop codons into the background plasmid is to eliminate RXR wild type background. When both cassettes are transformed into the PJ69-4A strain, as shown in Figure 5.5, the insert cassette combines with the background vector via homologous recombination, allowing the expression of multiply full length fusion protein, GBD-RXR, with an assortment of mutations. The transformants were then placed on nonselective plates, synthetic complete (SC) lacking leucine and tryptophan (SC-LW) to access the transformation efficiency and the success of homologous recombination. Transformants

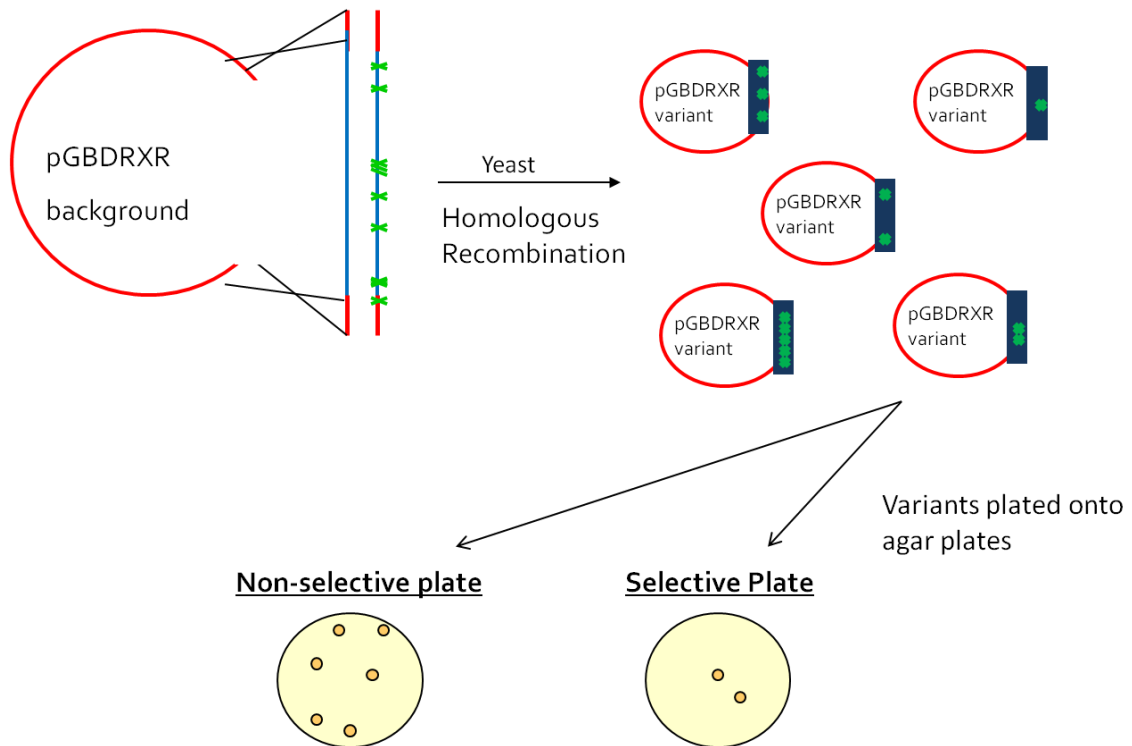


Figure 5.5: **Creation of RXR Library and transformation into PJ69-4A strain:** The background plasmid contains regions of homology with the insert cassette. The insert cassette contains a variety of mutations (x) at random positions. The insert cassette can combine with the background plasmid when transformed into yeast, creating various RXR variants. Variants are placed on non-selective and selective plates.

were also placed on adenine selective media, SC media lacking adenine, leucine and tryptophan (SC-ALW), containing a desired small molecules. If the small molecule can bind and activate the receptor, then ACTR-GAD will be recruited and turn on expression of the *ADE2* gene, allowing the survival of yeast in adenine selective media. Since the GRQCIMFI variant displays growth at a concentration of 1  $\mu$ M LG335 in CC, the adenine selective plates contained 100 nM LG335.

### 5.2.3 Results of RXR Error Prone Libraries

Most libraries displayed experimental transformation efficiencies and library size range from  $10^4$ - $10^5$  cfu/ $\mu$ g DNA and  $10^2$ - $10^4$  variants respectively, determined from the nonselective plate and are summarized in Table 5.1. However, RXRwt libraries had very low transformation efficiencies (275-950 cfu/ $\mu$ g DNA) and library sizes (14-48 variants), and produced no potential ligand-activated variants. The RXRwt libraries were repeated; however, no variants were produced with higher sensitivity towards LG335 than the QCIMFI variant.

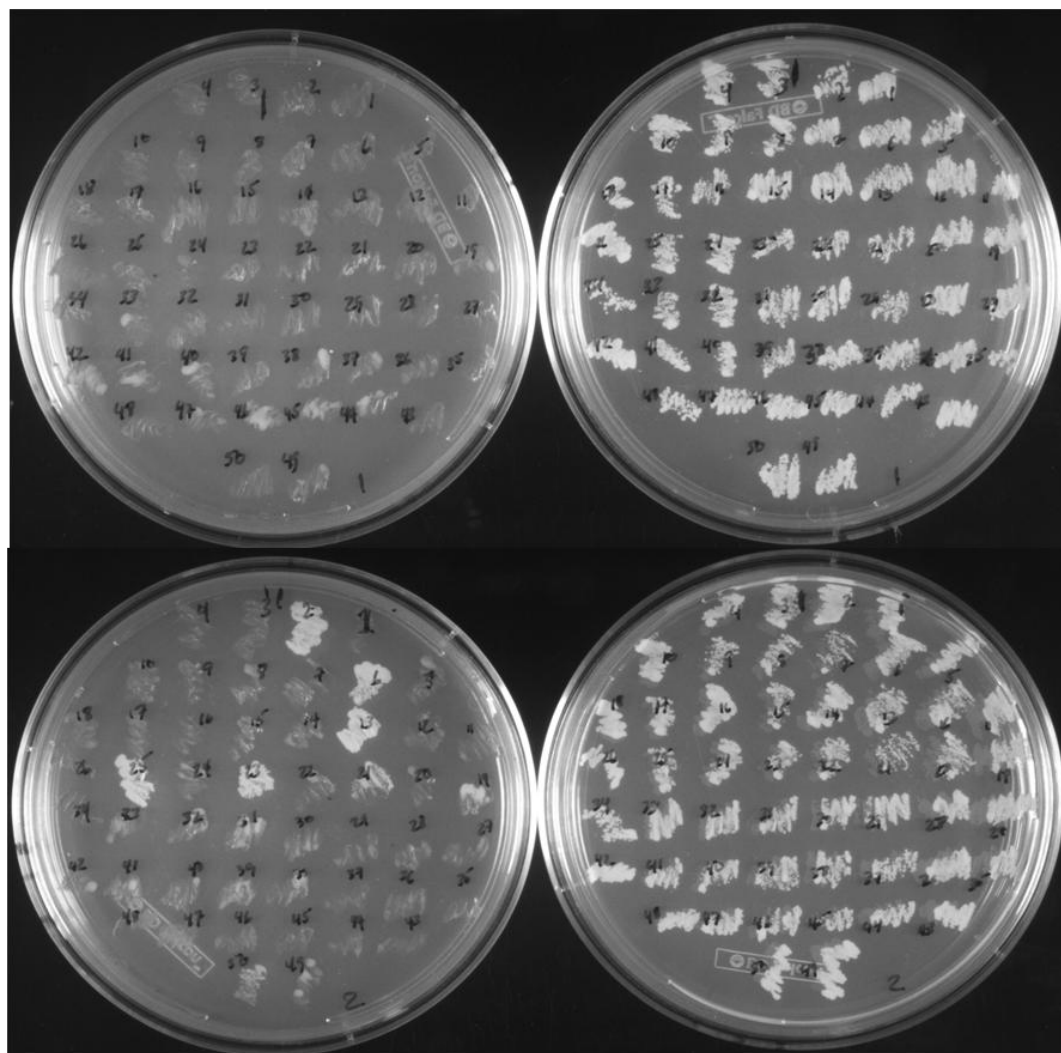
The GR130 and GRQCIMFI libraries resulted in several potential ligand-activated variants, since colonies formed on adenine selective plates with 100 nM LG335. Therefore, these variants were tested on solid media for constitutive activity. Constitutively active variants display growth regardless of the present of ligand. As shown in Figure 5.6, 100 colonies (~0.1-2% of each library) were streaked onto nonselective (SC-LW) and adenine selective (SC-ALW) plates. The streaking results showed that most of the colonies streaked were not constitutive active, displaying no growth on adenine selective plates without ligand and growth on nonselective plates.

Table 5.1: Transformation Results of RXR libraries			
Library Name	Concentration of $\text{MnCl}_2$ (mM)	Transformation Efficiency (cfu/ $\mu\text{g}$ VC)	Library Size (Variants)
GR130a	200	$2.8 \times 10^4$	784
GR130b	20	$1.6 \times 10^5$	$9.6 \times 10^3$
GR130c	2	$2.2 \times 10^5$	$1.3 \times 10^4$
QCIMFIa	200	$1.2 \times 10^5$	$7.3 \times 10^3$
QCIMFIb	20	$1.9 \times 10^5$	$1.1 \times 10^4$
QCIMFIc	2	$1.9 \times 10^5$	$1.1 \times 10^4$
RXRwta	200	275	14
RXRwtb	20	950	48
RXRwtc	2	400	20



## Adenine Selective Media without Ligand

## Nonselective Media



**Figure 5.6: Streaking Results of RXR Variants for Constitutive Activity:**  
Streaking results of RXR variants on adenine selective (SC-ALW) and nonselective (SC-LW) plates to test for constitutive activity.

The variants were further tested on solid media for activation at lower concentrations of LG335. Sixty potential colonies were streaked onto adenine selective plates with and without LG335. As shown in Figure 5.7, only three variants, circled in red, displayed ligand-activated growth, showing growth only on adenine selective plates with LG335. One variant was constitutively active, yellow arrow, growing regardless of the presence of ligand. As expected, Gal4, blue arrow, grew on both plates, since Gal4 is ligand independent, and RXRwt, purple arrow, did not grow on either plate since LG335 is not a strong agonist for this receptor.

#### 5.2.4 Liquid Quantitation Assay

For a more quantitative analysis, the variants that displayed ligand-activated growth at lower concentrations of LG335 were tested in liquid quantitation assays in chemical complementation. Yeast cells are transformed with both fusion proteins, GBD-RXR and ACTR-GAD, and grown in liquid adenine selective media with and without ligand. The same CC concept described previously applies to adenine selective liquid media, when a ligand binds to the GBD-RXR, ACTR-GAD is recruited, turning on expression of the *ADE2* gene. Yeast transformed with the RXR variants and ACTR-GAD were placed in 96-well plates with adenine-selective media (SC-ALW) and a range of ligand concentrations (Figure 5.8). Plates were incubated at 30°C with shaking, and optical density (OD) readings at the 630 nm wavelength were taken 0, 24, and 48 hours.

Figure 5.9 shows results of the 23b variant tested in liquid quantitation assays with the synthetic ligand LG335 and the natural ligand 9cRA. The 23b variant was compared to the QCIMFI variant, RXRwt, and Gal4. Gal4 (green line) showed ligand-activated growth regardless of ligand concentration, as expected. RXRwt (blue line)

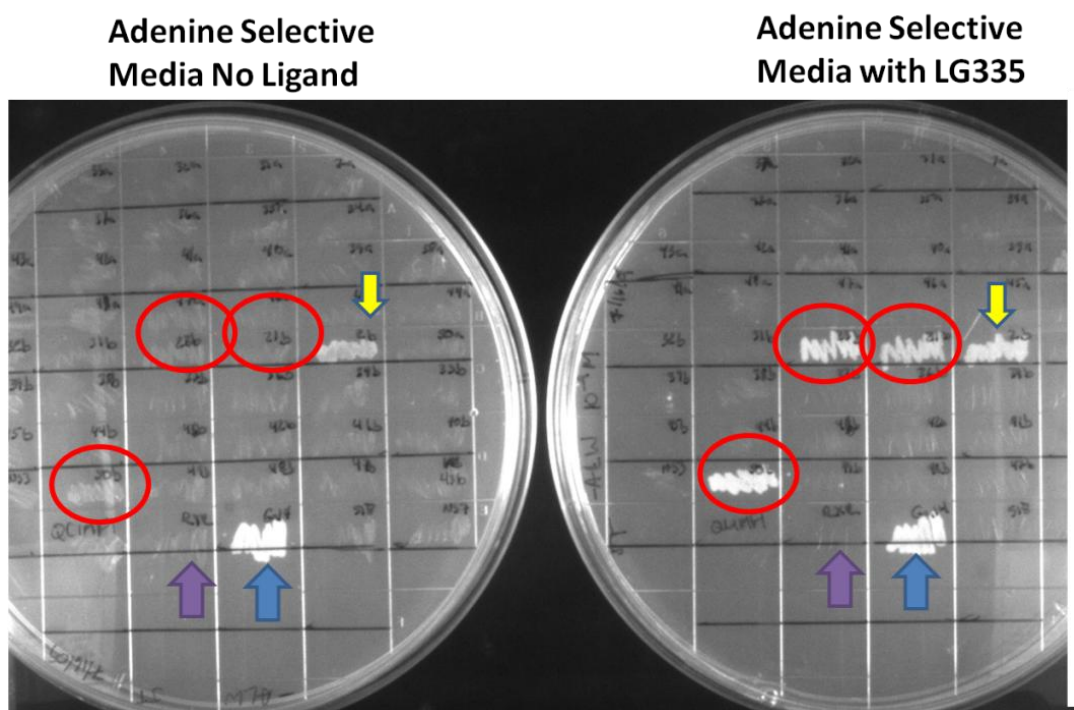


**Figure 5.7: Streaking Results of RXR Variants on Adenine Selective plates containing LG335:** Streaking results of RXR variants on adenine selective (SC-ALW) plates without ligand and with LG335. Red circles are ligand-activated variants, yellow arrow is a constitutively active variant, blue arrow is Gal4, and purple arrow is RXRwt.

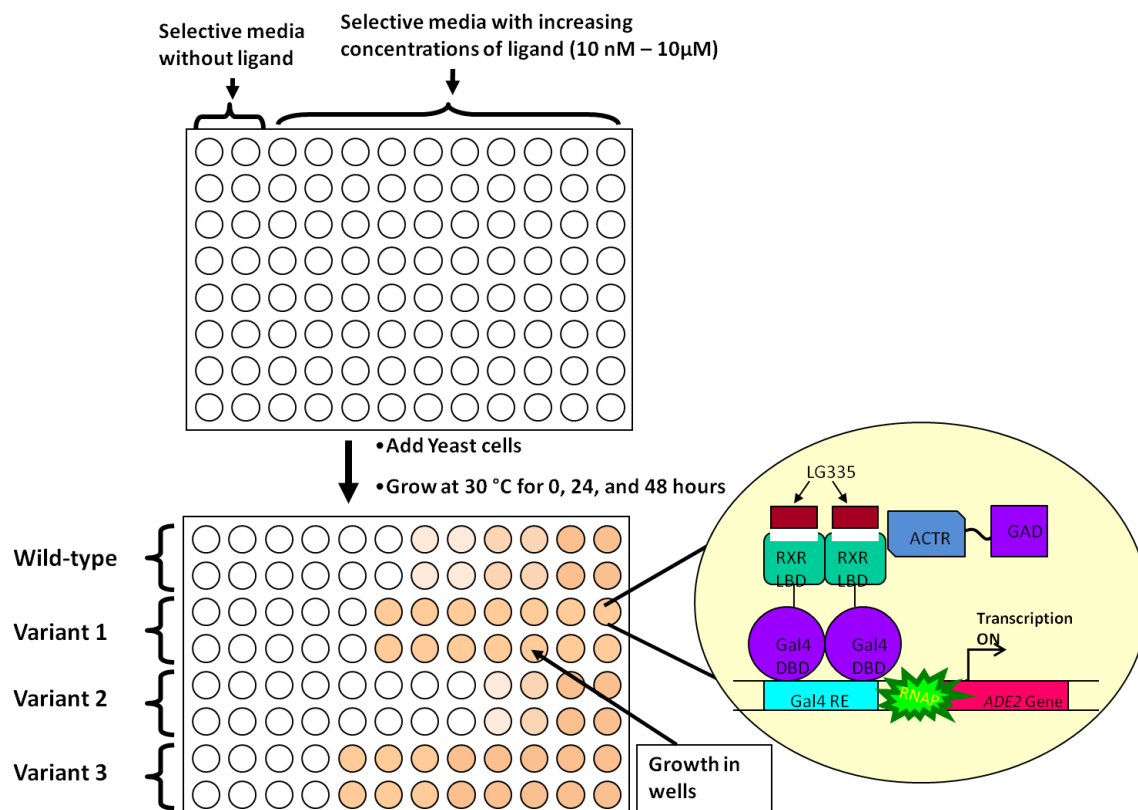


Figure 5.8: **Liquid Quantitation Assay:** Yeast transformed with RXR variants and ACTR-GAD are placed in 96-well plates with adenine selective media (SC-ALW) and a range of ligand concentrations. Plates are incubated at 30°C with shaking, and OD<sub>630</sub> readings are taken 0, 24, and 48 hours. Growth in wells indicates ligand activates expression of *ADE2* gene.

displayed ligand-activated growth at 1  $\mu$ M 9cRA (460 nM EC<sub>50</sub> value) with a 8.7 $\pm$ 0.5-fold activation and no growth was observed in LG335. Interestingly, the 23b variant (purple line) showed reverse specificity, no growth was observed with 9cRA and growth was observed at 10 nM LG335 (4 nM EC<sub>50</sub> value) with a 7.1 $\pm$ 0.3-fold activation. This variant displayed increased sensitivity towards LG335 when compared to the QCIMFI variant that shows ligand-activated growth at 1  $\mu$ M LG335 (300 nM EC<sub>50</sub> value) with a 7.0 $\pm$ 0.5-fold activation. No growth was observed with QCIMFI in response to 9cRA. Two other variants (21b and 50b), which displayed ligand-activated growth on solid media, were also tested in liquid quantitation assays (data not shown), but were constitutively active. Therefore, the results from these libraries possibly show a new variant that is activated at a lower concentration of LG335.

Several variants obtained from the nonselective and selective plates were sequenced. The sequencing of the nonselective variants determined the diversity and mutational limit of the error prone PCR method. The sequencing results shown in Table 5.2 reveal the wide diversity of mutations in the nonselective variants. Most nonselective variants displayed one to two mutations at a variety of positions, showing the range of mutational space put through selection. Although a limited number of variants were submitted for sequencing, an increase in mutations was observed as the MnCl<sub>2</sub> concentration increased, as expected. Most selective variants did not display additional mutations beyond the parent plasmid, GRQCIMFI, except for the 21b and 23b variants. The sequencing results showed the additional mutation I324V produced a constitutively active variant in the case of 21b, but the L455M additional mutation produced a variant with increase sensitivity towards LG335 (23b). From these random mutagenesis libraries,

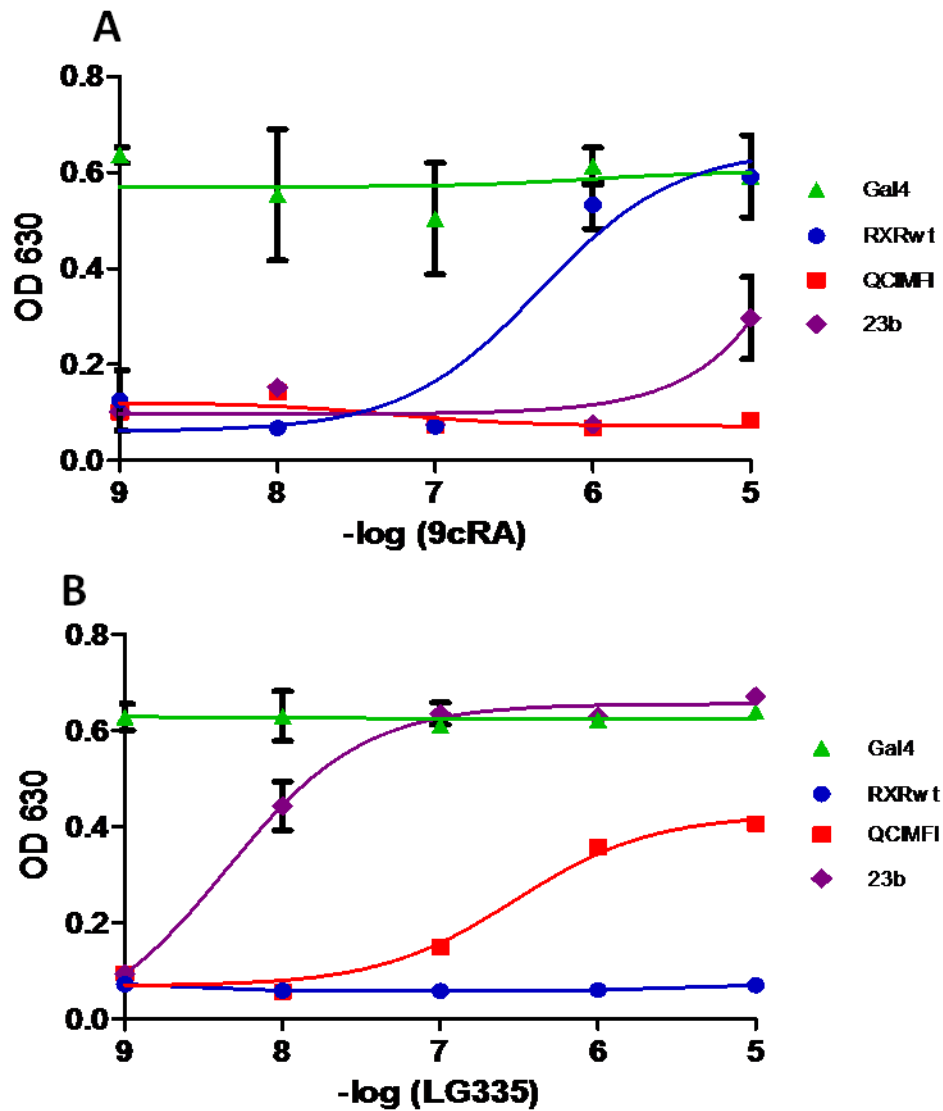


Figure 5.9: **Ligand-Activated Growth Profiles of Gal4, RXRwt, QCIMFI, and 23b:** Liquid quantitation assays in yeast with Gal4 ( $\blacktriangle$ ), RXRwt ( $\bullet$ ), variants 23b ( $\blacklozenge$ ), and QCIMFI ( $\blacksquare$ ) in response to (A) 9cRA or (B) LG335.

Table 5.2: Sequencing results of Error Prone Libraries		
Nonselective Variants		
NS3	Parent Plasmid is GR130: I268A, I310A, F313A, L436F	I292I
NS4	Parent Plasmid is GR130: I268A, I310A, F313A, L436F	L276H, G326G, F438S
NS5	Parent Plasmid is GR130: I268A, I310A, F313A, L436F	I299T, M452I
NS6	Parent Plasmid is GR130: I268A, I310A, F313A, L436F	No mutations
NS7	Parent Plasmid is GR130: I268A, I310A, F313A, L436F	E405G
NS8	Parent Plasmid is GR130: I268A, I310A, F313A, L436F	A272T, L433Q
Selective Variants		
S8	Parent Plasmid is GRQCIMFI: Q275C, I310M, F313I	V265L, L324H
S18	Parent Plasmid is GRQCIMFI: Q275C, I310M, F313I	No mutations
S19	Parent Plasmid is GRQCIMFI: Q275C, I310M, F313I	No mutations
S46	Parent Plasmid is GRQCIMFI: Q275C, I310M, F313I	No mutations
S48	Parent Plasmid is GRQCIMFI: Q275C, I310M, F313I	No mutations
S49	Parent Plasmid is GRQCIMFI: Q275C, I310M, F313I	N244I
S50	Parent Plasmid is GRQCIMFI: Q275C, I310M, F313I	No mutations
21b	Parent Plasmid is GRQCIMFI: Q275C, I310M, F313I	I324V
23b	Parent Plasmid is GRQCIMFI: Q275C, I310M, F313I	L455M

a new variant, Q275C, I310M, F313I, and L455M (QCIMFILM) was discovered to bind and activate in response to LG335 with a 4 nM EC<sub>50</sub> value. Also, the data shows that the epPCR method was successfully able to explore functional variants outside of the ligand binding pocket; however, the PCR conditions used were only able to create variants with one to two mutations.

### **5.2.5 Activation Profile of the GRQCIMFILM Variant in Mammalian Cell Culture**

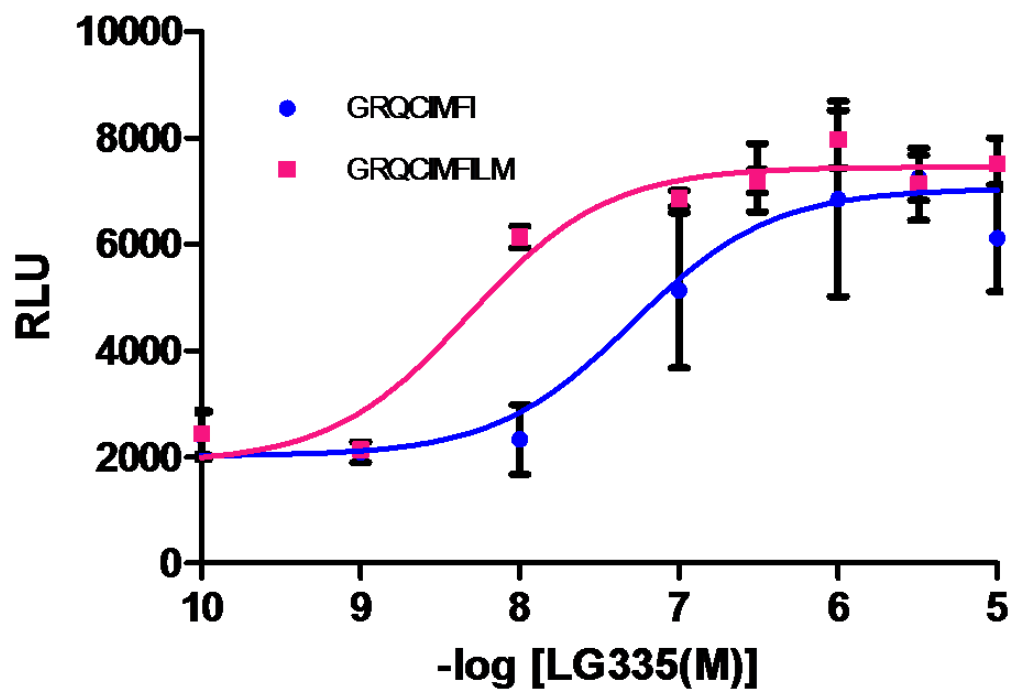
To confirm results observed in yeast, the quadruple variant (QCIMFILM) was then evaluated in mammalian cell culture assays for enhanced activity over the QCIMFI variant. The L455M mutation was added to the pMSCVGRQCIMFI plasmid via site-directed mutagenesis and primers containing the L455M mutation. The new plasmid, pMSCVGRQCIMFILM, which constitutively expresses GRQCIMFILM, was cotransfected in the HEK293T cells with the p17\*4TataLuc plasmid to test for luciferase activity. The p17\*4TataLuc plasmid contains Gal4 response elements controlling expression of the report gene *Renilla* Luciferase.

Results from the transfection (Figure 5.10) showed the new variant has a 10-fold increase in sensitivity towards the synthetic ligand LG335. QCIMFILM displays a 5 nM EC<sub>50</sub> value, compared to the 50 nM EC<sub>50</sub> value observed with QCIMFI. This data confirmed the results shown in yeast. The addition of the L455M mutation does increase the sensitivity of the receptor towards LG335; however, the increase is not as drastic as the 100-fold increase observed in yeast.

### **5.2.6 Libraries on the QCIMFILM variant**

In an effort to further increase the sensitivity of the quadruple variant to LG335, several libraries were created via epPCR using the QCIMFILM variant as the template





	LG335
Variant	EC <sub>50</sub> Value (nM)
QCIMFI	50
QCIMFILM	5

Figure 5.10: **Activation Profile of GRQCIMFI and GRQCIMFILM:** Activation profiles in HEK293T cells transfected with GRQCIMFI (●) and GRQCIMFILM (■) in response to LG335. Table is of EC<sub>50</sub> values for both variants.

and various concentrations of  $\text{MnCl}_2$ . The insert cassette was transformed into the PJ69-4A strain with the linearized background plasmid (pGBDRXRBP) and the coactivator plasmid (pGAD10BAACTR), and then plated on nonselective plates and adenine selective plates with 100 nM and 10 nM LG335. Table 5.3 shows each library produced sufficient transformation efficiencies ( $\sim 10^4$  cfu/  $\mu\text{g}$  of DNA) and library sizes ( $\sim 10^3$  variants). Approximately 1% of each library was tested for constitutive activity, by streaking colonies on adenine selective plates without ligand and nonselective plates. As shown in Figure 5.11, most variants were constitutively active; however a few variants displayed slight growth on the adenine selective plate, and they were further evaluated in liquid quantitation assays.

Variants were placed in adenine selective media with a range of ligand concentrations. Since the QCIMFILM variant is activated at 10 nM LG335, variants were evaluated at a lower concentration range to test for increased sensitivity towards LG335. As shown in Figure 5.12, no variants produced growth in response to 9cRA (Figure 5.12A), and no variants display ligand-activated growth at lower concentrations than the quadruple variant (Figure 5.12B). The variants 2-36 (red line), 2-43 (brown line), and 2-47 (black line) displayed ligand-activated growth at 100 nM LG335 ( $\sim 50$  nM  $\text{EC}_{50}$  value) with a  $\sim 9$ -fold activation, and no growth with 9cRA. The QCIMFILM variant displayed growth at 10 nM LG335 (6 nM  $\text{EC}_{50}$  value) with a  $12.5 \pm 0.3$ -fold activation, and no growth with 9cRA. The controls RXRwt and Gal4 were consistent with previous experiments. Gal4 (green line) displayed growth regardless of the presence of ligand, and growth was observed with RXRwt (blue line) at 1  $\mu\text{M}$  9cRA (420 nM  $\text{EC}_{50}$  value) with a  $11 \pm 1$ -fold activation, and no growth was observed with LG335. When sequencing these

Table 5.3: QCIMFILM Library Transformation Results			
Library Name	Concentration of MnCl <sub>2</sub> (μM)	Transformation Efficiency (cfu/ μg VC)	Library Size (Variants)
23a	200	7.3 x 10 <sup>4</sup>	2.3 x 10 <sup>3</sup>
23b	20	5.9 x 10 <sup>4</sup>	1.8 x 10 <sup>3</sup>
23c	2	5.8 x 10 <sup>4</sup>	1.8 x 10 <sup>3</sup>

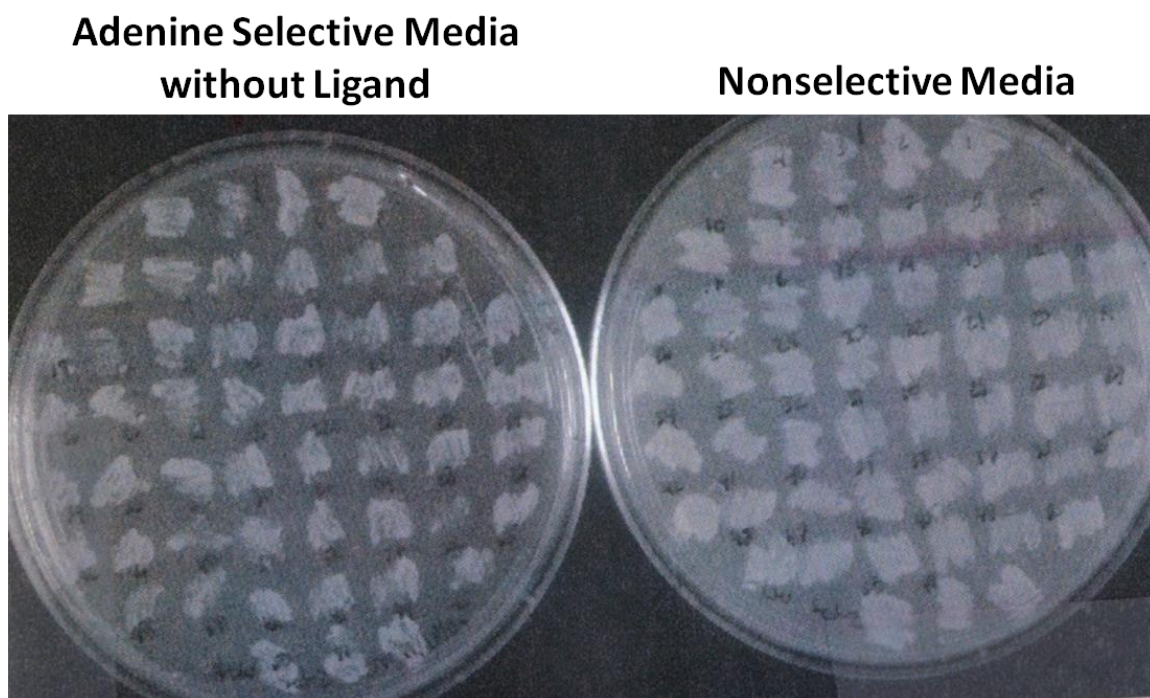


Figure 5.11: **Streaking results for Constitutive Activity from QCIMFILM libraries:** Streaking results of RXR variants from libraries 23a, 23b, and 23c on adenine selective (SC-ALW) and nonselective (SC-LW) plates to test for constitutive activity

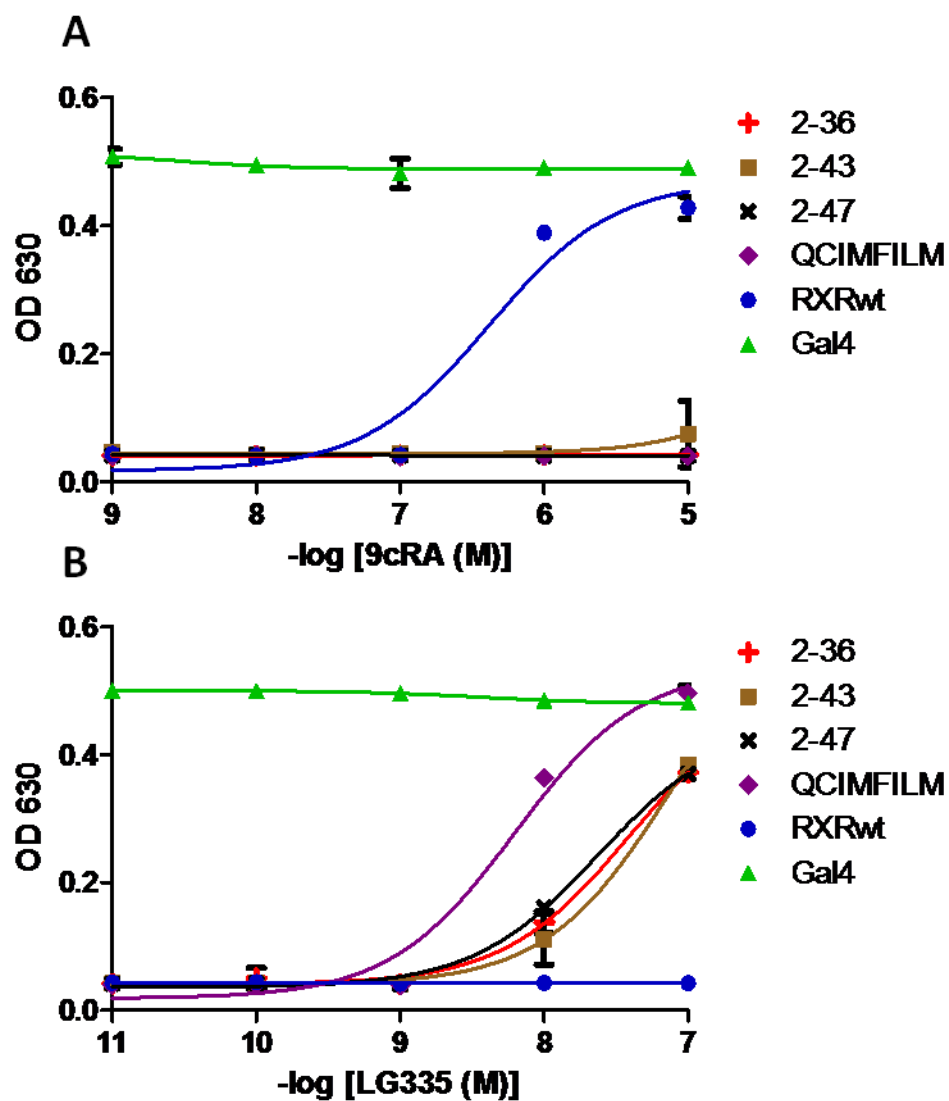


Figure 5.12: **Ligand-Activated Growth Profiles of Gal4, RXRwt, 2-36, 2-43, 2-47:** Liquid quantitation assays in yeast with Gal4 (▲), RXRwt (●), variants 2-36 (+), 2-43 (■), 2-47 (x), and QCIMFILM (◆) in response to (A) 9cRA or (B) LG335.

variant, all variants displayed the parent plasmid sequence (Q275C, I310M, F313I, and L455M). This library shows that perhaps the mutational tolerance of this receptor has been reached.

### 5.3 Determining the Role of the L455M Mutation

When looking at the L455 position in the crystal structure of RXR, the residue is not located in the ligand binding pocket. In fact, this residue is approximately 9.31 Å away from the ligand (Figure 5.13). However, the L455 residue is in helix 12 (H12), a helix critical for receptor activation. As stated in Chapter 1, when an agonist binds to the receptor a conformational change takes place, especially in H12, allowing the recruitment of the coactivator complex. Structurally, the L455M mutation is a part of the AF-2 domain, and does not directly interact with the ligand. However, previous findings have shown that this residue could also be involved in van der Waals interactions with surrounding residues.[21] Therefore, this mutation could increase the fold induction by stabilizing interactions in the ligand binding pocket, or by providing secondary interactions with coregulators for improved functionality of the receptor. To explore how the L455M mutation increased the activation of the receptor with LG335, the L455M position was added to single (Q275C, I310M, F313I), double (Q275C I310M, Q275C F313I, I310M F313I, and the triple (Q275C I310M F313I) variants, and tested for difference in receptor activation. The single, double, triple, and quadruple variants were created via site-directed mutagenesis into the pCMXRXRwt plasmid. The single, double, triple, and quadruple variants were then cotransfected into HEK293T cells with the pLuc\_CRBP<sub>II</sub> plasmid. The pLuc\_CRBP<sub>II</sub> plasmid contains RXR RE controlling expression of *firefly* luciferase.

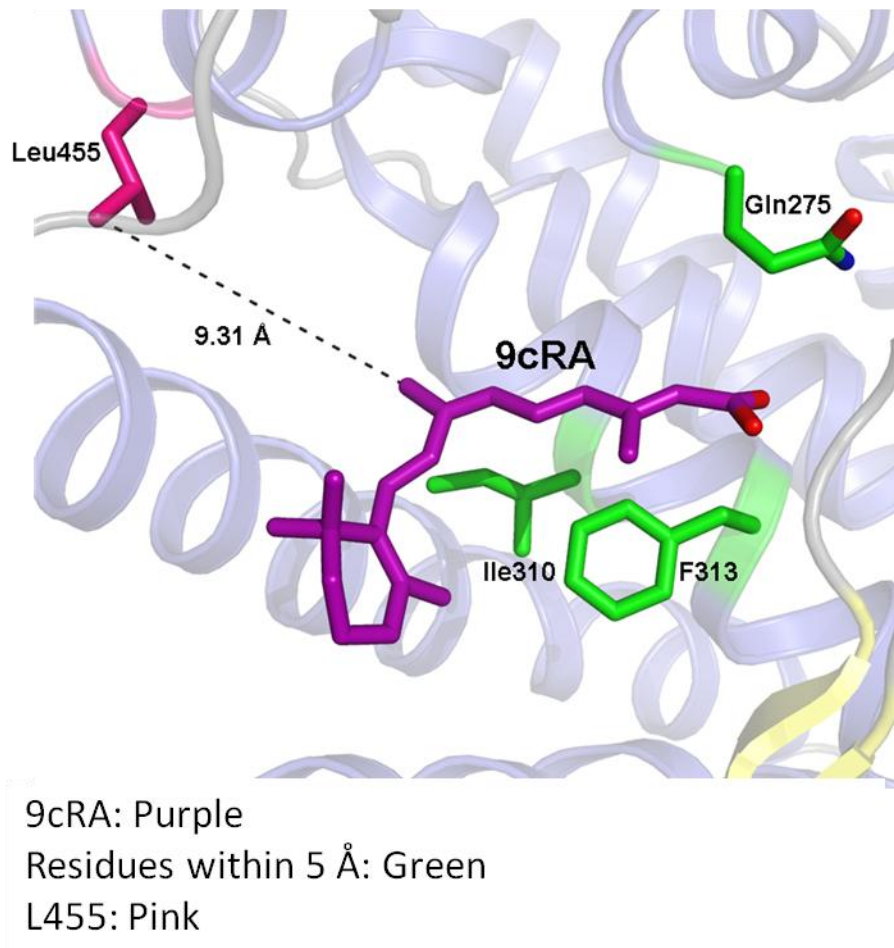


Figure 5.13: **Crystal structure of RXR bound to 9cRA:** Crystal structure of RXR with residues in the ligand binding pocket (green) and the L455 residue (pink), which is 9.31 Å away from the ligand. (PDB file: 1FBY).

Figure 5.14 shows the activation profiles of RXRwt and the single variants, Q275C and I310M, with and without the addition of L455M. A slight difference is observed in the activation profiles of RXRwt, Q275C, and I310M compared to when the L455M mutation is added. An increase in sensitivity with both ligands, 9cRA and LG335, is observed when the L455M is added to these variant. The  $EC_{50}$  value for RXRwt with 9cRA is 500 nM, and the addition of L455M showed slightly increases sensitivity with an  $EC_{50}$  value of 160 nM (Figure 5.14A). The same trend is observed with LG335 and the fold inductions with both ligands are comparable. A similar trend is observed with the addition of L455M to the Q275C and I310M variants. The Q275C and I310M displayed a 4,000 nM and 400 nM  $EC_{50}$  value, respectively, in response to 9cRA. However, the Q275C L455M and the I310M L445M showed increased sensitivity with 9cRA, displaying a 790 nM and 200 nM  $EC_{50}$  value, respectively (Figure 5.14B and 5.14C). The trend with increase in sensitivity was also observed when the same variants were tested with LG335.

Interestingly, the F313I is activated at 100 nM LG335 (50 nM  $EC_{50}$  value) with a  $16 \pm 3$ -fold induction, and only displays a 5,000 nM  $EC_{50}$  value and  $8 \pm 1$ -fold induction with 9cRA (Figure 5.15). Surprisingly, when L455M is added to the F313I variant, the receptor becomes constitutively active with no significant fold induction.

When looking at the double variants, a more pronounced increased in activity with LG335 is observed (Figure 5.16). The  $EC_{50}$  value for the Q275C I310M variant with 9cRA is greater than 10,000 nM and the fold induction is  $10 \pm 2$ -fold; only a 2,000 nM  $EC_{50}$  value and  $13 \pm 3$ -fold induction is observed in response to LG335. When the L455M



mutation is combined with the Q275C I310M variant, a 2-fold difference is seen in  $EC_{50}$  value with LG335 (1,000 nM) and the fold induction increases to  $20\pm3$ -fold.

A similar trend is observed in Figure 5.17, when L455M is combined with the Q275C F313I variants. The Q275C F313I displays a 160 nM  $EC_{50}$  value and a  $23\pm3$ -fold induction with LG335, and only a  $11\pm2$ -fold induction with 9cRA. However, the Q275C F313I L455M variant has a 5-fold difference in the  $EC_{50}$  values when compared to the Q275C I310M variant with LG335.

When L455M is added to the I310M F313I variant, a slight decrease in fold induction with LG335 is observed, whereas the  $EC_{50}$  values are very similar (Figure 5.18). The I310M F313I is activated at 100 nM LG335 (80 nM  $EC_{50}$  value) with a  $24\pm2$ -fold induction and 10,000 nM 9cRA with a  $10\pm5$ -fold induction. The I310M F313I L455M is activated at 100 nM LG335 (80 nM  $EC_{50}$  value) with a  $15\pm4$ -fold induction, and 10,000 nM 9cRA with a  $7\pm2$ -fold induction.

When comparing the triple variant (Q275C I310M F313I) to the quadruple variant (Q275C I310M F313I L455M), a 2-fold difference is observed in the  $EC_{50}$  value with LG335. The triple variant has a 100 nM  $EC_{50}$  value and a  $24\pm2$ -fold induction with LG335, while the quadruple variant has a 50 nM  $EC_{50}$  value and a  $31\pm7$ -fold induction with LG335. Both variants show low activation with 9cRA. Table 5.4 provides a summary of the  $EC_{50}$  values and fold inductions of all the variants. From these activation profiles, the most appropriate variant for the molecular switch system is the quadruple variant (Q275C I310M F313I L455M), which displays the highest fold-induction and lowest  $EC_{50}$  values with the LG335 ligand, and no activation with 9cRA. The next

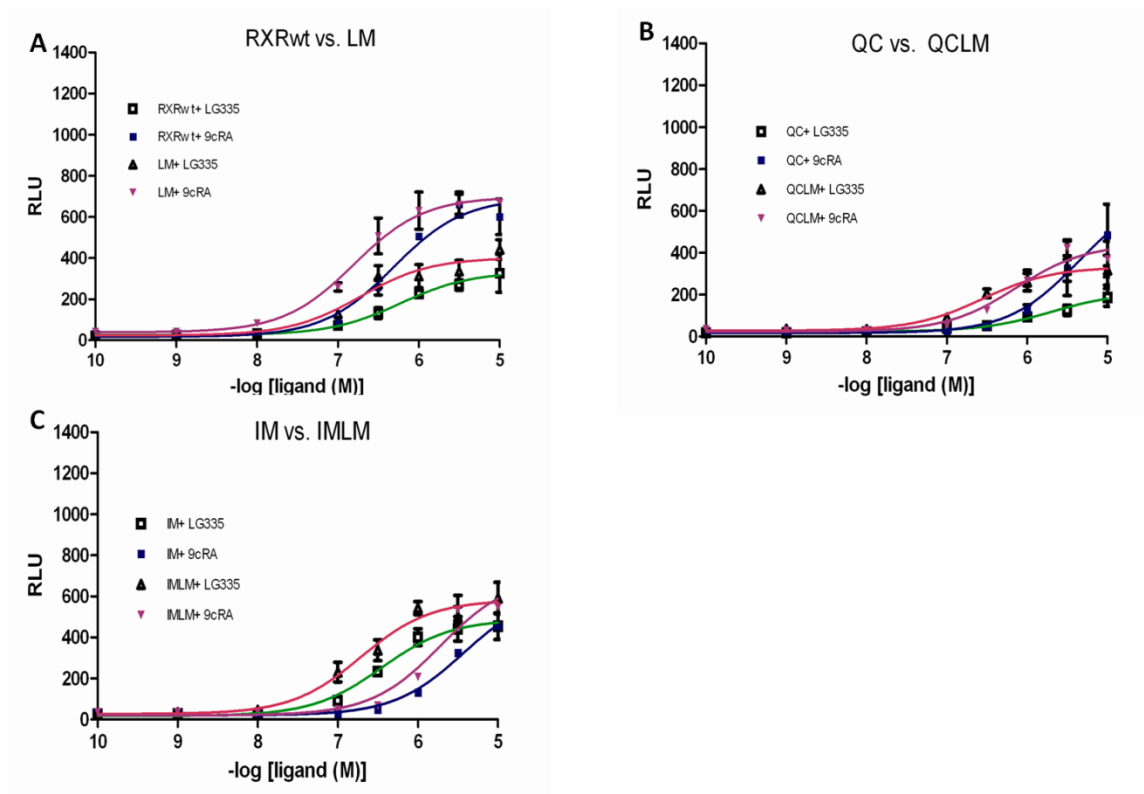


**Figure 5.14: Activation Profiles of RXRwt, L455M, Q275C L455M, I310M, and I310M L455M:** Activation profiles in HEK293T cells transfected with (A) RXRwt, L455M, (B) Q275C, Q275C L455M, (C) I310M, and I310M L455M in response to 9cRA and LG335.

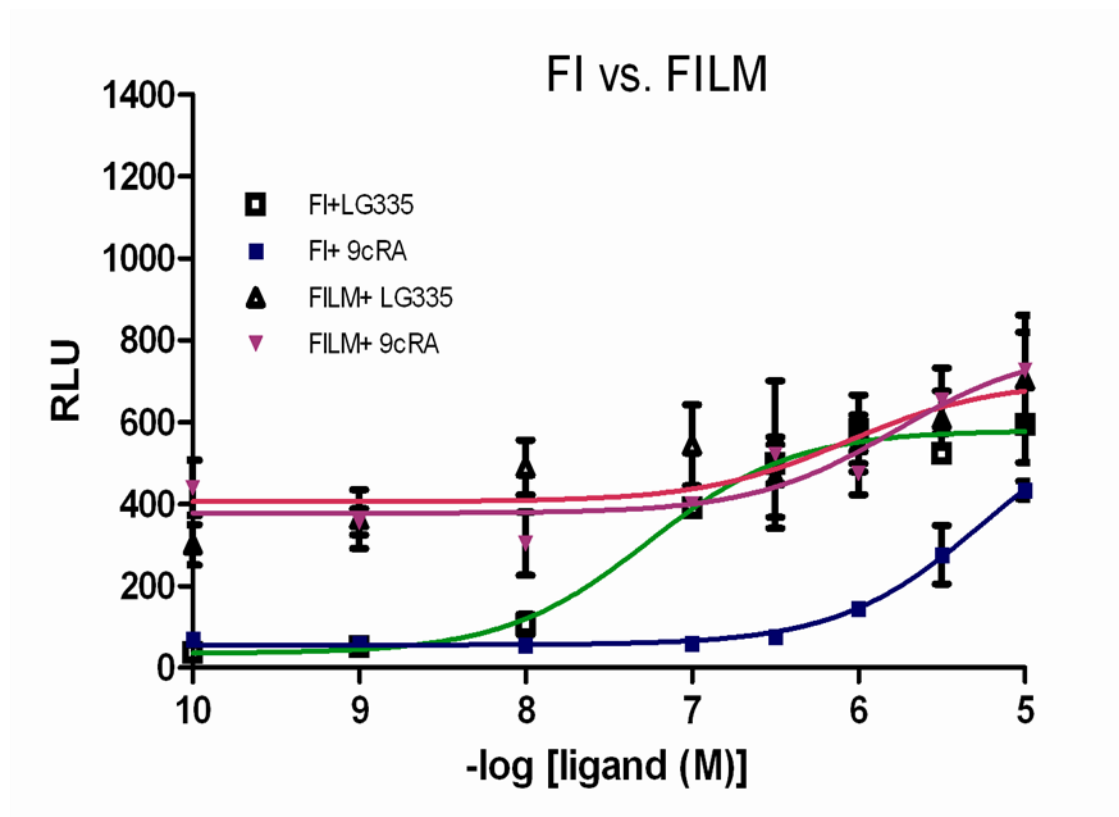


Figure 5.15: **Activation Profiles of F313I and F313I L455M:** Activation profiles in HEK293T cells transfected with F313I and F313IL455M in response to 9cRA and LG335.

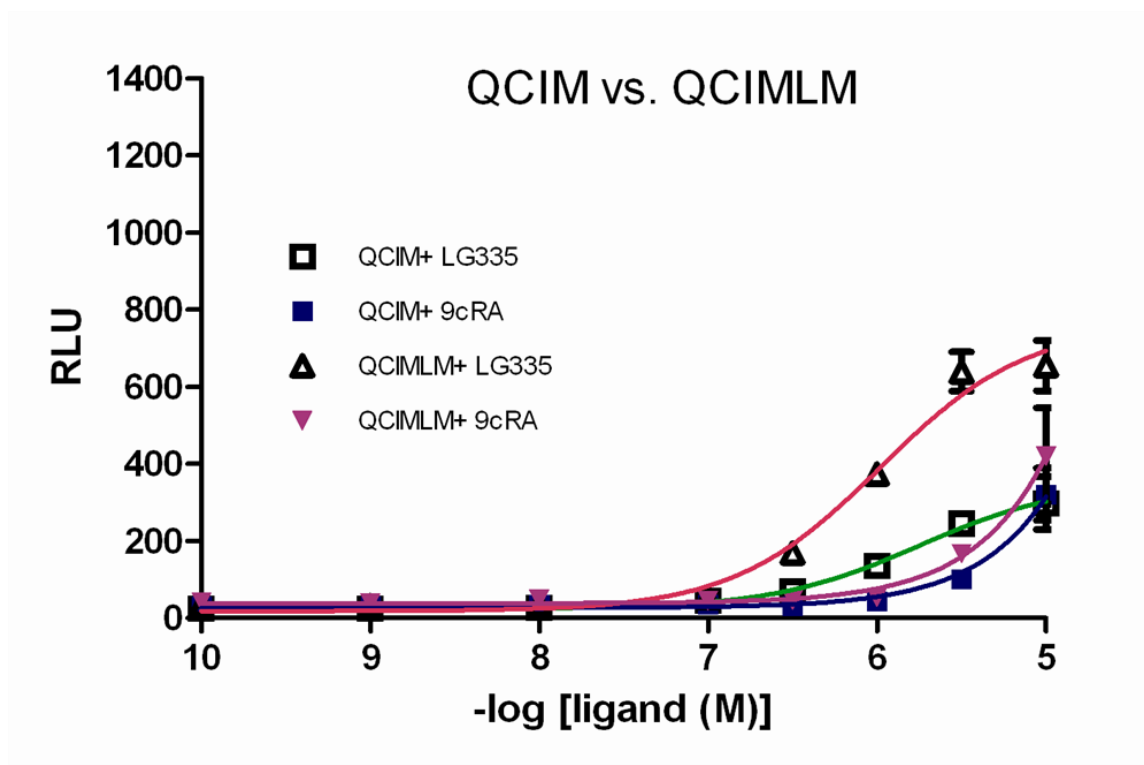


Figure 5.16: **Activation Profiles of Q275C I310M and Q275C I310M L455M:** Activation profiles in HEK293T cells transfected with Q275C I310M and Q275C I310M L455M in response to 9cRA and LG335.

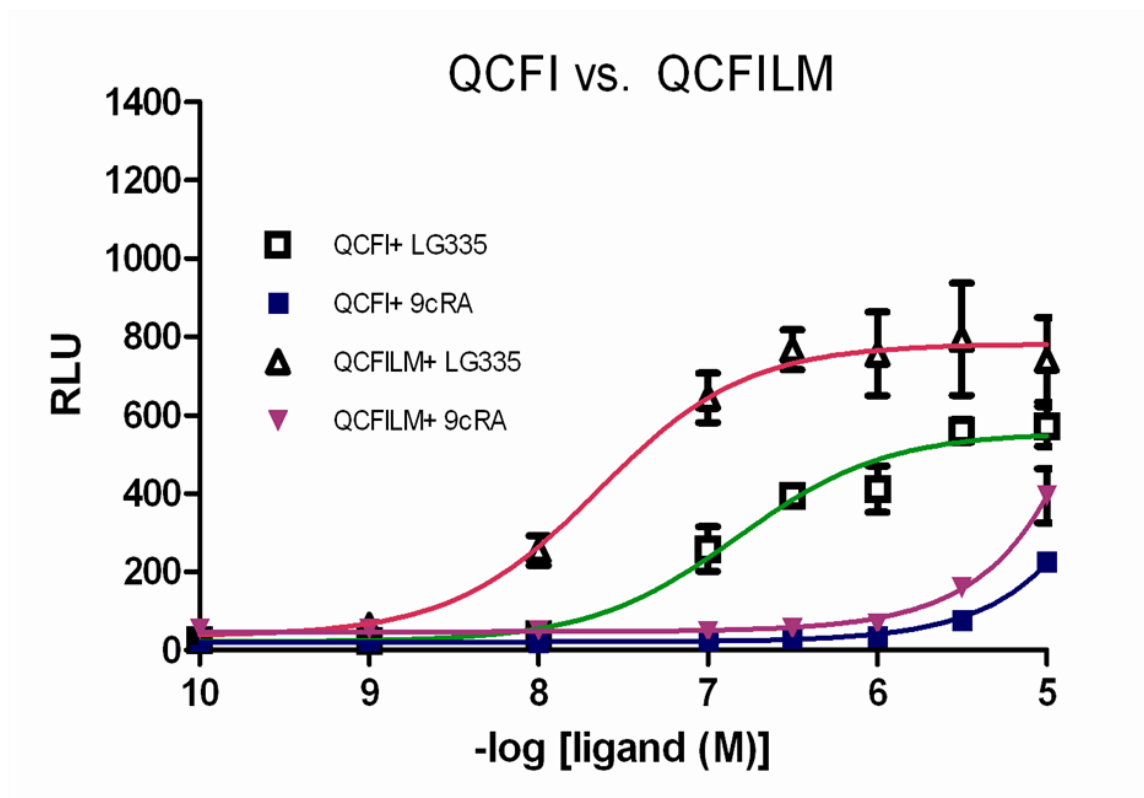


Figure 5.17: **Activation Profiles of Q275C F313I and Q275C F313I L455M:**  
Activation profiles in HEK293T cells transfected with Q275C F313I and Q275C F313I L455M in response to 9cRA and LG335.

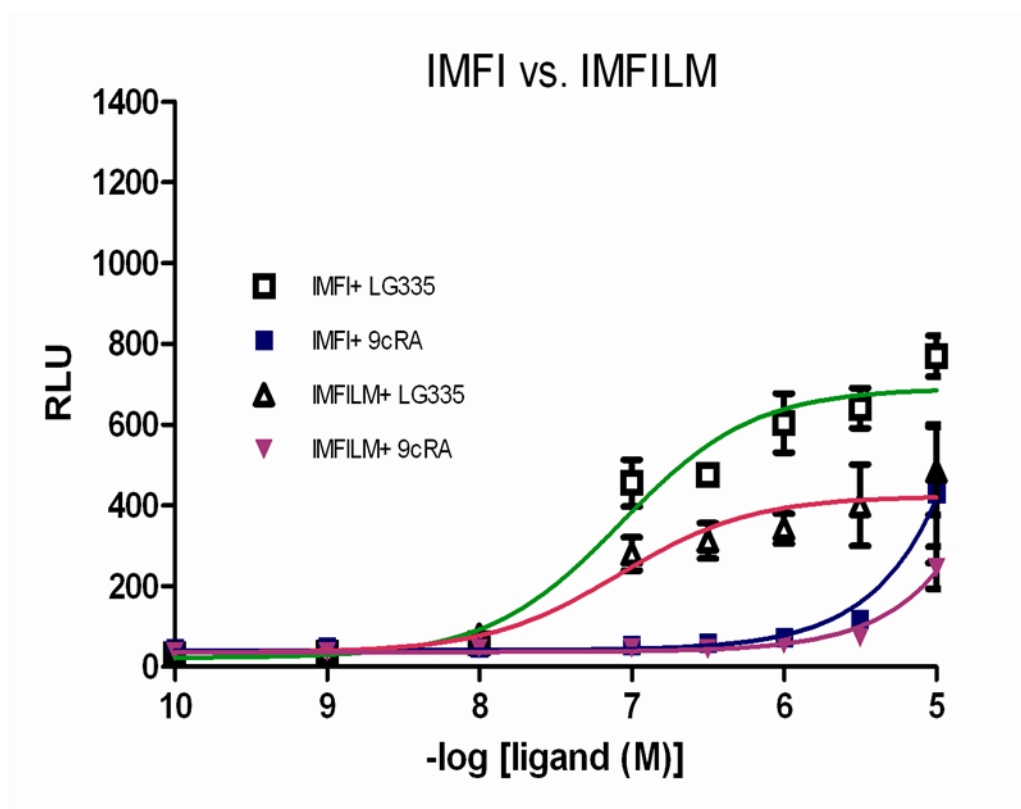


Figure 5.18: **Activation Profiles of I310M F313I and I310M F313I L455M:** Activation profiles in HEK293T cells transfected with I310M F313I and I310M F313I L455M in response to 9cRA and LG335.

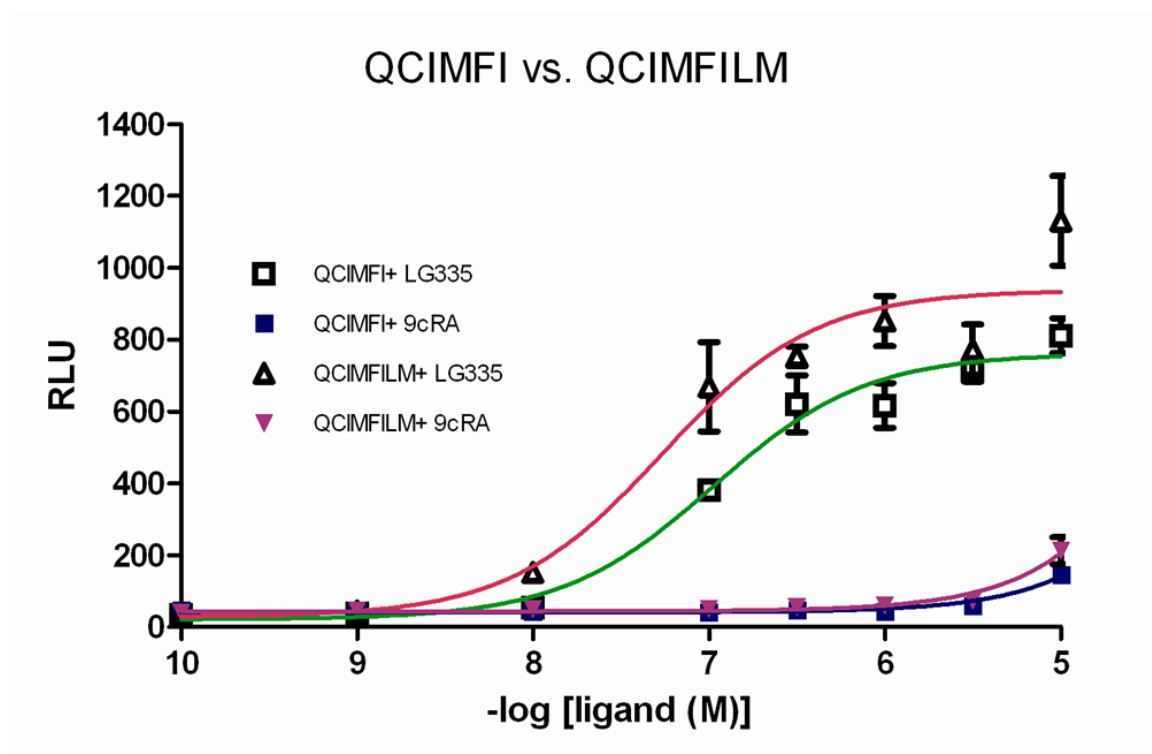


Figure 5.19: **Activation Profiles of Q275C I310M F313I and Q275C I310M F313I L455M:** Activation profiles in HEK293T cells transfected with Q275C I310M F313I and Q275C I310M F313I L455M in response to 9cRA and LG335.

**Table 5.4: Activation of RXR variant in Cell Culture**

RXR Variants	9cRA		LG335	
	EC50 Value (nM)	Fold Induction	EC50 Value (nM)	Fold Induction
WT	500	18±8	630	10±3
Q275C	3980	19±6	2000	8±2
I310M	3980	15±2	400	18±3
F313I	5010	8±1	50	16±3
L455M	160	16±1	200	15±2
Q275C, I310M	>10,000	10±2	2000	13±3
Q275C, F313I	>10,000	11±2	160	23±3
Q275C, L455M	790	14±2	250	10±3
I310M, F313I	>10,000	10±5	80	24±2
I310M, L455M	2000	15±1	200	21±3
F313I, L455M	>10,000	2±1	>10,000	2±1
Q275C, I310M, F313I	>10,000	3±0.3	100	24±2
Q275C, I310M, L455M	>10,000	11±3	1000	20±3
Q275C, F313I, L455M	>10,000	8±2	30	16±4
I310M, F313I, L455M	>10,000	7±2	80	15±4
Q275C, I310M, F313I, L455M	>10,000	5±1	50	31±7



chapter will examine the L455M mutation in more detail and how this mutation increases the fold-induction in the presence of LG335.

## 5.4 Summary

In summary, several processes were attempted to improve the molecular switch. The VP16 activation domain was fused to the N-terminus region of GRQCIMFI in an effort to increase the fold induction. However, the addition of the VP16 created a constitutively active protein, which would not be useful in the molecular switch system. The second approach used epPCR and chemical complementation to select for new variants with increases sensitivity towards LG335. This method produced a successful variant, Q275C, I310M, F313I, L455M (QCIMFILM), which displayed a 10-fold increase in sensitivity towards LG335 with a 50 nM  $EC_{50}$  value. Further mutagenesis on this variant did not increase sensitivity towards the ligand, suggesting that the mutational tolerance has been reached. Finally, the effect of L455M on the single, double and, triple, variants was explored for difference in activation. Overall, an increase in sensitivity with LG335 was observed when the L455M mutation was added. These results also confirmed that the most appropriate variant for the molecular switch system is the quadruple variant (QCIMFILM), since this variant has the lowest  $EC_{50}$  value and highest fold induction with LG335, and not activated by 9cRA.

Several other approaches could be evaluated for further improvement in the molecular switch system. For instance, enhancer sequences, such as the chicken insulator sequence could be inserted into our molecular switch system to facilitate the expression of two genes simultaneously. More techniques could also be examined to optimize the viral titer, or an alternative viral vector could be used. Lastly another control should be

developed to test the effectiveness of dual expression in the same vector. The Gal4 DBD should be fused to the VP16 activation domain, which is a chimeric protein that would turn on expression of genes controlled by the Gal4 response elements without the addition of ligand. This fusion protein would replace GRQCIMFI and could be used for comparing inducible gene expression in transient transfections, as well as retroviral transductions.

## 5.5 Materials and Methods

### Plasmid Construction

The *MfeI* and *AvrII* restriction sites were inserted into the pMSCVGRQCIMFI plasmid using the following primers: *MfeI**AvrII*for, CCT TCT CTA GGC GCC GGA CAA TTG ATT CGT TAA CCT CGA GAG ATC TCC TAG GAT GAA GCT ACT GTC TTC TAT CGA ACA AG; and *MfeI**AvrII*rev, CTT GTT CGA TAG AAG ACA GTA GCT TCA TCC TAG GAG ATC TCT CGA GGT TAA CGA ATC AAT TGT CCG GCG CCT AGA GAA GG. The VP16 insert cassette was amplified from the pVP16 plasmid (a gift from the Ortlund lab, Emory University) using the following primers containing the *MfeI* or the *AvrII* restriction site: *MfeI*VP16for, AAA CAA TTG ACC ATG GGC CCT AAA AAG AAG; and VP16*AvrII*rev, CTT CCT AGG GAA GCT TCT GCA GAC GCG TC. The insert cassette and the vector cassette was then digested with the *MfeI* and *SacII* restriction enzymes and ligated together using the Quick Ligase Enzyme (New England Biolab, Massachusetts).

### Mammalian Luciferase Assay

The pMSCV VP16-GRQCIMFI and the p17\*4TataLuc plasmids were cotransfected at a 1:2 molar ratio as described in Chapter 3. The single (Q275C, I310M, F313I, L455M), double (Q275C I310M, Q275C F313I, Q275C L455M, I310M F313I, I310M L455M, F313I L455M), triple (Q275C I310M F313I, Q275C I310M L455M, Q275C F313I L455M, I310M F313I L455M), the triple (Q275C I310M F313I L455M) variants, and RXRwt were also cotransfected into HEK293T cells with the pLuc\_CRBPII plasmid as previously described.

#### Error prone PCR

The RXR LBD gene was amplified from the pMSCVGRQCIMFI plasmid in a PCR using the following primers: Oligo1\_For, GGA TCC TGG AGG CTG AGC TGG CCG TGG AGC CCA AGA CCG AGA CCT ACG TGG AGG CAA ACA TGG GGC TGA ACC CCA GCT CG; and Oligo 10\_Rev, GGC CAG AAC GGG TGG GCA CAA AGG ATG GGC CCG CAG GCT TAA GCC TAA GTC ATT TGG TGC GGC GCC TCC AGC. The PCR solution also contained 10X Taq Buffer, dNTPs, MgCl<sub>2</sub>, 2, 20, or 200  $\mu$ M MnCl<sub>2</sub>, and the Taq polymerase. The annealing temperature used was 60°C.

#### Yeast Transformation

The insert cassette (1  $\mu$ g) and 0.3  $\mu$ g of the background plasmids pGBDRXRBP were transformed in the PJ69-4A strain using the TRAFCO yeast transformation protocol. The transformation mixture was placed onto nonselective plates (SC-LW) and adenine selective plates containing 100 nM LG335. Plates were incubated at 30°C for 3-4 days.

#### Liquid Quantitation Assay

Variants obtained from the yeast transformation were grown overnight in nonselective media SC-LW, at 30°C, shaking at 300 rpm. Variants were pelleted by centrifugation and resuspended in selective media SC-ALW with a range of ligand concentration and placed in 96-well plates. Plates were then incubated at 30°C, shaking at 170 rpm for 48 hours. Optical density readings were taken at a 630 nm wavelength after 0, 24, and 48 hours.

## 5.6 Literature Cited

1. Hall, D.B. and K. Struhl, *The VP16 activation domain interacts with multiple transcriptional components as determined by protein-protein cross-linking in vivo*. Journal of Biological Chemistry, 2002. **277**(48): p. 46043-46050.
2. Wysocka, J. and W. Herr, *The herpes simplex virus VP16-induced complex: the makings of a regulatory switch*. Trends Biochem Sci, 2003. **28**(6): p. 294-304.
3. Wang, Y.L., B.W. Omalley, and S.Y. Tsai, *A regulatory system for gene-transfer*. Proceedings of the National Academy of Sciences of the United States of America, 1994. **91**(17): p. 8180-8184.
4. Burcin, M.M., G. Schiedner, S. Kochanek, S.Y. Tsai, and B.W. O'Malley, *Adenovirus-mediated regulable target gene expression in vivo*. Proc Natl Acad Sci U S A, 1999. **96**(2): p. 355-60.
5. Nordstrom, J.L., *Antiprogestin-controllable transgene regulation in vivo*. Curr Opin Biotechnol, 2002. **13**(5): p. 453-8.
6. Schmitz, M.L. and P.A. Baeuerle, *The p65 subunit is responsible for the strong transcription activating potential of NF-kappa B*. EMBO J, 1991. **10**(12): p. 3805-17.
7. Palli, S.R., M.Z. Kapitskaya, and D.W. Potter, *The influence of heterodimer partner ultraspiracle/retinoid X receptor on the function of ecdysone receptor*. FEBS J, 2005. **272**(23): p. 5979-90.

8. Palli, S.R., M.Z. Kapitskaya, M.B. Kumar, and D.E. Cress, *Improved ecdysone receptor-based inducible gene regulation system*. European Journal of Biochemistry, 2003. **270**(6): p. 1308-1315.
9. Panguluri, S.K., P. Kumar, and S.R. Palli, *Functional characterization of ecdysone receptor gene switches in mammalian cells*. FEBS J, 2006. **273**(24): p. 5550-63.
10. Lipkin, S.M., T.L. Grider, R.A. Heyman, C.K. Glass, and F.H. Gage, *Constitutive retinoid receptors expressed from adenovirus vectors that specifically activate chromosomal target genes required for differentiation of promyelocytic leukemia and teratocarcinoma cells*. Journal of Virology, 1996. **70**(10): p. 7182-7189.
11. Schwimmer, L.J., P. Rohatgi, B. Azizi, K.L. Seley, and D.F. Doyle, *Creation and discovery of ligand-receptor pairs for transcriptional control with small molecules*. Proceedings of the National Academy of Sciences of the United States of America, 2004. **101**(41): p. 14707-14712.
12. Doyle, D.F., D.A. Braasch, L.K. Jackson, H.E. Weiss, M.F. Boehm, D.J. Mangelsdorf, and D.R. Corey, *Engineering orthogonal ligand-receptor pairs from "near drugs"*. Journal of the American Chemical Society, 2001. **123**(46): p. 11367-11371.
13. James, P., J. Halladay, and E.A. Craig, *Genomic libraries and a host strain designed for highly efficient two-hybrid selection in yeast*. Genetics, 1996. **144**(4): p. 1425-36.
14. Lohr, D., P. Venkov, and J. Zlatanova, *Transcriptional regulation in the yeast gal gene family - A complex genetic network*. Faseb Journal, 1995. **9**(9): p. 777-787.
15. Azizi, B., E.I. Chang, and D.F. Doyle, *Chemical complementation: small-molecule-based genetic selection in yeast*. Biochem Biophys Res Commun, 2003. **306**(3): p. 774-80.
16. Schwimmer, L.J., *Engineering ligand-receptor pairs for small molecule control of transcription*. 2005.
17. Azizi, B., *Chemical complementation a genetic selection system in yeast for drug discovery, protein engineering, and for deciphering and assembling biosynthetic pathways*. 2005.

18. Wang, T.W., H. Zhu, X.Y. Ma, T. Zhang, Y.S. Ma, and D.Z. Wei, *Mutant library construction in directed molecular evolution: casting a wider net*. Mol Biotechnol, 2006. **34**(1): p. 55-68.
19. Tindall, K.R. and T.A. Kunkel, *Fidelity of DNA synthesis by the Thermus aquaticus DNA polymerase*. Biochemistry, 1988. **27**(16): p. 6008-13.
20. Beckman, R.A., A.S. Mildvan, and L.A. Loeb, *On the fidelity of DNA replication: manganese mutagenesis in vitro*. Biochemistry, 1985. **24**(21): p. 5810-7.
21. Egea, P.F., A. Mitschler, N. Rochel, M. Ruff, P. Chambon, and D. Moras, *Crystal structure of the human RXR alpha ligand-binding domain bound to its natural ligand: 9-cis retinoic acid*. Embo Journal, 2000. **19**(11): p. 2592-2601.

## **CHAPTER 6**

### **THE EFFECT OF L455 VARIANTS ON RECEPTOR ACTIVATION AND COACTIVATOR ASSOCIATION**

#### **6.1 The Importance of H12**

The discovery of the QCIMFILM variant's enhanced sensitivity towards LG335 has prompted the further understanding of the L455 position. The L455 residue is located on helix 12 (H12), which plays a significant role in nuclear receptor (NR) function. When an agonist binds to a NR, H12 undergoes repositioning, allowing the association of coactivators [1, 2]. Besides the role H12 plays in coactivator association, the active conformation of H12 has been shown to be stabilized by residues in the ligand binding pocket (LBP) [3, 4].

The activation function 2 (AF-2) core found in H12 is a highly conserved motif throughout the nuclear receptor superfamily [5]. Mutational analysis has been performed at each of the positions in the AF-2 core of RXR to understand the impact of each residue on receptor activity and coregulator interactions. As shown in Figure 6.1, one key residue in this helix is the highly conserved glutamic acid (E), which clamps the coactivator to the receptor through electrostatic and dispersion interactions [6-9]. Electrostatic interactions occur between two oppositely charged molecules, whereas dispersion forces are weak attractive forces, which cause instantaneous polarization of a molecule. Conserved mutations at this position can completely abolish coactivator association; thus, eliminating receptor activity [10].

The L455 residue, which is well conserved within the retinoid receptors, has been shown not to eliminate coactivator association when mutated to an alanine. However, previous data has shown that substituting an alanine at this position decreases activation and enhances the receptor's interaction with corepressors [4, 11-13].

In Chapter 5, the addition of the L455M mutation to RXR variants led to increased activation with a novel small molecule, LG335. The quadruple variant (QCIMFILM) displayed a 10-fold increase in sensitivity towards LG335 (50 nM EC<sub>50</sub> value) and a 31±7-fold induction. The single variant L455M also showed a slight increase in sensitivity toward LG335 (200 nM EC<sub>50</sub> value and a 15±2-fold induction) when compared to RXRwt (630 nM EC<sub>50</sub> value with a 10±3-fold induction). Since the L455 position is located approximately 9 Å away from the ligand, and is on a helix known to associate with other proteins, initial thoughts were that this residue is involved in coactivator or corepressor association. However, the data from Chapter 5 also led to the consideration that this residue indirectly influences ligand binding. When L455M was added to some of the variants tested an increase in activation with LG335 was observed. For instance, when L455M was added to the Q275C F313I variant the EC<sub>50</sub> value was reduced by 5-fold. Also, the addition of the L455M mutation to the F313I variant produced a constitutively active receptor. These results and the location of L455 suggested that this residue perhaps interacts indirectly with the ligand through an allosteric mechanism affecting other residues in the ligand binding pocket (LBP). Two hypotheses were investigated in this chapter. First, the involvement of L455 with surrounding residues in the LBP was assessed by examining the interaction of L455 with L436.



	Helix 12						
hRXR $\alpha$	F	L	M	E	M	L	E
mRXR $\beta$	F	L	M	E	M	L	E
hRXR $\gamma$	F	L	M	E	M	L	E
hRAR $\alpha$	L	I	Q	E	M	L	E
hRAR $\beta$	L	I	Q	E	M	L	E
hRAR $\gamma$	L	I	R	E	M	L	E
hER	L	L	L	E	M	L	D
hPPAR $\alpha$	L	L	Q	E	I	V	R
hTR $\beta$	L	F	L	E	V	F	E
hPXR	L	N	Q	E	L	F	Q

Figure 6.1: **Sequence Alignment of H12 in Nuclear Receptor:** Sequence alignment of helix 12 of select nuclear receptors. Highlighted in yellow are the highly conserved glutamic acid and the leucine residue of interest.

The role of L455 in coactivator association was also assessed in yeast with two known coactivators to determine whether the activity of the variant differs from one coactivator to the other. The tolerance at this position was also assessed to determine if other mutations at that position could modify receptor activity, and perhaps lead to a molecular switch with enhanced activity with various ligands.

## **6.2 Tolerance at the L455 position**

### **6.2.1 Testing L455 Variants in Chemical Complementation**

To evaluate the receptor's tolerance for mutations at the L455 position, the residue was mutated to ten amino acids via site-directed mutagenesis with primers containing mutations at the L455 position. The amino acids that were chosen (alanine, cysteine, phenylalanine, histidine, lysine, methionine, serine, threonine, valine, and tyrosine) represent all classes of amino acids. The volume of the amino acids ranged from alanine (88.6 Å<sup>3</sup>) to tyrosine (193.6 Å<sup>3</sup>) [14], allowing the evaluation of the minimal and maximal space this residue can occupy without compromising receptor function. Each category of amino acids was also selected based on their chemical properties, such as hydrophobic, charged, and polar. These variants were first tested in yeast via chemical complementation (CC).

As stated in Chapter 5, CC is a genetic selection system that links the binding and activation of a nuclear receptor by a small molecule to the survival of yeast [15]. This selection system is a three-component system consisting of a Gal4 DNA DBD fused to the RXR LBD (GBD-RXR), a coactivator fused to the Gal4 activation domain (CoAc-GAD), and a small molecule. Gal4 is a yeast transcription factor that is ligand

independent [16]. When a ligand binds to GBD-RXR, a conformation change takes place, allowing the recruitment of CoAc-GAD, leading to the expression of an essential gene. RXR variants subjected to chemical complementation are grown on media lacking the essential nutrient adenine, but have the desired small molecule, 9cRA or LG335. Only functional variants that can be activated by the ligand should grow in the adenine selective media (ligand-activated growth).

Figure 6.2 shows L455 variants tested in liquid quantitation assays containing adenine selective media in response to either a range of 9cRA or LG335. All variants showed decreased ligand-activated growth compared to the wild-type receptor, except the L455M variant. RXRwt (blue circles) displayed an  $EC_{50}$  value of 43 nM with a 10-fold activation with 9cRA, and no ligand-activated growth was observed with LG335. As expected, changing L455 to the charged residues, histidine (green circles) and lysine (pink squares), produced no ligand-activated growth in response to 9cRA or LG335 ( $EC_{50}$  values is greater than 10,000 nM and a 1-fold activation was observed). The same result was observed with the smallest and largest hydrophobic residues, alanine (red triangles) and phenylalanine (green diamonds), indicating that the volume of the residue is important. The L455V variant (brown stars) that is slightly smaller than the wild type residue showed ligand-activated growth, but at higher concentrations of 9cRA than the wild type receptor (240 nM  $EC_{50}$  value), and no growth was observed with LG335. The growth observed with L455V showed that hydrophobic residues that occupy similar volume to leucine are tolerated at this position.

Interestingly, the polar residues, L455S and L455T, showed growth with both ligands. The L455S variant (purple downward triangles) displayed a 420 nM  $EC_{50}$  value

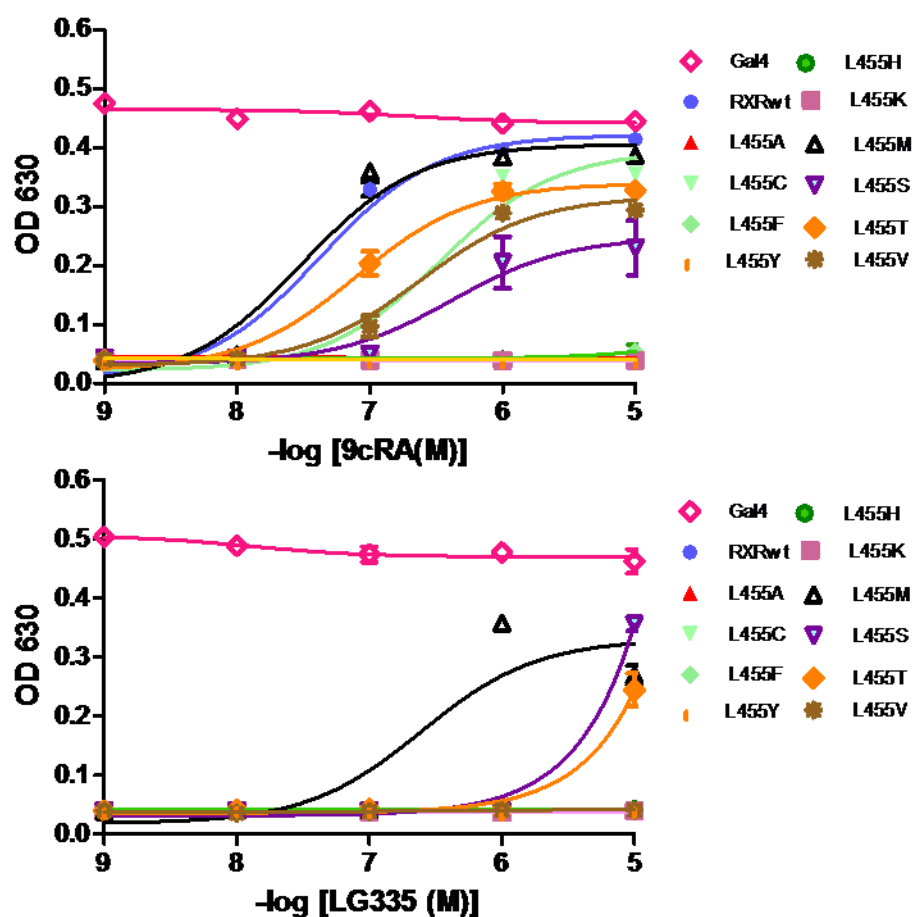


Figure 6.2: **Ligand-Activated Growth Profiles of L455 Variants:** Gal4, RXRwt, and L455 variants tested in liquid quantitation assays in adenine selective media (SC-ALW) and a range of (A) 9cRA or (B) LG335.

and a 5-fold activation with 9cRA. The EC<sub>50</sub> value with LG335 was greater than 10,000 nM and a 9-fold activation was detected. The L455T variant (gold diamonds) showed a 79 nM EC<sub>50</sub> value and an 8-fold activation with 9cRA. Again, the EC<sub>50</sub> value was greater than 10,000 nM, and a 6-fold activation was detected. The large polar residue, L455Y (gold lines), did not show ligand-activated growth with either ligands. These results show that polar residues are tolerated at this position; however, the residue must occupy a certain amount of space.

The L455C (green downward triangle) also showed ligand activated growth in response to 9cRA, displaying a 340 nM EC<sub>50</sub> value and a 9-fold activation. No growth was observed with LG335. Again, this result shows that the cysteine residue is tolerated at this position, but wild type receptor function is not achieved. As shown in Chapter 5, the L455M variant (black open triangle) displayed a similar growth profile with 9cRA as the wild type receptor, displaying a 31 nM EC<sub>50</sub> value and a 10-fold activation. Also, ligand-activated growth was observed at 1  $\mu$ M LG335 (250 nM EC<sub>50</sub> value) with a 9-fold activation. Table 6.1 is a list of EC<sub>50</sub> values and fold activations of all variants in the chemical complementation system.

These results indicate that tolerance is observed at the L455 position with hydrophobic and polar residues with limitations in the volume. Only the L455M variant displayed activity comparable to the wild type receptor. No other variants were able to enhance receptor activation with 9cRA, but three variants, L455M, L455S, and L455T, were able to show enhanced activity with LG335. Volume seems to be of particular importance at this position, where residues must occupy a particular amount of space (89-166 Å<sup>3</sup>).

**Table 6.1: EC<sub>50</sub> values and fold activations of L455 variants in yeast**

Variant	Volume (Å <sup>3</sup> )	Chemical Properties	9cRA		LG335	
			EC <sub>50</sub> Value (nM)	Fold-Activation	EC <sub>50</sub> Value (nM)	Fold-Activation
RXRwt	166.7	Hydrophobic	43	10	>10,000	1
L455A	88.6	Hydrophobic	>10,000	1	>10,000	1
L455F	189.9	Hydrophobic	>10,000	1	>10,000	1
L455M	162.9	Hydrophobic	31	10	250	9
L455V	140	Hydrophobic	240	7	>10,000	1
L455H	153.2	Charged	>10,000	1	>10,000	1
L455K	168.6	Charged	>10,000	1	>10,000	1
L455S	89	Polar	420	5	>10,000	9
L455T	116.1	Polar	79	8	>10,000	6
L455Y	193.6	Polar	>10,000	1	>10,000	1
L455C	108.5	Special	340	9	>10,000	1

Both hydrophobic and polar residues are tolerated at this position, as seen with L455T and L455V.

### 6.2.2 Testing L455 Variants in Mammalian Cell Culture

To verify the results observed in yeast, L455 variants were tested in mammalian cell culture assays. Each variant was made via site-directed mutagenesis on the pCMXRXRwt plasmid. As stated in Chapter 5, the pCMXRXRwt plasmid is a mammalian vector that constitutively expresses full length RXRwt under control of the CMV promoter. The single variants were then tested in a luciferase assay with the natural ligand, 9cRA, and the synthetic ligand LG335. HEK293T cells were cotransfected with the L455 variants along with the reporter plasmid, pLuc\_CRBPII at a 1:2 molar ratio. The pLuc\_CRBPII plasmid contains RXR response elements (RE) controlling expression of the reporter gene *Renilla* luciferase. RXRwt was also tested alongside as a positive control.

As shown in Figure 6.3, most of the variants did not display enhanced activation in comparison to the wild type receptor, confirming results seen in yeast. RXRwt (purple circle) is activated at 1  $\mu$ M 9cRA with a 400 nM EC<sub>50</sub> value and a 31 $\pm$ 9-fold induction. RXRwt shows decreased activation with LG335 having only a 12 $\pm$ 4-fold induction and a 540 nM EC<sub>50</sub> value. When L455 was mutated to charged or large aromatic residues, histidine (green diamonds), lysine (green circles), phenylalanine (yellow downward triangles), and tyrosine (gold diamonds), activation was completely abolished. On the other hand, the polar residues, serine (pink squares) and threonine (blue open triangle), showed comparable EC<sub>50</sub> values to RXRwt. However, activation was significantly

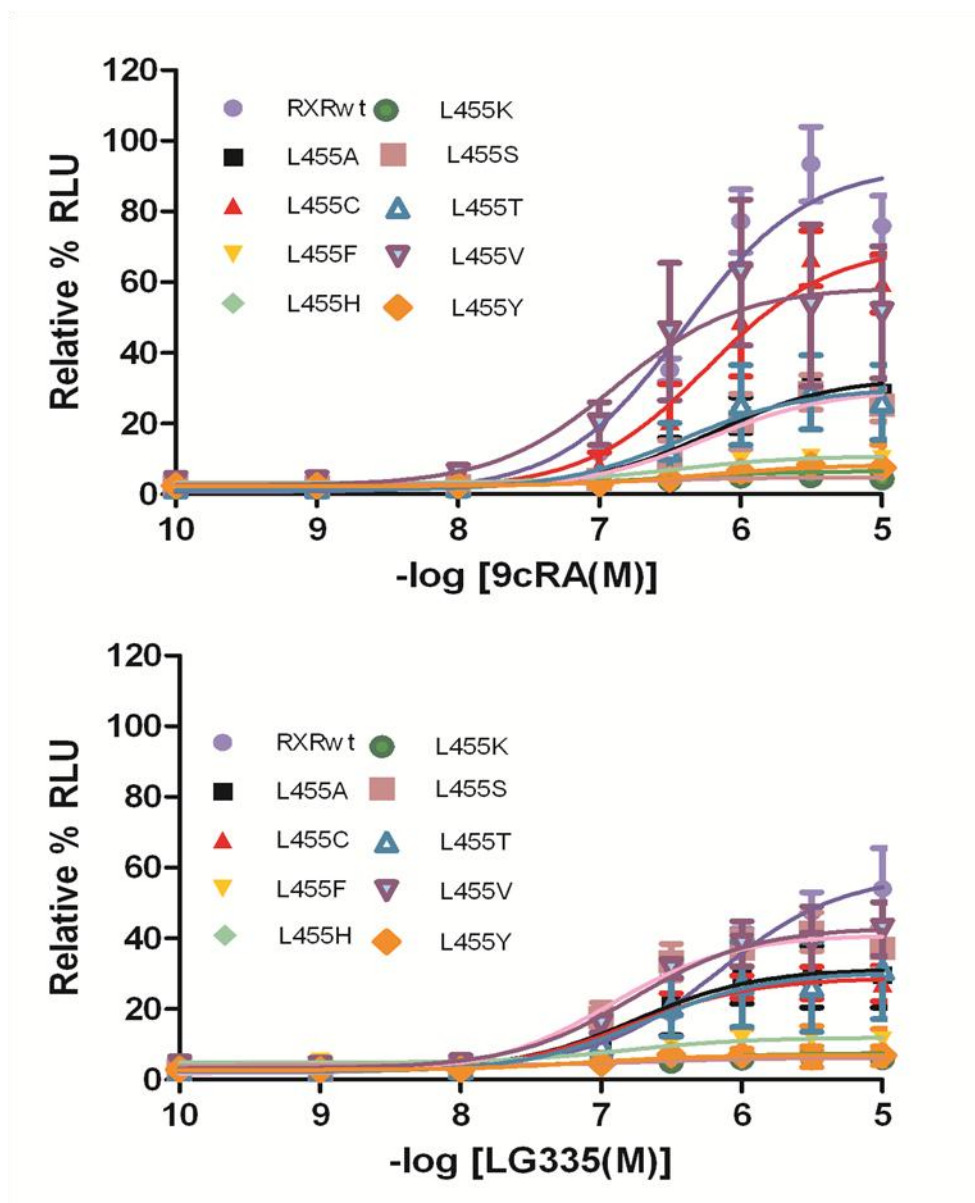


Figure 6.3: **Activation Profiles of L455 Variants in Cell Culture** Activation profiles in HEK293T cells transfected with RXRwt, L455A, L455C, L455F, L455H, L455K, L455S, L455T, L455V, and L455Y in response to 9cRA or LG335.



decreased, displaying a  $14\pm3$  and  $17\pm6$ -fold induction, respectively. Alanine (black squares), a smaller hydrophobic amino acid, did not show ligand-activated growth in yeast, and decreased activation was observed in mammalian cell with a  $13\pm6$ -fold induction and 630 nM EC<sub>50</sub> value. The cysteine and the valine residues showed the most comparable results to the wild type receptor, also seen in yeast. The cysteine residue (red triangles) displayed a  $23\pm6$ -fold induction and 580 nM EC<sub>50</sub> value in response to 9cRA, and valine (purple downward triangles) showed a  $17\pm6$ -fold induction and 130 nM EC<sub>50</sub> value with 9cRA. Table 6.2 list the EC<sub>50</sub> values and fold activations of all variants with 9cRA and LG335.

As shown in Figure 6.4, the L455M variant shows slightly increases sensitivity towards the natural ligand 9cRA, as well as, the synthetic ligand LG335, displaying a  $22\pm3$ -fold induction and 150 nM EC<sub>50</sub> value in the presence of 9cRA (pink downward triangles), and  $13\pm3$ -fold induction and 120 nM EC<sub>50</sub> value with LG335 (green diamonds shown in Figure 6.4). The methionine and leucine residue are similar since they both display hydrophobic properties, and the fact that their volume is approximately the same ( $\sim 165 \text{ \AA}^3$ ) could explain the similarities in the activation profiles.

Overall, the yeast assays and the luciferase assays evaluated the amino acid tolerance at the L455 residue. The data reveals that this residue is fairly tolerable, since five out of the ten variants displayed considerable growth or activation. However, activation is not comparable to the wild type receptor with most of the variants. Charged residues (histidine and lysine) and the residues with the largest volume (phenylalanine and tyrosine) are not tolerated at this position, but the hydrophobic residues with comparable volumes to leucine, display significant activation.

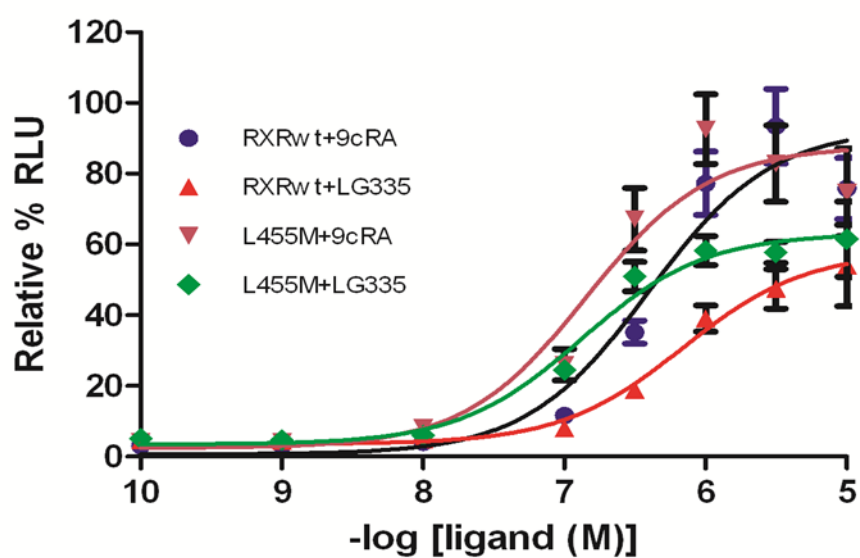


Figure 6.4: **Activation Profiles of L455M Variants in Cell Culture:** Activation profiles in HEK293T cells transfected with RXRwt and the L455M variants in response to 9cRA or LG335.

**Table 6.2: EC<sub>50</sub> values and fold activations of L455 variants in cell culture**

	9cRA		LG335	
Variant	EC <sub>50</sub> Value (nM)	Fold-Activation	EC <sub>50</sub> Value (nM)	Fold-Activation
RXRwt	400	31±9	690	12±3
LA	630	13±6	180	9.6±5.7
LF	>10,000	3±1	>10,000	2±1
LM	140	22±3	130	13±2
LV	130	17±6	170	11±4
LH	>10,000	2±1	>10,000	2.1±0.5
LK	>10,000	2±1	>10,000	1.6±0.3
LS	570	14±3	120	16±4
LT	390	16±6	200	11±6
LY	>10,000	3±1	>10,000	2.4±0.9
LC	580	23±3	170	9±3

The most surprising piece of data is that polar residues showed significant activation, indicating that the conserved hydrophobic nature of this residue could be changed such that activation profiles similar to the wild type receptor are achieved.

### **6.3 Assessment of the Double Variants L436V L455 and L436F L455**

#### **6.3.1 Testing of Double Variants in Chemical Complementation**

Recently, RXR crystal structures have been obtained with new ligands that have a mixture of agonist and antagonist properties, also known as nuclear receptor selective modulators. The analysis of these crystal structures showed the antagonistic properties of a ligand depends on the orientation of the L436 residue. Several studies have proposed that L436, a residue in the LBP of RXR, stabilizes H12 through van der Waals interaction with the L455 residue when a ligand binds [4, 17]. Ligands able to push L436 closer to L455 showed more antagonistic characteristics, due to steric interference with L455, causing the destabilization of H12 [18, 19]. Previously, Peet *et al.* have shown that mutating L436 to a valine, a smaller hydrophobic residue, severely decreases receptor activation [20]. The proposed reason for lost in activation was due to the fact that the L436V residue in the *holo* confirmation cannot effectively stabilize H12 since the interaction with the L455 residue is lost.

To further evaluate the effects of the L455 variants on receptor activity, these variants were tested in combination with the L436V residue, known to drastically reduce receptor activity. The idea was to investigate whether the L455M mutation (as well as other L455 mutations) could compensate for the lack of activation observed with the L436V mutation. The L436V mutation was added the L455 variants (L455A, L455C,

L455F, L455H, L455K, L455M, L455S, L455T, L455V, and L455Y) and RXRwt via site-directed mutagenesis. Primers containing the modified residue were used with the pGBDRXR plasmids to create the double variants of L436V L455, as well as the L436V single variant. The variants were then transformed into the PJ69-4A strain, grown on nonselective plates, and tested in ligand quantitation assays in adenine-selective media with a range of 9cRA and LG335 concentrations. As described in Chapter 3, in liquid quantitation assays, variants transformed into the PJ69-4A strain with the coactivator plasmid (pGAD10BAACTR) are placed in 96-well plates with adenine selective media with various concentrations of ligand and are incubated at 30°C with shaking. Optical density (OD) readings are taken at 630 nm at 0, 24, and 48 hours.

Figure 6.5 shows that the L436V single variant (brown squares) displayed no ligand-activated growth with either 9cRA or LG335, as expected, since this mutation was known to severely lower receptor activity [20]. Also, ligand-activated growth was not observed with any of the double variants in response to either ligand. The double variants are composed of the L436V mutation and one of the L455 mutations. The controls, Gal4 (green line) and RXRwt (blue circles) showed growth as expected. Gal4 grows regardless of the presence of ligand in the adenine selective media. RXRwt showed ligand-activated growth at 100 nM 9cRA (74 nM EC<sub>50</sub> value) with a 9-fold induction, and no growth with LG335, as observed in several other data sets. Therefore, the data shows that none of the L455 variants were able to compensate for the loss of activation when the L436V mutation is introduced.

Since the L436V variant is known to severely decrease receptor activity, perhaps the L455M or other L455 mutations could not compensate for such a dramatic loss in

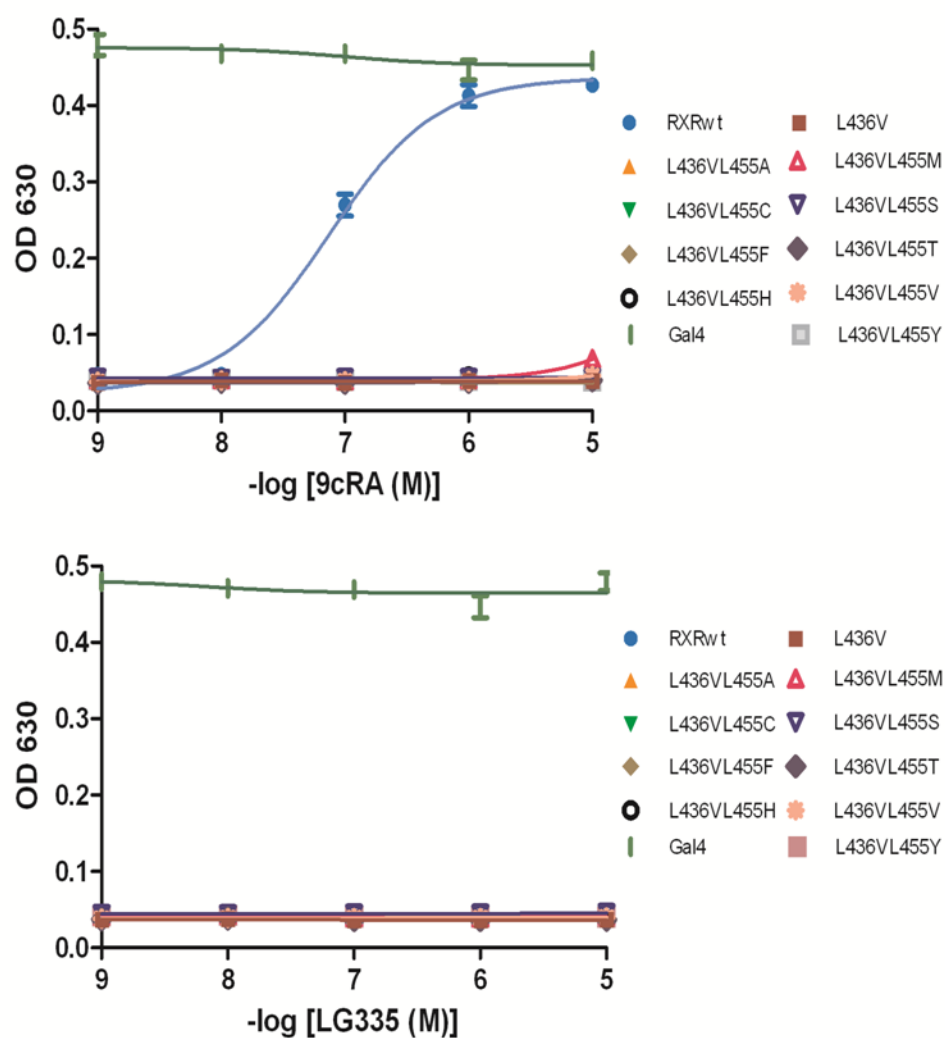


Figure 6.5: **Ligand-Activated Growth Profiles of L436V L455 Variants:** Gal4, RXRwt, L436V, L436VL455A, L436VL455C, L436VL455F, L436VL455H, L436VL455M, L436VL455S, L436VL455AT, L436VL455V, and L436VL455Y tested in liquid quantitation in adenine selective media (SC-ALW) with a range of 9cRA or LG335.

activation. Thus, the L436F mutation, which is also known to reduce receptor activity but not as drastically as the L436V mutation, was also tested. Again, the idea was that perhaps one of the L455 mutations could compensate for a slight loss of activity [20]. The L436F mutation was added to the L455 variants via site-directed mutagenesis. Variants were then transformed into the PJ69-4A strain, grown on nonselective plates, and tested in liquid quantitation assays in adenine-selective media with a range of 9cRA and LG335 concentrations as described above.

Figure 6.6 shows the single variant, L436F (brown square), with decreased ligand-activated growth, as expected, displaying growth at 1  $\mu$ M 9cRA (760 nM EC<sub>50</sub> value) with a 10-fold activation, and no growth with LG335. However, no growth was also observed with any of the double variants with either ligand. Again, Gal4 (green lines) showed growth independent of ligand, and RXRwt (blue circles) showed growth at 100 nM 9cRA (40 nM EC<sub>50</sub> value) with a 11-fold activation, and no growth with LG335. The results above show none of the double variants tested, L436V L455 or the L436F L455, were functional, indicating that the L455 mutations could not compensate for the loss of activation observed with the L436 variants. In fact, the addition of the L455 variants further destabilized the receptor, since all double variants displayed no ligand-activated growth.

### **6.3.2 Testing of Double Variants in Mammalian Cell Culture**

To confirm the results observed in yeast, a subset of L436V L455 variants were evaluated in mammalian cell assays. The double variants were created by adding the L436V mutation to the L455 variants on the pCMXRXRwt plasmids using site-directed mutagenesis and primers containing the L436V mutation. The double variant,

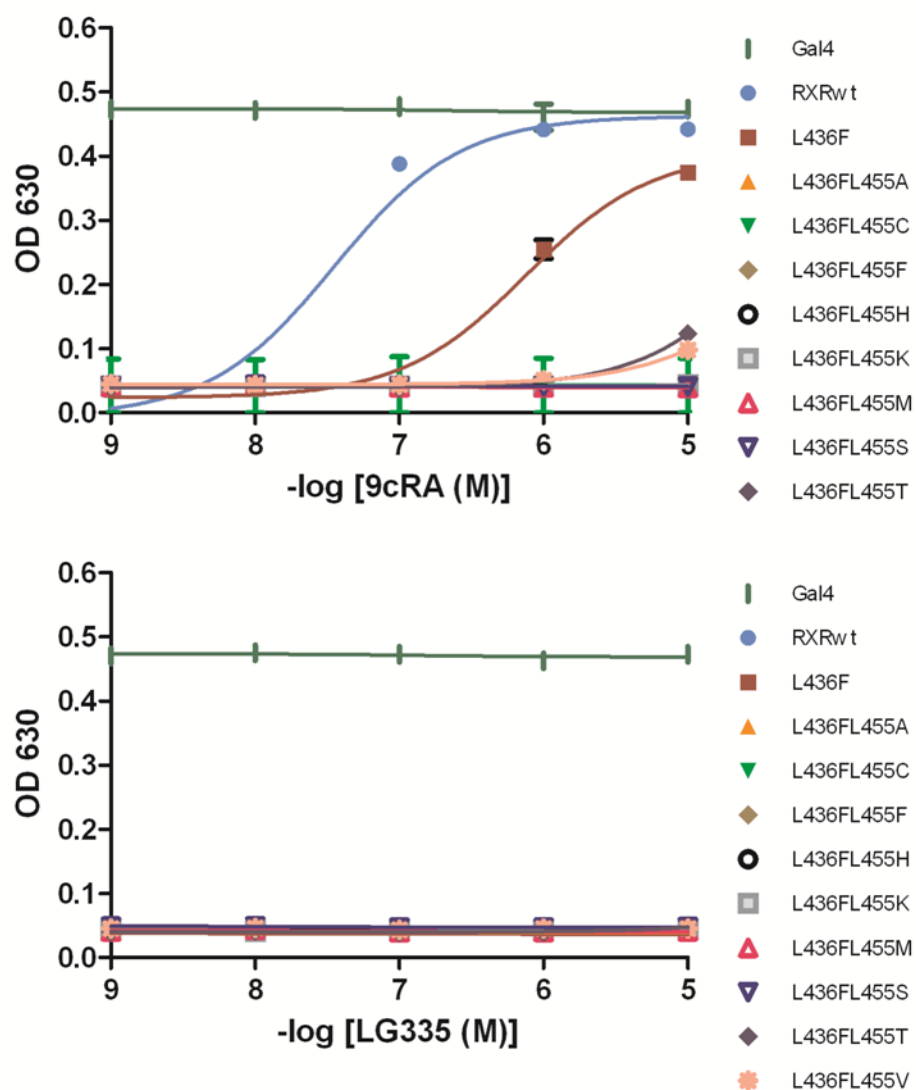


Figure 6.6: **Ligand-Activated Growth Profiles of L436F L455 Variants:** Gal4, RXRwt, L436F, L436FL455A, L436FL455C, L436FL455F, L436FL455H, L436FL455K, L436FL455M, L436FL455S, L436FL455T, and L436FL455Y tested in liquid quantitation in adenine selective media (SC-ALW) with a range of 9cRA or LG335.



L436VL455M, the single variants, L436V and L455M, and RXRwt were cotransfected with the pLuc\_CRBP<sub>II</sub> plasmid at a 1:2 molar ratio into HEK293T cells.

As shown in Figure 6.7, the L436V variant (purple squares) reduces the sensitivity and the function of the receptor with a 100-fold decrease in sensitivity towards 9cRA ( $EC_{50}$  value  $>10\text{ }\mu\text{M}$ ) and barely any activation with a  $6\pm 2$ -fold induction. The L436V variant also showed decrease activity with the synthetic ligand, LG335, displaying a  $1.7\text{ }\mu\text{M}$   $EC_{50}$  value and a  $5\pm 1$ -fold induction. The L455M variant showed enhanced activation, as expected, displaying a  $180\text{ nM}$   $EC_{50}$  value and a  $16\pm 1$ -fold induction with 9cRA, and a  $220\text{ nM}$   $EC$  value and a  $13\pm 3$ -fold induction in response to LG335. The double variant, L436V L455M (green diamonds), showed an  $EC_{50}$  value slightly lower than RXRwt. This variant displayed a  $100\text{ nM}$   $EC_{50}$  value in the presence of 9cRA (Figure 6.7), but with only  $8\pm 0.4$ -fold induction, significantly lower than wild type receptor. RXRwt displayed a  $410\text{ nM}$   $EC_{50}$  value and  $25\pm 3$ -fold activation in response to 9cRA. Interestingly, the double variant has a 10-fold increase in sensitivity towards LG335; a  $90\text{ nM}$   $EC_{50}$  value was observed with L436VL455M compared to the  $910\text{ nM}$   $EC_{50}$  value observed with RXRwt. The double variant also showed a  $17\pm 3$ -fold induction with LG335, comparable to RXRwt, which has a  $14\pm 4$ -fold induction. Also a lower  $EC_{50}$  values and similar fold activation was observe when comparing the double variant to RXRwt in the presence of LG335. Therefore, the L436VL455M variant restores activation of the receptor with lower  $EC_{50}$  values when compared to the L436V variant.

Two other variants were also evaluated for luciferase activity, L436V L455S and L436V L455T. Again, these variants were created by adding the L436V mutation to the pCMXRRL455S and pCMXRRL455T plasmids via site-directed PCR. The single

variants, the double variants, and RXRwt were cotransfected into HEK293T cells with pLuc\_CRBPII at a 1:2 molar ratio with a range of 9cRA. The activation profile of the L436V variant again showed an undetectable  $EC_{50}$  value and a low fold induction of  $7\pm 1$ -fold induction. As shown in Figure 6.8A, the single variant L455S has a 400 nM  $EC_{50}$  value with a  $9\pm 2$ -fold induction in response to 9cRA. When the L436V mutation is added to this variant, the receptor becomes practically nonfunctional, displaying a  $3\pm 2$ -fold induction. Therefore, the combination of the L455S and L436V leads to an inactive receptor.

When looking at the L436V L455T variant, a slight increase in sensitivity towards 9cRA and a higher fold induction is observed in comparison to the L436V variant (Figure 6.8B). The L436V L455T variant displays a 29  $\mu$ M  $EC_{50}$  value and a  $10\pm 1$ -fold induction in response to 9cRA. However, the activation is not comparable to the single variant L455T or RXRwt. The L455T variant displays a 480 nM  $EC_{50}$  value with a  $19\pm 3$ -fold induction, while RXRwt displays a 410 nM  $EC_{50}$  value and a  $14\pm 2$ -fold induction. Therefore, this variant is able to slightly compensate for the L436V mutation, but activation is not restored to wild type.

Our studies confirm that L436 is important for receptor activation and that the interaction of L436 and L455 is also crucial. The L455M variant is able to compensate for the loss of function when added to the L436V variant with 9cRA, and enhanced activation in the presence of LG335 is also observed. The L436V L455S double variant showed complete loss of activity; however, the L436V L455T double variant was able to show slightly enhanced activation over the L436V variant, but activation was still relatively low in comparison to RXRwt and the L455T single variant.

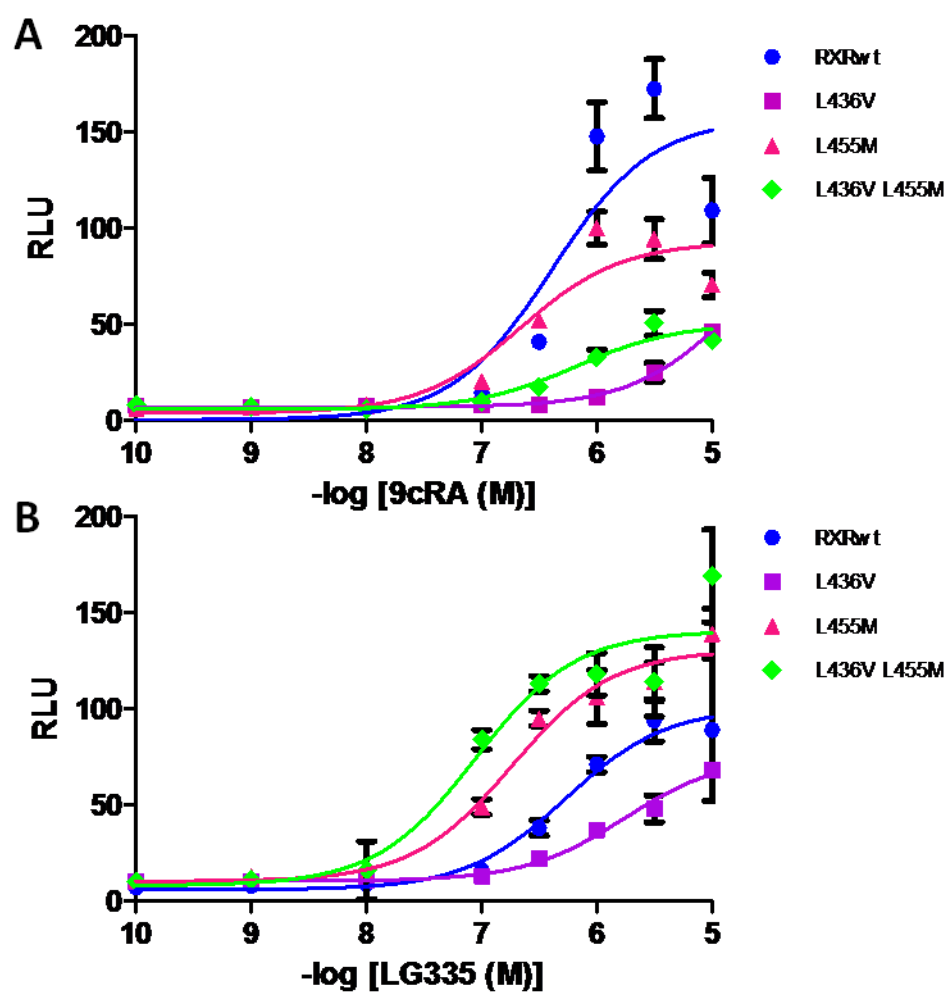
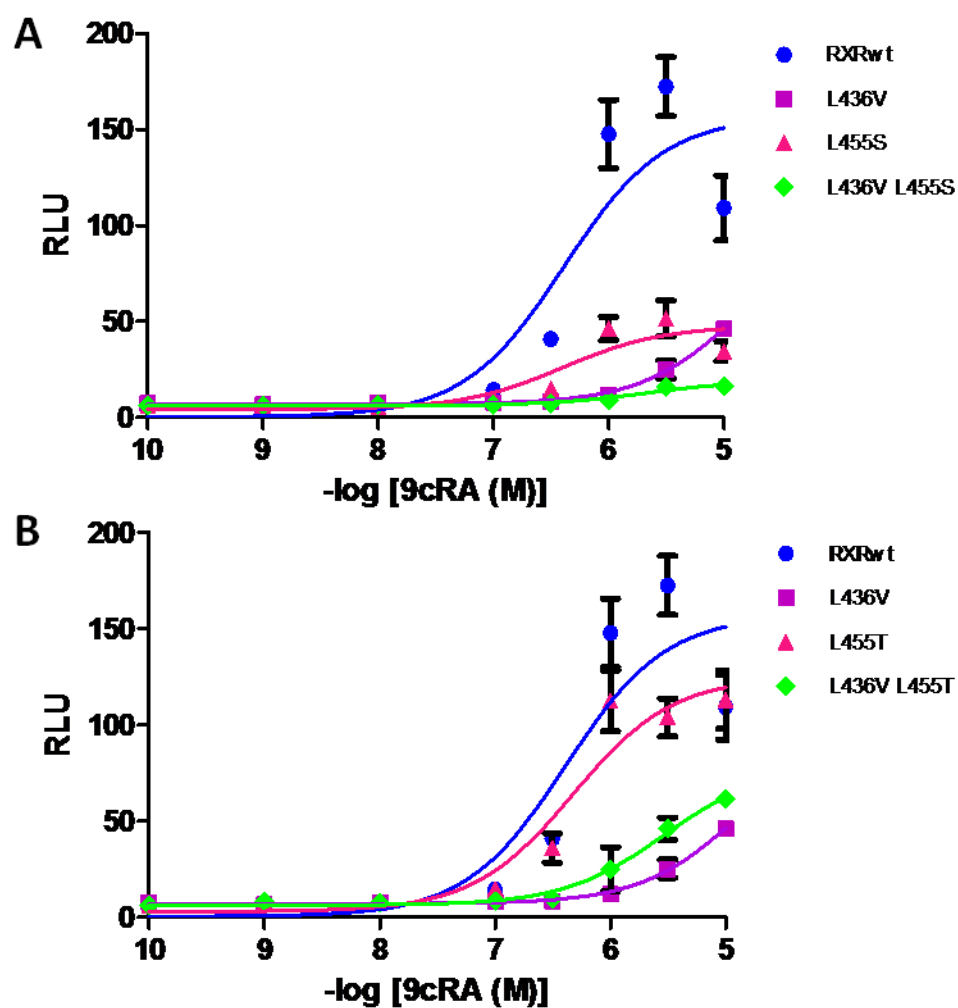


Figure 6.7: **Activation Profiles of L436V L455M in Cell Culture:** Activation profiles in HEK293T cells transfected with RXRwt, L436V, L455M, and L436VL455M in response to (A) 9cRA or (B) LG335.



**Figure 6.8 Activation Profiles of L436V L455S and L436V L455T in Cell Culture:**  
Activation profiles in HEK293T cells transfected with RXRwt, L436V, (A) L455S, L436V L455S, (B) L455T, and L436V L455T in response to 9cRA:

#### **6.4 Ligand-Activated Growth Profiles of L455 Variants with SRC-1 and ACTR**

As stated at the beginning of this chapter, once an agonist binds to the receptor, a conformational change takes place allowing coactivators to bind to the receptor for the initiation of transcription. The positioning of the AF-2 domain is crucial for coregulator interactions. An example of coregulators include the p160 steroid receptor coactivator (SRC) family, which directly interact with nuclear receptors, as well as, forms protein complexes with other factors that remodel chromatin or interact with general transcription factors. Therefore, these proteins provide a sophisticated process for gene regulation. Three members of the SRC family have been identified based on homology: SRC-1 (also known as NCoA-1), SRC-2 (also known as GRIP1, TIF2, or NCoA-2) and SRC-3 (also known as ACTR, p/CIP, RAC3, AIB1, TRAM-1) [21]. These coactivators are expressed in several types of tissues. The overexpression of the SRC proteins has been implicated in various cancers [21, 22], such as breast, ovarian and prostate cancer [23-26]. Therefore, several studies have investigated the interaction of coactivators with NR. Complete removal of the RXR AF-2 and mutational analysis on residues within this domain has lead to enhanced corepressor association and disassociation of coactivators [11, 27].

In relation to specific residues in RXR AF-2, the L455 residue has been mutated to an alanine, and a stronger association with corepressors was observed, correlating this residue to the functionality of H12 [11, 12]. H12 also plays an important role in inhibiting corepressor binding for RXR. The tetramer formed by RXR in the absence of ligand is partly due to the factor that H12 can bind to the corepressor binding site on an adjunct monomer, silencing the receptor [28, 29].

One of the proposed reasons why the L455M variant has increased sensitivity towards LG335 could be due to the enhanced interaction with coactivators. To investigate whether the different coactivators display various growth profiles, chemical complementation (CC) was used. CC provides the advantage of using yeast based assay, free of interference from endogenous receptors and coactivators seen in mammalian cells. Yeast are simple eukaryotes that have the essential transcription machinery, similar to mammalian cell, but lack nuclear receptors and certain coactivators [30, 31]. Therefore, this system is suitable for examining interaction of the RXR variants with known coactivators, since specific NR and coactivators can be introduced and analyzed without the possibility of interference from other proteins.

RXR variants subjected to chemical complementation were first transformed in the PJ69-4A strain with either SRC-1 or ACTR (activator for thyroid hormone and retinoid receptor, also known as SRC-3) and grown on nonselective media plates. Variants were then tested in liquid quantitation assays with media lacking the essential nutrient adenine, but have the desired small molecule 9cRA or LG335. Only functional variants that can be activated by the ligand and associate with the coactivator should grow in the adenine selective media.

As shown in Figure 6.9, the positive control full length Gal4, a ligand independent transcription factor [32], showed growth regardless of ligand or coactivator, as expected. Growth was observed for RXRwt at 100 nM 9cRA (~40 nM EC<sub>50</sub> value) regardless of which coactivator was present with approximately a 10-fold activation and no growth was observed with LG335. The single variants (Figure 6.10), L455A, L455F, L455H, L455K, and L455Y showed no ligand-activated growth with either ligand (9cRA or

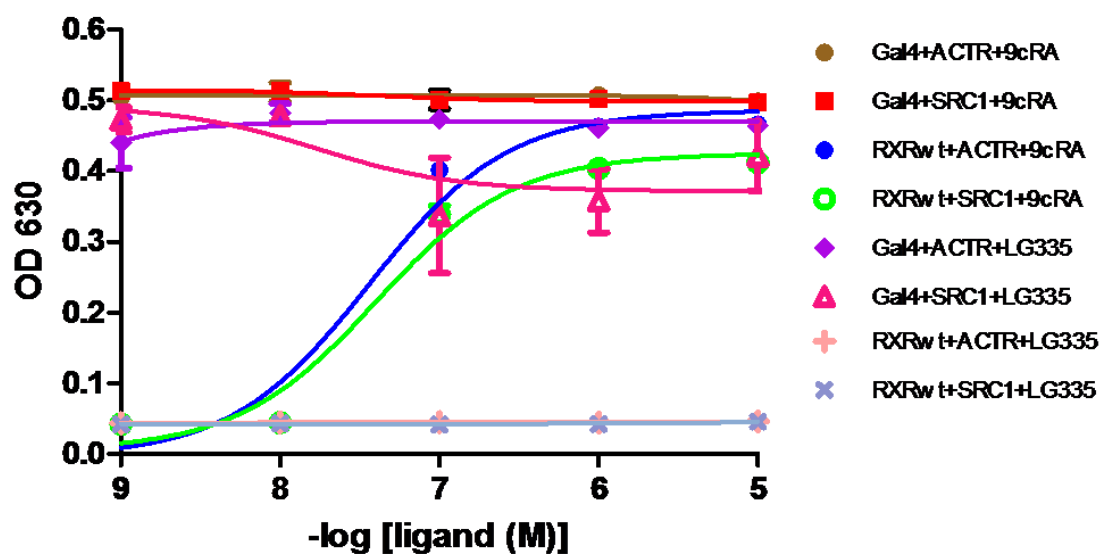


Figure 6.9: **Ligand-Activated Growth Profiles in Gal4 and RXRwt with ACTR and SRC-1:** Gal4 and RXRwt tested in liquid quantitation in adenine selective media (SC-ALW) and a range of 9cRA or LG335 and the ACTR and SRC-1 coactivator.

LG335) or coactivator (ACTR or SRC-1). These results were expected due to the factor that these variants either show no or very little activation in cell culture.

Some variants did not have a preference for either coactivator, as shown in Figure 6.11. The L455C variant is activated at 1  $\mu$ M 9cRA with both coactivators with a 9-fold activation, and no growth is observed with LG335 (Figure 6.11A). The single variant L455T also shows no preference for either coactivator displaying ligand-activated growth at 100 nM 9cRA ( $\sim$ 30 nM EC<sub>50</sub> value) (Figure 6.11B), and displayed growth at 10  $\mu$ M LG335 with this variant (EC<sub>50</sub> value >10  $\mu$ M).

The L455V variant exhibits a slight preference for the ACTR coactivator over the SRC-1 coactivator; a lower EC<sub>50</sub> value (48 nM) and higher fold activation (9-fold) was observed with ACTR than with SRC-1 (150 nM EC<sub>50</sub> value and 7-fold activation was observed with SRC-1) (Figure 6.11C). One of the most significant differences was observed with the L455S variant, which displayed growth at 1  $\mu$ M 9cRA with ACTR, and growth was also observed at 10  $\mu$ M LG335 (EC<sub>50</sub> value >10 $\mu$ M) (Figure 6.12). No growth was observed with either ligand when L455S was tested with the SRC-1 coactivator.

Another significant difference was observed with the L455M variant. Ligand-activated growth was observed at 10 nM 9cRA (33 nM EC<sub>50</sub> value), and at 1  $\mu$ M LG335 (344 nM EC<sub>50</sub> value) with the ACTR coactivator. However this variant is constitutively active with the SRC-1 coactivator (Figure 6.13). The enhanced interaction of the L455M variant with SRC-1 might explain the enhanced activity observed in mammalian cells. Table 6.3 is a list of EC<sub>50</sub> values and fold-activations of the L455 variants with ACTR and SRC-1 in response to 9cRA and LG335.



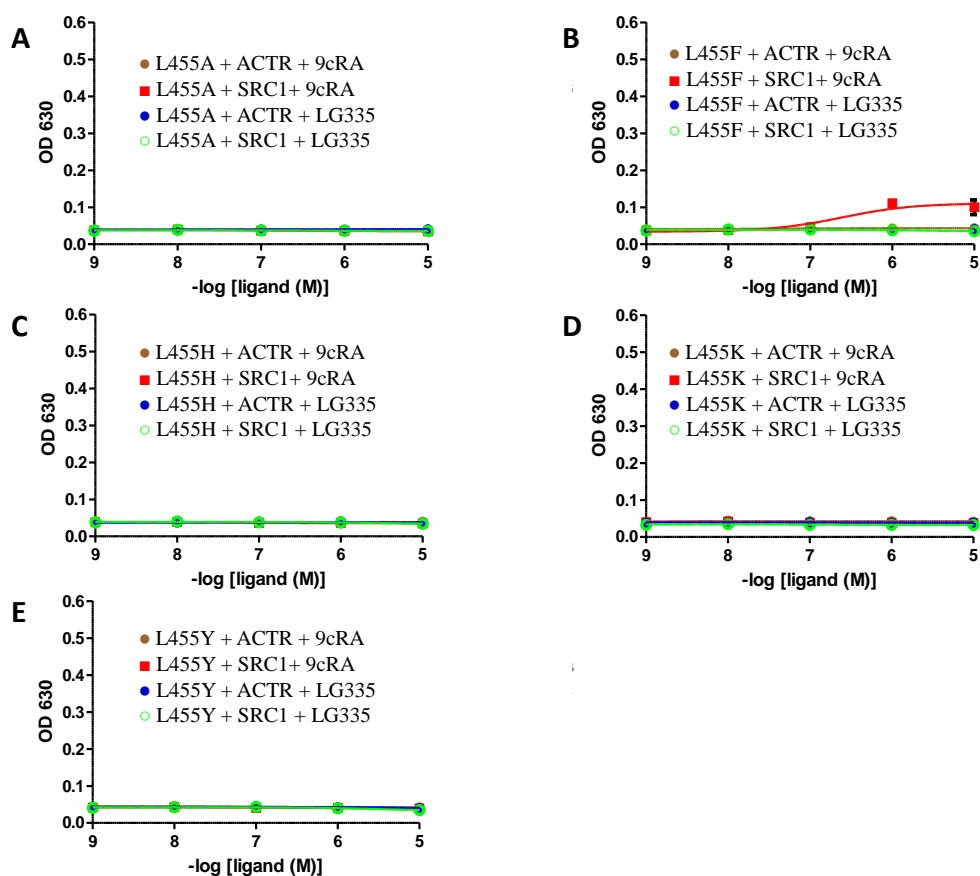


Figure 6.10: **Ligand-Activated Growth Profiles of L455A, L455F, L455H, L455K, and L455Y with ACTR and SRC-1:** (A) L455A, (B) L455F, (C) L455H, (D) L455K, and (E) L455Y tested in liquid quantitation in adenine selective media (SC-ALW) with a range of 9cRA or LG335 and either the ACTR or the SRC-1 coactivator.

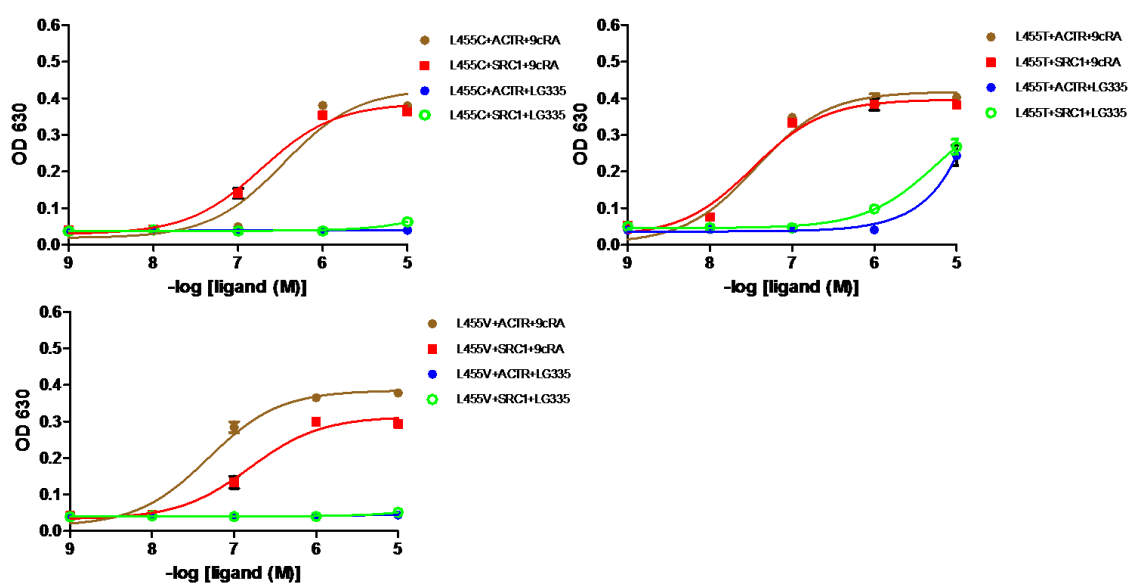


Figure 6.11: **Ligand-Activated Growth Profiles of L455C, L455T, and L455V with ACTR and SRC-1:** L455C, L455T, and L455V tested in liquid quantitation in adenine selective media (SC-ALW) with a range of 9cRA or LG335 and either the ACTR or the SRC-1 coactivator.

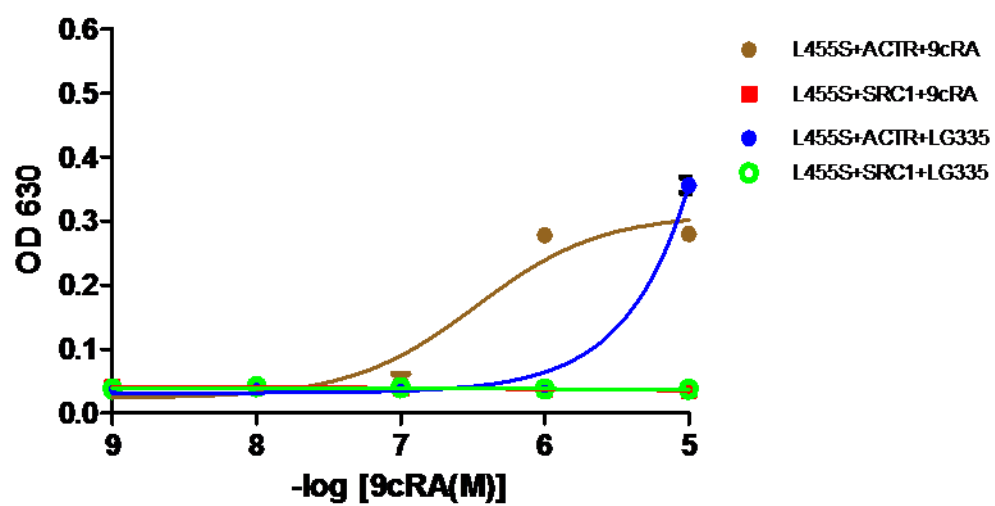


Figure 6.12: **Ligand-Activated Growth Profiles of L455S with ACTR and SRC-1:** L455S tested in liquid quantitation in adenine selective media (SC-ALW) with a range of 9cRA or LG335 and either the ACTR or the SRC-1 coactivator.

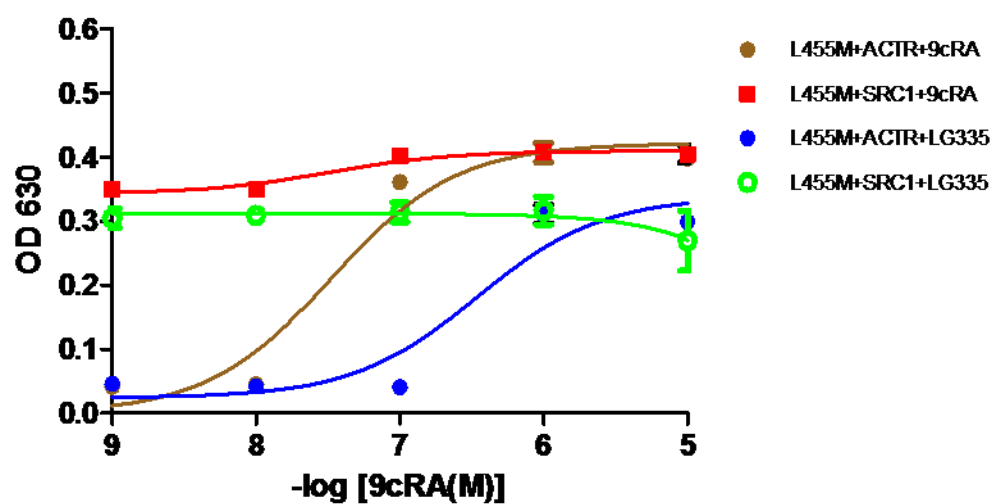


Figure 6.13: **Ligand-Activated Growth Profiles of L455M with ACTR and SRC-1:** L455M tested in liquid quantitation in adenine selective media (SC-ALW) with a range of 9cRA or LG335 and either the ACTR or the SRC-1 coactivator.

**Table 6.3: EC<sub>50</sub> values and fold activations of L455 variants in yeast**

	ACTR				SRC-1			
	9cRA		LG335		9cRA		LG335	
Variants	EC50 Value (nM)	Fold Activation	EC50 Value (nM)	Fold Activation	EC50 Value (nM)	Fold Activation	EC50 Value (nM)	Fold Activation
RXRwt	36	11	>10,000	1	40	10	>10,000	1
L455A	>10,000	1	>10,000	1	>10,000	1	>10,000	1
L455F	>10,000	1	>10,000	1	26	3	>10,000	1
L455M	33	10	344	8	>10,000	1	>10,000	1
L455V	48	9	>10,000	1	150	7	>10,000	1
L455H	>10,000	1	>10,000	1	>10,000	1	>10,000	1
>10,000	>10,000	1	>10,000	1	>10,000	1	>10,000	1
L455S	330	7	>10,000	9	>10,000	1	>10,000	1
L455T	36	9	>10,000	6	33	7	>10,000	6
L455Y	>10,000	1	>10,000	1	>10,000	1	>10,000	1
L455C	340	9	>10,000	1	190	9	>10,000	1

These results indicate that the mutations at the L455 position could potentially have an effect in selecting RXR's preference for different coactivators, such as in the case of the L455S variant, which shows a preference for ACTR in comparison to SRC-1. Surprisingly, the L455M variant is constitutively active with the SRC-1 coactivator, possibly the reason why enhanced activation is observed with this variant in cell culture. This study confirms the role of L455 in stabilizing the interaction of the receptor with their coregulators.

### **6.5 Ligand-Activated Growth Profiles of Double Variants with SRC-1 and ACTR**

A subset of double variants was also tested in chemical complementation with both coactivators. As controls, the single variants with mutations inside the ligand binding pocket, L436V and L436F, were also evaluated. The single variants (L436V and L436F) and a subset of double variants were transformed into the PJ69-4A strain with either ACTR or SRC-1 fused to the Gal4 activation domain (GAD) and grown on nonselective plates containing nonselective media. Variants were then tested in liquid quantitation assays in adenine selective media with either 9cRA or LG335.

The single variants, shown in Figure 6.14, had the same ligand-activated growth profile with both coactivators. The L436V variant showed no growth with either coactivator or ligand, and the L436F variant showed growth at 1  $\mu$ M 9cRA with both coactivators and no growth with LG335.

As expected, when evaluating the double variants L436VL455A and L436FL455A (Figure 6.15), no ligand activated growth was observed with either ligand or coactivator. This result was expected, since both mutations destabilize receptor

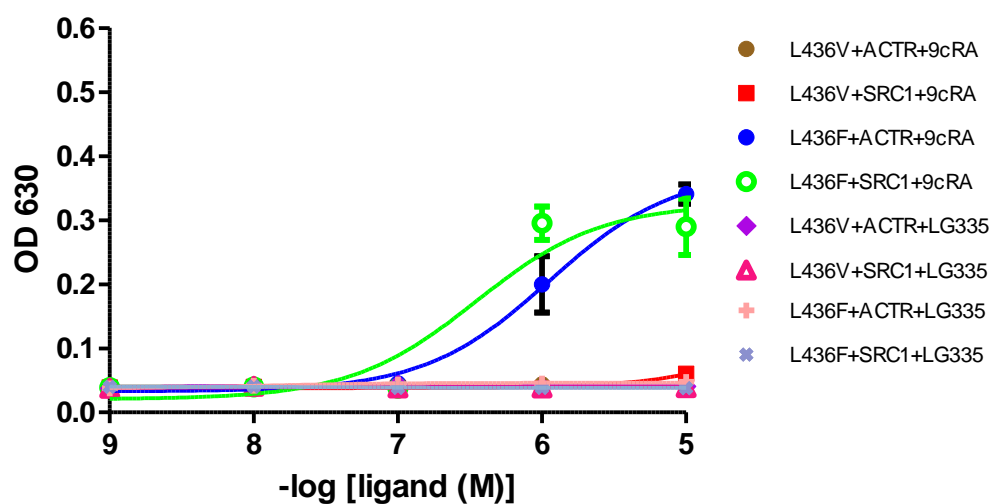


Figure 6.14: **Ligand-Activated Growth Profiles of L436V and L436F with ACTR and SRC-1:** L436V and L436F tested in liquid quantitation in adenine selective media (SC-ALW) with a range of 9cRA or LG335 and either the ACTR and or SRC-1 coactivator.

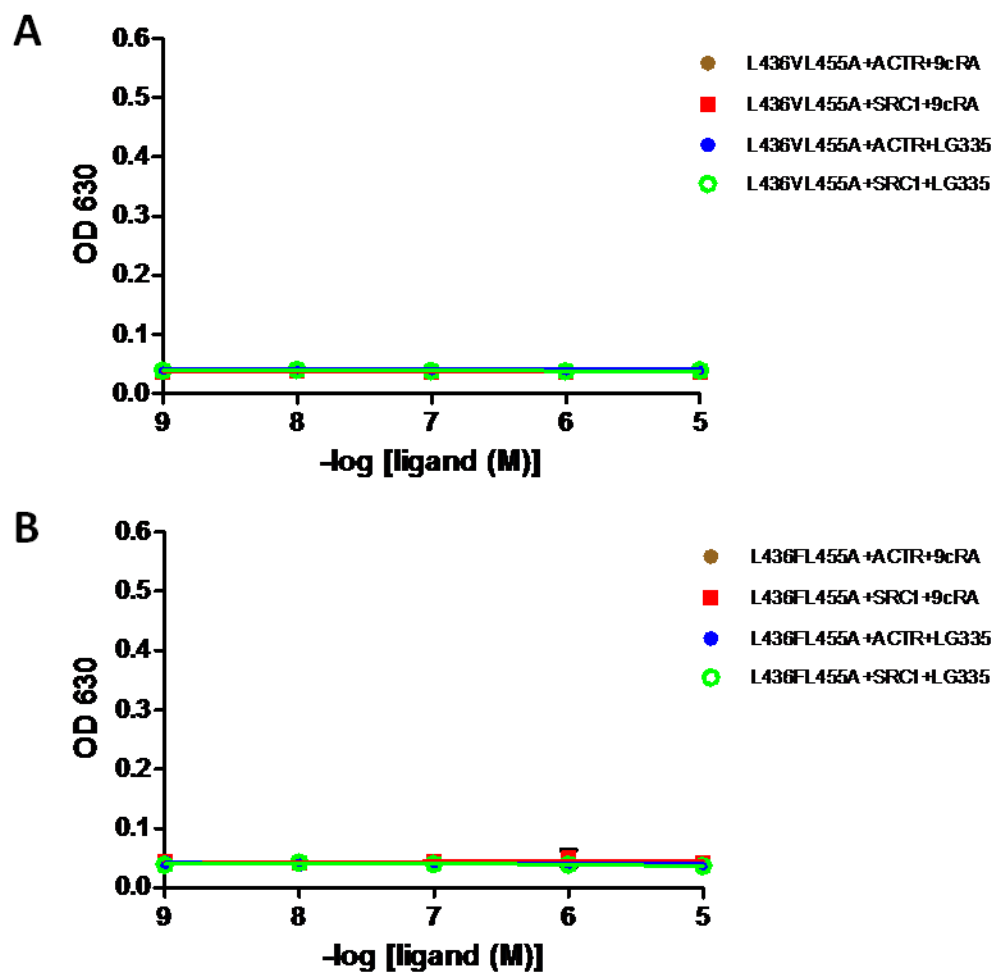


Figure 6.15: **Ligand-Activated Growth Profiles of L436V L455A and L436FL455A with ACTR and SRC-1:** (A) L436V L455A and (B) L436FL455A tested in liquid quantitation in adenine selective media (SC-ALW) with a range of 9cRA or LG335 and either the ACTR or the SRC-1 coactivator.



activity. As shown in Figure 6.16A, the double variant, L436VL455M, showed no growth with ACTR; however, growth is observed at 1  $\mu$ M 9cRA (3  $\mu$ M EC<sub>50</sub> value) and a 6-fold activation with the SRC-1 coactivator. Unfortunately, no growth is observed with either coactivator in response to LG335, which contradicts the cell culture data displayed in Figure 6.7, where the L436VL455M has the best activity in response to LG335. Since only two coactivators were tested this could be due to the association of this variant with other coactivators in the cells, or decreases interaction with corepressors. Also, the L436FL455M variant showed no growth with either coactivator or ligand (Figure 6.16B).

Interestingly, Figure 6.17 shows the L436VL455T variant preferred the SRC-1 coactivator, which was surprising since the single variant, L455T, did not have a preference for either coactivator. The L436VL455T variant showed ligand-activated growth at 1  $\mu$ M 9cRA (400 nM EC<sub>50</sub> value) and a 7-fold activation with SRC-1 and 10  $\mu$ M 9cRA (EC<sub>50</sub> value >10  $\mu$ M) and a 6-fold activation with ACTR (Figure 6.17A). The preference for the SRC-1 coactivator is also seen with the L436FL455T variants (Figure 6.17B), displaying a 290 nM EC<sub>50</sub> value and a 7-fold activation with 9cRA. The L436FL455T variant showed a 1.9  $\mu$ M EC<sub>50</sub> value and a 5-fold activation with the ACTR coactivator. Both the L436VL455T and the L436FL455T show no growth with the either coactivator in response to LG335. The preference for the SRC-1 coactivator was also seen in the L436VL455V and L436FL455V variants (Figure 6.18). The L436VL455V variant showed ligand-activated growth at 10  $\mu$ M 9cRA (EC<sub>50</sub> value >10  $\mu$ M) with a 4-fold activation with SRC-1 (Figure 6.18A). The L436FL455V variant displayed a 300 nM EC<sub>50</sub> value and a 7-fold activation in response to 9cRA with SRC-1 (Figure 6.18B), and

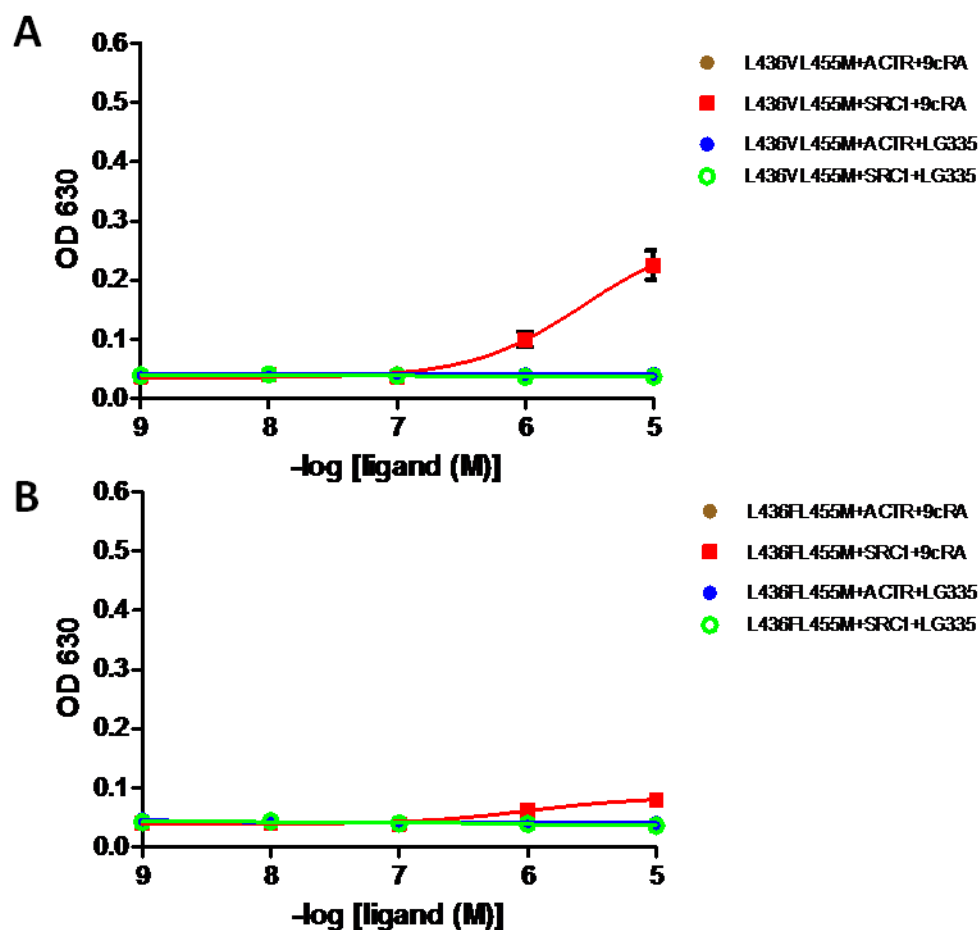


Figure 6.16: **Ligand-Activated Growth Profiles of L436V L455M and L436F L455M with ACTR and SRC-1:** (A) L436VL455M and (B) L436FL455M tested in liquid quantitation in adenine selective media (SC-ALW) with a range of 9cRA or LG335 and either the ACTR or the SRC-1 coactivator.

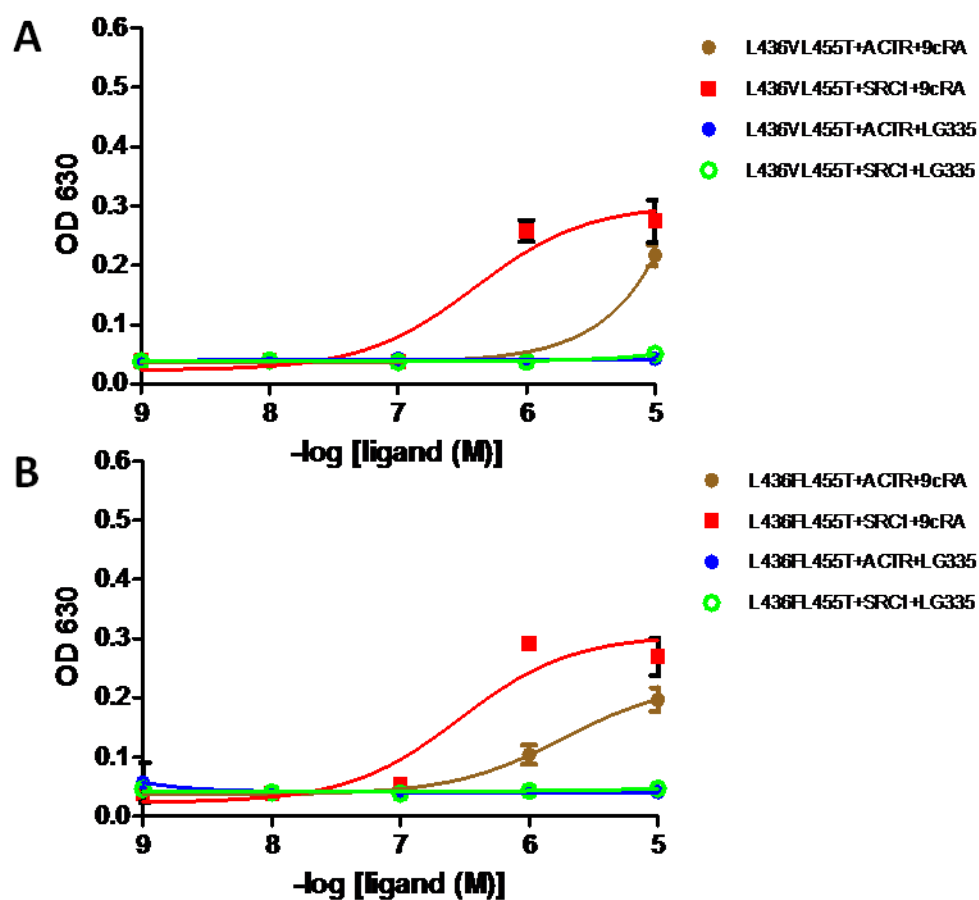


Figure 6.17: **Ligand-Activated Growth Profiles of L436V L455T and L436F L455T with ACTR and SRC-1:** (A) L436VL455T and (B) L436FL455T tested in liquid quantitation in adenine selective media (SC-ALW) with a range of 9cRA or LG335 and either the ACTR or the SRC-1 coactivator.

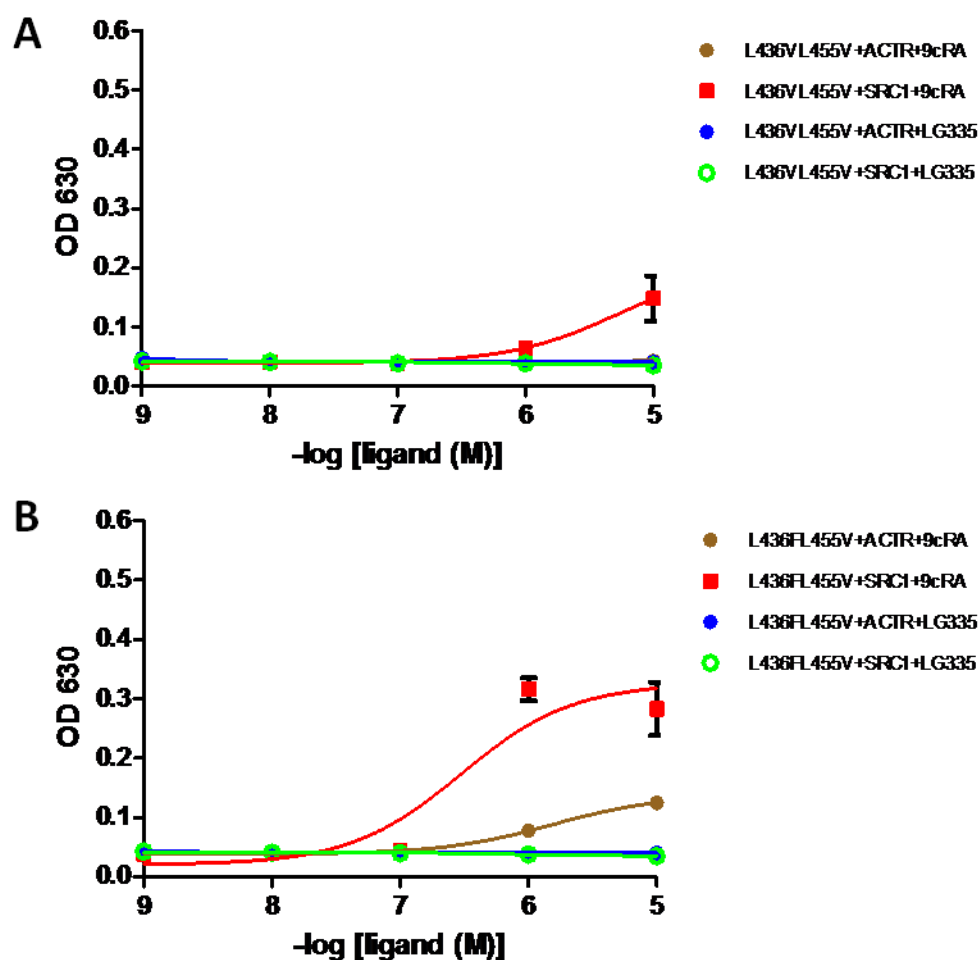


Figure 6.18: **Ligand-Activated Growth Profiles of L436V L455V and L436F L455V with ACTR and SRC-1:** (A) L436VL455V and (B) L436FL455V tested in liquid quantitation in adenine selective media (SC-ALW) with a range of 9cRA or LG335 and either the ACTR or the SRC-1 coactivator.

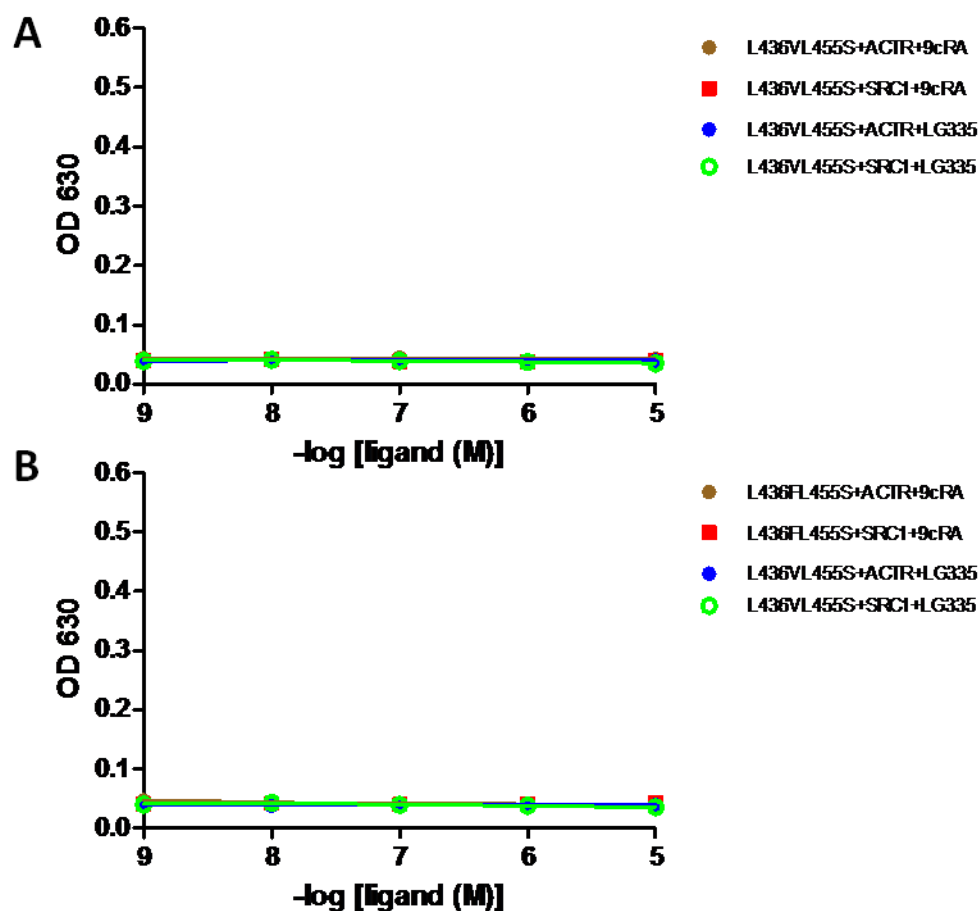


Figure 6.19: **Ligand-Activated Growth Profiles of L436V L455S and L436F L455S with ACTR and SRC-1:** (A) L436VL455S and (B) L436FL455S tested in liquid quantitation in adenine selective media (SC-ALW) with a range of 9cRA or LG335 and either the ACTR or the SRC-1 coactivator.

**Table 6.4: EC<sub>50</sub> values and fold activations of L436VL455 and L436FL455 variants in yeast**

	ACTR				SRC-1			
	9cRA		LG335		9cRA		LG335	
Variants	EC50 Value (nM)	Fold Activation	EC50 Value (nM)	Fold Activation	EC50 Value (nM)	Fold Activation	EC50 Value (nM)	Fold Activation
L436V	>10,000	1	>10,000	1	>10,000	1	>10,000	1
L436F	1100	9	>10,000	1	350	8	>10,000	1
L436VL455A	>10,000	1	>10,000	1	>10,000	1	>10,000	1
L436FL455A	>10,000	1	>10,000	1	26	3	>10,000	1
L436VL455M	>10,000	1	>10,000	1	2840	6	>10,000	1
L436FL455M	>10,000	1	>10,000	1	>10,000	1	>10,000	1
L436VL455S	>10,000	1	>10,000	1	>10,000	1	>10,000	1
L436FL455S	>10,000	1	>10,000	1	>10,000	1	>10,000	1
L436VL455T	>10,000	6	>10,000	1	>10,000	7	>10,000	1
L436FL455T	1900	5	>10,000	1	290	7	>10,000	1
L436VL455V	ND	1	>10,000	1	>10,000	4	>10,000	1
L436FL455V	1600	3	>10,000	1	300	7	>10,000	1

only showing a 3-fold activation with the ACTR coactivator. The L436VL455V and L436FL455V variants showed no growth in response to LG335 with both coactivators. Lastly, the L436VL455S variant showed no growth with either coactivator (Figure 6.19). This was not surprising since the previous results showed the single variant, L455S had a preference for ACTR, and most double variants did not displayed ligand-activated growth with the ACTR coactivator.

The data also shows that mutations within the ligand binding pocket do not exhibit a preference for either coactivator. The single variants, L455T and L455V, showed no preference for a coactivator; however, in the combination with the L436V or the L436F mutations, these double variants displayed a more pronounced preference to the SRC-1 coactivator. Interestingly, the L455M variant was found to be constitutively active with the SRC-1 coactivator, but ligand activation was observed when the L436V mutation was added to L455M at 1  $\mu$ M 9cRA. This data also infers that the L436 residue is directly affected by the presence of the L455 residue, since specific mutations at this position ultimately affect the association of the receptor and the coactivator. Overall, this data confirms that the L455 position is crucial for coactivator interactions.

In summary, this chapter looks into the importance of the L455 position and understanding the affect this residue has on the activity of RXR. First, the L455 position was mutated to several amino acids to analyze the tolerance at this position. Results from this section show that hydrophobic and polar residues that are similar in volume to leucine, displayed activation profiles comparable to RXRwt. The L455 variants were then analyzed with various L436 mutations to determine if one of the L455 mutations could rescue a nonfunctional variant. The results from this section showed that the

L436V L455M mutation could restore receptor activity, especially with LG335. Lastly, the interaction with the ACTR and the SRC-1 coactivators were examined in chemical complementation, where the L455 residue was shown to impact coactivator interaction with the receptor.

## **6.6 Materials and Methods**

### *Plasmid Construct*

The L455 mutations (L455A, L455C, L455F, L455H, L455K, L455M, L455S, L455T, L455V, and L455Y) were added to pGBDRXR and pCMXRXRwt plasmid by subjecting plasmids to site-directed mutagenesis with primers containing the appropriate mutation. The L436V and the L436F mutations were added to the single pGBDRXR and pCMXRXR plasmids using site-directed mutagenesis and primers containing either L436V or L436F mutation.

### *Liquid quantitation assays*

The single and double variants were tested in liquid quantitation assays by transforming the variants and the coactivator plasmid (pGAD10BAACTR or pGAD10BASRC1) into the PJ69-4A strain, and grown overnight in nonselective media (SC-LW) at 30°C with shaking at 300 rpm. Then testing in adenine selective media as described in chapter 5.

### *Mammalian Cell Culture assays*

The single and double variants were tested in cell culture assays by cotransfecting HEK293T cell with the pCMXRXR plasmid with the respective mutation and the



pLuc\_CRBP<sub>II</sub> plasmid at a 1:2 molar ratio. The transfection and the assessment for luciferase and  $\beta$ -galactosidase activity are described in Chapter 3.

## 6.7 Literature Cited

1. Chambon, P., *The nuclear receptor superfamily: a personal retrospect on the first two decades*. Mol Endocrinol, 2005. **19**(6): p. 1418-28.
2. Gronemeyer, H., J.A. Gustafsson, and V. Laudet, *Principles for modulation of the nuclear receptor superfamily*. Nat Rev Drug Discov, 2004. **3**(11): p. 950-64.
3. Egea, P.F., A. Mitschler, N. Rochel, M. Ruff, P. Chambon, and D. Moras, *Crystal structure of the human RXR  $\alpha$  ligand-binding domain bound to its natural ligand: 9-cis retinoic acid*. Embo Journal, 2000. **19**(11): p. 2592-2601.
4. Nahoum, V., E. Perez, P. Germain, F. Rodriguez-Barrios, F. Manzo, S. Kammerer, G. Lemaire, O. Hirsch, C.A. Royer, H. Gronemeyer, A.R. de Lera, and W. Bourguet, *Modulators of the structural dynamics of the retinoid X receptor to reveal receptor function*. Proceedings of the National Academy of Sciences of the United States of America, 2007. **104**(44): p. 17323-17328.
5. Chambon, P., *A decade of molecular biology of retinoic acid receptors*. Faseb Journal, 1996. **10**(9): p. 940-954.
6. Collingwood, T.N., O. Rajanayagam, M. Adams, R. Wagner, V. Cavailles, E. Kalkhoven, C. Matthews, E. Nystrom, K. Stenlof, G. Lindstedt, L. Tisell, R.J. Fletterick, M.G. Parker, and V.K.K. Chatterjee, *A natural transactivation mutation in the thyroid hormone beta receptor: Impaired interaction with putative transcriptional mediators*. Proceedings of the National Academy of Sciences of the United States of America, 1997. **94**(1): p. 248-253.
7. Jurutka, P.W., J.C. Hsieh, L.S. Remus, G.K. Whitfield, P.D. Thompson, C.A. Haussler, J.C.G. Blanco, K. Ozato, and M.R. Haussler, *Mutations in the 1,25-dihydroxyvitamin D-3 receptor identifying C-terminal amino acids required for transcriptional activation that are functionally dissociated from hormone binding, heterodimeric DNA binding, and interaction with basal transcription factor IIB, in vitro*. Journal of Biological Chemistry, 1997. **272**(23): p. 14592-14599.

8. Ito, M., K. Fukuzawa, T. Ishikawa, Y. Mochizuki, T. Nakano, and S. Tanaka, *Ab initio fragment molecular orbital study of molecular interactions in liganded retinoid X receptor: specification of residues associated with ligand inducible information transmission*. J Phys Chem B, 2008. **112**(38): p. 12081-94.
9. Tone, Y., T.N. Collingwood, M. Adams, and V.K. Chatterjee, *Functional analysis of a transactivation domain in the thyroid hormone beta receptor*. J Biol Chem, 1994. **269**(49): p. 31157-61.
10. Ito, M., K. Fukuzawa, Y. Mochizuki, T. Nakano, and S. Tanaka, *Ab initio fragment molecular orbital study of molecular interactions between liganded retinoid X receptor and its coactivator; part II: influence of mutations in transcriptional activation function 2 activating domain core on the molecular interactions*. J Phys Chem A, 2008. **112**(10): p. 1986-98.
11. Ghosh, J.C., X.F. Yang, A.H. Zhang, M.H. Lambert, H. Li, H.E. Xu, and J.D. Chen, *Interactions that determine the assembly of a retinoid X receptor/corepressor complex*. Proceedings of the National Academy of Sciences of the United States of America, 2002. **99**(9): p. 5842-5847.
12. Thompson, P.D., L.S. Remus, J.C. Hsieh, P.W. Jurutka, G.K. Whitfield, M.A. Galligan, C. Encinas Dominguez, C.A. Haussler, and M.R. Haussler, *Distinct retinoid X receptor activation function-2 residues mediate transactivation in homodimeric and vitamin D receptor heterodimeric contexts*. J Mol Endocrinol, 2001. **27**(2): p. 211-27.
13. Liu, H., C.K. Shaw, E.L. Reineke, Y. Liu, and H.Y. Kao, *Retinoid X receptor alpha (RXRalpha) helix 12 plays an inhibitory role in the recruitment of the p160 co-activators by unliganded RXRalpha/retinoic acid receptor alpha heterodimers*. J Biol Chem, 2004. **279**(43): p. 45208-18.
14. Reichert, J. and J. Suhnel, *The IMB Jena Image Library of Biological Macromolecules: 2002 update*. Nucleic Acids Res, 2002. **30**(1): p. 253-4.
15. Azizi, B. and D.F. Doyle. *Chemical complementation: a genetic selection system in yeast for drug discovery, protein and enzyme engineering*. 2006: Federation Amer Soc Exp Biol.
16. Lohr, D., P. Venkov, and J. Zlatanova, *Transcriptional regulation in the yeast gal gene family - A complex genetic network*. Faseb Journal, 1995. **9**(9): p. 777-787.

17. Santin, E.P., P. Germain, F. Quillard, H. Khanwalkar, F. Rodriguez-Barrios, H. Gronemeyer, A.R. Lera, and W. Bourguet, *Modulating Retinoid X Receptor with a Series of (E)-3-[4-Hydroxy-3-(3-alkoxy-5,5,8,8-tetramethyl-5,6,7,8-tetrahydronaphthalen-2-yl)phenyl]acrylic Acids and Their 4-Alkoxy Isomers*. Journal of Medicinal Chemistry, 2009. **52**(10): p. 3150-3158.
18. Nahoum, V., E. Perez, P. Germain, F. Rodriguez-Barrios, F. Manzo, S. Kammerer, G. Lemaire, O. Hirsch, C.A. Royer, H. Gronemeyer, A.R. de Lera, and W. Bourguet, *Modulators of the structural dynamics of the retinoid X receptor to reveal receptor function*. Proc Natl Acad Sci U S A, 2007. **104**(44): p. 17323-8.
19. Perez Santin, E., P. Germain, F. Quillard, H. Khanwalkar, F. Rodriguez-Barrios, H. Gronemeyer, A.R. de Lera, and W. Bourguet, *Modulating retinoid X receptor with a series of (E)-3-[4-hydroxy-3-(3-alkoxy-5,5,8,8-tetramethyl-5,6,7,8-tetrahydronaphthalen-2-yl)phenyl]acrylic acids and their 4-alkoxy isomers*. J Med Chem, 2009. **52**(10): p. 3150-8.
20. Peet, D.J., D.F. Doyle, D.R. Corey, and D.J. Mangelsdorf, *Engineering novel specificities for ligand-activated transcription in the nuclear hormone receptor RXR*. Chemistry & Biology, 1998. **5**(1): p. 13-21.
21. Xu, J. and Q. Li, *Review of the in vivo functions of the p160 steroid receptor coactivator family*. Mol Endocrinol, 2003. **17**(9): p. 1681-92.
22. Xu, J., R.-C. Wu, and B.W. O'Malley, *Normal and cancer-related functions of the p160 steroid receptor co-activator (SRC) family*. Nat Rev Cancer, 2009. **9**(9): p. 615-630.
23. Hussein-Fikret, S. and P.J. Fuller, *Expression of nuclear receptor coregulators in ovarian stromal and epithelial tumours*. Mol Cell Endocrinol, 2005. **229**(1-2): p. 149-60.
24. Hudelist, G., K. Czerwenka, E. Kubista, E. Marton, K. Pischinger, and C.F. Singer, *Expression of sex steroid receptors and their co-factors in normal and malignant breast tissue: AIB1 is a carcinoma-specific co-activator*. Breast Cancer Res Treat, 2003. **78**(2): p. 193-204.
25. Gregory, C.W., B. He, R.T. Johnson, O.H. Ford, J.L. Mohler, F.S. French, and E.M. Wilson, *A mechanism for androgen receptor-mediated prostate cancer*

- recurrence after androgen deprivation therapy*. Cancer Res, 2001. **61**(11): p. 4315-9.
26. Gnanapragasam, V.J., H.Y. Leung, A.S. Pulimood, D.E. Neal, and C.N. Robson, *Expression of RAC 3, a steroid hormone receptor co-activator in prostate cancer*. Br J Cancer, 2001. **85**(12): p. 1928-36.
  27. Liu, H., C.K. Shaw, E.L. Reineke, Y. Liu, and H.Y. Kao, *Retinoid X receptor alpha (RXR alpha) helix 12 plays an inhibitory role in the recruitment of the p160 co-activators by unliganded RXR alpha/retinoic acid receptor alpha heterodimers*. Journal of Biological Chemistry, 2004. **279**(43): p. 45208-45218.
  28. Kersten, S., P.R. Reczek, and N. Noy, *The tetramerization region of the retinoid X receptor is important for transcriptional activation by the receptor*. J Biol Chem, 1997. **272**(47): p. 29759-68.
  29. Kersten, S., D. Kelleher, P. Chambon, H. Gronemeyer, and N. Noy, *Retinoid X receptor alpha forms tetramers in solution*. Proc Natl Acad Sci U S A, 1995. **92**(19): p. 8645-9.
  30. Malik, S. and R.G. Roeder, *Transcriptional regulation through Mediator-like coactivators in yeast and metazoan cells*. Trends Biochem Sci, 2000. **25**(6): p. 277-83.
  31. Guarente, L., *Transcriptional coactivators in yeast and beyond*. Trends Biochem Sci, 1995. **20**(12): p. 517-21.
  32. Traven, A., B. Jelacic, and M. Sopta, *Yeast Gal4: a transcriptional paradigm revisited*. Embo Reports, 2006. **7**(5): p. 496-499.

## CHAPTER 7

### CONCLUSIONS AND FUTURE WORK

#### 7.1 The Molecular Switch System

##### 7.1.1 Conclusions

Two orthogonal ligand receptor pairs (OLRP) were characterized as molecular switches to provide controlled gene expression and potentially benefit gene therapy applications. One of the major challenges in gene therapy is the lack of transcriptional control of exogenously introduced genes. Thus, creating molecular switch systems with the ability to regulate target genes through activation by a small molecule should provide a pathway for controlling gene expression. One potential target gene is the homeobox gene *HOXB4*, which has been shown to repopulate hematopoietic stem cells in mice, and potentially could be used to treat patients with immune deficiency disorders [1-3].

OLRP were designed and created using nuclear receptors by taking advantage of the modular structure of these receptors and their function in gene regulation. As ligand-activated transcription factors, these receptors serve as regulators of transcription in various cells, regulating metabolic and physiological processes. Previous work had manipulated the structure of these modular proteins by developing variants capable of activating in response to the synthetic ligand LG335 rather than the natural ligand 9-*cis* retinoic acid (9cRA). These constructs were then further modified to contain a Gal4 DNA binding domain (DBD) fused to either the RXR variant 130 (I268A, I310A, F313A, and L436F) ligand binding domain (LBD) (also known as GR130) or the RXR variant QCIMFI (Q275C, I310M, and F313I) LBD (also known as GRQCIMFI). Gal4 is a yeast

transcription factor that binds Gal4 RE, a sequence not present in mammalian cells. Both molecular switches are able to bind Gal4 RE in response to LG335 and activate expression of a reporter gene in either a two- or one-component system. The two-component system has the molecular switch on one plasmid, and the artificial promoter and reporter gene on a separate plasmid. While the one-component system contains all system components on a single plasmid. When characterizing the GR130 variant in the two-component system, orthogonal characteristics were observed since no activation occurred with the natural ligand 9cRA, and activation occurs in response to the synthetic ligand LG335. This variant displayed a  $19 \pm 5$ -fold activation and a 50 nM  $EC_{50}$  value in the presence of LG335. When GR130 was tested in the one-component system with the luciferase gene, reduced luciferase activity was observed in the presence of LG335, displaying a 2-fold increase in the  $EC_{50}$  value (100 nM) compared to the two-component system, and a lower fold activation of  $3 \pm 1$ -fold. The data with the green fluorescent protein (GFP) in the one-component system, where the reporter gene was switched from luciferase to GFP, was inconclusive, as the sequence of the variant tested was not confirmed to be GR130. GR130 displayed insufficient gene expression in the one-component system with the luciferase reporter gene and was not successfully characterized with the GFP reporter gene. Therefore GRQCIMFI was selected as the appropriate variant to use as this variant was characterized in both the two- and one-component systems.

When the GRQCIMFI variant was evaluated in the two-component system, activation was observed in the presence of LG335 with a 10 nM  $EC_{50}$  value and a  $6 \pm 2$ -fold induction, and 9cRA induced activation only at the highest concentration. A comparable

fold induction was observed when the GRQCIMFI variant was cloned into the one-component system, displaying a  $6\pm 1$ -fold induction but a higher  $EC_{50}$  value of 270 nM. The GRQCIMFI variant was also characterized in a transient transfection with a one-component system containing the reporter gene GFP, and showed green fluorescence in 30% of the cells in the presence of 10  $\mu$ M LG335. The one-component system can also be introduced virally into NIH3T3 cells, and 30% of the cells were able to stably express GFP in the presence of 10  $\mu$ M LG335. However, the fluorescence intensity was significantly decreased in the cells stably transduced with retrovirus in comparison to cells that were transiently transfected.

A comparison of the two variants revealed advantages and disadvantages for each molecular switch. The GR130 variant is not activated by the natural ligand 9cRA; therefore this variant should not influence endogenous pathways. This variant also displays a higher fold induction when compared to the GRQCIMFI variant in the two-component system. The GR130 variant displays a  $19\pm 5$ -fold induction, whereas GRQCIMFI displays a  $6\pm 2$ -fold induction. GRQCIMFI is activated at slightly lower concentrations of LG335 in the two-component; displaying a 10 nM  $EC_{50}$  value whereas the GR130 variant displays a 50 nM  $EC_{50}$  value. In the one-component system, GRQCIMFI exhibits a consistent fold induction of  $6\pm 1$ -fold whereas the fold induction of GR130 significantly decreases to  $3\pm 1$ -fold.

Since GRQCIMFI was more accurately assessed, this variant was further characterized to determine whether the criteria for molecular switch systems discussed in Chapter 2 were met. The first criterion included the ability to turn on and off transgene expression upon the addition of ligand. As was discussed in the section above,

GRQCIMFI was able to control gene expression of both the luciferase and GFP reporter genes. However, a significant amount of basal expression was observed which lowered the fold induction and leaky expression could be problematic if this system is analyzed in animal model studies. The molecular switch could be further developed by increasing the fold induction, which can be achieved by either lowering the basal activity or increasing the amount of activation. Activation of the molecular switch at lower concentrations of ligand would also be advantageous as low drug dosages are desirable in gene therapy trials.

One approach taken to improve the fold induction of GRQCIMFI was to add an activation domain, a protein domain that is known to stimulate transcription. Several molecular switch systems have incorporated an activation domain as a means to improve fold induction. In the initial development of the GeneSwitch® system, the VP16 activation domain was fused to the C-terminus region of this chimeric protein, enhancing the activation approximately 50-fold [4]. The most current Rheoswitch® system, which consists of two fusion proteins: a hybrid DBD fused to an EcR LBD, and a RXR LBD fused to the VP16 activation domain, displays approximately a 10,000-fold induction [5]. The VP16 activation domain was fused to the N-terminus region of GRQCIMFI in an effort to increase the fold induction. However, the addition of the VP16 created a constitutively active protein, since the luciferase gene was expressed regardless of the presence of ligand. A constitutively active receptor is ineffective in a molecular switch system since the target gene cannot be turned off.

VP16 is known to be a potent activation domain; therefore, alternate activation domains should be assessed with the molecular switch to determine whether a higher fold



activation could be achieved. For example, the GeneSwitch® system was optimized by replacing the VP16 activation domain with the human p65 activation domain, which reduced the basal activity levels and minimized potential immunogenic reactions [6]. Several activation domains have been characterized, such as Oct1, Oct2, Sp1, p65, and ITF-1, that are able to stimulate transcription [7].

Another approach used to enhance the fold-activation and sensitivity of the molecular switch incorporated error-prone PCR and chemical complementation to select for new variants with increased sensitivity towards LG335. This method produced a successful variant, Q275C, I310M, F313I, L455M (QCIMFILM), which displayed a 10-fold increase in sensitivity towards LG335 with a 5 nM EC<sub>50</sub> value. The additional mutation at the L455 position was further examined by assessing the location in the receptor. The RXR crystal structure revealed this residue is located outside of the ligand binding pocket and on helix 12 (H12), which was interesting since the residue lacks direct contact with the ligand but is able to significantly enhance receptor function. The QCIMFILM variant should next be characterized in the one-component system to show gene expression also takes place at lower levels of LG335.

The second criterion for a successful molecular switch system examines the specificity of the ligand to the molecular switch, and the specificity of the switch to the artificial promoter region. This is particularly important for ensuring that the molecular switch does not interfere with any endogenous pathways, preventing adverse side effects. The ligand or the molecular switch should not activate expression of endogenous genes, and conversely endogenous ligands or receptors should not activate expression of the target gene in the molecular switch system. The results presented in this work have

successfully shown that the molecular switch presented is specific to the artificial promoter region containing the Gal4 RE, since activation was not observed with endogenous RXR RE. Conversely, RXRwt is unable to activate genes controlled by the Gal4 RE, so endogenous receptors should not activate expression of the target gene in the molecular switch. However, improvements in the specificity of the ligand to the molecular switch are needed. The synthetic ligand LG335 is able to activate gene expression with the wild-type receptor with a  $4\pm 1$ -fold induction, but the fold induction is substantially lower than the  $10\pm 3$ -fold observed with RXRwt and the natural ligand 9cRA. The data also shows that  $10\text{ }\mu\text{M}$  9cRA activates GRQCIMFI, which could initiate transcription of genes controlled by the molecular switch in gene therapy applications. Although the concentration of endogenous 9cRA remains controversial, studies have revealed nanomolar concentration of 9cRA in animal models, which is much lower than the levels that activate the molecular switch [8, 9]. The effect of endogenous ligands on the molecular switch cannot be fully assessed until the molecular switch is characterized in an animal model. In the future, new OLRP should be discovered with new ligands to avoid the potential inference dilemma.

Although the specificity of the molecular switch system to the Gal4 response elements have been successfully shown, alternative DNA binding domains can also be engineered. While the Gal4 DBD does not bind to endogenous sequences, Gal4 is a yeast protein that may cause an immunogenic response if introduced in human gene therapy applications. The development of a novel DNA binding domain can be pursued by engineering zinc finger motifs to bind an exogenous DNA sequence. Several studies have constructed novel DBD that can bind unique 18 bp sequences and have the ability to

regulate gene expression [10-13]. Creation of an artificial DBD may eliminate immunogenic response if introduced in human gene therapy applications.

One other criteria for a successful molecular switch system looks at whether ligand dosage correlates to the expression of the target gene. The addition of ligand should rapidly induce target gene expression, while the removal of ligand should rapidly suspend target gene expression. When using transient transfections to characterize the ligand time course, the molecular switch system shows rapid induction, where activation levels are observed 16 hours after the addition of ligand. However, the removal of LG335 shows steady decline in transgene expression. The steady decrease to basal levels was expected when considering the stability of LG335. LG335 has a high melting temperature of 250-252°C, therefore rapid decomposition is unlikely in cell culture assays [14]. Since transient transfections were used to characterize the ligand time course, the amount of time permitted to evaluate the ligand was limited to three and a half days. In the future, the ligand time course should be determined upon stable expression of the molecular switch system in a given cell line or animal model. Stable expression allows a more accurate assessment of the rate of gene expression since transient transfection factors are eliminated, such as plasmid retention. This will provide a more comprehensive examination of the ligand's ability to turn on or off gene expression. Also to further understand the pharmacology of LG335, *in vivo* analysis is essential to determine toxicity as well as the rate of metabolism of LG335; however, it is assumed that the pharmacological properties of this ligand would be very similar to the analog Targretin.

### **7.1.2 Future Work**

Although a molecular switch system has been characterized that can proficiently regulate gene expression, several other approaches could be implemented for further improvements in this system. One area of improvement could be the introduction of a control to test the efficiency of dual expression in the same vector. In the current molecular switch system, the expression of the reporter gene relies on the expression of GRQCIMFI as well as the binding of LG335 to GRQCIMFI. This system is functional in transient transfections; however, GFP expression is decreased when virally introduced. An appropriate control to develop would consist of a constitutively active receptor controlling expression of the reporter gene. This control allows the evaluation of maximal activation from the inducible system by eliminating the need of a small molecule to turn on gene expression. This control can be developed by fusing the Gal4 DBD to the VP16 activation domain, which is a chimeric protein capable of inducing expression of genes controlled by the Gal4 response elements without the addition of ligand. This fusion protein would replace GRQCIMFI in the one-component system and could be used for comparing inducible gene expression in transient transfection as well as retroviral transductions.

The one-component system is the preferred vector for the molecular switch system, since this vector would increase transduction efficiency while confining all components to one segment of DNA. However, several issues have arisen when using a vector containing multiple components. One of the issues with constructing this retroviral vector is determining the proper arrangement of genes when expressing two genes simultaneously. Several groups have observed “positional effects” or different expression patterns when expressing two genes within the same vector [15, 16]. These groups have

observed that the transgene at the 3' region is expressed in a lower quantity than the transgene expressed at the 5' region [15, 16]. In the current molecular switch system (Figure 7.1A), the molecular switch GRQCIMFI is located near the 5' region and is constitutively expressed under the control of a strong promoter. GRQCIMFI can then bind the Gal4 RE upon the addition of LG335 and control expression of the reporter gene, which is near the 3' region. Since the reporter gene is downstream in the molecular switch system, the decrease in gene expression observed in retrovirally transduced cells could result from inefficient gene expression due to positional effects. A possible method to increase expression of the reporter gene is to reorder the gene sequence, where the Gal4 RE and the reporter gene are cloned downstream from the 5' region, and a different strong promoter and the molecular switch are cloned upstream from the 3' region (Figure 7.1B).

Transcriptional interference may also be the cause of decreased expression of downstream transgenes. Transcriptional interference occurs when multiple transgenes contained on a single plasmid are controlled by two separate internal promoters [16, 17]. Interestingly, the insertion of enhancer sequences, such as termination signaling sequences, has also been used as a molecular tool to overcome transcriptional interference and is able to elevate expression levels of the downstream transgene [16]. For example, the chicken insulator sequence (cHS4) has been inserted into the Tet-On system to improve expression of the target gene [18]. Inserting insulator sequence(s) between the reporter gene and molecular switch, as shown in Figure 7.1B, could further enhance gene expression within this system.

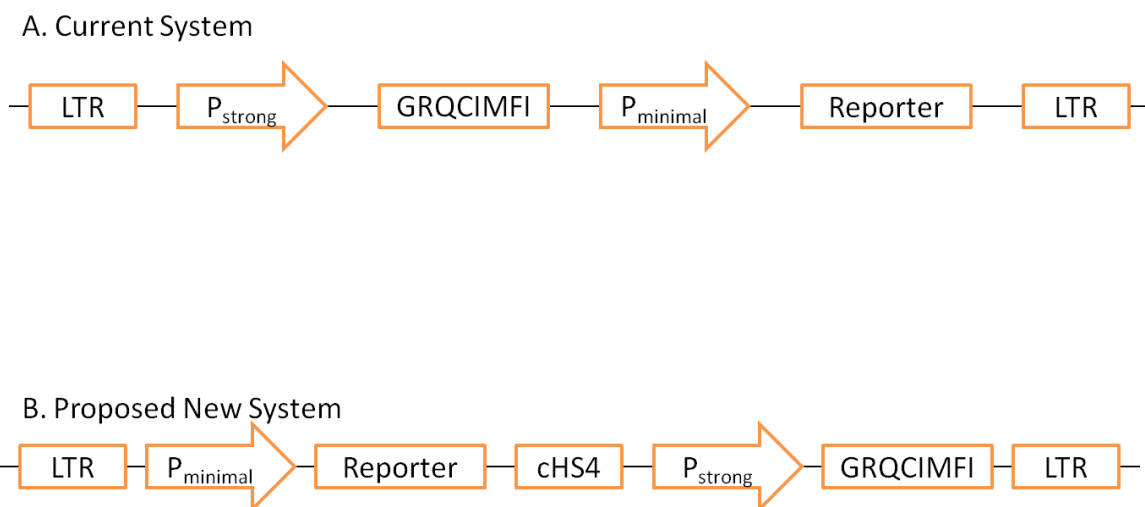


Figure 7.1: **Improvements in molecular switch system:** (A) Diagram of the current molecular switch system. (B) Diagram of a proposed new molecule switch system that would possible enhance gene expression of the reporter gene.

Another possible approach to improve gene expression in the molecular switch system is to use an alternate viral vector to stably transduce cells and express both the molecular switch and the reporter gene. Gene silencing is known to take place in retroviral systems due to methylation of viral promoter regions, which may be the cause of reduced gene expression with the reporter gene in the current molecular switch system [19]. A solution to this problem could be the utilization of a lentiviral system rather than a retroviral system. Lentiviruses are RNA viruses within the *Retroviridae* family; therefore, this viral system has the same advantages as retroviruses. In addition, this viral system is able to infect both dividing and nondividing cells whereas retroviruses only infect nondividing cells. The lentiviral system has successfully transduced a variety of cell types, such as mice, rats, chickens, and monkeys without stimulating complete gene silencing, whereas retroviruses have been only successful in transducing specific strains of mice [20]. Therefore, lentiviral systems offer an alternative method to create cell lines that stably express the molecular switch system. This viral system can also be used when characterizing the molecular switch system in small and large animal model studies.

## **7.2 The L455 Project**

### **7.2.1 Conclusions**

Chapter 6 examined the significance of the L455 position and the effect this residue exerts on RXR activity. First, the L455 position was mutated to several amino acids to analyze the tolerance at this position. Hydrophobic and polar residues that are similar in volume to leucine displayed activation profiles comparable to RXRwt. The L455 variants were then analyzed with various L436 mutations to determine whether one

of the L455 mutations could compensate for a nonfunctional variant. Results showed that the L436V L455M mutation could restore receptor activity, especially with LG335. Lastly, the interactions between L455 variants and the coactivators ACTR and SRC-1 indicated that perhaps the L455 residue is able to impact the interaction between the receptor and the coactivator.

Previous studies have focused primarily on mutating residues that line the binding pocket in order to enhance receptor function. However, this research provides a significant contribution in regards to protein engineering as this work reveals the capability of mutations outside of the ligand binding pocket to enhance protein function. The L455M variant, a residue on H12, was able to enhance receptor activation, compensate for a nonfunctional variant, as well as influence coactivator association. Applications of this study can lead to further comprehension of the role of nuclear receptors in transcriptional regulation.

### **7.2.2 Future Work**

To further develop a comprehensive and holistic understanding of the role of L455 in receptor function, future work should be conducted to confirm the results previously observed. The testing of the single and double variants with other coactivators should be performed, which could aid in the identification of the dominant coactivator associated with RXR and also facilitate understanding of gene regulation in a specific cell type. These variants could also be tested in chemical complementation with corepressors fused to the Gal4 activation domain in order to understand corepressor association, since nuclear receptors are known to interact with both coactivators and corepressors. Most importantly, *in vitro* binding studies should also be performed with coactivator peptides



and the L455M variant, to confirm the stronger interaction observed between L455M and the SRC-1 coactivator. Residues analogous to this position in other nuclear receptors should be tested to determine whether mutations at this position can affect coactivator preference. Receptors having similar activity can perhaps provide some evolutionarily insight into the possible role of residues in helix 12 influencing coactivator association.

### 7.3 Literature Cited

1. Sauvageau, G., U. Thorsteinsdottir, C.J. Eaves, H.J. Lawrence, C. Largman, P.M. Lansdorp, and R.K. Humphries, *Overexpression of HOXB4 in hematopoietic cells causes the selective expansion of more primitive populations in vitro and in vivo*. Genes Dev, 1995. **9**(14): p. 1753-65.
2. Thorsteinsdottir, U., G. Sauvageau, and R.K. Humphries, *Enhanced in vivo regenerative potential of HOXB4-transduced hematopoietic stem cells with regulation of their pool size*. Blood, 1999. **94**(8): p. 2605-12.
3. Antonchuk, J., G. Sauvageau, and R.K. Humphries, *HOXB4 overexpression mediates very rapid stem cell regeneration and competitive hematopoietic repopulation*. Exp Hematol, 2001. **29**(9): p. 1125-34.
4. Wang, Y.L., B.W. Omalley, and S.Y. Tsai, *A regulatory system for gene-transfer*. Proceedings of the National Academy of Sciences of the United States of America, 1994. **91**(17): p. 8180-8184.
5. Panguluri, S.K., P. Kumar, and S.R. Palli, *Functional characterization of ecdysone receptor gene switches in mammalian cells*. FEBS J, 2006. **273**(24): p. 5550-63.
6. Burcin, M.M., G. Schiedner, S. Kochanek, S.Y. Tsai, and B.W. O'Malley, *Adenovirus-mediated regulable target gene expression in vivo*. Proc Natl Acad Sci U S A, 1999. **96**(2): p. 355-60.
7. Seipel, K., O. Georgiev, and W. Schaffner, *Different activation domains stimulate transcription from remote ('enhancer') and proximal ('promoter') positions*. EMBO J, 1992. **11**(13): p. 4961-8.

8. Goldstein, J.T., A. Dobrzyn, M. Clagett-Dame, J.W. Pike, and H.F. DeLuca, *Isolation and characterization of unsaturated fatty acids as natural ligands for the retinoid-X receptor*. Archives of Biochemistry and Biophysics, 2003. **420**(1): p. 185-193.
9. Wolf, G., *Is 9-cis-retinoic acid the endogenous ligand for the retinoic acid-X receptor?* Nutr Rev, 2006. **64**(12): p. 532-8.
10. Magnenat, L., L.J. Schwimmer, and C.F. Barbas, *Drug-inducible and simultaneous regulation of endogenous genes by single-chain nuclear receptor-based zinc-finger transcription factor gene switches*. Gene Therapy, 2008. **15**(17): p. 1223-1232.
11. Gonzalez, B., L.J. Schwimmer, R.P. Fuller, Y.J. Ye, L. Asawapornmongkol, and C.F. Barbas, *Modular system for the construction of zinc-finger libraries and proteins*. Nature Protocols, 2010. **5**(4): p. 791-810.
12. Beerli, R.R. and C.F. Barbas, *Engineering polydactyl zinc-finger transcription factors*. Nature Biotechnology, 2002. **20**(2): p. 135-141.
13. Beerli, R.R., U. Schopfer, B. Dreier, and C.F. Barbas, *Chemically regulated zinc finger transcription factors*. Journal of Biological Chemistry, 2000. **275**(42): p. 32617-32627.
14. Schwimmer, L.J., P. Rohatgi, B. Azizi, K.L. Seley, and D.F. Doyle, *Creation and discovery of ligand-receptor pairs for transcriptional control with small molecules*. Proceedings of the National Academy of Sciences of the United States of America, 2004. **101**(41): p. 14707-14712.
15. Sadaie, M.R., M. Zamani, S. Whang, N. Sistrone, and S.K. Arya, *Towards developing HIV-2 lentivirus-based retroviral vectors for gene therapy: dual gene expression in the context of HIV-2 LTR and Tat*. J Med Virol, 1998. **54**(2): p. 118-28.
16. Osti, D., E. Marras, I. Ceriani, G. Grassini, T. Rubino, D. Vigano, D. Parolaro, and G. Perletti, *Comparative analysis of molecular strategies attenuating positional effects in lentiviral vectors carrying multiple genes*. Journal of Virological Methods, 2006. **136**(1-2): p. 93-101.

17. Villemure, J.F., N. Savard, and A. Belmaaza, *Promoter suppression in cultured mammalian cells can be blocked by the chicken beta-globin chromatin insulator 5' HS4 and matrix/scaffold attachment regions*. Journal of Molecular Biology, 2001. **312**(5): p. 963-974.
18. Tian, X.B., G.M. Wang, Y. Xu, P. Wang, S.S. Chen, H. Yang, F. Gao, A.J. Xu, F. Cao, X.G. Jin, A. Manyande, and Y.K. Tian, *An Improved Tet-On System for Gene Expression in Neurons Delivered by a Single Lentiviral Vector*. Human Gene Therapy, 2009. **20**(2): p. 113-123.
19. Jahner, D. and R. Jaenisch, *Retrovirus-induced de novo methylation of flanking host sequences correlates with gene inactivity*. Nature, 1985. **315**(6020): p. 594-7.
20. Pfeifer, A., T. Lim, and K. Zimmermann, *Lentivirus transgenesis*. Methods Enzymol, 2010. **477**: p. 3-15.